Universidad de Córdoba

Departamento de Biología Celular, Fisiología e Inmunología

Doctoral Thesis

Analysis of the roles of kisspeptins and the tachykinin receptor, Tacr2, in the control of Reproduction: novel interactive pathways, regulatory mechanisms and metabolic implications.

Encarnación Torres Jiménez

Córdoba, 9 de febrero de 2021

TITULO: *Analysis of the roles of kisspeptins and the tachykinin receptor, Tacr2, in the control of Reproduction: novel interactive pathways, regulatory mechanisms and metabolic implications*

AUTOR: *Encarnación Torres Jiménez*

Campus de Rabanales
Ctra. Nacional IV, Km. 396 A
14071 Córdoba

https://www.uco.es/ucopress/index.php/es/
ucopress@uco.es

Universidad de Córdoba

Departamento de Biología Celular, Fisiología e Inmunología

Analysis of the roles of kisspeptins and the tachykinin receptor, Tacr2, in the control of Reproduction: novel interactive pathways, regulatory mechanisms and metabolic implications.

Memoria de Tesis Doctoral presentada por **Encarnación Torres Jiménez**, graduada en Bioquímica por la Universidad de Córdoba, para optar al grado de **Doctora** en Biomedicina por la Universidad de Córdoba.

Los Directores,

TENA SEMPERE MANUEL JOSE - 30534904N
Firmado digitalmente por TENA SEMPERE MANUEL JOSE - 30534904N
Fecha: 2021.02.09 11:43:05 +01'00'

Dr. Manuel Tena Sempere
Catedrático de Fisiología de la Universidad de Córdoba

ROMERO RUIZ ANTONIO - 79221402H
Digitally signed by ROMERO RUIZ ANTONIO - 79221402H
Date: 2021.02.09 11:16:05 +01'00'

Dr. Antonio Romero Ruiz
Investigador Postdoctoral Senior
Programa "Nicolás Monardes"

Título de la Tesis: Analysis of the roles of kisspeptins and the tachykinin receptor, Tacr2, in the control of Reproduction: novel interactive pathways, regulatory mechanisms and metabolic implications.

Doctoranda: Encarnación Torres Jiménez

Informe razonado de los directores de la Tesis

El trabajo de Tesis Doctoral titulado "Analysis of the roles of kisspeptins and the tachykinin receptor, Tacr2, in the control of Reproduction: novel interactive pathways, regulatory mechanisms and metabolic implications" ha sido completado de forma muy satisfactoria por la doctoranda Encarnación Torres Jiménez en la Sección de Fisiología del Departamento de Biología Celular, Fisiología e Inmunología de la Universidad de Córdoba, entre los años 2015 y 2021, bajo nuestra dirección. El objetivo general de esta Tesis doctoral ha sido ampliar el conocimiento sobre los mecanismos de acción de las kisspeptinas y el papel de las taquiquininas en la regulación de la función reproductiva mediante el uso de modelos murinos novedosos, genéticamente modificados. En concreto, se ha avanzado en la definición del papel fisiológico de la señalización del receptor 2 de taquiquininas, NK2R, en el control reproductor y metabólico, y se ha identificado una nueva vía de señalización de kisspeptins en los astrocitos, como posibles mediadores de al menos parte de las acciones biológicos de las kisspeptinas en el control de la reproducción.

Durante el período predoctoral, la doctoranda no sólo ha cumplido ampliamente el objetivo general propuesto, sino que también ha aprovechado esta etapa formativa para (i) adquirir una considerable destreza en el manejo de diferentes técnicas de biología molecular y neuroendocrinología experimental, (ii) reforzar sus conocimientos en el área de estudio, (iii) estimular su pensamiento crítico y (iv) colaborar activamente en líneas de investigación estrechamente relacionadas con su línea de Tesis Doctoral.

La excelente labor investigadora de la doctoranda durante este periodo se ha traducido hasta hasta la fecha en: (i) 1 artículo científico como primera autora publicado en la revista *American Journal of Physiology -Endocrinology and Metabolism*, en primer cuartil del área de Fisiología, y otro que se anticipa que será completado en breve a fin de proceder con su envío a evaluación, a una revista de primer decil, en el primer semestre del año en curso; (ii) 4 artículos científicos como co-autora, todos en primer decil (*Cell Metabolism*, *American Journal of Obstetrics and Gynecology*, *Metabolism* y *Human Reproduction*), (iii) 11 comunicaciones a congresos nacionales e internacionales; (iv) 2 becas para asistencia y participación, "Research Visit Grant" (2017) y "International Conference Travel Fund" (2019) ambas concedidas por la Sociedad Británica de Neuroendocrinología; y (v) 2 estancias financiadas en centros de prestigio: *University of Stanford*, California (2018) y *University of Cambridge*, Reino Unido (2019).

Por todo lo anteriormente expuesto, se autoriza la presentación de esta Tesis Doctoral.

Córdoba, 9 de febrero de 2021

Firma de los directores

TENA SEMPERE MANUEL JOSE - 30534904N
Firmado digitalmente por TENA SEMPERE MANUEL JOSE - 30534904N
Fecha: 2021.02.09 11:44:05 +01'00'

ROMERO RUIZ ANTONIO - 79221402H
Digitally signed by ROMERO RUIZ ANTONIO - 79221402H
Date: 2021.02.09 11:17:08 +01'00'

Fdo.: Manuel Tena Sempere

Fdo.: Antonio Romero Ruiz

Agradecimientos

Esta tesis está llena de serendipia, mucha. Ahora os cuento, pero antes aclaro que me voy a dejar llevar un poco por la entropía. Empezando por el final quiero concluir que no sólo he descubierto la magia de la ciencia sino también del valor del trabajo constante y en equipo. Ahora sí. En esta historia, el primer hallazgo afortunado e inesperado del que os hablado es el de formar parte del grupo GCIO. De él diré que ha sido mi casa; y de mis compañeros, mi familia, esa misma que te enseña, te apoya, te acompaña, celebra contigo, mucho, y también te riñe si viene al caso.

El primer gracias de los muchos que diré es para mis directores de tesis, Manolo Tena y Antonio Romero. Me siento afortunada de haber tenido y aprendido de un jefe de grupo como Manolo, excepcional ejemplo de científico y líder, al que admiro mucho. Gracias Manolo por fomentar el más que deseado ambiente de trabajo con el que contamos. Antonio, gracias por implicarte siempre, durante mi etapa como alumna interna, como estudiante de máster y durante la tesis. Gracias por enseñarme, apoyarme y equilibrar la balanza con tu constante positividad.

Gracias también a ti, Leo, por tu cercanía, tus consejos y por celebrar nuestros logros como la que más. Contigo aprendí que si alguien te importa, hacerle el camino más fácil no hará que la persona se esfuerce y aprenda tanto como debiera. Y de jefa a otra jefa, Chus, gracias por enseñarnos (al equipo Ratatouille y a mí) que da igual si eres postdoc, si tienes mil clases o reuniones de departamento, que si hay que arremangarse y ponerse la bata se hace. Por proximidad de despacho, el siguiente gracias va para Juan o también conocido como el Sensei. Gracias por dejarme molestarte siempre con mis dudas científicas y a veces no tan científicas y terminar haciendo de psicólogo junto con Chus. No muy lejos está Rocio o Encarni, no sé, depende del lío en el que se haya metido o de las escaleras por las que suba o baje. Gracias por tu ayuda, tu siempre disposición y por alegrarnos el lab con letras de carnaval mientras genotipas. Anita, a ti también gracias, por tu cariño y enseñarnos todo lo que sabemos del subsuelo (animalario). Si vamos a la sala de postdocs, gracias Curro, por rescatarnos una y otra vez, con los congeladores, los ordenadores, las in situs,...! Patxi, Marisol, Vero, Miguel Ángel, David y Silvia (sí, lo sé, somos un supergrupo y aún no he terminado) gracias por vuestra ayuda y consejos.

Gracias a mi mami del lab, Mª Jesús, por cuidarme, ayudarme y preocuparte siempre, y por reñirme cuando hace falta. Rafa, gracias por todo, por enseñarme tanto, dentro y también fuera del lab, por ser crítico conmigo y hacer que quiera ser mejor. ¡Serendipia contigo! Que sepas que seguiré al gato (referencia a Susurros del Corazón, estudios Ghibli). ¡Gracias, gracias!

¡Equipo Ratatouille allá vamos! Amiga Alexia, gracias por tu cariño, por tus divertidas ocurrencias y tu admirable entusiasmo. Estoy feliz de poder compartir contigo un año más de trabajo bata con bata. Niño Miguel, gracias por *estar a hierros* con nosotras y con nuestros dilemas científicos, y por regalarnos joyitas como «estar cabañoso» y «ser taleguero» aunque después hagas que tenga que poner fechas antiguas a las soluciones de incubación, ajam ajam. Cecilia, tenerte como compi de mesa ha sido como pipetear y vortear, ¡gracias! Además, abejita, sí que damos pie con *bolo* consiguiendo los mejores duplicados de absorbancia ever, ¡yuju! Sarini, eres muy brava amiga. Gracias

por acogerme en la bellisimisima Italia! Violetii, hermana del lab y hasta en casa también, gracias por darnos vida con tus líos, por todos los momentos y viajes que hemos compartido. Eres genial! ¿Y de la mejor guiri del mundo qué digo? ¿Qué pasará, qué misterio habrá...? Delphine, gracias por formar parte de todo lo divertido que tramamos, por la visita a Cambridge, por los viajes, las risas en el pádel y por ser para mí un ejemplo a seguir como científica. ¡Delphine, Violeta, os echo mucho de menos amigas! Pequeña Elvi, es una fantasía tenerte como amiga y como compi del lab. Gracias por todo, risas, pádel, viajes, ideas locas que terminan en ser influencers de ciencia, y las maldades, que se nos acumulan eh, aunque... ¡pues ni tan mal! Inmi, eres única. Si tuviera que resumirlo sería algo así como: #niunplansininma #lapulsatilidadcontigoesmenospulsatilidad #mejorcompidelíos #dandomieditoporellab #estefaníanostienecaladas #laspreferidasdecarmen #ponunainmaentuvida. Gracias por enseñarme tanto. He aprendido muchísimo contigo. ¡Te admiro amiga! Hey, no voy a olvidarme de ti Adelaida. Gracias por dejarnos usar tu nombre para cualquier incidente de lab del que no conocemos al causante, muy amable. ¡Gracias EQUIPO, os quiero!

Quiero agradecer también a todos los colaboradores nacionales como internacionales que han contribuido al desarrollo de esta Tesis: Stephania Meine, Ariane Sharif, Giuliana Pellegrino, Paco Gaytán por vuestra inestimable ayuda. A Antonio Carlos por enseñarme a trabajar con cultivos y cuidar de las células. Ha sido un *plaser* trabajar contigo, outlier. De mi estancia en Cambridge, quiero agradecerle a Bill Colledge la hospitalidad en su laboratorio y su colaboración en el proyecto de la glía. Gracias también a Stephen y Ya-Ling por acogerme en Cambridge y compartir conmigo una experiencia única y enriquecedora.

Sigo...gracias a Caro, Teru, Crece, Sandra, Noe, Diego y a mi familia que, apoyándome desde las gradas, son mis incondicionales. Papá, mamá, hermanas, tata, gracias por apoyarme y cuidarme siempre. Abuelas, ¡cuánto se ha perdido el mundo de vosotras, por no dejaros volar tan alto como queríais! Gracias por ser mis *referentas* de mujeres fuertes y trabajadoras, por hacer que trabaje incansablemente para conseguir las metas que me proponga y por hacerme feliz sabiendo lo orgullosas que siempre estáis de lo que hago. Gracias también a mi compi de piso José Joaquín, por cuidarme, apoyarme y aguantar cada «no, hoy tampoco me ha salido el experimento». ¡Gracias FAMILIA, os quiero!

Y así aquí termino dándoos las gracias a todos, porque acabo esta etapa y empiezo otra que no sería posible, o como mínimo no sería lo mismo, sin vuestra ayuda y apoyo. ¡Gracias¡

I’m sorry I know so little. I’m sorry we all know so little.
But that’s kind of the fun, isn’t it?

Vera Rubin 1928-2016

Index

Index

Summary

Summary

1. Introduction

The reproductive function in mammals is indispensable for the perpetuation of the species. Thus, it is safeguarded by sophisticated regulatory networks. The neuroendocrine system responsible for controlling this function is the so-called hypothalamic-pituitary-gonadal (HPG) axis, also known as reproductive axis[1,2]. Within the HPG axis, the gonadotropin-releasing hormone (GnRH) neurons conform the major hierarchical hub, integrating endogenous (e.g., metabolic hormones) and exogenous (e.g., nutritional cues) factors, and whose neuro-secretory activity is regulated by a variety of trans-synaptic and glial inputs, including glutamate, prostaglandins, GABA, GnIH and NPY. Likewise, proper reproductive capacity depends on the pulsatile secretion of GnRH[3,4].

Among the numerous neuropeptides and transmitters that are regulating the secretion of GnRH, kisspeptins are recognized as master regulators. Kisspeptins are a family of structurally related peptides derived from a common precursor, whose biological actions are mediated through Gpr54, a G protein-coupled receptor[5,6]. Kisspeptins have been described to play a major role in sexual differentiation, timing of puberty and gonadotropin pulsatile secretion[6,7]. However, our current knowledge about the mechanisms and down-stream targets whereby kisspeptins conduct their central regulatory actions is rather incomplete. Thus, the identification and characterization of novel co-transmitters and effector pathways are important, since these may provide a deeper understanding of the mode of action of kisspeptins and of their roles in the regulation of reproductive function.

Tachykinins (TACs) have also emerged as key regulators of GnRH neuro-secretion and of different aspects of reproductive function, via close interaction with the kisspeptin pathway[8-10]. However, due to the considerable crosstalk and partial redundancy of the elements of TAC system, as defined by multiple ligands (SP, NKA, NKB) and receptors (NK1R, NK2R, NK3R), teasing apart the individual roles of the specific TAC pathways has been difficult and remains to date elusive[11]. In this context, the putative physiological role of NK2R signaling in the control of reproduction persists particularly ill-defined and its characterization has been so far mostly based on pharmacological analyses or studies in murine models with congenital ablation of the *Tac1* gene, which encodes both SP and NKA[12,13].

In the above context, the aims of this Doctoral Thesis have been to explore (i) the role of NK2R signaling in the control of reproductive function, by characterizing a novel mouse line with a congenital ablation of the *Tacr2* gene; and (ii) novel mediators for the effects of kisspeptins in the hypothalamus, by implementing proteomic analyses in a suitable genetic model. The latter analyses led also to (iii) the assessment of the physiological roles of kisspeptin signaling in astrocytes, as putative novel mechanism for regulating the reproductive axis, using, among other approaches, a novel mouse line with a selective ablation of *Gpr54*, the gene encoding the canonical kisspeptin receptor, in GFAP-positive cells.

2. Research contents

For sake of clarity, this Doctoral Thesis has been divided in 3 main experimental sets:

In the **Experimental Set 1**, a comprehensive series of phenotypical, pharmacological, behavioral and histological analyses were conducted in a novel mouse line with congenital ablation of *Tacr2*, namely, the Tacr2 KO mouse, to unravel the physiological role of neurokinin 2 receptor (NK2R) signaling, and its eventual interplay with kisspeptins, in the control of the HPG axis.

Our initial pharmacological studies documented the capacity of the agonist of NK2R to evoke acute LH responses after icv administration in control mice, which was comparable with those elicited by the other TAC agonists as well as kisspeptin (Kp-10). Similar pharmacological studies in Tacr2 KO mice revealed that the LH responses to the NK1R and NK3R receptor agonists and Kp-10 were not affected by *Tacr2* ablation. On the contrary, the LH response to a NK2R agonist was sexually dimorphic, so that Tacr2 KO female mice displayed an attenuated LH response while, despite effective ablation of NK2R, Tacr2 KO male mice displayed a grossly conserved LH responsiveness to NK2R agonist, which, nonetheless, was abrogated after blockade of NK3R.

Next, we carried out a thorough reproductive characterization of Tacr2 null mice of both sexes, which documented that the congenital lack of NK2R signaling does not compromise the timing of puberty onset or the fertility either in males or females. Yet, a trend for increased breeding intervals together with partially alteration in LH pulsatility were observed in Tacr2 KO female mice in adulthood; the latter consisting in the suppression of basal LH levels, but no changes in the number of LH pulses. On the other hand, histological analyses suggested the existence

of a defective function of Sertoli cells in their interaction with spermatids in adult Tacr2 KO male, but no gross morphological alterations in the ovary or the uterus of females KO mice.

In addition, Tacr2 KO female mice failed to display a significant increase of LH levels at 2 days after ovariectomy (OVX), although no differences were detected at later periods, nor did OVX Tacr2 KO female mice showed differences in terms of tail skin temperature as compared with littermate controls. On the other hand, LH levels in Tacr2 KO mice subjected to conditions of energy deficit caused by 24-h fasting were significantly lower than in controls.

A three-chamber social sex preference and female urine sniffing tests were also applied to adult male and female null mice and their controls. Yet, no differences in any of the behavioral parameters explored, including velocity, distance moved and time spent in the vicinity of the same or opposite-sex mouse, were noted between control and KO mice. Additionally, to assess the impact of the lack of NK2R signaling on key metabolic parameters, we monitored body weight gain in both adult female and male Tacr2 KO mice, which was similar to that of control littermates. Likewise, body composition analyses demonstrated similar fat and lean mass in Tacr2 KO and control mice; energy expenditure and respiratory quotient, total and nocturnal locomotor activity, and the day/night feeding patterns during 24 hours were also similar in control and Tacr2 KO mice. Moreover, measurement of blood pressure demonstrated that Tacr2 KO mice display values of systolic blood pressure similar to their control littermates. Finally, metabolic analyses addressing glucose homeostasis after challenge mice with an obesogenic diet revealed a significant increase in the basal glucose levels in Tacr2 KO males.

In the **Experimental Set 2**, a series of proteomic, molecular and immunohistochemical analyses were implemented using genetically modified mouse lines to explore novel targets mediating kisspeptins actions. We performed a first proteomic analysis in samples from the preoptic area (POA) of Kiss1 KO male mice icv injected with Kp-10, which pointed out a set of 30 differentially-expressed proteins involved in cellular metabolism and energy balance, cell signaling, protein folding and synaptic plasticity; the later revealed that glial fibrillary acidic protein (GFAP), an astrocyte marker, was modified in response to Kp-10. In a second proteomic analysis using a next-generation technology, we found that astrocyte markers including GFAP were again modified in response to Kp-10; a finding that was also confirmed by RT-qPCR and western blot analyses. These findings led us to analyze and demonstrate for the first time the expression of *Gpr54* and the presence of functional kisspeptin receptors in astrocytes. On the latter, we found in both primary astrocyte cultures from neonatal rats and

mice the activation of downstream signaling pathways in response to kisspeptin. Our data also demonstrated the co-expression of *Gpr54* in GFAP-positive cells in mouse brain tissue, with a substantial enrichment in the % of co-location in the hypothalamic regions of the vascular organ of lamina terminalis (VOLT) and anteroventral periventricular nucleus (AVPV). In addition, in two models of congenital ablation of *Gpr54*, we observed changes in astrocytic GFAP labelling by immunohistochemistry in the arcuate nucleus (ARC) of these mouse models, although immunoreactivity of S100 calcium binding protein B (S100β), another astrocytic marker protein, was not affected.

Finally, in the **Experimental Set 3**, a series of phenotypic and pharmacological analyses were conducted in a novel mouse line with selective ablation of *Gpr54* in GFAP-positive cells, namely, the G-KiRKO mouse (for **G**FAP cell-specific **Ki**sspeptin **R**eceptor **KO**), to evaluate the physiological role of kisspeptin signaling in astrocytes in the control of the reproductive axis. First, we carried out a set of molecular and immunohistochemical analyses that involved the use of a reporter mouse line and primary astrocyte cultures for the validation of our G-KiRKO model. These analyses confirmed effective ablation of Gpr54 in astrocytes. However, despite the effective disruption of kisspeptin signaling in astrocytes, characterization of G-KiRKO mice revealed normal pubertal timing, and preserved LH levels and estrous cyclicity in the adulthood of G-KiRKO mice. Yet, challenging of G-KiRKO mice with icv injection of Kp-10 demonstrated an enhancement of LH responses, suggesting a repressive role of astrocyte signaling in mediating kisspeptin actions in terms of gonadotropin secretion.

The measurement of the metabolic parameters (i.e., body weight gain and body composition analysis) did not show differences in G-KiRKO vs. control mice. Nevertheless, the glucose tolerance test (GTT) revealed a subtle improvement of the response to a glucose bolus in G-KiRKO mice, without showing alterations in insulin sensitivity. On the other hand, obesogenic conditions defined by chronic exposure to HFD evidenced a delay in the vaginal opening (VO), external marker of puberty in female rodents, in HFD-fed G-KiRKO mice in comparison to HFD-fed control mice. In contrast, no differences were detected in term of first estrus, indirect marker of first ovulation, neither in the age of balano-preputial separation (BSP), external marker of puberty in male rodents, in HFD-fed KO mice versus controls. In adulthood, only HFD-fed G-KiRKO female mice displayed the LH hyper-response to Kp-10, as observed in lean conditions. In addition, high-fat diet exposure induced estrous cycle irregularities in G-KiRKO female mice, as evidenced by longer cycle length and a higher number of days in diestrus and reduced number of days in estrus. The metabolic parameters, such as body weight

gain and body composition remained unaltered in G-KiRKO mice. In HFD-fed G-KiRKO males, the levels of glucose during the GTT were lower than those observed for control mice, as already registered in conditions of normal feeding. In contrast, no differences in terms of insulin sensitivity (assessed by ITT) were detected. In the case of HFD-fed G-KiRKO female mice, no differences in basal glucose levels, neither in the response to glucose or insulin boluses, were detected. Finally, GFAP immunoreactivity was not different in the ARC nucleus of G-KiRKO male mice fed HFD in comparison to their controls. By contrast, GFAP immunoreactivity responses to acute exposure to HFD were significantly lower in the ARC of G-KiRKO male mice.

3. Conclusions

The major conclusions of this Doctoral Thesis are the following:

1. Congenital ablation of the tachykinin receptor, NK2R, namely the canonical receptor for NKA, causes discernible, albeit moderate deficits in the functioning of the reproductive axis, including the suppression of basal and mean LH levels, trend for lengthening of breeding intervals and defective function of Sertoli cells, together with a moderate perturbation of glucose homeostasis in obesogenic conditions, but without preventing normal fertility or social sex behavior. These findings reveal a modest, albeit detectable role of NK2R signaling in the control of the reproductive axis, with partially overlapping and redundant functions with other tachykinin receptors.

2. Our data are the first to document the capacity of kisspeptins to activate hypothalamic glial responses *in vivo* and the existence of a previously unsuspected, functional kisspeptin receptor pathway in astrocytes, which utilizes canonical signaling factors, such as ERK, and regulates glial cell markers. Effective disruption of kisspeptin signaling in astrocytes *in vivo* induced only modest alterations in the functioning of the reproductive axis in basal conditions, denoted by enhancement of LH secretion after kisspeptin stimulation, but perturbed some reproductive responses to metabolic stress induced by HFD, including altered pubertal timing and estrous cyclicity in female mice, and attenuated indices of reactive gliosis after short-term exposure to high fat content diet.

4. Bibliography

1. Fink, G. in *Neuroendocrinology in Physiology and Medicine* (eds. Conn, P. M. & Freeman, M. E.) 14, 107–133 (Humana Press, 2000).

2. Schwartz, N. B. in *Neuroendocrinology in Physiology and Medicine* (eds. Conn, P. M. & Freeman, M. E.) 139, 135–145 (Humana Press, 2000).
3. Carmel, P. W., Araki, S. & Ferin, M. Pituitary Stalk Portal Blood Collection in Rhesus Monkeys: Evidence for Pulsatile Release of Gonadotropin-Releasing Hormone (GnRH). *Endocrinology* 99, 243–248 (1976).
4. Tsutsumi, R. & Webster, N. J. G. GnRH Pulsatility, the Pituitary Response and Reproductive Dysfunction. *Endocrine Journal* 56, 729–737 (2009).
5. Bilban, M. Kisspeptin-10, a KiSS-1/metastin-derived decapeptide, is a physiological invasion inhibitor of primary human trophoblasts. *Journal of Cell Science* 117, 1319–1328 (2004).
6. Pinilla, L., Aguilar, E., Dieguez, C., Millar, R. P. & Tena-Sempere, M. Kisspeptins and Reproduction: Physiological Roles and Regulatory Mechanisms. *Physiological Reviews* 92, 1235–1316 (2012).
7. Terasawa, E., Guerriero, K. A. & Plant, T. M. in *Kisspeptin Signaling in Reproductive Biology* (eds. Kauffman, A. S. & Smith, J. T.) 784, 253–273 (Springer New York, 2013).
8. Navarro, V. M. *et al.* Regulation of Gonadotropin-Releasing Hormone Secretion by Kisspeptin/Dynorphin/Neurokinin B Neurons in the Arcuate Nucleus of the Mouse. *J. Neurosci.* 29, 11859–11866 (2009).
9. Navarro, V. M. *et al.* The Integrated Hypothalamic Tachykinin-Kisspeptin System as a Central Coordinator for Reproduction. *Endocrinology* 156, 627–637 (2015).
10. León, S. & Navarro, V. M. Novel Biology of Tachykinins in Gonadotropin-Releasing Hormone Secretion. *Semin Reprod Med* 37, 109–118 (2019).
11. León, S. *et al.* Redundancy in the central tachykinin systems safeguards puberty onset and fertility. 51, 523–36 (2019).
12. Maguire, C. A. *et al.* Tac1 Signaling Is Required for Sexual Maturation and Responsiveness of GnRH Neurons to Kisspeptin in the Male Mouse. *Endocrinology* 158, 2319–2329 (2017).
13. León, S. *et al.* Characterization of the Role of NKA in the Control of Puberty Onset and Gonadotropin Release in the Female Mouse. *Endocrinology* 160, 2453–2463 (2019).

Resumen

Resumen

1. Introducción

En mamíferos, la reproducción es una función indispensable para la perpetuación de las especies, y dada su importancia, es asegurada por una red sofisticada de señales reguladoras. El sistema neuroendocrino encargado de controlar esta función es el denominado eje hipotálamo-hipófiso-gonadal o también conocido eje reproductivo[1,2]. Dentro de este eje, a nivel hipotalámico, las neuronas GnRH son el principal centro de integración de factores tanto endógenos (p. ej. hormonas metabólicas) como exógenos (p. ej. señales nutricionales). A su vez, su actividad secretora es regulada por múltiples señales de origen neuronal y glial. De hecho, para el correcto funcionamiento del eje reproductivo es esencial la secreción pulsátil de GnRH[3,4].

De entre los numerosos neuropéptidos y transmisores que modulan la actividad neuro-secretora de las neuronas GnRH, las kisspeptinas destacan como reguladores principales. En concreto, las kisspeptinas son una familia de péptidos relacionados, derivados de un precursor común, que realizan su función a través de Gpr54, un receptor acoplado a proteínas G[5,6]. Las kisspeptinas desempeñan un papel importante en la diferenciación sexual, la pubertad y la secreción pulsátil de gonadotropinas[6,7]. Sin embargo, el conocimiento que tenemos sobre los mecanismos y dianas de acción de las kisspeptinas requiere de más investigación, siendo de gran interés la identificación de nuevas rutas de señalización y elementos mediadores de las kisspeptinas en el control de la función reproductiva.

Por otro lado, las taquiquininas (TACs) son también reconocidas como factores reguladores clave de la secreción de GnRH y de otros aspectos de la función reproductiva, en una estrecha interacción con las kisspeptinas[8-10]. No obstante, la redundancia y el solapamiento de las distintas taquiquininas (SP, NKA, NKB) y sus receptores (NK1R, NK2R, NK3R), dificulta el estudio individual de cada uno de los elementos de este sistema[11]. De hecho, el papel de la señalización por el receptor 2 de taquiquininas (NK2R) en el control de la función reproductiva sigue sin ser caracterizado en detalle, a excepción de aproximaciones basadas en estudios farmacológicos o de modelos murinos con eliminación congénita del gen *Tac1*, que codifica tanto para SP como para el ligando preferencial de NK2R, que es NKA[12,13].

En base a lo anteriormente expuesto, el objetivo de esta Tesis Doctoral es (i) caracterizar el papel de NK2R en el control de la función reproductiva, mediante estudios en un modelo

novedoso de eliminación congénita de *Tacr2*; y (ii) identificar nuevas dianas mediadoras de los efectos de kisspeptinas en el hipotálamo mediante estudios proteómicos en modelos murinos genéticamente modificados. Por otro lado, derivado de este último, en esta Tesis se pretende igualmente (iii) caracterizar el papel de la señalización por kisspeptina en astrocitos, mediante la generación de un modelo novedoso de eliminación selectiva de *Gpr54* en células GFAP-positivas.

2. Contenido de la investigación

Esta Tesis Doctoral se ha dividido en tres bloques experimentales principales:

En el **Bloque Experimental 1**, se ha realizado una caracterización fenotípica, farmacológica y comportamental exhaustiva, incluyéndose también análisis histológicos, del modelo de ratón con ablación congénita de *Tacr2*, denominado Tacr2 KO, para desvelar la implicación de la señalización por NK2R, y su interacción con kisspeptinas, en el control de la función reproductiva.

Los estudios farmacológicos iniciales documentaron la capacidad del agonista de NK2R para evocar una respuesta en términos de secreción de LH tras su administración icv en ratones control, en la misma medida que lo hacen los otros agonistas de taquiquininas y la kisspeptina (Kp-10). Estudios farmacológicos similares en el modelo Tacr2 KO no mostraron alteraciones en la respuesta de LH a los agonistas de NK1R y NK3R así como de Kp-10. No obstante, en la respuesta de LH al agonista de NK2R se observó un dimorfismo sexual; esto es, mientras que en hembras la respuesta apareció parcialmente atenuada, en los machos Tacr2 KO esta respuesta estuvo prácticamente conservada, siendo esta última suprimida tras el bloqueo de la señalización por NK3R.

La caracterización reproductiva de este modelo reveló que el inicio de la pubertad y la fertilidad no están comprometidas por la ausencia de señalización por NK2R, aunque sí se detectó una tendencia al incremento en el intervalo de cría, así como un deterioro en la función en las células de Sertoli en su interacción con las espermátides en los ratones macho adultos Tacr2 KO, aunque ninguna alteración en ovario ni útero en el caso de las hembras KO. Por otro lado, los ratones hembra Tacr2 KO presentaron niveles basales de secreción pulsátil de LH significativamente bajos, sin cambios aparentes en el número de pulsos de LH. Además, en las hembras Tacr2 KO, no se observó el incremento de los niveles de LH tras dos días después de la ovariectomía (OVX) que sí es detectado en las hembras controles. En estas mismas hembras

Tacr2 KO ovariectomizadas, el perfil de temperatura de la cola monitorizado no reveló diferencias con respecto a los controles.

En el caso de los machos Tacr2 KO, en condiciones de déficit energético consecuencia de un ayudo de 24 horas de duración, se registraron niveles de LH significativamente más bajos que los de los controles. Por otro lado, los estudios de comportamiento de preferencia por el sexo opuesto y de orina de hembras, en los que se incluye la monitorización de la velocidad y distancia recorrida durante el test, no mostraron ninguna respuesta diferencial entre los ratones KO y los controles. Adicionalmente, se analizaron indicadores metabólicos para valorar el impacto de la ausencia de señalización por NK2R sobre la homeostasis metabólica. Entre ellos la ganancia de peso corporal fue similar entre ratones Tacr2 KO y sus controles. Del mismo modo, los análisis de composición corporal indicaron que no había diferencias en el porcentaje de masa grasa y magra entre KO y controles, ni tampoco en el gasto energético, coeficiente respiratorio, actividad locomotora total y nocturna, ni en los patrones de ingesta durante el día y la noche registrados durante 24 horas. La medida de la presión sanguínea tampoco evidenció diferencias entre animales controles y KO. Finalmente, se observaron niveles basales de glucosa significativamente más elevados en los ratones macho Tacr2 KO tras la exposición crónica de estos a una dieta obesogénica.

En el **Bloque Experimental 2**, se llevaron a cabo una serie de análisis proteómicos, moleculares e inmunohistoquímicos en modelos de ratón modificados genéticamente dirigidos a identificar nuevas dianas de acción de las kisspeptinas. En el primer estudio proteómico realizado en muestras del área preóptica del hipotálamo de ratones deficientes para kisspeptina, Kiss1 KO, inyectados intracerebroventriculamente (icv) con Kp-10, se observó la expresión diferencial de 30 proteínas implicadas en el metabolismo celular y balance energético, señalización celular, plegamiento de proteínas y plasticidad sináptica; identificándose en esta última categoría a la proteína acídica fibrilar glial (GFAP), marcador de astrocitos. En el segundo estudio proteómico, en el que se empleó una tecnología de nueva generación, se detectó de nuevo que la expresión de GFAP y otros indicadores de astrocitos eran modificados en respuesta a la administración de kisspeptina; efecto que fue confirmado también por análisis de RT-qPCR y western blot. A partir de estas evidencias, implementamos una serie de análisis que permitieron demostrar por primera vez en cultivos primarios de astrocitos de rata y ratón la expresión del receptor de kisspeptina, *Gpr54*. Además, se comprobó que la señalización por kisspeptinas era funcional en estas células. *In vivo* se detectó la co-expresión de *Gpr54* y GFAP

en cerebro de ratón, registrándose un enriquecimiento del porcentaje de co-localización Gpr54-GFAP en las áreas hipotalámicas del órgano vascular de la lámina terminal (VOLT) y del área anteroventral periventricular (AVPV). Por último, mediante análisis por inmunohistoquímica se observaron cambios en el marcaje de GFAP en el núcleo arcuato (ARC) en dos modelos de ratón con eliminación congénita de *Gpr54*, si bien dichos cambios no fueron extensibles a la proteína S100B de unión a calcio, otro marcador de astrocitos.

Finalmente, en el **Bloque Experimental 3**, se llevaron a cabo una serie de estudios fenotípicos y farmacológicos en un modelo novedoso de ratón con deleción selectiva del receptor *Gpr54* en células GFAP-positivas, modelo de ratón denominado como G-KiRKO (del inglés ***G****FAP cell-specific* ***Ki****sspeptin* ***R****eceptor* ***KO***), a fin de caracterizar el papel fisiológico de la señalización por kisspeptinas en astrocitos en el control de la función reproductiva. Primero, se validó el modelo mediante análisis moleculares e inmunohistoquímicos empleando una línea reportera de ratón y cultivos primarios de astrocitos; análisis que confirmaron la eficiente eliminación de *Gpr54* de astrocitos. Sin embargo, la eliminación efectiva de la señalización de kisspeptina en astrocitos en el modelo G-KiRKO, no afectó la edad de llegada a la pubertad, ni modificó la secreción de LH ni alteró el ciclo estral en la edad adulta. En cambio, los ratones G-KiRKO presentaron respuestas significativamente aumentadas de LH tras la administración icv de Kp-10.

Por otro lado, los ratones G-KiRKO tampoco presentaron alteraciones en parámetros metabólicos como son el peso y composición corporal, pero sí se registró una respuesta glucémica mejorada en el test de sobrecarga de glucosa, sin verse afectada la respuesta a insulina. A su vez, los ratones hembra G-KiRKO mostraron una atenuación del efecto de una dieta obesogénica (HFD) sobre el adelanto de la edad de apertura vaginal, marcador externo de llegada a la pubertad en roedores hembra. No obstante, no se afectó la edad de primer estro, indicador de la primera ovulación en roedores, ni tampoco la edad de la separación balano-prepucial en el caso de los ratones macho. En la edad adulta, solo en el caso de las hembras G-KiRKO se detectó un aumento excesivo de la respuesta de LH tras la administración con Kp-10, que previamente se había observado en condicionales basales. Además, con la exposición a la dieta rica en grasas, el ciclo estral en hembras KO se vio comprometido, registrándose ciclos más largos, con un mayor número de días en la fase de diestro y menos en estro. Por otro lado, los valores de parámetros metabólicos como el peso y la composición corporal en los ratones G-KiRKO fueron comparables a los de los controles. Bajo esta condición de estrés

metabólico, solo los machos G-KiRKO mostraron una respuesta glucémica mejorada, similar a la observada en condiciones fisiológicas, sin alteraciones en la respuesta a insulina, y sin diferencias en la respuesta de glucosa ni de insulina entre las hembras controles y G-KiRKO. Por otro lado, los ratones macho G-KiRKO presentaron una respuesta disminuida en términos de inmunoreactividad de GFAP en el ARC tras exposición aguda a HFD.

3. Conclusiones

Las principales conclusiones de esta Tesis Doctoral son:

1. La eliminación congénita del receptor de taquiquininas, NK2R, receptor preferencial de NKA, causa alteraciones moderadas pero detectables en el funcionamiento del eje reproductivo, evidenciadas por unos niveles basales y medios de LH más bajos, una tendencia al incremento en el intervalo de cría y una función deficiente de las células de Sertoli, junto con una alteración modesta en el control homeostático de la glucosa en condiciones obesogénicas, aunque sin comprometer el éxito reproductivo ni afectar al comportamiento sexual. Los resultados de este estudio ponen de manifiesto un papel moderado de la señalización de NK2R en el control del eje reproductivo, en el que se aprecia la redundancia y solapamiento entre los receptores de taquiquininas en la regulación de la función reproductiva.

2. Los datos obtenidos en este estudio documentan por primera vez la capacidad de kisspeptinas de inducir una respuesta en las células hipotalámicas de la glía, además de identificar la presencia de su receptor en astrocitos y la funcionalidad de este, a través de rutas de señalización en las que interviene ERK, y en las que se regula la expresión de marcadores gliales. La eliminación eficiente de la señalización de kisspeptina en astrocitos *in vivo* conlleva ligeras alteraciones del funcionamiento del eje reproductivo en condiciones basales, evidenciadas por una mayor secreción de LH en respuesta a kisspeptina, pero en condiciones obesogénicas, se hacen evidentes alteraciones en la edad de llegada a la pubertad y del ciclo estral en ratones hembras deficientes en la señalización de kisspeptina en astrocitos, así como una respuesta atenuada de la reactividad de astrocitos tras una exposición aguda a una dieta rica en grasas.

4. Bibliografía

1. Fink, G. in *Neuroendocrinology in Physiology and Medicine* (eds. Conn, P. M. & Freeman, M. E.) 14, 107–133 (Humana Press, 2000).
2. Schwartz, N. B. in *Neuroendocrinology in Physiology and Medicine* (eds. Conn,

P. M. & Freeman, M. E.) 139, 135–145 (Humana Press, 2000).
3. Carmel, P. W., Araki, S. & Ferin, M. Pituitary Stalk Portal Blood Collection in Rhesus Monkeys: Evidence for Pulsatile Release of Gonadotropin-Releasing Hormone (GnRH). *Endocrinology* 99, 243–248 (1976).
4. Tsutsumi, R. & Webster, N. J. G. GnRH Pulsatility, the Pituitary Response and Reproductive Dysfunction. *Endocrine Journal* 56, 729–737 (2009).
5. Bilban, M. Kisspeptin-10, a KiSS-1/metastin-derived decapeptide, is a physiological invasion inhibitor of primary human trophoblasts. *Journal of Cell Science* 117, 1319–1328 (2004).
6. Pinilla, L., Aguilar, E., Dieguez, C., Millar, R. P. & Tena-Sempere, M. Kisspeptins and Reproduction: Physiological Roles and Regulatory Mechanisms. *Physiological Reviews* 92, 1235–1316 (2012).
7. Terasawa, E., Guerriero, K. A. & Plant, T. M. in *Kisspeptin Signaling in Reproductive Biology* (eds. Kauffman, A. S. & Smith, J. T.) 784, 253–273 (Springer New York, 2013).
8. Navarro, V. M. *et al.* Regulation of Gonadotropin-Releasing Hormone Secretion by Kisspeptin/Dynorphin/Neurokinin B Neurons in the Arcuate Nucleus of the Mouse. *J. Neurosci.* 29, 11859–11866 (2009).
9. Navarro, V. M. *et al.* The Integrated Hypothalamic Tachykinin-Kisspeptin System as a Central Coordinator for Reproduction. *Endocrinology* 156, 627–637 (2015).
10. León, S. & Navarro, V. M. Novel Biology of Tachykinins in Gonadotropin-Releasing Hormone Secretion. *Semin Reprod Med* 37, 109–118 (2019).
11. León, S. *et al.* Redundancy in the central tachykinin systems safeguards puberty onset and fertility. 51, 523–36 (2019).
12. Maguire, C. A. *et al.* Tac1 Signaling Is Required for Sexual Maturation and Responsiveness of GnRH Neurons to Kisspeptin in the Male Mouse. *Endocrinology* 158, 2319–2329 (2017).
13. León, S. *et al.* Characterization of the Role of NKA in the Control of Puberty Onset and Gonadotropin Release in the Female Mouse. *Endocrinology* 160, 2453–2463 (2019).

Abbreviations

Abbreviations

2D-DIGE: two-dimensional difference gel electrophoresis

3V: third ventricle

ABP: androgen-binding protein

AC: anterior commissure

ACTH: adrenocorticotropic hormone

AHA: anterior hypothalamic area

AMPA: α-amino-3-hydroxy-5-methyl-4-isoxazolepropionic acid

APP: amyloid precursor protein

AR: androgen receptor

ARC: arcuate nucleus

AUC: area under the curve

AVPV: anteroventral periventricular nucleus

BAC: bacterial artificial chromosome

BBB: blood-brain barrier

BC: body composition

bFGF: basic fibroblast growth factor

bp: base pair

BP: blood pressure

BPS: balano-preputial separation

BW: body weight

cAMP: cyclic adenosine monophosphate

CL: corpora lutea

CNS: central nervous system

CRYAB: small heat shock protein αB-crystallin

CT: cycle threshold

D: diestrus

DAB: 3,3'-diaminobenzidine

DAG: diacylglycerol

DDA: data-dependent acquisition

DHA: dorsal hypothalamic area

DHT: 5α-dihydrotestosterone

DIA: data-independent acquisition

DIO: diet-induced obesity

DLPO: dorsolateral preoptic area

DMH: dorsomedial nucleus

Dyn: dynorphin

E: estrus

E_2: estradiol

EAA: excitatory amino acid

EE: energy expenditure

EGF: epidermal grown factor

ELISA: enzyme-linked immunosorbent assay

EOPs: endogenous opioid peptides

ER: estrogen receptor

EREs: estrogen-responsive elements

EU: European union

F: follicles

FDR: false discovery rate

FE: first estrus

FSH: follicle-stimulating hormone

FSHR: follicle-stimulating hormone receptor

FUST: female urine sniffing test

Fw: forward

G: endometrial glands

GABA: gamma-amino butyric acid

GDX: gonadectomized

GFAP: glial fibrillary acidic protein

GH: growth hormone

GHS-R: growth hormone secretagogue receptors

Glu: glutamate

GnIH: gonadotropin-inhibiting hormone

GnRH-R: gonadotropin-releasing hormone receptor

GnRH: gonadotropin-releasing hormone

GO: gene ontology

GPCR: G protein-coupled receptor

GTT: glucose tolerance test

hCG: human chorionic gonadotropin

HFD: high-fat diet

HH: hypogonadotropic hypogonadism

HPG: hypothalamic-pituitary-gonadal

HTLA: hypothalamus

icv: intracerebroventricular

IEF: isoelectric focusing

IF: immunofluorescence

IGF-1: insulin-like growth factor 1
IHC: immunohistochemistry
ip: intraperitoneal
IP_3: inositol 1,4,5-trisphosphate
IR: insulin receptor
IRES: internal ribosome entry site
ISH: *in situ* hybridization
ITT: insulin tolerance test
IU: international units
KA: kainite
KI: knock-in
KO: knockout
Kp: kisspeptin
Kp: kisspeptins
L: uterine lumen
LC: leyding cells
LepR: leptin receptors
LH: luteinizing hormone
LHA: lateral hypothalamic area
LHR: luteinizing hormone receptor
LRR: leucine-rich repeats
LV: lateral ventricle
MAM: mammillary nuclei
MAPKs: mitogen-activated protein kinases
MBH: medial basal hypothalamus
ME: median eminence
mGLUR: metabotropic glutamate receptors
MNPO: median preoptic nucleus
MPO: medial preoptic area
MS: mass spectrometer
MSH: melanocyte stimulating hormone
MT3: metallothionein 3
NCAM: neural cell adhesion molecule
nf H_2O: nuclease-free water
NK1R: neurokinin 1 receptor
NK2R: neurokinin 2 receptor
NK3R: neurokinin 3 receptor
NKA: neurokinin A
NKB: neurokinin B
NMDA: N-methyl-D-aspartate
NPK: neuropeptide K
NPY: neuropeptide Y
NPγ: neuropeptide γ
NRGs: neuregulins
ob: obese
OC: optic chiasm nucleus
OVX: ovariectomy
PRO: proestrus
P4: progesterone
PBS: phosphate buffered saline
PBS-T: phosphate buffered saline-Tween 20
PCR: polymerase chain reaction
PFA: paraformaldehyde
PG: prostaglandin
PGE_2: prostaglandin E_2
PHA: posterior hypothalamic area
PI3K: phospatidyl-inositol-3-kinase
PIP_2: phosphatidyl-inositol bisphosphate
PKA: protein kinase A
PKC: protein kinase C
PLC: phospholipase C
PND: postnatal day
POA: preoptic area
POMC: proopiomelanocortin
PPI: protein-protein interaction
PRs: progesterone receptors
PRL: prolactin
PVH: paraventricular hypothalamic nucleus
QMR: quantitative magnetic resonance
RPs: ribosomal proteins
RPTPβ: receptor-like protein tyrosine phosphate-β
RQ: respiratory quotient
RT: reverse transcription
RT-qPCR: real time polymerase chain reaction
Rv: reverse
S100β: S100 calcium-binding protein B
SAEX: animal service for experimentation
sc: subcutaneous

SCN: suprachiasmatic nucleus
SEM: standard error of the mean
SHBG: sex hormone-binding-globulin
SON: supraoptic nucleus
SP: substance P
ST: seminiferous tubules
SUM: supramammillary nucleus
SynCAM1: synaptic cell adhesion molecule
TACs: tachykinins
TBS: Tris-buffered saline
TGF-α: transforming growth factor alpha
TGF-β: transforming growth factor beta
TMN: tuberomammillary nucleus
TSH: thyroid-stimulating hormone
VCO_2: carbon dioxide production rate
Veh: vehicle
VLPO: ventrolateral preoptic nucleus
VMH: ventromedial nucleus
VO: vaginal opening
VO_2: oxygen consumption rate
VOLT: vascular organ of lamina terminalis
WB: western blot
WT: wild-type
YFP: yellow fluorescent protein
β-END: β-endorphin

Introduction

Introduction

The perpetuation of the species is the main aim of the mammalian reproductive system and, as indispensable capacity to maintain the population, is under a complex and refined network of central and peripheral regulatory signals that integrate at the so-called hypothalamic-pituitary-gonadal (HPG) axis, also known as the gonadotropin axis[1,2]. Proper reproductive capacity depends on the pulsatile release of gonadotropin-releasing hormone (GnRH) from GnRH neurons at hypothalamic level, which conform the major hierarchical hub of this neuro-hormonal system. Indeed, these neurons are the final output for the brain control of reproduction, and integrate a large range of endogenous and exogenous factors that affect the HPG axis, such as energy balance, stress, hormonal status, developmental and environmental cues[4,14].

1. Hypothalamic-pituitary-gonadal axis

The physiological organization of the HPG axis is conserved across vertebrate species and is defined by three hierarchical elements: i) the hypothalamus, where a small population of neurons synthesizes and releases the gonadotropin-releasing hormone (GnRH); ii) the anterior pituitary, in which gonadotropic cells secrete the gonadotropins, luteinizing hormone (LH) and follicle-stimulating hormone (FSH); and iii) the gonads, testes and ovaries, responsible for the production of sex steroids and gametes. The elements of the reproductive axis are linked by feedforward loops in which GnRH stimulates the release of LH and FSH, and these enhance gonadal secretion and promote gametogenesis. In turn, gonadal hormones, via negative and positive feedback loops, the latter being exclusive of females, regulate GnRH secretion from the hypothalamus; and also of LH and FSH secretion from the pituitary (**Figure 1**). From early life to adulthood, the sexual dimorphism of the HPG axis contributes to the developing and organization of the reproductive centers of the nervous system in the two sexes[15]. Clear examples of this are the female-specific functional changes of the neuroendocrine reproductive axis that occur during the ovarian cycle, pregnancy and lactation[16].

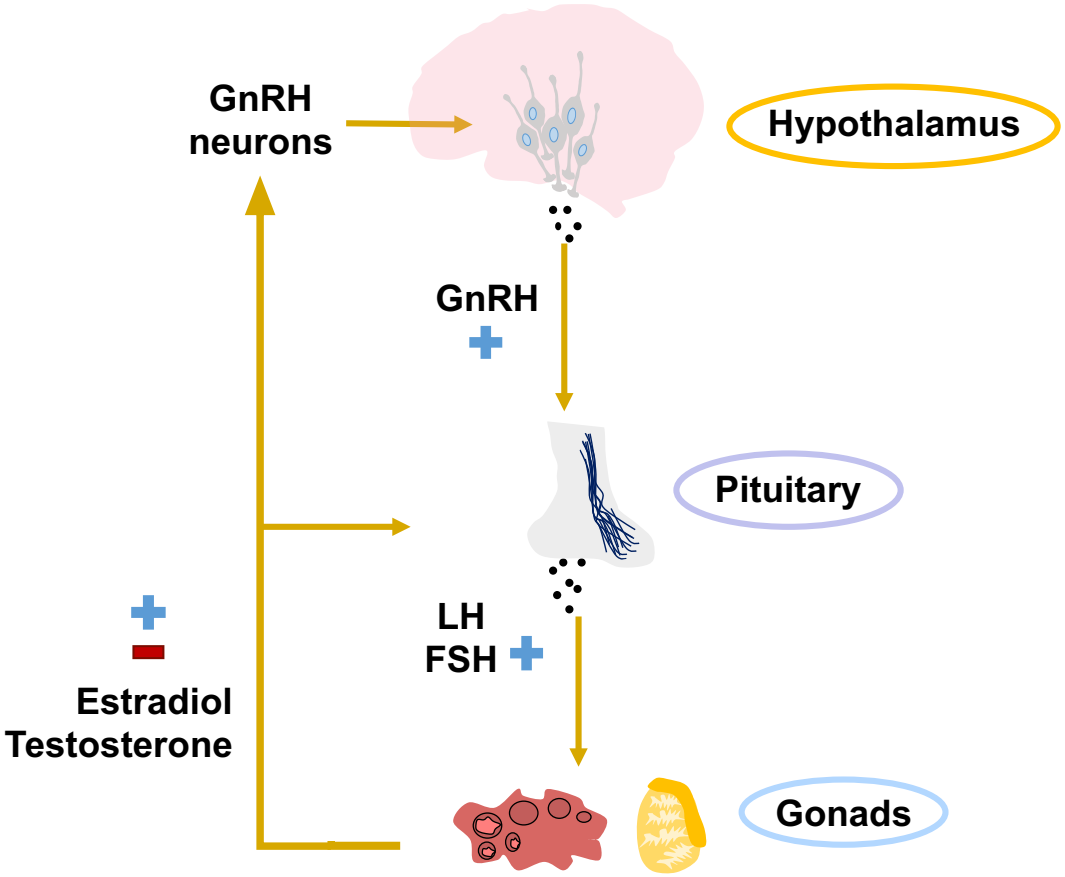

Figure 1. Schematic representation of HPG axis. Adapted from L. Pinilla *et al.*[6]

1.1. Hypothalamus

The hypothalamus is a small region of the brain that controls basic processes of life, including reproduction, metabolic homeostasis and thermoregulation[17-19]. Anatomically, the hypothalamus is lying below the thalamus and above the pituitary, with the third ventricle (3V) separating the hypothalamus into two symmetrical sides. Structurally, the hypothalamus is divided from rostral to caudal into three regions: i) the rostral region; ii) the tuberal hypothalamus and iii) the caudal or mammillary region. An overview of the hypothalamus regions and nuclei are described below (**Figure 2**)[20].

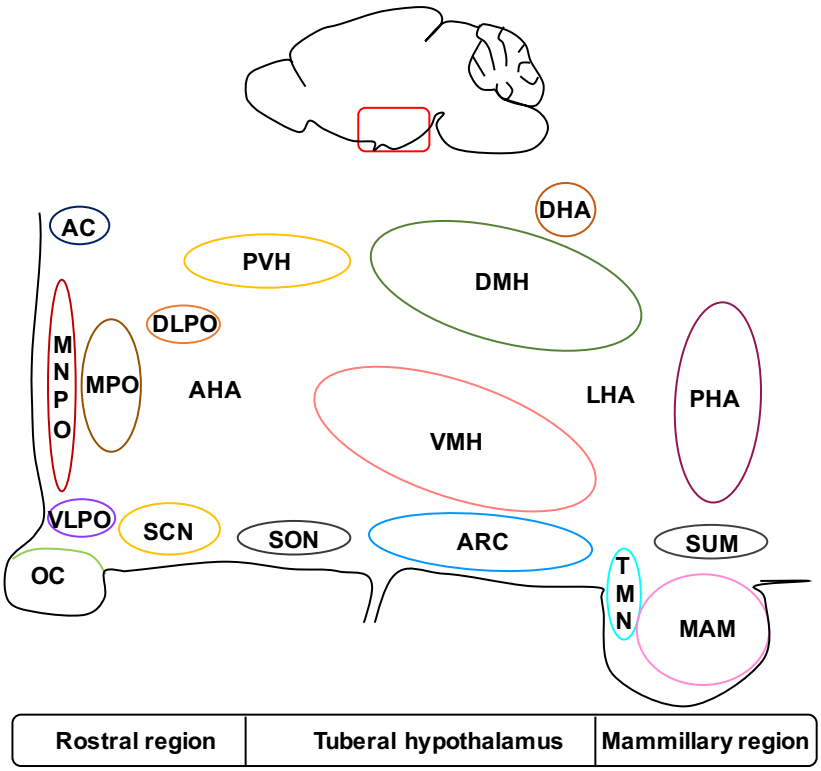

Figure 2. Sagittal schematic representation of the major hypothalamic nuclei. Adapted from Saper, C. B. *et al.*[20]. AC: anterior commissure; AHA: anterior hypothalamic area; ARC: arcuate nucleus; DHA: dorsal hypothalamic area; DLPO: dorsolateral preoptic area; DMH: dorsomedial hypothalamic nucleus; LHA: lateral hypothalamic area; MAM: mammillary nuclei; MNPO: median preoptic nucleus; MPO: medial preoptic nucleus; OC: optic chiasm nucleus; PHA: posterior hypothalamic area; PVH: paraventricular hypothalamic nucleus; SCN: suprachiasmatic nucleus; SON: supraoptic nucleus; SUM: supra-mammillary nucleus; TMN: tuberomammillary nucleus; VLPO: ventrolateral preoptic nucleus; and VMH: ventromedial hypothalamic nucleus.

The rostral region, lying above the optic chiasm (OC), includes the preoptic area (POA), suprachiasmatic nucleus (SCN), paraventricular hypothalamic nucleus (PVH), supraoptic nucleus (SON) and the anterior hypothalamic area (AHA)[20]. This region contains key elements in the control of thermoregulation, circadian rhythms, reproduction and sexual behavior.

The tuberal hypothalamus contains the anterior (AHA) and lateral hypothalamic areas (LHA), as well as the arcuate (ARC), dorsomedial (DMH), ventromedial (VMH), paraventricular (PVH) and supraoptic (SON) nuclei[20]. This region is a critical area where metabolic and reproductive signals communicate[21].

The caudal region includes mainly the mammillary bodies and the areas above them, such as the posterior, tuberomammillary (TMN) and supramammillary nuclei (SUM). This region seems to be involved in regulating wakefulness and stress responses, together with a potential a role in memory[20].

In terms of integration with other areas, many neurons of the hypothalamus project their axons to the third ventricle (3V) at the emergence of the pituitary stalk or median eminence (ME). These neurons synthesize hormones that are released into the hypophysial portal blood to control the secretion of pituitary hormones[1,20,22]. Among them, gonadotropin-releasing hormone (GnRH), the hypothalamic decapeptide, stimulates the synthesis and release of the gonadotropins, LH and FSH, from the gonadotrope cells in the adenohypophysis.

1.1.2. Gonadotropin-releasing hormone

GnRH, also referred as luteinizing hormone-releasing hormone, is a neuropeptide consisting of 10 amino acids ((pyro)Glu-His-Trp-Ser-Tyr-Gly-Leu-Arg-Pro-Gly-NH_2), which plays a primary role in regulating reproduction[23-25]. Over 23 variants of this peptide exist across species, evolutionarily conserving several residues that are essential for the receptor binding and activation[26]. In vertebrates, there are three paralogous forms of GnRH (GnRH-I, GnRH-II and GnRH-III), although mammals only express GnRH-I and GnRH-II[27,28]. GnRH-I, referred herein to as GnRH, is the hypothalamic variant and the final output of the central hypothalamic regulation that drives the reproductive axis. Nevertheless, GnRH-II is the most ubiquitous form, identified in brain but also in peripheral tissues, likely playing a divergent role from GnRH-I. GnRH-II has been also proposed to participate in the regulation of reproduction behavior based on energy status[29,30]. However, it is noted that in many species (e.g., rat, mouse, sheep, rabbit and/or cow) the presence of coding errors for *GnRH-II* gene has led to a functionally inactive form, while other species including human, horse or pig maintain its active form[28]. Eventually, GnRH-III is a forebrain variant, present in the *nervus terminalis*, which has been also involved in the mediation of sexual behavior, but only in fish and amphibians at date[31,32].

Focusing in the hypothalamic variant, GnRH is synthesized and processed in a small population of neurons scattered from the rostral preoptic area to the caudal hypothalamus. GnRH-secreting neurons originate in the nasal placode and subsequently migrate along the olfactory bulb to enter the hypothalamus and turn towards the caudal region to project to the external zone of the median eminence[33]. While in primates GnRH bodies are mainly located in medial basal hypothalamus (MBH) and project to the infundibular nucleus, in rodents, GnRH neurons are in the POA with their projections along the arcuate nucleus reaching the median eminence in which GnRH is released[34].

GnRH gene expression follows an intermittent pattern, under the regulation of a 300-base pair

promoter named neuron-specific enhancer[35]. In addition, the pattern of GnRH secretion fluctuates over development. In humans and rodents, GnRH secretion in the late fetal and early neonatal period is detected at higher levels than the pre-pubertal stage. Then, in the onset of puberty, a gradual increase in the frequency and amplitude of GnRH pulses into the hypophyseal portal blood is observed. In adult mammalian species, the secretion of GnRH occurs in two different modes: the surge and the pulse modes[36]. The surge mode occurs exclusively in the females by the positive feedback of estrogen, which is important for the induction of the preovulatory peak of gonadotropins. On the other hand, the pulsatile secretion of GnRH, which stimulates gonadotropins secretion to drive gametogenesis and steroidogenesis, is negatively regulated by sex steroids. In this context, an appropriate GnRH secretion pattern is essential for the success of reproduction[4,37,38].

The biological effects of GnRH are mediated via a G protein-coupled receptor (GPCR), termed GnRH receptor (GnRH-R), primarily expressed in the pituitary, although GnRH-R is also present in other tissues, including specific brain nuclei and the gonads[39]. There exist various types of GnRH-R (GnRH-RI, GnRH-RII and GnRH-RIII), although mammals only express GnRH-RI and GnRH-RII variants. In many species (e.g., human, bovine, sheep, mouse and/or rat) the GnRH-RI is the only functional variant, and although the *GnRH-RII* gene is retained, the presence of coding errors leads to a disrupted and non-functional variant. By contrast, in other species such as the marmoset, rhesus monkey and/or some non-mammalian vertebrates the type II, GnRH-RII, is also functional[40,41]. Despite the non-functionality of GnRH-RII in some mammalian species, in humans, it has been proposed that the fragments of GnRH-RII may be modulating the activity of the type I GnRH receptor[40].

Regarding the ligand-receptor interaction, the NH_2- and COOH- terminal domains of the decapeptide, GnRH, are involved in the binding to its receptor, whereas the NH_2-terminal domain of GnRH alone is involved in the receptor activation[42]. In its role controlling the reproductive axis, the protein expression of GnRH-R on the plasma membrane of pituitary gonadotrophs determines their responsiveness, and is regulated by GnRH itself and/or sex steroids, fluctuating during several physiological periods, such as development, estrous cycle, pregnancy and lactation[43].

1.2. Pituitary

The pituitary, also called hypophysis, is an endocrine gland that plays a major role in controlling the endocrine system in the body. The gland is located in the sella turcica and it is

suspended from the hypothalamus by the infundibulum or pituitary stalk. The pituitary consists of two anatomically and functionally different lobes: the posterior pituitary (neurohypophysis) and the anterior pituitary (adenohypophysis)[44].

The posterior pituitary is anatomically an extension of the axons and nerve terminals of the paraventricular (PVH) and supraoptic (SON) nuclei of the hypothalamus. Both nuclei synthesize oxytocin and vasopressin that are released into the systemic circulation at the posterior pituitary.

In contrast to the posterior pituitary, the adenohypophysis is not anatomically connected with the hypothalamus, but is functionally linked via the hypophyseal portal system. The anterior pituitary is itself divided into three distinct regions: the *pars distalis*, the *pars intermedia* and the *pars tuberalis*. The anterior lobe secretes hormones regulated by hypothalamic neurons: gonadotropins (LH and FSH), produced by the gonadotrope cells[45], the product of the proteolytic processing of proopiomelanocortin (POMC), namely, adrenocorticotropic hormone (ACTH); prolactin (PRL); growth hormone (GH) and thyroid stimulating hormone (TSH)[44].

1.2.1. Gonadotropins: LH and FSH

The gonadotropins, LH and FSH, are members of the glycoprotein hormone family, which share a common α subunit and a distinct β subunit[46]. LH and FSH are synthesized by pituitary gonadotropes, whereas human chorionic gonadotropin (hCG), which is also member of the family of glycoprotein hormones, is synthesized by the placenta. The two gonadotropins act via two different G protein-coupled receptors, luteinizing-hormone receptor (LHR) and follicle-stimulating hormone receptor (FSHR). These receptors are characterized by a large extracellular domain that contains leucine-rich repeats involved in the binding to their ligands. Gonadotropin receptors are mainly expressed in gonads, but also in others extra-gonadal tissues[47,48]. LHR recognizes both LH and hCG, while FSHR is specific for FSH[49,50]. LH receptor is expressed in theca, granulosa and luteal cells in the ovary and Leydig cells in the testis. The FSH receptor is expressed in granulosa cells in the ovary and testicular Sertoli cells[51,52]. In the ovaries, LH stimulates the production of steroid hormones, ovulation and corpus luteum formation; in the testes, it stimulates the production of testosterone. FSH stimulates the expression of the aromatase and follicular development in the female gonads, whereas, in the male, FSH promotes spermatogenesis.

1.3. The Gonads

The gonads, the primary reproductive organs, are the ovaries in the female and the testes in the male. Mammalian gonads serve a dual function: they are responsible for the synthesis and secretion of sex steroids and protein hormones, and also the production of germ cells[53].

1.3.1. The ovary

Mammalian ovaries are a bilateral pair of small and oval-shaped organs located within the pelvic cavity and connected to the uterus by the uterine tubes. They are surrounded by connective tissue, named tunica albuginea, and beneath that, the ovary has a stromal matrix of cells supporting the oocytes, the female germ cells. The oocyte wrapped by epithelial cells forms the ovarian follicle that comprises the functional unit of the ovaries[54].

The ovaries have three primary functions; i) to produce estrogens and progesterone; ii) to control the development and maturation of follicles (folliculogenesis); and iii) to release the oocytes for fertilization (ovulation)[53,55]. The ovarian follicular development begins in-utero, and by the time reproductive life begins, the human ovaries contain approximately 400,000 primordial follicles. Most of the primordial follicles undergo atresia, meaning follicle death, before birth[56].

The follicular development takes places in the peripheral cortex of the ovary, and it proceeds sequentially in a gonadotropin-independent (preantral stages) and -dependent manner. The primordial follicle, the first level of follicular organization, is formed by a primary oocyte surrounded by a single layer of cells called granulosa cells. Primordial follicles can stay at this level for years. After puberty, a cohort of few primary follicles begins to grow, increasing in diameter and secreting glycoproteins that form an acellular layer called the *zona* pellucida, located between the oocyte and the granulosa cells. Secondary follicles, also known as preantral follicles, are characterized by the oocyte growth, granulosa cell proliferation and an increase in the size and complexity of ovarian stromal cells, which form the so-called theca layer. Tertiary follicles, also referred as antral follicles, continue to proliferate, resulting in an increase of granulosa cells, enlargement of the follicle size and the beginning of the secretion of muco-polysaccharides that form the follicular fluid, collected into a large pool, called antrum. Several follicles reach the antral phase at the same time but, most of the early antral follicles undergo atresia. The antral follicles that mature further and become ready to enter its pre-ovulatory phase are called Graaf follicles. When a mature ovarian follicle is stimulated by

gonadotropins, it is ruptured and the oocyte is released into the uterine tubes[54].

The early follicular growth occurs in a gonadotropin-independent manner, supported by local growth factors. It is not until the early antral follicle phase when FSHR and LHR expression enable the secondary follicles to respond to gonadotropins. FSH stimulates the follicle growth and promotes the aromatization of androgens, whose secretion is previously stimulated by LH[54]. Follicular estrogens feedback on the hypothalamus and pituitary, triggering the LH surge that precedes ovulation[57].

In women, ovulation occurs approximately every 28 days while in rodents this cycle, called the estrous cycle, lasts 4-5 days. After ovulation, the residual part of the follicle within the ovary is transformed into a corpus luteum, formed by collapsed layers of granulosa and theca lutein cells. These lutein cells secrete progesterone and estrogens to support the fecundation. If fertilization does not occur, the corpus luteum in the non-pregnant female degenerates into the corpus albicans that is absorbed by the stroma of the ovary (**Figure 3**).

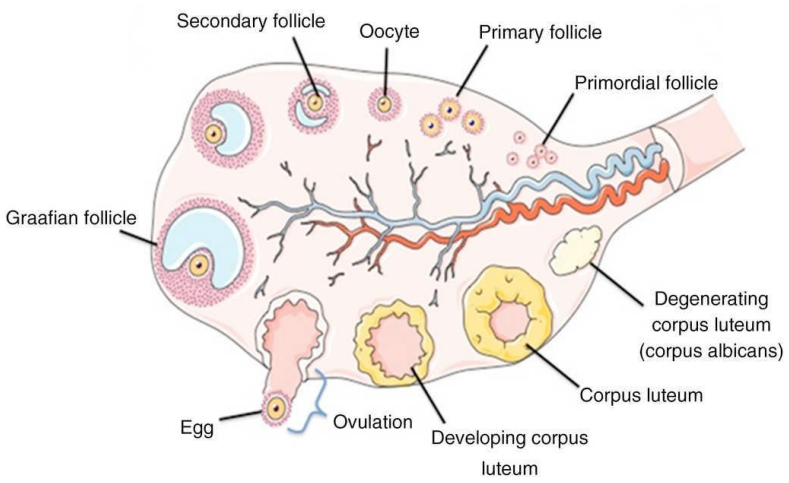

Figure 3. Diagram showing the anatomical structure of the ovary. Taken from Gildas Tetaping *et al*.[58].

In rodents, the estrous cycle is divided into four phases: proestrus; estrus; metestrus and diestrus (D), which can be identified by vaginal cellularity. Proestrus is characterized by predominant nucleated epithelial cells and marked by the LH/FSH surge at the afternoon of the preovulatory day. Estrus consists predominantly of cornified squamous epithelial cells and corresponds to ovulation as a result of the preovulatory surge of gonadotropins. In metestrus, there are mainly leucocytes and a few nucleated epithelial and/or estrus cells. The diestrus phase is characterized mainly by the presence of leucocytes (**Figure 4**)[59,60].

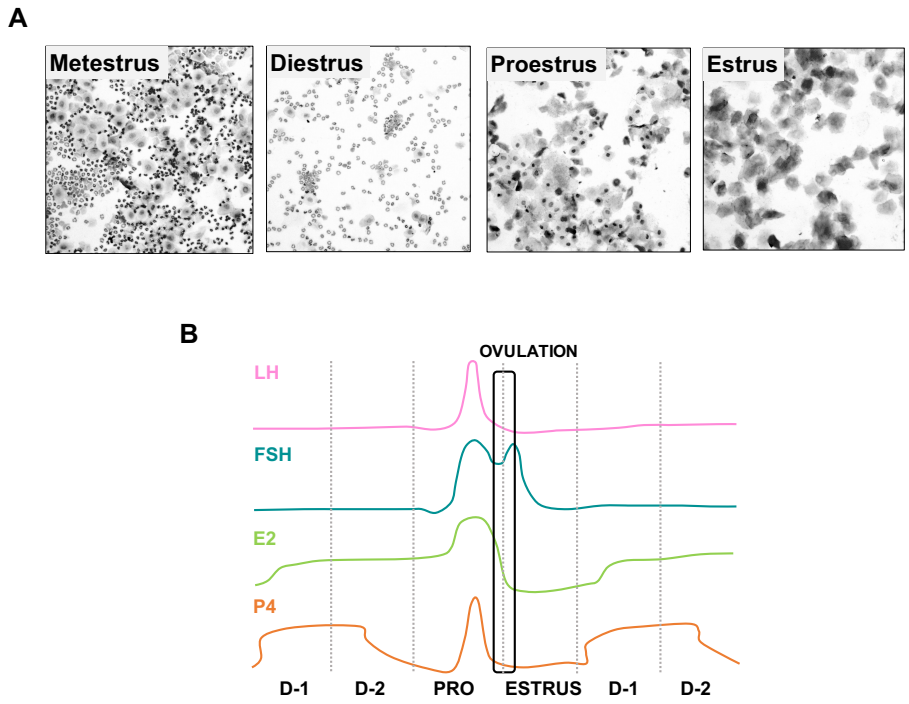

Figure 4. The estrous cycle of rodents. (**A**) Images from estrous cycle cellularity in mice: metestrus (D-1), diestrus (D-2), proestrus (PRO) and estrus. (**B**) Levels of LH, FSH, estradiol (E_2) and progesterone (P4) in the phases of estrous cycle.

1.3.2. The testis

The male reproductive tract consists of the paired testes, epididymis, vas deferens and the accessory glands (paired seminal vesicles, prostate, ampullary glands, bulbourethral glands, preputial glands and the penis)[61].

The adult mammalian testis is a paired oval structure covered by a fibrous capsule, called tunica albuginea. Histologically, testicular tissue can be divided into two compartments: the seminiferous tubules and the interstitial compartment, separated by cellular barriers. The seminiferous tubules consist of an outer layer of peritubular tissue and an inner layer of seminiferous epithelium interspersed with a basement membrane. The tubules contain various developing germ cell types and Sertoli cells, which are essential for spermatogenesis. The interstitial compartment between the seminiferous tubules contains the blood and lymph vessels, macrophages, fibroblasts and Leydig cells, the latter being the primary cell type of the testis whose function is the synthesis of testosterone (**Figure 5**)[62,54].

Figure 5. Illustration of testicular tissue organization, consisting of the Leydig cells (LC) within the interstitial compartment between the seminiferous tubules (ST).

The testes have two important functions, namely, sperm and sex hormone production. Spermatogenesis occurs in the seminiferous tubules of the adult testis with a sequence of events that include mitotic proliferation, meiotic division and cytodifferentiation phases. The spermatogenesis involves the most primitive germ cell, named type A spermatogonia, which sequentially transforms into type B spermatogonia, preleptotene or primary spermatocyte, secondary spermatocyte, and spermatids, until they mature into haploid spermatozoa. During the process, Sertoli cells, which extend from the basement membrane to the lumen of the tubules, are in close contact with germ cells, supporting their structural transformations and mobilization through the seminiferous epithelium[62]. The spermatogenic process depends on endocrine support. FSH and androgens interact within the seminiferous tubules to modulate the developing germ cells and their interaction with Sertoli cells. In addition, in Sertoli cells, FSH stimulates the synthesis of key proteins, such as the androgen-binding protein (ABP) or activins and inhibins, which in turn regulate FSH release at the pituitary level[63,64].

In the interstitial compartment, Leydig cells, the main interstitial cell type, produces testosterone from acetate and cholesterol, under the stimulatory action of LH[65]. Testosterone, as the main testicular androgen of adult testis, is required to stimulate spermatogenesis, although a substantial fraction leaves the testis by different routes. Testosterone enters the bloodstream, where a high percentage binds to plasma proteins, such as sex hormone-binding globulin (SHBG) (not found in rodents). In addition, testosterone enters the lymph system, and also passes through the tissues of the testis mainly by simple diffusion, thereby entering the tubule lumen upon binding to ABP, which carries it into the testicular fluid[54]. That luminal fluid and spermatozoa move out the seminiferous tubules through the rete testis and efferent

ducts into the epididymis that are involved in the maturation, accumulation and storage of mature spermatozoa[66,67]. The epididymis lies on the posterior aspect of the testis that terminates in the ductus deferens[68]. The fluid in the ductus deferens empties into the urethra through the prostate to the outside.

Many peripheral effects of testosterone require its metabolization via the enzyme 5α-reductase into dihydrotestosterone (DHT), whose functions include the acquisition and maintenance of secondary sex characteristics after puberty. In contrast, the central actions of testosterone require its aromatization via the enzyme aromatase into estradiol. The negative feedback of testosterone on the HPG axis occurs mainly via conversion to E_2[69]. Other important actions of androgens are associated with sexual differentiation of the central nervous system (CNS) during the pre- and early postnatal development, thereby contributing to set key functional differences between the adult female and male.

2. Regulation of the HPG axis

The hypothalamic-pituitary-gonadal axis is characterized by an initial activation during the late gestational development and early postnatal stages of life, followed by a period of restrain during childhood, which finally leads to its prominent reactivation before puberty onset to complete sexual maturation and achieve fertility. The precise control of the HPG axis, and hence of reproductive function, relies on the integration of a wide range of central and peripheral signals, resulting in the regulation of the pulsatile secretion of GnRH/LH.

2.1. Central regulators

GnRH neurons are considered the major hierarchical element in the HPG axis. Given the relevance of the pulsatile release of GnRH in the reproductive function, here we highlight some of the most prominent factors than control GnRH release:

2.1.1. Stimulatory signals

A large number of signals have been identified as upstream stimulatory regulators of GnRH neurons, thereby participating in the control of puberty and reproductive function. For sake of concision, we review herein few of the most important ones, especially those related with the contents of this Thesis.

Kisspeptins: These neuropeptides are recognized as the principal regulator of GnRH, and play a key role in the control of essential aspects of reproductive function, including the onset of

puberty, gonadotropin secretion, the regulation of sex steroid feedbacks and sexual behavior[7,70,71]. Given their special relevance in this Thesis, the kisspeptin system will be described in detail in Section 4.

Tachykinins: This family of neuropeptides have emerged as potent modulators of GnRH/LH release[9,72]. Given its importance in this Thesis, the tachykinin system will be described in detail in Section 5.

Glutamate (Glu): This amino acid is the most important excitatory neurotransmitters in the mammalian central nervous system (CNS)[73]. This neurotransmitter is synthesized by two different pathways: i) via transamination of an intermediate of the tricarboxylic acid cycle, and ii) the most common pathway, involving the metabolization of glutamine released by glial cells. The biological actions of glutamate are mediated by its binding to two receptor types, ionotropic and metabotropic receptors. Ionotropic glutamate receptors are ligand-gated ion channels and depending on their ligand affinities they are named as N-Methyl-D-Aspartate (NMDA), α-amino-3-hydroxy-5-methyl-4-isoxazolepropionic acid (AMPA) and kainite (KA) receptors. In contrast, metabotropic glutamate receptors are a varied group of G protein-coupled receptors that are classified into three main groups depending on the sequence, signal pathway and pharmacology[74,75].

The main actions of Glu signaling in the control of reproductive axis are conducted by its binding to NMDA, KA and AMPA receptors in GnRH neurons at the level of the POA and also at GnRH terminals in the ME, where it modulates GnRH/LH secretion[76,77]. But also, these ionotropic glutamate receptors are also expressed in other hypothalamic neurons involved in the control of GnRH secretion[76]. Gonadal steroids appear to modulate the glutamatergic inputs on GnRH/LH secretion; likewise, it has been described that Glu plays a role mediating the E_2 feedback on Kiss1 neurons over GnRH[78,79].

The glutamatergic inputs via metabotropic glutamate receptors (mGluR) that modulate the activity of GnRH neurons are less known and remain poorly characterized. Indeed, despite the fact that GnRH cell lines cultures respond to glutamate agonists via mGluR mechanism, direct *in vivo* evidence for a regulatory action on GnRH neurons remains scarce[80]. However, in astrocytes, mGluR interact with estrogen receptors as part of estradiol signaling facilitating the synthesis of neuro-progesterone needed for the LH surge[81].

Prostaglandin E_2 (PGE_2): This is a member of the prostaglandin (PG) family, that includes derivatives of C_{20} fatty acids; PGE_2 being a ubiquitous molecule and the most abundant PG in the body. It is synthesized from arachidonic acid via the phospholipase A_2 and the cyclo-oxygenase enzymes[82]. This prostanoid regulates many biological functions by its binding to G protein-coupled membrane receptors, called EP receptors[83]. In the regulation of the HPG axis, the release of glial PGE_2 in response to astrocyte-GnRH neurons communication stimulates the secretion of GnRH, via the EP2 receptor; PGE_2 being considered an important regulator of GnRH neuronal activity[84]. In mice, ablation of astrocytic PGE_2 synthesis leads to decrease the activity of GnRH neurons[84]. The relevance of glial cells, mainly as facilitatory signals, in the stimulation of GnRH secretion will be covered in detail in Section 6.

2.1.2. Inhibitory signals

As is the case for stimulatory factors, different inhibitory signals modulating GnRH secretion have been described to date. Relevant examples of such inhibitory factors are provided below.

Gonadotropin-inhibiting hormone (GnIH): This peptide, which was originally identified in birds, is a hypothalamic dodecapeptide (SIKPSAYLPLRF-amide) that inhibits gonadotropins secretion[85]. Its biological functions are mediated via a G protein-coupled receptor named GPR147. In mammals, GnIH orthologs acts at pituitary and hypothalamic levels, but also at the gonadal level, regulating the production of sex steroids and gametes[86].

Gamma-amino butyric acid (GABA): This compound is synthesized primarily from glutamate and it is the predominant inhibitory neurotransmitter in the adult CNS. GABA acts via two types of receptors, ionotropic ($GABA_A$ and $GABA_C$) and metabotropic ($GABA_B$) receptors. GnRH neurons express $GABA_A$ and $GABA_B$ receptors that mediate the secretion of GnRH. Although most *in vivo* animal studies have reported an inhibitory effect of GABA on GnRH/LH secretion, stimulatory actions of GABA on GnRH neurons have been reported also[87].

Endogenous opioid peptides (EOPs): These are a group of neuropeptides that include dynorphins (Dyn), β-endorphins (β-END) and enkephalins that bind preferentially to κ, μ and δ receptors. EOPs play an important role inhibiting GnRH/LH secretion and mediating the negative feedback of progesterone[88,89]. EOPs act at the hypothalamic level upon neuronal populations that regulate GnRH neuron activity. Dyn, synthesized and released by KNDy (i.e., producing kisspeptin/neurokinin B/dynorphin) neurons in the arcuate nucleus, plays a role

regulating the secretion of kisspeptin, and thereby, the pulsatile secretion of GnRH[8,90]. For further details on the roles of Dyn in KNDy neurons, see Section 4.

Neuropeptide Y (NPY): This is a 36-amino acid peptide, conserved across species and best known as a potent stimulant of food intake, which is also considered a key regulator of the reproductive axis[91]. NPY is expressed throughout the hypothalamus, pituitary and gonads, where it acts via different types of G protein-coupled receptors (Y1, Y2, Y4, Y5 and Y6); Y1 and Y5 receptors being the ones primary involved in the regulation of the HPG axis. In the hypothalamus, NPY exerts direct actions on GnRH cell bodies and terminals, but also indirectly on other neurons connected with GnRH neurons. In many species, NPY inhibits the secretion of GnRH/LH in conditions of low E_2 and P4, such as gonadectomy, whereas in gonadectomized animals supplemented with E_2, NPY stimulates LH secretion. Those opposite effects of NPY on GnRH release are thought to depend on the endocrine state, the type of receptor activated and the pattern of administration (acute or chronic)[92].

2.2. Peripheral signals

Integration of peripheral inputs that regulate the HPG axis is needed for proper reproductive maturation and function. The main peripheral signals regulating the reproductive axis are produced by the gonads, but include also those informing on the metabolic state of the body.

2.2.1. Gonadal factors

Sex steroids: These are essential signals for the generation and maintenance of sexual differentiation of the brain, secondary sex characteristics, sexual behaviors and for the regulation of GnRH/gonadotropin secretion by feedback loops at the hypothalamic-pituitary axis. Sex steroids include three groups: estrogens, progesterone and androgens; and all sex steroids being synthetized from cholesterol. The majority of sex steroid production occurs in the gonads, and to a lesser extent in non-reproductive organs/tissues such as the brain, adrenal glands, fat and liver. Additionally, the production, regulation and actions of sex steroids are sexually dimorphic[54].

- **Estrogens:** These include estradiol (E_2), estrone and estriol, and exert their actions mainly via two nuclear estrogen receptors (ERs), ERα and ERβ, that modulate the transcription of target genes after binding to their estrogen-responsive elements (EREs). Aside from nuclear receptors, estrogens can also act through estrogen membrane signaling, such as Gpr30, but its physiological role in the control of reproduction remains contentious[93-95]. The ERs are

widely expressed in the hypothalamus and pituitary, where they are involved in the control of reproductive function and sexual behavior[96]. Estrogens have a bimodal effect on GnRH secretion; in females, they stimulate the preovulatory surge of GnRH/LH, whereas in males and during the main part of the ovarian cycle in females, estrogens inhibit GnRH secretion, which results in a decrease of the release of LH. The effects of estrogens in regulating the hypothalamic-pituitary axis can be direct on GnRH neurons via ERβ, but mainly through indirect E_2-sensitive neurons and astrocytes[96-99], with an overall predominant action via ERα in mediating the feedback control of gonadotropins.

- **Progesterone (P4):** This steroid acts via two nuclear progesterone receptors (PRs), PRA and PRB, and also through membrane progesterone receptors (mPRs)[100,101]. In the control of reproductive function, P4 operates as a suppressor of GnRH/LH secretion in an E_2-dependent manner[102]. On the other hand, preovulatory P4 is involved in the initiation of the LH surge. The source of this progesterone, named neuro-progesterone, is primarily from astrocytes stimulated via estrogen membrane signaling and needed for estrogen positive feedback[81].

- **Androgens:** These include mainly testosterone and 5α-dihydrotestosterone (DHT) and operate through their binding to nuclear/cytosolic androgen receptors (AR), to modulate the expression of multiple genes. Yet, androgens act also through the membrane signaling pathways[103]. Androgens have an inhibitory effect on GnRH/LH secretion, mainly through interneurons expressing androgen receptors in the hypothalamus[104].

Gonadal peptides: These include activins, inhibins and follistatin, and are important regulators of gonadotropin (mainly FSH) release acting upon the HPG axis. Although they were originally described in the gonads, the three gonadal peptides are expressed in extra-gonadal tissues, including the brain and pituitary[105]. Hence, their effect on gonadotropin secretion can be conducted via endocrine actions at pituitary and hypothalamic levels of the gonadal-born hormones, but also via paracrine-autocrine regulation[64].

- **Activins:** These are members of the transforming growth factor β (TGF-β) family of proteins, and exert a stimulatory effect on FSH secretion and on GnRH-R expression at pituitary level[64]. Activin effects are modulated by inhibins and follistatin.

- **Inhibins:** These are also members of TGF-β family of proteins, but carry out a negative effect on FSH synthesis and secretion, as well as on GnRH-R expression[64].

- **Follistatin:** This is a glycoprotein hormone, which inhibits FSH secretion and GnRH-R gene expression via the blockade of activins[64].

2.2.2. Metabolic factors

Reproductive function demands a high energy support, which is supplied by the body energy stores. Metabolic factors, such as insulin, leptin and ghrelin, play important roles in the metabolic control of reproduction, connecting energy balance and reproduction. States of sustained energy imbalance usually results in pubertal alterations and/or reproductive dysfunction[18].

Insulin: This peptide is secreted by pancreatic β-cells into the bloodstream after food intake, and its main function is to enhance glucose uptake in the target cells by its binding to insulin receptors (IR). In terms of HPG axis control, particularly in obesity conditions, insulin stimulates GnRH/LH secretion, which might contribute to reproductive impairment[106]. Importantly, neuronal ablation of IR not only causes severe metabolic impairment but also infertility, denoting a major role of central insulin actions in the control of the reproductive axis[107]. Insulin signaling has been reported to be direct on GnRH neurons, modulating GnRH gene expression, but also via other afferent neurons, such as NPY and POMC (pro-opiomelanocortin) neurons[108-110]. Additionally, a limited number of kisspeptin neurons also express the insulin receptor, and congenital ablation of IR in these neurons has a minor importance on reproductive parameters[111,112]. Notably, astrocytic insulin sensing plays an important role in the regulation of the reproductive axis. While the lack of insulin signaling in GnRH does not affect puberty onset and fertility, IR ablation in glial cells leads to delayed puberty onset, low fecundity and causes reproductive impairment associated with low levels of PGE_2 and deficits in glucose metabolism[113,114].

Leptin: This peptide is synthesized by the adipose tissue and secreted into the bloodstream in proportion to the magnitude of body fat stores. It plays a key role in the control of energy balance, by suppressing appetite and enhancing energy expenditure[115]. Leptin integrates the metabolic state of the body and reproductive capacity. It is encoded by the obese (*ob*) gene. Its binds to leptin receptors (LepR) in the hypothalamus, as main site of action for regulating body weight, energy homeostasis and reproduction, as well as facilitating puberty onset. The genetic inactivation of leptin leads to hyperphagia, insulin resistance and infertility, which can be corrected by the administration of exogenous leptin[116,117]. The absence of functional LepR expression in GnRH neurons suggests the existence of afferent pathways to these neurons.

Among them, the leptin-kisspeptin pathway appears to play a prominent role, which will be discussed in detail in Section 4.

Ghrelin: This peptide hormone is secreted mainly by the stomach and released into the circulatory system. It binds to growth hormone secretagogue receptors (GHS-R) and it is involved in meal initiation and in the regulation of food intake and energy balance[118]. In term of regulation the HPG axis, ghrelin has emerged as a signal of energy insufficiency and thus, its predominant action is suppressing gonadotropin secretion. Its chronic central administration has been reported to delay of puberty onset in rats[119].

3. Neuroendocrine control of Puberty

In the reproductive lifespan of multiple species, including humans, puberty is defined as the state of transition between childhood and adulthood, in which the reproductive capacity is acquired; a process that encompasses multiple, coordinated physiological, morphological and psychological changes[120]. From a neuroendocrine perspective, puberty critically relies on the proper activation of the neuro-secretory activity of GnRH neurons, as major driving force for the full activation of the HPG axis[121,122].

Indeed, the timing of puberty onset is determined by genetics and environmental factors, and characterized by a remarkable increase in the secretory activity of GnRH neurons, as a result of an increase of neuronal and glial facilitatory inputs, that takes place together with a loss of inhibitory signals to GnRH neurons network[121-123]. Among these, kisspeptins are recognized as master regulator for the central control of puberty; given their importance in pubertal control, this function will be detailed in Section 4[6]. As extensively discussed in that section, the effect of kisspeptins are mainly direct on GnRH neurons since those cells express the kisspeptin receptor, Gpr54, even though indirect actions of kisspeptins modulating glutamate and GABA transmission to GnRH neurons, in an estrogen-dependent manner have been also reported[6,124,125]. During the pubertal transition, the physiological role of kisspeptin has been document by an increase in the kisspeptin tone in the hypothalamus, an increase in the sensitivity to the excitatory effects of kisspeptin on GnRH/LH release, an increase in the efficiency of Gpr54 signaling on GnRH neurons coupled to resistance to desensitization after long-term kisspeptin stimulation; and an increase in the number of kisspeptin neurons in the hypothalamus and of their projections to GnRH neurons in a sexually dimorphic manner[126-128].

Also there exists differences between male and female in terms of the pattern of expression of kisspeptin mRNA around the time of puberty[129].

Additionally, there are other central excitatory factors regulating the GnRH neuron activity, such as tachykinins and glial factors, that will be detailed in Sections 5 and 6, as well as inhibitory factors that include GABAergic and opiatergic neurons (**Figure 6**). Worthy of note, peripheral and environmental factors, as well as complex molecular mechanisms, including epigenetic regulation, via DNA methylation and histone modifications and microRNAs, also play an important role in the regulation of the timing of puberty[122]. Importantly, among puberty-controlling factors, those related with the metabolic state and the magnitude of energy stores of the body, signaled mainly by hormones, such as insulin, leptin or ghrelin, are known to have a clear impact on the timing of puberty, as mentioned in previous Section 2[130].

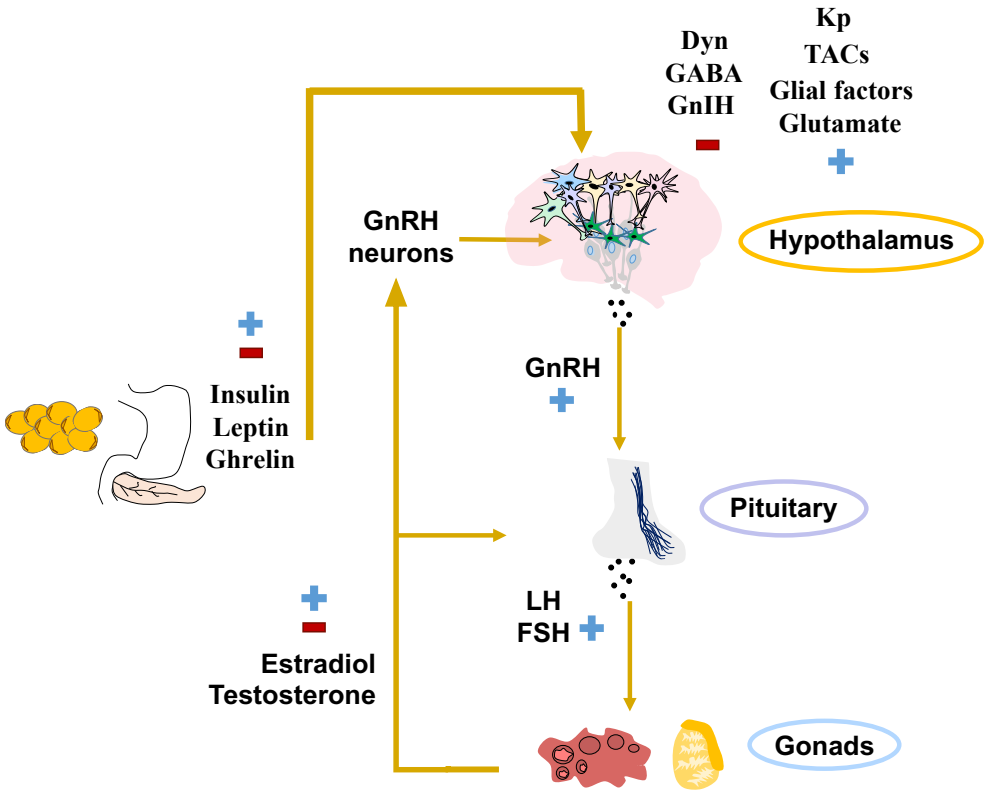

Figure 6. Schematic representation of the main signals participating in the control of puberty onset. Adapted from Pinilla *et al.* [6]

4. The Kiss1/Gpr54 system

Kisspeptins and their receptor, Gpr54, form the so-called Kiss1/Gpr54 system. This system is now recognized as a powerful stimulator of GnRH/LH secretion, an essential player for the onset of puberty, a key regulator of sex steroid-feedback and a critical factor for fertility[6].

In order to unify criteria regarding the nomenclature used in this Thesis, we will use *KISS1* and

Kiss1 to denote the gene and its transcripts (mRNA) in primates and rodents, respectively. The protein products of the *KISS1/Kiss1* gene are termed kisspeptins (Kp). Additionally, the kisspeptin receptor is referred as GPR54 and Gpr54 in primates and rodents, respectively, while *GPR54* and *Gpr54* are used to name the corresponding genes/mRNA. To refer to the ligand/receptor system without references to any given species, the term Kiss1/Gpr54 system will be used.

4.1 Overview of Kiss1/Gpr54 system

Kisspeptins are a family of structurally related peptides, including Kp-54, in human, or Kp-52, in rodents, Kp-14, Kp-13 and Kp-10, derived from a differential proteolytic processing of a single precursor[5]. All the members of kisspeptin share a common COOH-terminal region that contains a RF-amide motif implicated in the activation of their receptor. They are encoded by the *Kiss1* gene, and their biological actions are mediated through Gpr54, a G protein-coupled receptor, also known as Kiss1R[6]. Kisspeptins were initially identified between 1996 and 2001 by their capacity to suppress tumor metastasis, but the reproductive roles of Kiss1/Gpr54 system were not identified until 2003, when inactivating mutations of *GPR54* were observed in patients with hypogonadotropic hypogonadism (HH), a clinical syndrome that entails impuberism and infertility of central origin[131]. Further studies in genetically engineered mouse models with congenital elimination of *Gpr54* or *Kiss1* replicated the pathological phenotype of affected patients, highlighting the relevance of the Kiss1/Gpr54 system in the control of reproduction in mammals[132]. Departing from these initial observations, several studies have addressed the role of the Kiss1/Gpr54 system in the control of puberty onset and reproductive axis.

4.2. Expression of Kiss1/Gpr54 system

The patterns of expression of the elements of the Kiss1/Gpr54 system have been studied in a wide range of species. While some differences have been reported among the species, expression has been detected both in the SNC and peripheral organs. In humans, similar to rodents, *KISS1/Kiss1* is widely expressed throughout the brain but also in other tissues such as placenta, small intestine, pancreas, pituitary, liver and gonads[133,134]. Anyhow, for obvious reasons, it is the brain of rodents (and particularly, the hypothalamus) where the neuroanatomy of the Kiss1/Gpr54 system is by far the best characterized. In detail, the distribution of *Kiss1* within the hypothalamus was located in two main populations of neurons that are consequently termed as Kiss1 neurons, one residing in the arcuate nucleus (ARC), which is the equivalent to

the infundibular region found in primates, and another one in the anteroventral periventricular nucleus (AVPV), in the rostral hypothalamus[6]. Likewise, it is worthy of note that there are species differences in the precise location of these Kiss1 neurons in the HPG. In the case of sheep and primates, Kiss1 neurons are scattered throughout the preoptic area (POA) instead of being exactly located in the AVPV[135]; while the population of Kiss1 neurons located in the ARC (or its equivalent infundibular region in primates and humans) remain consistent across different mammalian species. Additionally, it has been reported an additional extra-hypothalamic population of Kiss1 neurons located in the amygdala[136,137]. Regarding the *GPR54*/*Gpr54* distribution is to a large extent similar to *KISS1*/*Kiss1*. It is mainly expressed in placenta, pituitary, pancreas, liver, skeletal muscle, gonads and brain, especially in GnRH neurons, in which kisspeptin acts via Gpr54 stimulating GnRH secretion[138,139].

Likewise, the expression patterns of Kiss1/Gpr54 system has been characterized across development. Numerous studies have detailed the temporally and spatially expression of this system required for the pubertal transition, ovulation and pregnancy, being this last one characterized by the striking increase of kisspeptin levels in plasma[6,139,140]. Regarding its role in metastasis, it has been also reported changes in the transcript levels of this system, having detected a remarked decrease of these ligands and receptor in a variety of metastatic cancers such as epithelial ovarian, pancreatic, melanoma or choriocarcinoma[141].

4.3. Mechanism of action

In both human and rodents, the binding of kisspeptin to Gpr54, a $G_{q/11}$ coupled-receptor abundantly expressed in GnRH neurons, leads to the activation of phospholipase C (PLC) and, subsequently, to the hydrolysis of phosphatidyl-inositol bisphosphate (PIP_2) into inositol 1,4,5-trisphosphate (IP_3) and diacylglycerol (DAG). IP_3 boosts the mobilization of intracellular Ca^{+2} and DAG activates protein kinase C (PKC) contributing to the secretion of GnRH (**Figure 7**). Furthermore, kisspeptins also activate phosphatidyl-inositol-3-kinase (PI3K)/Akt cascade, leading to the phosphorylation of mitogen-activated protein kinases (MAPKs), such as ERK1/2 and p38. In addition, the Kiss1/Gpr54 signaling can also regulate the expression of the other molecules such as matrix metalloproteinase 9 or the signaling pathways by interacting with other receptors (e.g., chemokine receptors)[142,143]. Possibly via these alternative pathways, kisspeptins have been proposed to play an important role not only in the regulation of reproductive function, but also in cell proliferation and migration[6,143].

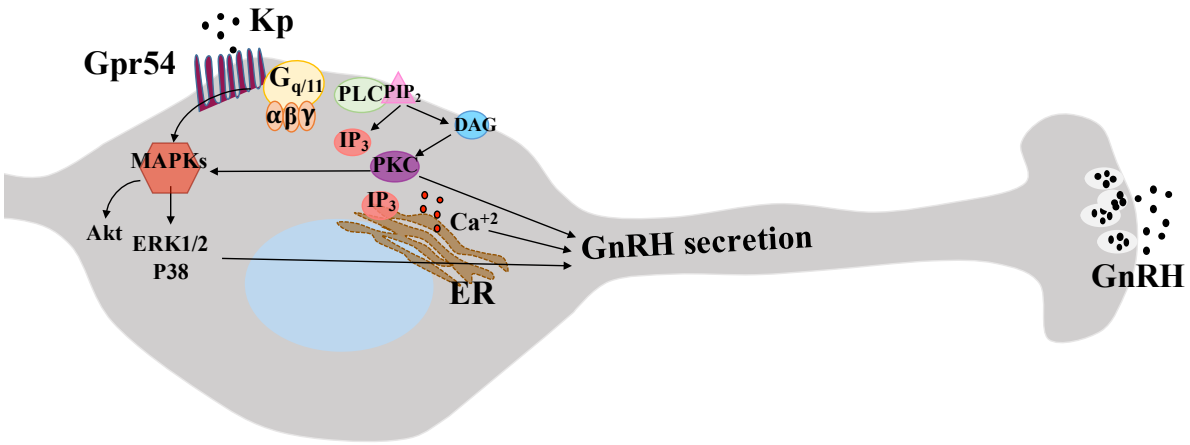

Figure 7. Diagram of Gpr54 signaling in the control of reproduction. Adapted from Pinilla *et al.* [6]

4.4. Kiss1 neurons

In rodents, AVPV and ARC populations of Kiss1 neurons differ physiologically, playing different roles in the control of HPG axis, and exhibit distinct sensitivity to sex steroids. AVPV Kiss1 neurons show a clear sexual dimorphism, with higher numbers of Kiss1 neurons in females than in males. Besides, AVPV Kiss1 neuronal population is known for mediating the positive feedback effect of estradiol in the generation of preovulatory GnRH/LH surge, since estrogen through ERα upregulate *Kiss1* expression in this hypothalamic area[144]. In contrast, ARC Kiss1 neurons have been described to be consistently detected in male and female rodents, orchestrating the pulsatile secretion of GnRH/LH[145]. This Kiss1 population mediates the negative feedback effect of sex steroids upon GnRH/LH secretion[146,147]; in fact, sex steroids are known to potently suppress *Kiss1* expression in the ARC. Furthermore, a substantial proportion of ARC Kiss1 neurons co-express the tachykinin named neurokinin B (NKB; for additional details, see Section 5), and dynorphin (Dyn), and, consequently, they are named as KNDy neurons (as they co-express **K**iss1, **N**KB and **Dy**n). The expression of both NKB and Dyn receptors in this neuronal population, but not of Gpr54, led to the proposal that both signals act in an auto- or para-synaptical manner on KNDy neurons to modulate the kisspeptin release and, subsequently, the stimulation of GnRH/LH secretion[8]. This model is further supported by the profuse network of connections between KNDy neurons, and the proven capacity of NKB to activate and of Dyn to inhibit the GnRH/LH system, respectively, as described in detail in Section 5. Additionally, the extra-hypothalamic population of Kiss1 neurons located in the medial amygdala has been also proposed to play a role modulating gonadotropin secretion, so

that these neurons would be mediating the effects of sexual olfactory signals that lead to an increase in LH levels[148,149]. Besides, it has been also demonstrated that these amygdala Kiss1 neurons are involved in puberty onset, ovulation and GnRH/LH surges[150].

4.5. Kiss 1 neurons as metabolic sensors

Notably, Kiss1 neurons are not only key elements in the control of the HPG axis, but also contribute to the functional link between energy homeostasis and reproduction. Several studies have reported that Kiss1 neurons are sensitive to conditions of metabolic stress, ranging from subnutrition, to diabetes and obesity, and they have been proposed as targets of metabolic regulators[151]. Indeed, studies in pubertal rats showed suppressed hypothalamic *Kiss1* mRNA levels in conditions of negative energy balance associated with decreased gonadotropin levels[151]. In this context, ARC Kiss1 neurons have been shown to express leptin receptor (LepR) that appears to be modulating the expression of kisspeptins, while insulin receptor has been found in both AVPV and ARC populations[112,152]. Nevertheless, single or double ablation of those receptors from Kiss1 neurons do not overtly impair fertility[153]. In detail, congenital ablation of LepR in Kiss1 neurons does not appear to disrupt the timing of puberty, and some reports suggested that leptin signaling in Kiss1 neurons is only detectable after sexual maturation[154,155]. However, the fact that leptin modulates LH and *Kiss1 mRNA* levels in different metabolic conditions strongly suggests that leptin effects are mediated, at least in part, via kisspeptins signaling, even if that regulatory action is conducted via indirect connections. In the contrary, insulin signaling in Kiss1 neurons alters the timing of puberty but without altering the capacity of reproduction in the adulthood. On the other hand, the orexigenic peptide, ghrelin, appears to reduce *Kiss1* expression, thereby contributing to the suppression of the HPG axis under fasting conditions, in which ghrelin levels increase[156]. In the ARC, it has been described that Kiss1 neurons express GHS-R, whose responsiveness to ghrelin is mediated by E_2[157]. Besides the direct action of ghrelin in Kiss1 neurons, indirect ghrelin actions to modulate these neurons have been proposed also. Yet, further studies are required to characterize the full spectrum of ghrelin-Kiss1 neurons interactions.

5. The tachykinin system

Tachykinins (TACs) constitute a neuropeptide family that is widely distributed throughout the central nervous system and periphery, playing a wide array of functions that include

modulation of neural activity, control of behavioral responses, maintenance of fertility, vasodilation and smooth muscle contraction[158,159].

5.1. Overview of the TAC system

The mammalian TAC family is composed by a number of neuropeptides, which include substance P (SP), neurokinin A (NKA), neurokinin B (NKB), neuropeptide K (NPK) and neuropeptide γ (NPγ), all having the characteristic C-terminal sequence, Phe-X-Gly-Leu-Met-NH2[159]. To date, most attention in TAC research has focused on the biological effects of SP, NKA (both encoded by a single gene, *Tac1*, in rodents) and NKB (encoded by *Tac2* in rodents), which bind preferentially to the G protein-coupled receptors, NK1R, NK2R and NK3R, respectively (see **Table 1**)[159,160]. Notwithstanding this ligand preference, some degree of cross-reactivity between TACs and their receptors has been documented[10,161].

TACs have been identified as key elements in the central control of GnRH/LH secretion in numerous mammalian species[9,162-164]. Indeed, genetic studies in humans found that inactivating mutations in *TAC3* or *TACR3* genes, encoding NKB and NK3R respectively, led to impaired fertility, with a similar phenotype than that observed in patients with mutations in the Kiss1/Gpr54 system[165].

Table 1. Gene nomenclature for tachykinins and their receptors in human and rodent.

Gene encoding ligands			Gene encoding receptors		
Ligand	**Human**	**Rodent**	**Receptor**	**Human**	**Rodent**
SP	*TAC1*	*Tac1*	NK1R	*TACR1*	*Tacr1*
NKA	*TAC1*	*Tac1*	NK2R	*TACR2*	*Tacr2*
NKB	*TAC3*	*Tac2*	NK3R	*TACR3*	*Tacr3*

5.2. Hypothalamic expression of the elements of the TAC system

Given the role of the TAC system in the control of reproduction, the expression of all the elements of this system has been well characterized within the hypothalamus, with particular attention to their eventual co-localization with Kiss1 and GnRH neurons. In this context, *Tac1* expression has been detected mainly in the ventromedial nucleus (VMH) and the ARC, without any detectable co-localization with Kiss1 neurons, but reported expression in neurons in close contact with them in ovariectomized (OVX) female mice[9]. On the other hand, as mentioned in the previous section, *Tac2* expression has been identified in ARC Kiss1 neurons in several

species, including humans[9,166]. Regarding the expression of their receptors, *Tacr1* has been found in about half of ARC Kiss1 neurons, whereas *Tacr3* is expressed in 100% of them in mice. In the AVPV and rostral hypothalamus, *Tacr1* is expressed in approximately one-fourth of Kiss1 neurons and GnRH neurons, while *Tacr3* in one-tenth. However, *Tacr2* is absent in both Kiss1 and GnRH neurons, even if NKA effects on LH secretion appear to be kisspeptin-dependent, which would suggest the presence of unidentified intermediate neurons upstream of Kiss1 neurons, connecting Tacr2 and Kiss1 pathways. On the other hand, expression of NK2R has been identified in both ARC and VMH, having partial co-location with VMH Tac1 neurons[13]. Therefore, it is suggested that this population of Tac1 neurons expressing NK2R may be, at least in part, stimulating ARC Kiss1 neurons, and hence GnRH/LH secretion, via activation of SP/NK1R signaling, as well as via the stimulation of an as yet unidentified NKA-responsive neuron that in turn regulates ARC Kiss1 neuronal activity (**Figure 8**)[13]. Nevertheless, further investigation is needed to fully clarify this complex TAC/Kiss1 pathway.

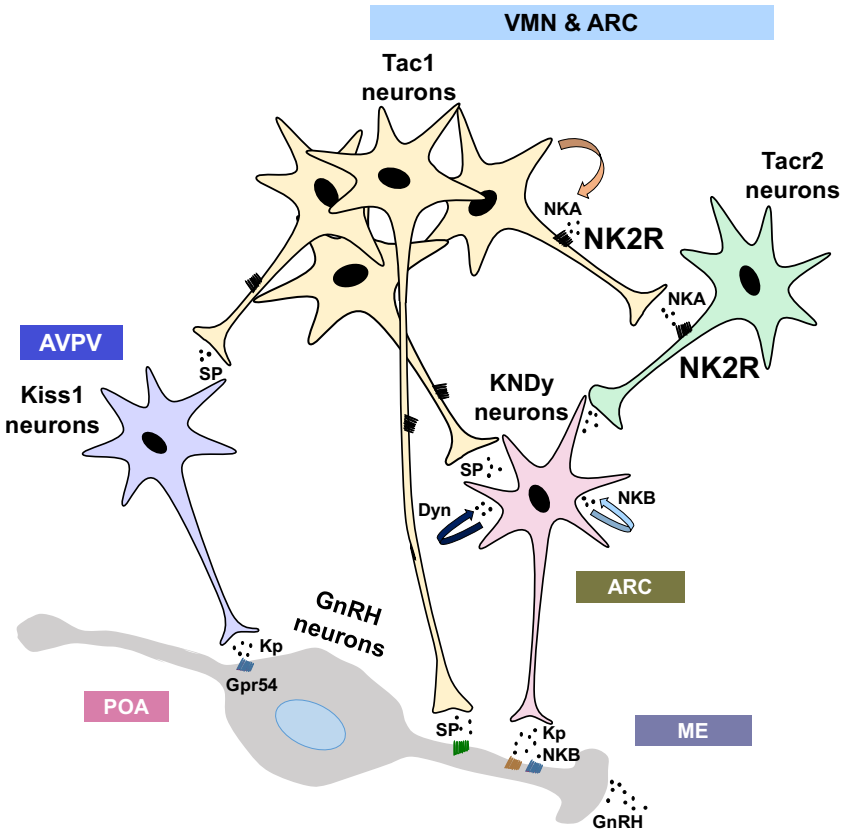

Figure 8. Schematic representation of a hypothalamic neuronal network comprising Kiss1 neurons, GnRH neurons and TAC neurons in mice. Adapted from Fergani C. *et al.*[13]

5.3. TAC system in the control of HPG axis

The tachykinin effects on GnRH/LH secretion have been documented in multiples mammalian species (e.g., rodents, rabbits and humans)[10,72,167]. Their effects are mainly conducted at the hypothalamic level, but some TACs may stimulate also LH release on the anterior pituitary gland, depending on gonadal steroids levels[168,169]. We summarize below the involvement of each TAC ligand and its receptor in the regulation of the HPG axis.

- The NKB/NK3R system

Rodent studies have demonstrated that NKB has a dual effect on LH secretion depending on the physiological levels of E_2. For instance, in intact rodents, NKB increases LH levels while under conditions of low levels of E_2 (e.g., after ovariectomy), NKB inhibits LH secretion[9]. Regarding its mode of action, it has been demonstrated that NKB acts via kisspeptin to modulate GnRH neurons, since the stimulatory effects of the NKB agonist, Senktide, were absent in Gpr54 null mice, while desensitization of Gpr54 disables the effect of Senktide on gonadotropin secretion in monkeys[9,170,171]. On the other hand, it has been also proposed that NKB induces LH release in a kisspeptin-independent manner through neurons expressing NK3R in the posterodorsal medial amygdala[172].

Besides its role as regulators of pulsatile GnRH secretion in adulthood, NKB also plays an important role regulating the timing of puberty, as documented by the increase of the hypothalamic expression of NKB/NK3R system along postnatal maturation and by the detectable (albeit moderate) delay of puberty onset after chronic central blockade of NK3R signaling[173].

As mentioned above, initial reports documented that inactivating mutations in humans of the genes encoding NKB (*TAC3*) or NK3R (*TACR3*) were associated with hypogonadotropic hypogonadism (HH) and lack of puberty[165,174]. Despite this human phenotype, genetic inactivation of *Tac2* or *Tacr3* caused a less severe reproductive impairment in mice[175,176]. For instance, Tacr3 null female mice were only sub-fertile, whereas Tacr3-deficient males attained fertility. Alike, Tac2 null female mice displayed delayed puberty but were otherwise fertile at adulthood, while males showed no overt reproductive defects. Altogether, these features resemble the human phenotype of some mutations of the NKB pathway, in which forms of partial or complete reversal of their HH state have been also reported[177]. As a plausible explanation, it has been proposed that, because of some degree of redundancy among TAC

pathways, SP/NK1R and/or NKA/NK2R signaling may compensate the congenital absence of NKB actions, thereby preserving fertility in mice, and permitting reversal of the hypogonadal state in humans with genetic inactivation of the NKB pathway. Additionally, this redundancy of the TAC system has been recently exposed by phenotypic analyses on double Tac1/Tac2 KO mice, which displayed more profound reproductive defects than mice lacking one of the two TAC genes[178]. In line with this, it has been described that while TAC effects on LH release are blunted by central administration of an antagonist for all three of receptors, administration of each TAC receptor antagonist alone did not affect the LH induced secretion by TAC agonists[163]. In the same vein, full blockade of NKB actions on GnRH neuron firing was only achieved when combined suppression of all three TAC receptors was applied[161].

Interestingly, as it was mentioned in Section 4, studies in rodents, sheep and humans found NKB to be co-expressed in a substantial fraction of ARC Kiss1 neurons, termed KNDy neurons, as they co-express not only Kiss1 and NKB, but, to a variable degree, also Dynorphin (Dyn)[179]. This defines a sort of oscillatory network, in which NKB activates and Dyn preferentially inhibits kisspeptin output to GnRH neurons[6,9,180]; this neuronal setup has been recently proven as essential component of the GnRH pulse generator[181]. Additionally, this network has been associated with the generation of hot flushes in women and rodents; the latter have documented also the critical involvement of NK3R signaling in the heat dissipation response[182-185]. In this context, studies in rodents have shown that the administration of Senktide to ovariectomized mice increases tail skin temperature. By contrast, OVX mice supplemented with E_2 exhibited lower sensitivity to this thermoregulatory action[183].

- The SP/NK1R system

Compelling evidence supports the involvement of SP/NK1R in the control of reproduction, acting at the hypothalamic, pituitary and gonadal levels[10,185]. Although in humans, no mutations in *TAC1* or *TACR1* genes associated to reproductive impairment have been reported to date, SP has been shown to significantly increase LH levels[186]. In addition, also in humans, a subset of Kiss1 neurons has been identified in the infundibular region that co-expresses SP[187]. As for the other TACs, the effect of SP on LH secretion has been shown to mainly kisspeptin-dependent[9]. Of note, this TAC system seemingly has variable effects on LH secretion depending on the species, so that NK1R agonists stimulated LH secretion in intact male mice, as well as in OVX female mice, supplemented or not with estradiol, whilst in adult rats no LH responses to NK1R activation were detected[9,188]. In any event, recent evidence from rodent

studies have further documented a role of the SP/NK1R pathway in the modulation of puberty and fertility. Thus, in prepubertal female mice, central injection of a NK1R agonist elicited gonadotropin secretion, while its repeated exposure advanced puberty onset. In turn, Tac1 KO female mice displayed delayed puberty and subfertility[189]. Notably, SP/NK1R signaling seems to be also involved in the control of sexual behavior, as injection of SP into the midbrain central grey facilitated lordosis[190], and Tacr1 KO male mice showed decreased pheromone-induced sexual approach behavior[191].

- The NKA/NK2R system

In contrast to the other TAC systems, described above, the physiological roles of the NKA/NK2R system in the control of the reproductive axis remain largely unexplored. Anyhow, although NK2R does not appear to be expressed in Kiss1 or GnRH neurons, NKA agonists have been found capable to regulate gonadotropin secretion in a sex steroid- and kisspeptin-dependent manner, with stimulatory and inhibitory actions on LH release being reported[9,192]. As reported also for NKB, the effect of NKA on LH release is stimulatory on physiological levels of E_2 and inhibitory in their absence (e.g. after ovariectomy)[9]. More recently, a putative role for the NKA/NK2R pathway in the control of puberty and the gonadotropic axis was suggested by pharmacological studies showing that activation of NK2R in pre-pubertal female mice advanced puberty onset and stimulated LH release in the adulthood[13]. In the same line, the state of delayed puberty and subfertility observed in Tac1 null mice might be caused, at least partially, by the lack of endogenous NKA, since this neuropeptide, together with SP, is ablated in this mouse line[189]. Nonetheless, the overlapping functions of other TAC pathways, the partial promiscuity at the receptor level, and the lack of more incisive genetic models have prevented further elucidation of the specific biological roles and actual physiological relevance of NK2R signaling in the control of the reproductive axis.

5.4. TACs in the peripheral control of reproductive function

In multiple mammalian species, tachykinins and their receptors have been found in the reproductive tract, being expressed in the placenta, ovary, uterus, testes and prostate[193]. TACs play a role enhancing the uterine contraction, the motility of spermatozoa, the dilatation of blood vessels in the uterine vasculature and modulating gonadal steroids secretion[193,194]. In the female reproductive tract, the expression of most of the elements of the TAC system has been detected to change during the ovarian cycle and the pregnancy[195,196]. However, in humans and rats, the expression of *NK2R* remains stable despite hormonal changes or gestational status;

NK2R seemingly being the most important receptor stimulating the contractility of the uterus[197,198]. Despite this, further research is needed to elucidate the relative importance of NK2R signaling preserving the fertility. In male gonads, TACs play a role stimulating the secretory activity of Sertoli cells and inhibiting the testosterone secretion by Leydig cells[199,200]. Furthermore, in humans, the TAC system appears to be enhancing the motility of spermatozoa in order to facilitate the fertilization[194]. Nevertheless, the specific role of NK2R signaling in testes remains large unknown.

Overall, tachykinins have been shown to exert multiples functions that contribute to the regulation of the reproductive function at central levels of the HPG axis, but also in the rest of reproductive tissues. Given the overall importance of TAC system in fertility, the adobe data supports the need to clarify the role of each component of this system in reproductive control, noting that, to date, little is known about the specific functions of NKA/NK2R system.

6. Glial elements and the control of the GnRH network

Glial cells, also known as neuroglia, are composed of astrocyte, microglia, tanycyte, radial glial cell, pituicyte and oligodendrocyte lineage cells. Glial cells are the major components of the mammalian brain. Initially considered as non-functional supporter elements for neurons, decades of research have documented that, instead of a passive function, glial cells play an essential and active role in controlling multiple brain functions[201, 202]. Moreover, glial cells are responsive to gonadal steroids and contribute to the sexual differentiation of the brain[203].

Astrocytes, the most abundant glial cell type in the adult brain, are a heterogeneous group that exhibit distinct shapes, gene expression profiles and functions associated with the neural networks in which they are involved. They participate in the control of energy balance, water and ion homeostasis, in the tripartite synapse and contribute to the blood-brain barrier (BBB) maintenance[204]. In recent decades, it has been demonstrated that astrocytes play a critical role in the regulation of the reproductive function in which the bi-directional interaction astrocyte-GnRH neuron and their adhesiveness are essential for the proper regulation of the HPG axis (**Figure 9**)[205,206]. Furthermore, the responsiveness of astrocytes to gonadal steroids also modulates the release of gliotransmitters that promotes the neuro-secretory activity of GnRH neurons[207].

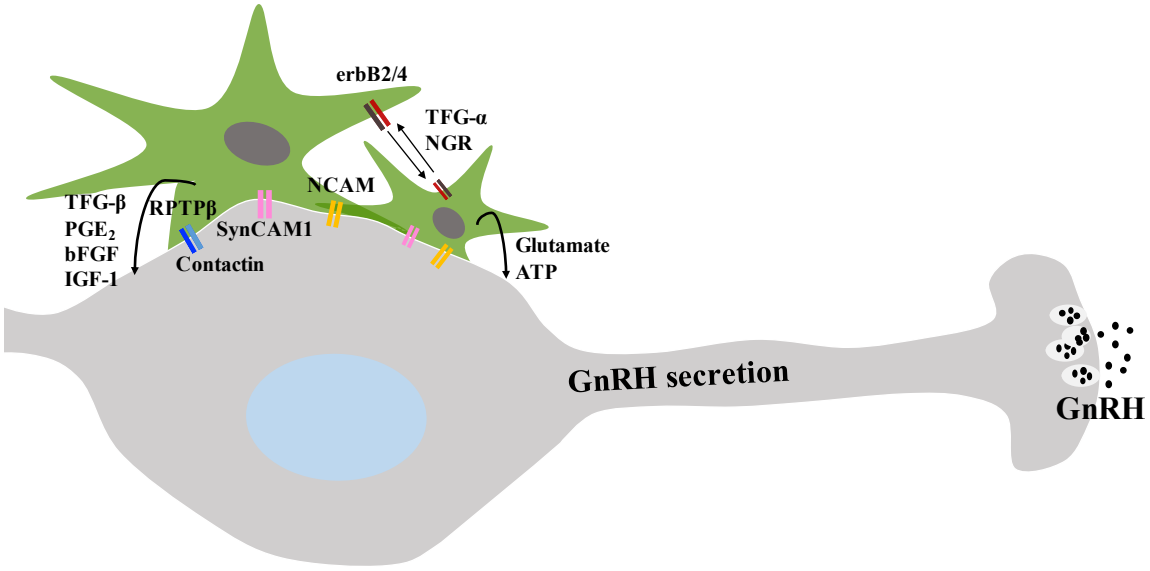

Figure 9. Glia-to-GnRH-neuron interaction at the level of GnRH cell body. Control of the GnRH secretion by gliotransmitters, such as PGE_2, growth factors and small molecules.

6.1. Astrocytes-GnRH neurons direct contacts

Astrocytes have been described to be wrapping GnRH neurons. Their adhesiveness to these neurons is achieved via different astrocyte-GnRH neuron interaction mechanisms. Among them, synaptic cell adhesion molecule 1 (SynCAM1), expressed in both astrocytes and GnRH neurons, promotes their homophilic interactions. Notably, this communication is enhanced in astrocytes by ligand-dependent activation of erbB4 receptors, which play a critical role in the regulation of puberty onset, the preovulatory surge of LH and fertility[205,208]. Another cell-cell adhesion between astrocytes and GnRH neurons is mediated by glial receptor-like protein tyrosine phosphate-β (RPTP-β) and its interaction with contactin in GnRH neurons. In addition, there is another homophilic interaction via neural cell adhesion molecule (NCAM) that is expressed in both astrocytes and GnRH neurons.

These adhesive interactions, in addition to provide direct astrocyte-GnRH neuron contacts, facilitate intracellular cascades into astrocytes and GnRH neurons, resulting in the release of transmitters that regulate the secretion of GnRH[205,209]. Furthermore, it has been described that the astrocytic appositions to GnRH neurons are, in turn, remodeled by the sex steroid milieu in both primates and rodents[210,211]. A clear example of this phenomenon happens in the ARC of rodents, in which E_2 increases the astrocytic surface apposing to non-GnRH neurons, suggested

to be related to their participation in the reduction of the number of inhibitory synaptic inputs to GnRH neurons[205].

Astrocytes are known to undergo plastic changes in response to a wide range of stimuli, a feature that comprises morphological changes that modifies the synaptic activity and neuronal excitability, and changes in the protein expression profile[212]. In the hypothalamus of rodents, the morphology of astrocytes is modulated during the estrous cycle by sex steroids. In addition, the cytoskeletal glial fibrillary acidic protein (GFAP), an intermediate filament, is also modulated over the estrous cycle[213]. Furthermore, the astrocytes in apposition to GnRH neuron bodies appear to exhibit morphological changes across the estrous cycle in both primates and rodents[214].

6.2. Growth factor-dependent glial signaling

The bioactive molecules released by astrocytes include growth factors, such as transforming growth factor beta (TGF-β), insulin-like growth factor 1 (IGF-1), basic fibroblast growth factor (bFGF) and epidermal growth factor (EGF)-like family ligands. The transforming growth factor alpha (TGF-α) and neuregulins (NRGs), both members of EGF-like peptide family, are considered the major regulators of GnRH secretion and act indirectly via erbB receptors in astrocytes, promoting the secretion of other gliotransmitters, such as TGF-β and PGE_2, that, in turn, regulate the release of GnRH[84,215]. Moreover, it has been described that afferent neuronal activation of ionotropic and metabotropic glutamate receptors on astrocytes stimulates erbB signaling by promoting the recruitment of the receptors and their ligands.

6.3. Prostaglandin E_2 glial signaling

PGE_2 is considered an important upstream regulator of GnRH neuronal function. As mentioned above, astrocyte-GnRH neuron communication leads to the secretion of glial PGE_2 that is also released upon activation of hypothalamic astrocytic oxytocin receptors. The binding of PGE_2 to EP2 receptors in GnRH neurons activate the cyclic adenosine monophosphate/protein kinase A (cAMP/PKA) cascade, with the concomitant depolarization of the neurons, which ultimately drives the secretion of GnRH[84,216]. Additionally, PGE_2 has been also implicated in the modulation of the GABAergic afferents to GnRH neurons[217].

6.4. Astrocytes as metabolic sensors

Astrocytes have been proposed as metabolic mediators in the CNS. Throughout their membrane surface, astrocytes express insulin, leptin and ghrelin receptors[218,219]. At the

hypothalamic level, it has been shown that astrocytic insulin signaling not only acts to sense glucose in the CNS and to regulate glucose uptake through the blood-brain barrier (BBB), but is also critical for the proper function of the reproductive axis[113,114]. In astrocytes, the loss of leptin receptors alters glial morphology, reduces glial coverage and modifies the physiological responses to ghrelin and leptin-regulated feeding behaviors[218]. Furthermore, it has been described that hypothalamic astrocytes undergo hyperplasia and hypertrophy, a process termed as reactive astrogliosis, in response to obesity in both humans and rodents[220,221]. Indeed, either acute or chronic exposure to HFD leads to produces gliosis that has been associated with an increase in *GFAP* expression in rodents[221-223]. Likewise, this gliosis in response to obesity seemingly modulates also leptin signaling[223]. Nevertheless, the underlying mechanisms by which HFD induces reactive gliosis and the involvement of astrocytes in obesity require further research.

Objectives

Objectives

The reproductive function in mammals is indispensable for the perpetuation of the species and is safeguarded by sophisticated regulatory networks in accordance with the relevance of this function. Tachykinins (TACs) and kisspeptins have emerged in the last decade as key regulators of the neuronal networks governing GnRH secretion and, hence, controlling reproduction. However, despite thorough investigations detailing the role of the tachykinin and Kiss1/Gpr54 systems in the central regulation of reproduction, including their involvement in sexual differentiation, puberty onset and pulsatile gonadotropin secretion, many questions on their actual physiological roles remain unsolved. In this sense, the majority of the studies reported to date on the roles of TACs in the control of GnRH/LH secretion has focused on the NKB/NK3R system and to a lesser extent on SP/NK1R. In contrast, the physiological roles of the NKA/NK2R system in the control of the reproductive axis remain largely unexplored. In addition, further research is needed to fully decipher the complex regulation and the downstream effectors of kisspeptin actions that participate in the control of GnRH release.

In this context, the **general objective** of this Thesis was to deepen our knowledge on the physiological role of Neurokinin 2 Receptor (NK2R) signaling, and its eventual interplay with kisspeptins, in the control of the HPG axis, and to describe novel putative kisspeptin actions and effectors in the reproductive axis through a series of phenotypical, pharmacological, behavioral and histological studies in novel genetically modified mouse lines. To cover this general objective, the following **specific objectives** have been addressed:

1. To characterize the physiological roles of NK2R in regulating the reproductive axis by characterizing a novel mouse line with congenital ablation of the neurokinin 2 receptor gene (*Tacr2)*.

2. To explore novel mediators for the effects of kisspeptins in the hypothalamus by proteomic analyses.

3. To assess the physiological roles of kisspeptin signaling in astrocytes in regulating the reproductive axis by characterizing a novel mouse line with a selective ablation of *Gpr54* in GFAP-positive cells.

Materials and Methods

Materials and methods

1. Ethics statement

The experiments and animal protocols included in this Thesis have been approved by the Ethical Committee of the University of Córdoba; all experiments were conducted in accordance with Spanish Royal decree 53/2013 on animal welfare in experimentation and European Union (EU) normative for the use and care of experimental animals (EU Directive 2010/63/UE, September 2010).

2. Animals

Mice were housed in the Animal Service for Experimentation (SAEX) of the University of Córdoba. All animals were maintained in constant conditions of light, 12-h light/dark cycle, at standard temperature (22 ± 2ºC) and given ad libitum access to standard laboratory mouse chow (A04, Panlab) and water, unless mentioned otherwise. The day the litters were born was considered as day 1 of age (postnatal day 1, -PND1-); animals were weaned at PND21. For the diet-induced obesity studies, adult mice were fed with high-fat diet (HFD, #D12451 or #D12331; Research Diets, New Brunswick, NJ) with 45% or 58%, 20% or 17%, and 35% or 25% calories from fat, protein and carbohydrate, respectively, for a period of 10 weeks or until the end of the experiment in the adulthood. Further details on the use of 45% or 58% HFD on specific experiments are provided in the Experimental design section.

Mouse models

The use of genetically engineered mouse models has been crucial to reaching the objectives of this Thesis. The genotyping required to identify the different mouse models is detailed in Section 3 of Materials and Methods.

Tacr2 KO mice

Mice with congenital ablation of *Tacr2* gene, named hereafter Tacr2 KO, were obtained from UCDavis KOMP Repository (referenced as *tm1(KOMP)Wtsi, tm1(KOMP)Mbp*). This mouse line was made available via a basic research collaborative agreement with Menarini Ricerche S.p.A. (Italy); notably, the company had no role in the design of the studies, nor was involved in the analysis or discussion of the data presented herein. In this model, the strategy for disrupting *Tacr2* gene was to replace exons 2 and 3 with a LacZ/neo cassette (**Figure 10**).

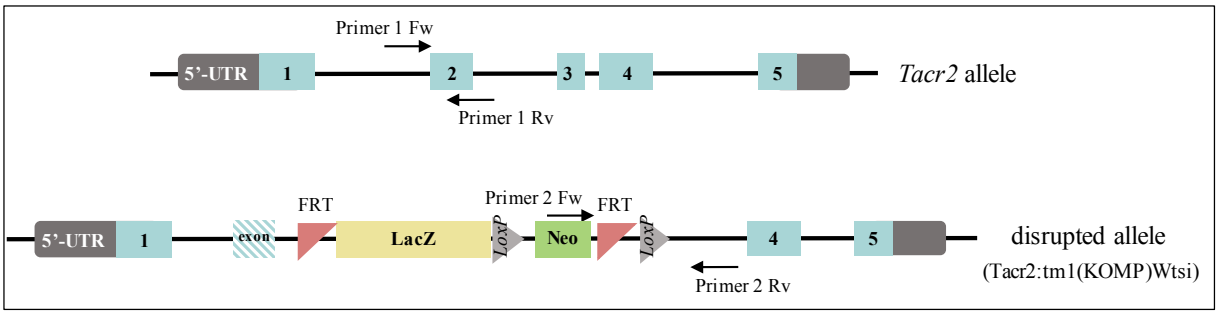

Figure 10. Diagram representative of designing the Tacr2 KO mouse line. The strategy for genotyping of Tacr2 KO mice, using a combination of primers to detect the WT and the disrupted alleles of *Tacr2* is shown. Primer sequences and further details will be described in the Genotyping section.

Generation of GFAP-specific Gpr54 null mice line

Two transgenic mouse lines described below were crossed to generate a novel mouse line, named herein G-KiRKO (for **G**FAP cell-specific **Ki**sspeptin **R**eceptor **KO**), with conditional ablation of *Gpr54* targeted to GFAP-positive cells. These two mouse lines were: i) GFAP-Cre mice obtained from the University of Seville[224,225], which express Cre recombinase under the control of the human glial fibrillary acidic protein (hGFAP) promotor and, ii) Gpr54^{loxP} mice from Lexicon Pharmaceuticals (The Woodlands, Texas, USA), in which *Gpr54* gene is flanked by *loxP* sites (**Figure 11**); the latter mouse line have been previously used in studies of our group to general global Gpr54 KO mice[170]. After the first generation of the breeding, GFAP-Cre:Gpr54^{loxP} male mice were crossed with homozygous Gpr54^{loxP} female mice to generate the G-KiRKO line. GFAP-Cre:Gpr54^{loxP} mice littermates lacking Cre expression were used as controls.

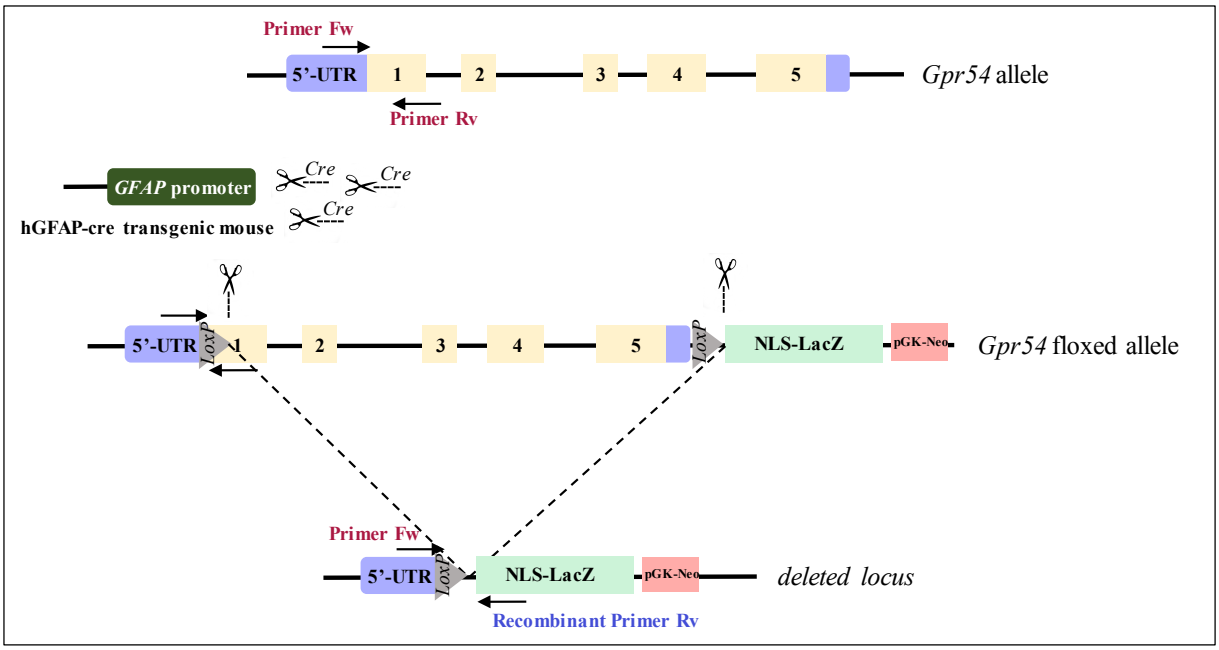

Figure 11. Diagram of the strategy for G-KiRKO mouse line generation. The strategy for genotyping of G-KiRKO mice, using a combination of primers to detect the WT and the *loxP* flank alleles of *Gpr54*, the presence of Cre transgene and the recombinant event is shown. Primer sequences and further details will be described in the Genotyping section.

Generation of a GFAP-YFP reporter mouse line

The reporter mouse line, termed herein YFP-GFAP Cre, was generated by crossing the GFAP-Cre transgenic line, described above for generating the G-KiRKO model, with the YFP^{loxP} mouse line (B6.129X1-Gt(ROSA)26Sor$^{tm1(EYFP)Cos}$/J. -The Jackson Laboratory-) which contains an enhanced yellow fluorescent protein (YFP) gene blocked by a *loxP*-flanked STOP sequence.

Kiss1 KO mice

Mice with global ablation of the *Kiss1* gene, termed here as Kiss1 KO, were obtained from professor W. H. College's lab (University of Cambridge). The model was generated by the replacement of *Kiss1* gene with an internal ribosome entry site (IRES)-LacZ reporter gene, as described in detail elsewhere[226].

Gpr54 null mice (Gpr54 KO)

Mice with global ablation of Gpr54 signaling, referred herein as Gpr54 KO, with Gpr54^{tm1SPR} background and a 52-bp region deleted in exon 2, were used. This mouse model was generated by Schering Plough Research and included the insertion of (IRES)-LacZ cassette that allows

detecting the expression of *Gpr54* by histochemical staining of X-gal. Detailed description of this model can be found in previous publications of our team[170].

Gpr54 knock-in (KI) mice

This model was obtained by engineering mice with the previous Gpr54 KO background, in which selective expression of *Gpr54* in GnRH neurons was achieved; termed here Gpr54 knock-in (KI) mice. They were generated by inserting a bacterial artificial chromosome (BAC) in Gpr54 KO mice and validated by the groups of G. Schuzt and M. Kirilov (German Cancer Research Center, Heidelberg, Germany) and A. E. Herbison (Centre of Neuroendocrinology, University of Otago, NZ). Our group has also experience in the neuroendocrine characterization of this Gpr54 KI mouse line[124].

3. Genotyping

Genomic DNA was isolated from mouse-ear tissue. The tissue was digested 2 hours at 56°C in lysis buffer (1 M Tris pH 8.5; 0.5 M EDTA pH 8; ClNa 1M and SDS 10%) supplemented with proteinase K (20 mg/ml Tris-ClH 0.01 M. Promega, Madison, WI, USA). After the digestion, the tissue lysate was centrifuged for 5 min at 13,000 rpm, and the supernatant moved to a new tube for DNA precipitation with 2-propanol (EMSURE® ACS, ISO, Reag. Ph Eur) in 1:1 volume ratio. A second centrifugation step was run followed by the decantation of supernatant and a washing step with 70% ethanol. The DNA extracted was resuspended in 50 µl nuclease-free water (nf H_2O) and stored at -20°C until its further usage. DNA of animals for primary cultures was isolated from neonatal mouse-tail tissue. The incubation in lysis buffer was for 2-4 hours, followed by the same protocol as described above. DNA extracted from neonatal mouse-tail tissue was resuspended in 100 µl nf H_2O.

Polymerase chain reaction (PCR)

The PCR was performed using the specific primers listed in **Table 2**. The stock vials of primers used were resuspended to a final concentration of 100 µM in nf H_2O and diluted 1:10 for the PCR amplifications.

Table 2. Sequences of PCR primers to genotype the mouse models mentioned above.

Primers name	Sequence (5'-3')
Gpr54-Flox Forward Reverse	 AGCGCAAGGCTCTGAAGCGGC CAATGTCGCCTCGGTGGCCAT
GFAP-Cre Forward Reverse	 ACGGGCACTGTGTCCAG TGTTCAGGGATCGCCAG
GFAP-Cre:Gpr54 Reverse	 AACAACCCGTCGGATTCTCCG
EYFP WT Forward Reverse	 AAAGTCGCTCTGAGTTGTTAT GGAGCGGGAGAAATGGATATG
EYFP mutant Forward Reverse	 AAAGTCGCTCTGAGTTGTTAT AAGACCGCGAAGAGTTTGTC
Tacr2 WT Forward Reverse	 CTCCTGACCATCACCCAATCC GGCTGGAAAGGGTGGACAATGG
Tacr2 KO Forward Reverse	 TGGATTCATCGACTGTGGCCG TGAGTCTCAAGCCTAGCTCCCTAG
Gpr54 KO Forward Reverse	 GGGTGGGATTAGATAAATGCCTGCTCT CGCGTACCTGCTGGATGTAGTTGAC
Gpr54 KI Forward Reverse	 GGTTTCAGGGAACCCAAATTA ACCAATGAGTTTCCGACCAG

For genotyping of the Tacr2 KO mouse model, two PCR amplifications per mouse were set: one to detect the WT allele and another one for detecting the disruption of the *Tacr2* allele (**Figure 12**). The Tacr2 WT primers produced a 210-pb band indicating the WT allele; and Tacr2 KO primers generated an 875-pb band, which indicates the mutant allele.

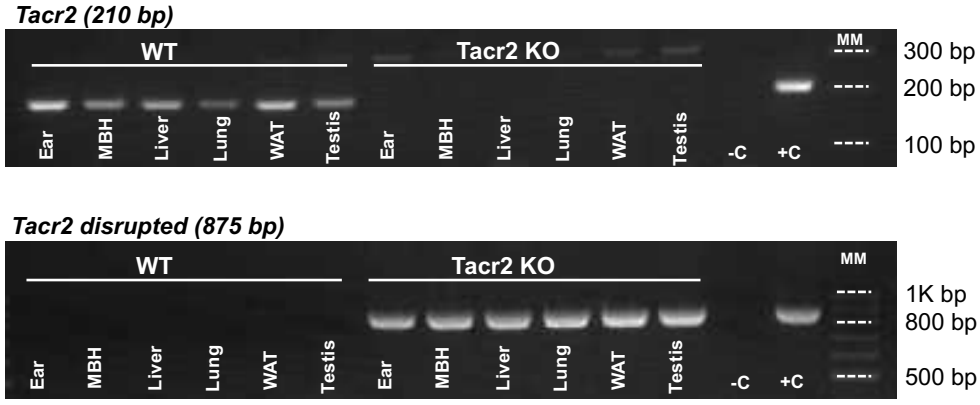

Figure 12. *Genotyping and screening of the Tacr2 KO mouse model*. Gel 1: PCR products for detecting the WT allele (210 bp band). Gel 2: PCR products for detecting the disrupted *Tacr2* gene (875 bp band).

For genotyping of the G-KiRKO mouse model, three PCR amplifications per mouse were set: one to detect the wild-type (WT) and/or *loxP* flanked Gpr54 allele, another to detect the *Cre* transgene and the third one to detect the recombination event (**Figure 13**). The Gpr54-Flox primers were designed to produce a 288-bp band to indicate WT allele and a 326-bp band for the *Gpr54* allele flanked with *LoxP* sites. GFAP-Cre primers produced a 788-bp band that denotes the presence of the *Cre* transgene. Finally, Gpr54-Flox (forward) and GFAP-Cre:Gpr54 (reverse) primers were designed to generate a 750-bp band to indicate the recombination event due to the action of Cre over *LoxP* sequences.

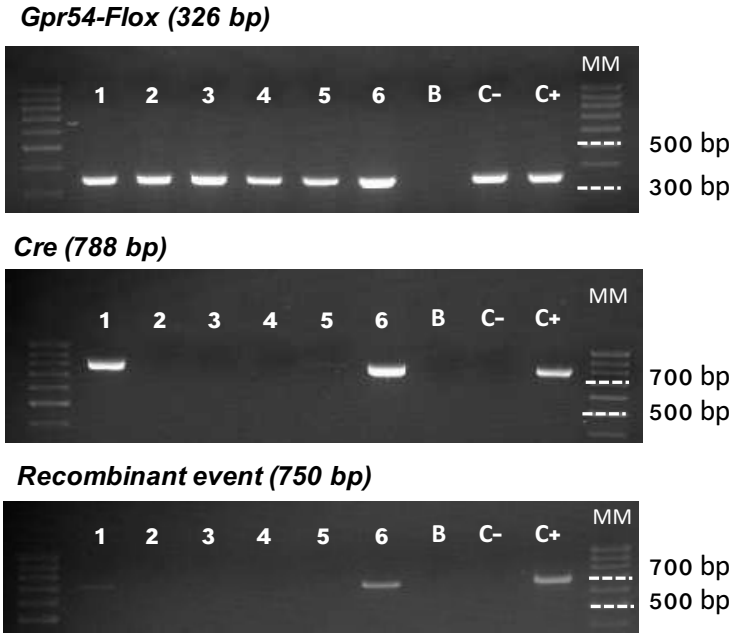

Figure 13. *Genotyping of G-KiRKO mouse model*. Gel 1: PCR products for *loxP* flanked Gpr54 allele (326 bp band). Gel 2: PCR products for detecting the presence of the Cre transgene (mouse nº 1 and nº 6 were positives for Cre band -788 bp-). Gel 3: PCR products for denoting the recombination even (mouse nº 1 and nº 6 were also positives for recombinant band -750 bp-).

Genotyping of the YFP-GFAP Cre reporter mouse model required three PCR amplifications per mouse: one to detect the WT allele, another for the mutant allele and the last one for detecting *Cre* transgene (**Figure 14**). The EYPF WT primers were designed to produce a 600-bp amplicon to indicate the WT allele. The EYFP mutant primers produced a 320-bp amplicon that indicates EYFP construction allele. As described in the previous mice model, GFAP-Cre primers were used to detect the presence of the Cre transgene (788-bp band).

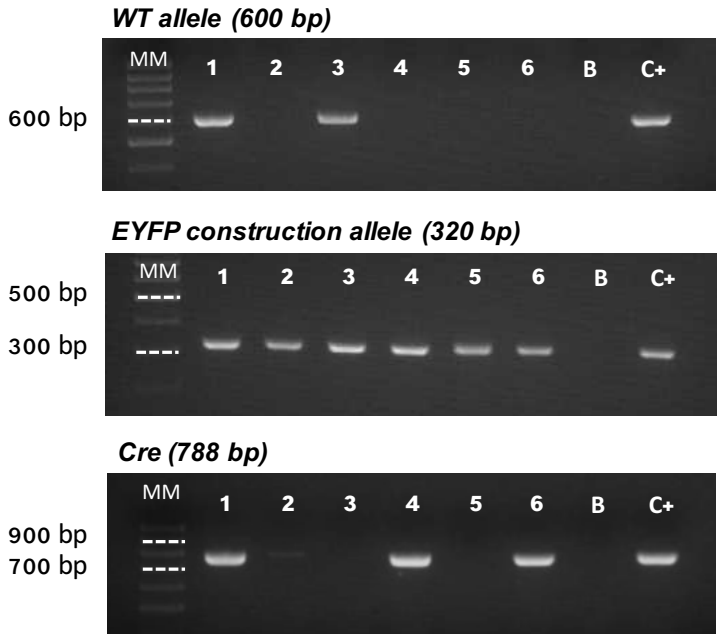

Figure 14. *Genotyping of the YFP-GFAP Cre mouse model*. Gel 1: PCR products for detecting the WT allele (600 bp band). Gel 2: PCR products for indicating the EYPF construction allele (320 bp band). Gel 3: PCR products for detecting the presence of the Cre transgene (788 bp band).

Each PCR was prepared by mixing 4 µl genomic DNA, 10 µl PCR buffer (5X Green GoTaq® Flexi Reaction Buffer -Promega-), 4 µl 25 mM $MgCl_2$ (Promega), 2 µl 5mM dNTPs (Canvax), 1 µl of each primer pair [forward (Fw) and reverse (Rv)], 0.25 µl DNA polymerase and nf H_2O up to a 50 µl final volume. Negative controls were included with all reagents except DNA sample. The PCR reactions were carried out in a T100™ thermal Cycler (Bio-Rad, Hercules, CA, USA) using the following cycling conditions: 5 min at 95°C followed by 30 cycles of 95°C for 30 s, except to detect the Tacr2 KO amplicon, which needed 38 cycles and 35 cycles for Tacr2 wild-type band; 60°C for 30 s, and 72°C for 10 s or 45 s for Tacr2 genotyping. A final extension step at 72°C for 5 min was performed. After this step, samples were kept at 10°C until being electrophoresed in 2% agarose 1X TBE (TBE 10X: 10% Tris-HCl, 5% boric acid and 4% EDTA) gels. For visualization of electrophoresed PCR products, gels were stained with RedSafe™ Nucleic Acid Staining Solution (INtRON), and digital images were captured in a Molecular Imager® Gel Doc™ XR System (Bio-Rad).

4. Drugs

The NK1R agonist (GR 73632), NK2R agonist (GR 64349), NK3R agonist (Senktide) and NK3R antagonist (SB 222200) were purchased from Tocris Bioscience (Bristol, UK). Kisspeptin (110–119)-NH2 (referred as kisspeptin-10 or Kp-10) was obtained from Phoenix

Pharmaceuticals Inc. (Burlingame, CA, USA). 17β-estradiol (E_2), testosterone, glucose and insulin were obtained from Sigma-Aldrich (St. Louis, MO, USA). Kp-10, NK2R agonist, NK1R agonist and Senktide were dissolved in physiological saline (0.9% sodium chloride); estradiol and testosterone were dissolved in olive oil; glucose and insulin were dissolved in water for injections; and NK3R antagonist was dissolved in 50% dimethyl sulfoxide (DMSO). The doses for the different drugs administered via intracerebroventricular (icv) route were: Kp-10 (50 pmol), GR 73632 (3nmol), GR 64349 (600 pmol), Senktide (600 pmol) and SB222200 (7 nmol). The drugs were administered in a final volume of 5 µl. The intraperitoneal (ip) bolus of glucose used in GTT was 2 g/kg of body weight (BW) per mouse; and the bolus of insulin administered ip for ITT was 0.75 international units (IU). For further details, see below.

5. General experimental procedures

5.1. Sample collection

For LH assays, 4 µl of blood samples were obtained from the mouse-tail and diluted in 46 µl of 0.1 M PBS (phosphate buffered saline) with 0.05% Tween 20, snap-frozen on dry ice and stored at -80°C until assayed using a super-sensitive LH enzyme-linked immunoabsorbent assay (ELISA)[227]. For analyses of pulsatile LH secretion, female mice were bilaterally ovariectomized (OVX), replaced or not estradiol (E_2), under isoflurane anesthesia. Mice were handled, 5 min per mouse, every day for 3 weeks before blood sampling in order to habituate them for tail-tip bleeding. During blood sample collection, mice were restrained in a cardboard tube every 5-min interval during 3 hours for taking serial tail-tip blood samples (**Figure 15**).

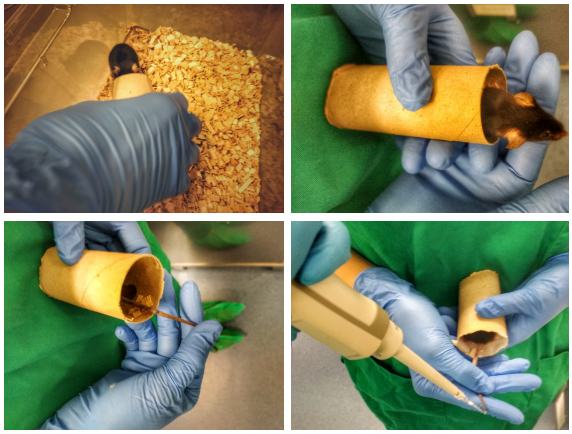

Figure 15. Representative sequential images of the blood sampling procedure for hormonal determinations.

For studies involving real time PCR (RT-qPCR) and western-blot (WB), hypothalami were dissected out, immediately upon the decapitation of the animals, frozen in liquid nitrogen and stored at -80°C until used for molecular analyses. Within the hypothalamus, medial basal hypothalamus (MBH) was dissected following the limits of the rostral border of the mammillary bodies and rostral end of the optic chiasm; and preoptic area (POA) was dissected following the optic chiasm and the intersection to the decussation of the optic nerves; as shown in **Figure 16**. Total RNA was extracted using a commercial kit for RNA extraction (Favorgen Tissue Total RNA Extraction Mini Kit, FATRK001) according to the manufacturer's recommendations. For the protein extracts, the flow-through obtained from the RNA-binding column of *"Favorgen Tissue Total RNA Extraction Mini Kit"* was collected from each sample, and precipitated by adding four volumes of acetone. The protein pellet was resuspended in lysis buffer (7 M urea (Sigma-Aldrich); 2 M thiourea (Sigma-Aldrich); 1 M Tris (Sigma-Aldrich) and CHAPs (PanReac)) until further used for molecular analyses.

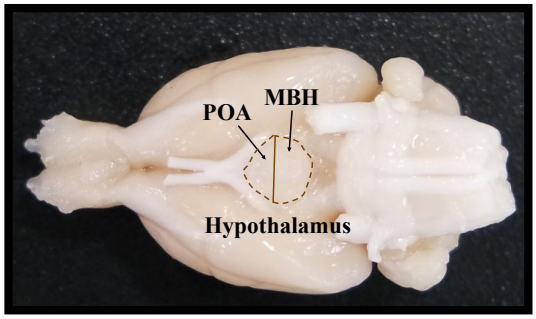

Figure 16. Schematic dissection of rat hypothalamus: POA and MBH.

For immunohistochemistry (IHC) analyses, mice were anesthetized by ip injection of a mixture of ketamine/xylazine and perfused intracardially with 0.9% saline followed by 4% paraformaldehyde (PFA) in PBS pH 7.4. Brains were collected upon the intracardiac fixation of the animals and post-fixed in 4% PFA for 24 hours at 4ºC. Then, the brains were washed in PBS for 24 hours for removing PFA remains. After that, brains were dehydrated by immersion in 30% sucrose in PBS for 48 hours at 4ºC. Then they were frozen at -80°C until further use for immunohistochemistry.

5.2. Phenotypic evaluation of pubertal maturation

After weaning, 3-week-old mice were checked for phenotypic markers of puberty onset on a daily basis. Somatic and reproductive indices of pubertal development were monitored

including body weight (BW), age of vaginal opening (VO) and balano-preputial separation (BPS), the latter two ones being considered external markers of puberty in female and male rodents, respectively. Once the vaginal opening occurred, vaginal cytology was performed daily to identify the age of the first estrus (FE), a marker of first ovulation in female rodents.

5.3. Reproductive assessment of adult mice

Adult virgin female mice were monitored daily by vaginal cytology for at least 3-4 weeks to characterize the estrous cyclicity. In Tacr2 KO mice, fertility studies were performed by breeding adult knock-out mice with control counterparts. Litter size, time-lapse until successful pregnancy in female and pregnancy rates were monitored. At the age of 4-5 months, gonads from adult males and females at diestrus were dissected immediately after euthanasia. The tissues were incubated in Bouin's solution (VWR Chemicals) and stored at room temperature until their further processing and assays.

5.4. Three-chamber sex preference test

To test sex preference, Tacr2 KO mice were individually put into the Social Box (PanLab, Harvard Apparatus) and allowed to acclimate for 5 min. After the habituation stage, mice were allowed to explore during 10 min the arena where non-familiar female and male conspecifics were placed in opposite corners of the cage into a closed wire basket (**Figure 17**). The non-familiar mice used in the sex preference test were previously habituated to the wire basket for 3 days. The time spent by the mouse in each chamber and in close interaction were recorded using Debut Video Capture Software (NCH® Software) and calculated automatically by a video tracking software (EthoVision XT, Noldus). Social Box cage was cleaned with 70% ethanol followed by double distilled water after each test.

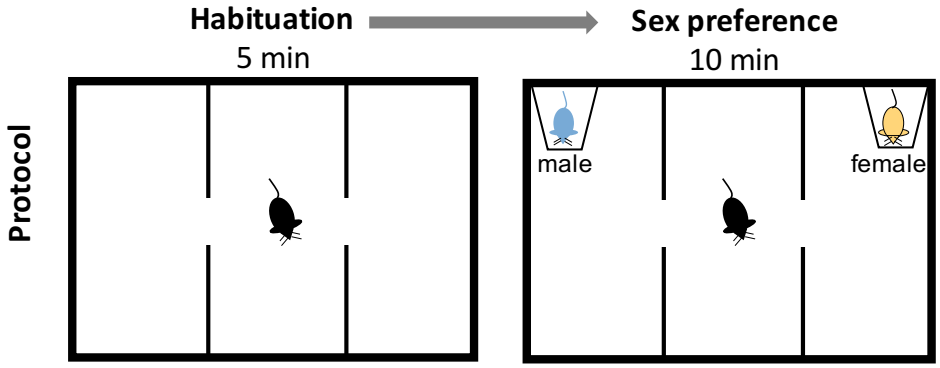

Figure 17. Diagram of sex preference test in the Social Box.

5.5. Female urine sniffing test (FUST)

To check whether Tacr2 KO male mice can distinguish between a sex odor (female urine, 10 µl) and non-social odor (tap water, 10 µl) on cotton pads located in opposite corners of the cage in comparison to WT counterparts, female urine sniffing test (FUST) was performed, as adapted from previous references[228,229]. For this test, urine samples were collected from mature WT female mice at diestrus from different cages; pooled was conducted for decreasing variability in sniffing time. Mice were individually placed into the Social box and habituated for 5 min. After the acclimation period, mice were presented to the social odor and a non-social odor (**Figure 18**). The time spent sniffing each cotton pad was recorded using Debut Video Capture Software (NCH® Software) and digitally determined by using a video tracking software (EthoVision XT, Noldus). Social Box cage was cleaned with 70 % ethanol followed by double distilled water after each test.

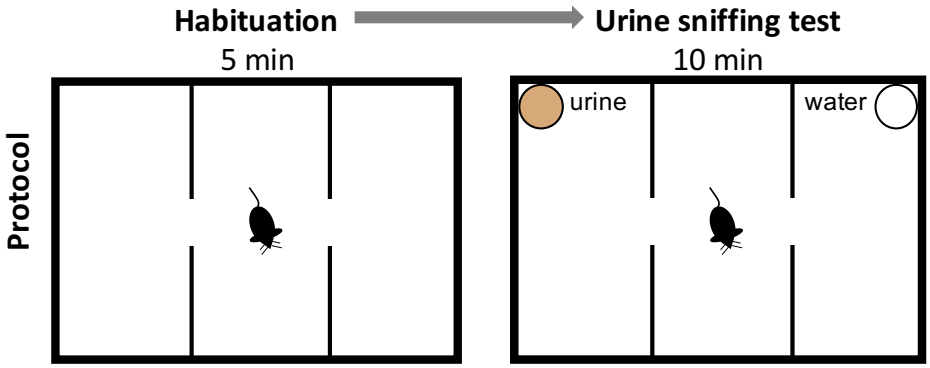

Figure 18. Diagram of FUST in the Social box.

5.6. Evaluation of metabolic parameters

For analyzing the body composition, quantitative magnetic resonance (QMR) using the EchoMRI™ 700 analyzer (Houston, TX, software v.2.0) was performed. In addition, in Tacr2 KO mice, non-invasive measures of food intake, energy expenditure (EE), respiratory quotient (RQ) and locomotor activity were obtained using OxiletPro equipment (PanLab, Harvard Apparatus) in adult mice of both sexes, fed with standard chow (low-fat content; <8.5%). To determine the EE and RQ, after 24-hour acclimation period to the metabolic cages, mice were monitored for an additional period of 24 hours with ad-libitum access to standard laboratory mice chow and water. Animal O_2 consumption rate (VO_2) and CO_2 production rate (VCO_2) were measured every 40 minutes, allowing calculation of EE and RQ. Locomotor activity of

each animal and measurement of food intake were recorded every 3 minutes.

For the glucose tolerance test (GTT) and insulin tolerance test (ITT), mice were fasted for 4 h and subsequently received an ip bolus of glucose or insulin, as described in previous sections. Glucose concentrations from tail-tip bleeding were monitored before (basal) and 20, 60 and 120 minutes after ip injections, using a handheld glucometer (ACCU-CHECK Aviva; Roche Diagnostics). For plasma glucose concentrations, the total area under the curve (AUC) were determined by the trapezoidal method during the 120 min following glucose and/or insulin administration.

5.7. Astrocyte primary culture

Newborn (PND1-3) G-KiRKO mice were used to generate astrocyte primary cell cultures. Animals were euthanized and the hypothalami were collected in cold DMEM/F12 medium with L-glutamine (Lonza, #BE12-719F). Mechanical dissociation of hypothalamic tissue was done by gentle scraping using a cell scraper (Sarstedt®) over a 40 nm mesh. The cell suspension was centrifuged (5 min at 3200 rpm, 4°C) and the resulting cell pellet resuspended with 4 ml in growth medium (DMEM/F12 with L-glutamine; 1% Gentamicin/Amphotericin (GIBCO, #R01510) and 10% Fetal bovine serum (Sigma-Aldrich). Cells were plated on uncoated T25 flasks and left growing for the first 5 days without changing the medium. After that period, fresh growth medium was added and after 48 hours, the flasks were placed at 300 rpm in a shaker incubator at room temperature for 24 hours (done to remove oligodendrocytes and microglial cells from culture), having a period of incubation at 37 ºC for 1 hour to adjust the temperature and gas content after 12 hours of shaking. After shaking, the medium was replaced with fresh medium and cells were again incubated in growth medium and changed every 3 days until they reached the 75-85% confluence (**Figure 19**). Once the confluence was optimal, astrocytes were washed with PBS, trypsinized, centrifuged (5 min at 1000 rpm, room temperature) and placed in 6-well cell culture plates for assessing the astrocytic response to Kp-10. RNA and protein from astrocytes were collected for RT-qPCR and WB analyses.

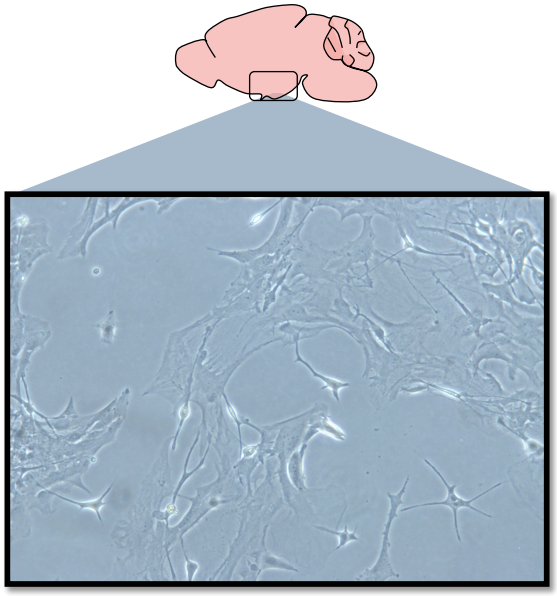

Figure 19. Morphological overview of primary astrocyte culture.

5.8. Blood pressure determination

Systolic blood pressure measurements were performed in conscious Tacr2 KO mice using a tail-cuff sphygmomanometer (CIBERTEC Niprem 645 Non-Invasive Blood Pressure System) that inflates the blood pressure cuff for occluding the tail-vessel and once the inflation point is reached it slowly deflates the cuff, displaying a linear drop in pressure. Briefly, mice were kept warm with an overhead heating lamp, and systolic blood pressure was recorded as a substantive pulse. For each mouse, four-seven blood pressure readings were obtained and averaged, being expressed as mmHg. A systolic blood pressure ≤125 mmHg was considered normotensive.

5.9. Monitoring tail skin temperature

In OVX Tacr2 KO mice, tail skin temperature was monitored using a Star-Oddi DST (data storage tag) Nano-T temperature probe (EMKA Technologies, Falls Church, VA). The small temperature data logger was attached to the ventral surface of the tail. The mice were housed individually and the skin temperature was recorded every 15 min during 20 hours.

6. General surgical procedures

6.1. Cannulation and icv administration

For hormonal studies involving icv administration of drugs, mice were cannulated 48 hours before the beginning of the experiment. Cannulae (Intrademic polyethylene tubing, Becton

Dickinson, Sparks, MD, USA) were set at a depth of 2 mm beneath the surface of the skull, with an insert point at 1 mm posterior and 1.2 mm lateral to Bregma according to a mouse brain atlas to target the lateral ventricle (LV). After cannulation, mice were individually housed until the end of the experiments.

6.2. Ovariectomy and hormonal supplementation

To examine the negative feedback effects of sex steroid on LH release, Tacr2 KO mice were subjected to bilateral ovariectomy via abdominal incision under isoflurane anesthesia. In addition, for avoiding the effect of endogenous fluctuation of sex steroids in the determination of LH levels, mice were ovariectomized (OVX) and supplemented with a fixed dose of estradiol known for restoring the physiological range. To this end, capsules (SILASTIC brand silicon tubing, 12.5 mm length, 1.98 mm in inner diameter, 3.18 mm in outer diameter; Dow Corning) filled with E_2 (10 μg/ml) were implanted subcutaneously via a small incision at the base of the neck; threads were used to close the incision.

7. General analytical procedures

7.1. RNA extraction, reverse transcription (RT) and real-time PCR (RT-qPCR)

***Total RNA extraction*:** Total RNA was extracted from tissues using a commercial kit for RNA extraction (Favorgen Tissue Total RNA Extraction Mini Kit, FATRK001) according to the manufacturer's recommendations. RNA concentration of each sample was determined using Nanodrop ND-1000 v3.5.2 spectrophotometer (Nanodrop Technology®, Cambridge, UK).

Reverse transcription for mRNA: For removing potential genomic DNA contamination from intronless target genes, 1 μg of RNA was DNase-treated following manufacturer's instruction (RQ1 RNase-Free DNase. Promega, WI, USA). DNA digestion consisted of 1 μg total RNA, 1 μl RQ_1 RNase-Free DNase and 1 μl RQ DNase 10X Reaction Buffer in a final volume of 10 μl. The reaction mix was incubated at 37°C for 30 min (DNA digestion), and after that, 1 μl Stop Solution was added. The mix was incubated at 65°C for 10 min to terminate the reaction. Then, the reverse transcription reaction was prepared using the iScript™ cDNA Synthesis Kit (1708891; Bio-Rad Laboratories Inc., USA). Each RT mixture consisted of 11 μl DNase-treated RNA sample, 1 μl iScript Reverse Transcriptase and 4 μl 5x iScript Reaction Mix in a final volume of 20 μl. For intron-containing genes, specific qPCR primers, spanning over intron regions, were designed in order to avoid genomic DNA contamination. Similar RT reactions using iScript™ cDNA Synthesis Kit were performed: 1 μg RNA sample, 1 μl iScript

Reverse Transcriptase and 4 µl 5x iScript Reaction Mix in a final volume of 20 µl. Negative controls were used with all reagents except RNA sample. In both intronless and intro-containing genes determinations, the RT reaction mix was incubated in a T100™ thermal cycler (Bio-Rad, Hercules, CA, USA) following the protocol of 5 min at 25°C, 60 min at 42°C and 5 min at 85°C. Once RT was over, the reaction volume was diluted in 80 µl of nuclease free water and stored at -20°C.

Real time PCR for mRNA quantification: RNA reversed transcribed into cDNA was analyzed by quantitative RT-PCR using specific primers pairs listed in **Table 3**. Go Taq qPCR Master mix (A6102; Promega Corporation, USA) in a CFX96 Touch Real-Time PCR Detection System (Bio-Rad Laboratories Inc., USA) was used for RT-PCR. PCR reactions were performed in duplicates for each experimental sample and consisted of 5 µl cDNA, 0.5 µl specific primer forward (Fw), 0.5 µl specific primer reverse (Rv), 6.25 µl Go Taq qPCR Master mix and 2.75 µl of nuclease free water in a final volume of 15 µl. Negative controls for genomic DNA, RT and RT-qPCR were included. The mRNA input values of each target gene were normalized to ribosomal protein S11 content and the resulting values were expressed as fold change above control levels. Primer-specific amplification and quantification cycles were run as follows: 1 cycle of Hot-Start activation at 95°C for 2 min, followed by 40 cycles of denaturation at 95°C for 30 s; annealing at a specific temperature for 30 s; extension at 72°C for 20 s and a final extension of 72 °C for 10 min, unless otherwise indicated (see **Table 3**).

Calculation of the expression levels of each target was conducted based on the cycle threshold (CT) method. The CT for each sample was calculated using the iCycler iQ™ Real-time PCR detection system software with an automatic fluorescence threshold setting. The CT from each sample was referred to S11 mRNA content/sample. The slope of the standard curve, constructed from a serial dilution of pool cDNA samples from selected tissues, was represented as a semi-log regression line plot of CT value vs. log of input nucleic acid, and used to estimate the PCR amplification efficiency.

Table 3. Primers used for RT-qPCR analyses.

Targets	Sequence (5'-3')	Annealing Temperature (° C)	Amplification Cycles	Amplicon Size (bp)
NK1R (NM_009313.5)				
Forward	GCCAGAACATCCCAACAGGA	60	40	175
Reverse	GGCAGAGACTTGCTCATGGT			
NK2R (NM_009314.4)				
Forward	TCAACTTCATCTATGCCAGTCAC	65	40	199
Reverse	ATGACAGCAATAACCGCCTTG			
NK3R (NM_021382.6)				
Forward	GCCATTGCAGTGGACAGGTAT	60	40	159
Reverse	ACGGCCTGGCATGACTTTTA			
NKB (NM_009312.2)				
Forward	CAGCTTGGCATGGACCTTC	57	40	167
Reverse	TAGCCTTGCTCAGCACTTTCA			
Kiss1 (NM_178260.3)				
Forward	GCTGCTGCTTCTCCTCTGTG	60	40	129
Reverse	TCTGCATACCGCGATTCCTT			
GnRH (NM_008145.3)				
Forward	GCATTCTACTGCTGACTGTGT	60	36	144
Reverse	GTTCTGCCATTTGATCCACCT			
Pdyn (NM_018863.4)				
Forward	AGCTTGCCTCCTCGTGATG	57	40	122
Reverse	GGCACTCCAGGGAGCAAAT			
GFAP (NM_010277.3)				
Forward	CACCTACAGGAAATTGCTGGAGG	60	35	137
Reverse	CCACGATGTTCCTCTTGAGGTG			
Gpr54 (NM_001359010.1)				
Forward	CGGAAACTCATTGGTCA	60	35	214
Reverse	TGTGGCTTGCACCGAGA			
S11 (NM_013725.4)				
Forward	CATTCAGACGGAGCGTGCTTAC	58	40	240
Reverse	TGCATCTTCATCTTCGTCAC			

7.2. Immunohistochemistry (IHC)

Coronal sections throughout the hypothalamus were cut at 30 µm thicknesses in a 1:3 series using a cryotome (Leica CM1850 UV). The sections were collected in cryoprotectant and stored at -20°C until their further usage. For the immunohistochemistry, one set of free-floating sections was washed three times (10 min per wash) in Tris-buffered saline (TBS) pH 7.6 at room temperature with gentle agitation; followed by a blocking step for 45 min at room temperature with blocking buffer (2% normal donkey/goat serum (Merck Millipore), TBS, 0.3% Triton-X (PanReac), 0.25% bovine serum albumin (BSA) (Sigma-Aldrich) and 0.01% sodium azide (NaN_3) (Scharlau)). After blocking, sections were incubated with the primary antibody diluted in blocking buffer for 1h at room temperature and overnight at 4°C with gentle agitation (**see Table 4**). On the next day, sections were washed three times (10 min per wash) in TBS and incubated with the secondary antibody, diluted 1:500 in blocking buffer for 90 min

at room temperature with gentle agitation (**see Table 5**). After three more washes in TBS (10 min per wash), the sections were mounted on microscope slides, air dried and coverslipped with Vectashield fluorescence mounting medium (Vector Laboratories). For double-labelling immunohistochemistry, a similar protocol was run. Primary antibodies were raised in different species and incubated at the same time. Secondary antibodies were used in a sequential way. Each secondary antibody was tested in the absence of the primary antibody, as negative control, to discard cross-reactivity with the tissue.

For nickel-3,3'-diaminobenzidine (nickel-DAB) immunohistochemistry, the protocol was similar to the one described above for immunofluorescence, with slight modifications. Prior to the incubation with the primary antibody, sections were blocked for endogenous peroxidases for 10 min. After the incubation with the second antibody diluted in blocking buffer without NaN_3, sections were incubated in A/B Vectastain Elite solution (Vectastain® Elite® ABC Kit reagents; Vector Laboratories, Burlingame, CA, USA), at room temperature for 90 min in blocking buffer without NaN_3. After three washes in TBS (5 min per wash), three further washes in acetate buffer 0.1 M (5 min per wash) were required. Subsequently, sections were incubated with glucose oxidase and nickel-DAB for 20 min at room temperature in dark environment. Finally, sections were washed with acetate (5 min wash) and TBS (10 min wash). For double nickel-3,3'-diaminobenzidine (nickel-DAB)-DAB immunohistochemistry, the above protocol was repeated, from the step of blocking of endogenous peroxidase activity onwards. The main difference was that the first incubation with DAB was without nickel, to incubate after, in the additional step in the third day of protocol, with nickel-DAB. After that, wash steps were performed and sections were mounted in microscope slides, air dried, dehydrated in ascending concentration of ethanol (70%, 90% and 100%) and xylene, and cover-slipped using Eukitt mounting medium (MICROPTIC S.L., Barcelona).

Table 4. Primary antibodies used.

Name	Reference	Host specie	Dilution
GFAP	3670S	mouse	1/200
YFP	ab13970	chicken	1/5000
cFos	226 003	rabbit	1/20000
S100B	ab41548	rabbit	1/3000 (IF) 1/80000 (IHC)

Table 5. Secondary antibodies used.

Name	Reference	Host specie	Dilution
FITC	715-096-150	donkey	1/200
Biotin-SP conjugated anti-rabbit	711-066-152	donkey	1/500
Anti-Chicken Alexa 488	A-11039	goat	1/500
Anti-Rabbit Rhodamine (TRITC)	AB_2337926	goat	1/500

7.3. Immunohistochemistry image processing

Images were captured with a Leica DM2500 microscope in JPEG format and processed using the open source image processing software, ImageJ (National Institutes of Health, Bethesda, Maryland). For image quantification, representative images of the areas of interest were delimited using as reference the mouse section from Allen Brain Atlas[230]. Both sides of bilateral structures (e.g., arcuate nucleus) were counted on a similar number of sections per analyzed nucleus and animal, and replicate values were averaged for further determination of group means. The number of cells was counted manually in the areas of interest in ImageJ and/or the staining was quantified measuring the intensity within a defined region of interest.

7.4. LH Enzyme-linked immunosorbent assay (ELISA)

For the assessment of circulating LH levels, a sandwich ELISA was performed. The coating of the microplate (Corning® 96 Well Clear Flat Bottom Polystyrene High Bind Microplate) was conducted using 50 µl of anti-LH antibody (monoclonal antibody, anti-bovine LHβ 518B7; University of California, Davis) diluted 1:1000 in 0.1 M PBS (1.09 g of Na_2HPO_4 [anhydrous], 0.32 g of NaH_2PO_4 [anhydrous], and 9 g of NaCl in 1000 ml of distilled water) and incubated overnight at 4°C in a humidified chamber. On the next day, the microplate was blocked with 5% skim milk powder in PBS-T (0.1M PBS and 0.05% Tween-20, pH 7.4) for 2 hours at room temperature on an orbital shaker. For the data analyses, a standard curve was prepared using a serial dilution of mouse LH reference preparation (AFP5306A; provided by Dr. A.F. Parlow and the National Hormone and Peptide program) in PBS-T. After three washes in PBS-T, 50 µl of blood samples and LH standards were incubated for 2 hours at room temperature in gentle agitation. After three-time washes, the plate was incubated with 50 µl of anti-LH antibody (polyclonal antibody, rabbit LH antiserum, AFP240580Rb; provided by Dr. A.F. Parlow and the National Hormone and Peptide program) diluted 1:10000 in blocking buffer (5% skim milk powder in PBS-T) for 90 min at room temperature in agitation. After three-time washes, the plate was incubated with 50 µl of horseradish peroxidase-conjugated antibody (polyclonal goat

anti-rabbit, DakoCytomation) diluted 1:1000 in 50% blocking buffer and 50% PBS for 90 min at room temperature in agitation. After peroxidase-conjugated antibody incubation, 100 µl of o-phenylenediamine (Invitrogen) diluted in 48 ml citrate buffer (0.1 M citric acid monohydrate and 0.2 M sodium phosphate, pH 5.0) with 20 µl of 30% solution of H_2O_2 was added to each well and incubated for 30 min at room temperature on an orbital shaker in dark. The reaction was stopped with 50 µl of 3 M HCl. The absorbance was read at a wavelength of 490 nm and 650 nm using a standard absorbance plate reader (iMark™ Microplate Absorbance Reader). The concentration of LH was determined by interpolating the optical density values of tested samples against a nonlinear regression of LH standard curve.

7.5. Gonadal removal for histology

At 4-5 months of age, gonads from adult males and females at diestrus were dissected, immediately upon the decapitation of the animals. The tissues were incubated in Bouin's solution and stored at room temperature until used further. For histological analysis, the fixed gonads were dehydrated and embedded in paraffin wax. Serial (7 µm-thick) sections were cut, stained with hematoxylin and eosin, and evaluated under microscope, using previously validated procedures in our group[231].

7.6. Western Blot

Total protein from hypothalamic nuclei and astrocyte cultures was extracted, as previously described (see "Sample collection" and "Astrocyte primary culture" sections). The protein concentration of each sample was determined using RC DC™ Protein Assay (Bio-Rad). The absorbance was read at a wavelength of 750 nm in a standard spectrophotometer (Beckman DU530). Briefly, total protein lysates (10 and/or 20 µg) were subjected to SDS-PAGE on 9% polyacrylamide gels, electro-transferred on polyvinylidene difluoride membranes (Millipore) and probed overnight at 4°C in the presence of the corresponding primary antibody (**Table 6**). For protein detection, horseradish peroxidase-conjugated secondary antibodies, as listed in **Table 7**, were used and chemiluminescence ECL Western Blotting Substrate (Thermo Scientific) was applied. Protein levels were normalized to actin. Densitometric analysis of protein bands was conducted using ImageJ.

Table 6. Primary antibodies used.

Name	Reference	Host specie	Dilution
GFAP	3670S	mouse	1/1000
Vimentin (D21H3)	5741	rabbit	1/1000
Anti-Akt	9272	rabbit	1/1000
Anti-pAkt	9271	rabbit	1/1000
Anti-ERK	sc-154	rabbit	1/1000
Phosphi-p44/42 MAPK	4370	rabbit	1/1000
anti-β-Actin	A5441	mouse	1/2000

Table 7. Horseradish peroxidase-conjugated secondary antibodies used.

Name	Reference	Host specie	Dilution
Anti-mouse	ab6789	goat	1/5000
Anti-rabbit	ab6721	goat	1/5000

7.7. Two-Dimensional Difference Gel Electrophoresis (2D-DIGE) labeling & electrophoresis

The protein concentration of the extracts obtained from hypothalami of Kiss1 KO mice was determined using RC DC™ Protein Assay (Bio-Rad). The absorbance was read at a wavelength of 750 nm in a standard spectrophotometer. Proteins (50 µg) were labelled with 400 pmol of either Cy3 or Cy5 dyes (GE Healthcare) (pH 8.0). A 50 µg protein mix containing an equal amount of each protein extract used in the experiment was labelled with 400 pmol of Cy2 dye (GE Healthcare), to define the internal standard sample. Labelled samples were immediately subjected to isoelectric focusing (IEF). A total 150 µg of labelled protein containing three equal amount extracts (Cy3-labeled sample, Cy5-labeled sample and the internal standard) was complemented with 0.5% IPG buffer (pH 3-11), 0.3% DTT and traces of bromophenol blue and applied on Immobiline™ DryStrip (pH 3-11), 18 cm strips (rehydrated in DeStreak™ Rehydration Solution, GE Healthcare) using Ettan™ IPGphor™ Cup Loading Manifold (GE Healthcare). Focusing was performed in the Ettan™ IPGphr™ IEF System following four steps: 3 hours at 300 V (step and hold), 6 hours at 3000 V (gradient); 3 hours at 8000 V (gradient) and 8000 V until steady state was reached. After isoelectric focusing, the IPG strips were incubated in equilibration solution-1 (50 mM Tris-HCl (Sigma-Aldrich), 6 M urea (Sigma-Aldrich), 30% glycerol (Sigma-Aldrich), 2% SDS (Sigma-Aldrich) and 10 mg/mL DTT (Sigma-Aldrich) (pH 8.8)) and equilibration solution-2 (50 mM Tris-HCl, 6 M urea, 30% glycerol, 2% SDS and 25 mg/mL iodoacetamide (pH 8.8)) for 15 min, respectively, and then applied to 5-20% gradient SDS polyacrylamide gel electrophoresis bands (SDS-PAGE) using SE-600 electrophoresis system (GE Healthcare). Strips were cut by 1 cm at each end to adjust to SE-600 width. For DIGE analysis, fluorescent gel images were obtained using a Typhoon

9400 Scanner and analyzed with the DeCyder Differential analysis software (GE Healthcare) by applying default parameters. For preparative gel, Immobiline™ DryStrips were rehydrated in the presence of 0.5-1 mg of protein and 0.5% IPG buffer, pH 3-11, 0.3% DTT, and DeStreak reagent (GE Healthcare). Both focusing and second dimension were performed as described above for the analytical gel. The proteins selected were analyzed by MALDI-MS(/MS) compatible with silver (GE Healthcare) or SYPRO (Bio-Rad) staining to allow subsequent protein identification in the MS Unit of the Central Service for Research Support (SCAI) of the University of Córdoba.

7.8. SWATH-MS protein quantitation

Protein extracts obtained from hypothalami of Kiss1 KO mice were precipitated with trichloroacetic acid (TCA)/acetone and solubilized in 0.2% RapiGest SF (Waters, Milford, MA, USA) in 50 mM ammonium bicarbonate. Total protein was measured using the Qubit™ Protein Assay Kit (Thermo Fisher Scientific); 50 µg of protein extract was subjected to trypsin digestion following the protocol described by Ortea *et al*[232]. Samples were analyzed using a SWATH data-independent acquisition (DIA) approach for massive protein quantitation. Equal amount of all samples from each group were pooled and subjected to shotgun analysis in order to build a peptide spectral library. Each pooled sample was analyzed twice by data-dependent acquisition (DDA) nanoscale liquid chromatography, followed by tandem mass spectrometry (nano LC-MS/MS) runs, using a LC system Ekspert™ nanoLC400 (Eksigent, Dublin, CA, USA) coupled to a Triple TOF® 5600+ (Sciex, Redwood City, CA, USA) mass spectrometer system. A top 65 method (250 ms MS survey scan in the range 350-1250 m/z, followed of 65 MS/MS with 60 ms acquisition time in the range 230-1700 m/z) was applied. On each run, 1 µg of protein was analyzed using a 120 min gradient from 5 to 30% buffer B (buffer A: 0.1% FA in water; buffer B: 0.1% FA in ACN) at a flow rate of 300 nL/min, with a 25 cm x 75 µm Acclaim PepMap100 column (Thermo Fisher Scientific). Peptide and protein identifications from all the DDA runs together were performed using Protein Pilot software v5.0.1 (Sciex) with a mouse SwissProt concatenated target-reverse decoy database, specifying iodoacetamide as cysteine alkylation. The false discovery rate (FDR) was set to 0.01 for both peptides and proteins. The MS/MS spectra of the identified peptides were used to generate a spectral library for SWATH peak extraction using the add-in for PeakView Software v2.1 (Sciex) MS/MSALL with SWATH Acquisition MicroApp v2.0 (Sciex). Peptides with a confidence score above 99% as reported from Protein Pilot database search were included in the spectral library. Depleted serum samples (1 µg per sample) were individually analyzed by a SWATH method

using the same LC-MS system and LC gradient, described above for the generation of the spectral library. A variable SWATH method, consisting on a cycle of a TOF MS scan (350-1200 m/z, 50 ms acquisition time) plus 60 MS/MS scans (230-1500 m/z, 90 ms acquisition time) of variable width windows covering the 350 to 1200 mass range was optimized according to the ion density found on the previous DDA runs. The targeted data extraction of the SWATH raw runs was performed by PeakView, using the MS/MSALL with SWATH Acquisition MicroApp v2.0 and the spectral library created from the shotgun data, with the following parameters; up to seven peptides per protein and ten fragment ions per peptide; shared and modified peptides excluded; six-minute XIC windows; 20 ppm XIC width; 1% FDR threshold. All the SWATH runs were retention time-realigned using peptides from the RePliCal iRT peptides (PolyQuant GmbH, Bad Abbach, Germany), that had been previously spiked on each vial according to the manufacturer's instructions. Protein quantitation was calculated by adding the peak areas of the ion fragments of each of the corresponding peptides.

7.9. Prediction of protein interactions and pathways enrichment analysis

The differentially expressed proteins listed from the SWATH quantitative analysis were selected as the target gene list. Then, the target gene list was imported into STRING[233] for network reconstruction and visualization. As the interactions between proteins are a required analysis for proteomics studies, in this Thesis, the STRING open database has been used to assemble, evaluate and disseminate protein-protein association information. For this analysis, medium confidence, as the minimum required interaction scored, was selected (0.400). In addition, ClueGO from the most updated version of Cytoscape[234] was used for an enrichment pathways analysis, where the biological processes and cellular components working in the target gene list described above were noted.

7.10. RNAScope in situ hybridization combined with immunohistochemistry

Single-molecule fluorescent *in situ* hybridization was performed on 14 μm brain sections of 3 adult female mice (C57BL/6) in diestrus, using the RNAScope® Multiplex Fluorescent V2 Assay according to the manufacturer's protocols (Advanced Cell Diagnostics, Inc., Newark, CA, USA). Specific probes were used to detect GnRH-I (Probe- Mm-Gnrh1-O1-C3, Cat No. 476281-C3) and Gpr54 (Probe-Mm-Kiss1r, Cat No. 408001) mouse mRNAs. Sections were then processed for immunohistochemistry, as follows: after washing in PBS, sections were incubated for 1 hour at room temperature in blocking solution containing PBS 1X, 0.4% normal donkey serum and 0.3% Triton X-100. Afterwards, sections were incubated with primary

antibody (rabbit polyclonal anti-GFAP, 1:100, Z0334, DakoCytomation, Glostrup, Denmark) diluted in blocking solution, overnight at 4°C in a humid chamber. After rinsing in PBS, the secondary antibody (Alexa Fluor 488-conjugated anti-IgG, 1:500, Molecular Probes) diluted in blocking solution was deposited on sections and incubated at room temperature for 2 hours. After washing in PBS, cell nuclei were stained with DAPI according to the RNAScope Assay.

7.11. Images acquisition and qualitative analysis of RNAScope samples

Mouse brain tissue was analyzed in coronal sections and mapped using as reference the Allen Brain Atlas[230]. Fluorescent signals of *Gpr54* and *GnRH* transcripts (*in situ* hybridization) and GFAP immunofluorescence were imaged with 20X objective lens on a Zeiss LSM 710 confocal system. All settings were identical for all images. The color label for far red was assigned for *GnRH* mRNA and the color label to red was assigned for *Gpr54* mRNA hybridization signal. The color label green was assigned for GFAP signal. The numbers of *Gpr54* mRNA positive/GFAP astrocyte marker cells were quantified in two microscopic fields per brain section using ImageJ.

8. Statistical analyses

Statistical analyses were performed using Prism software (GraphPad Prism). All data are presented as mean ± standard error of the mean (SEM). An unpaired *t*-test was applied for assessment of differences between two groups and ANOVA followed by post hoc Bonferroni tests were applied for comparisons of more than two groups. The significance level was set at $P \leq 0.05$ and different letters or asterisks have been used to indicate statistical significance.

9. Experimental design

In order to cover the specific objectives of this Thesis, the following experimental designs were applied. These are individually presented per each of the major Parts of this work.

9.1. Part I: Addressing the physiological roles of NK2R in regulating the reproductive axis by characterizing a novel mouse line with congenital ablation of Tacr2

9.1.1. Experimental set #1: Characterization of the neuroendocrine reproductive axis in Tacr2 KO mice

A first set of experimental studies included in this Thesis aimed to address the physiological roles of NK2R signaling in the regulation of the neuroendocrine reproductive axis, as well as

related functions, through a comprehensive series of analyses in a novel line with congenital ablation of *Tacr2*, the Tacr2 KO mouse.

9.1.1.1. Experiment 1: Pharmacological studies in adult control and Tacr2 KO mice

Adult WT (n=6-12) and Tacr2 KO (n=8-12) male and female mice were icv injected with NK2R and NK3R agonists (600 pmol), NK1R agonist (3 nmol) or Kp-10 (50 pmol). For time-course analyses, blood samples were collected before injections (basal) and at 15, 30 and 60 after icv administration (**Figure 20**). Doses and routes of administration were selected on the basis of previous references[9].

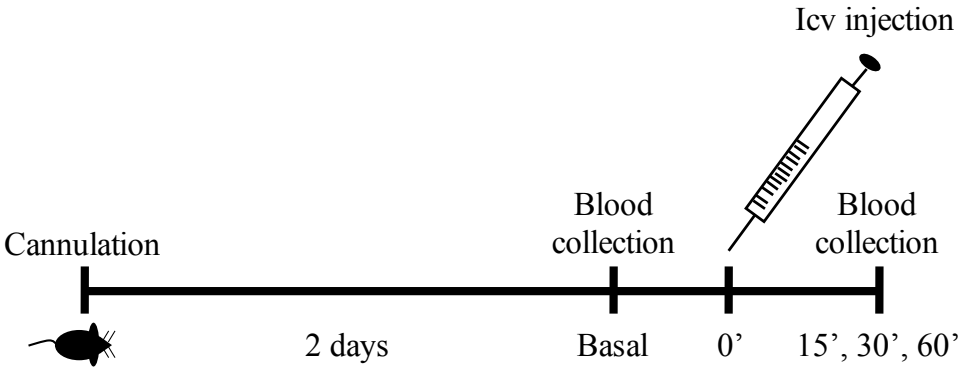

Figure 20. Experimental scheme of experiment 1.

In an additional experiment, we intended to assess LH responses to the NK2R agonist, GR 64349, after pharmacological blockade NK3R, using the selective antagonist, SB222200 (7 nmol). To this end, adult WT (n=4) and Tacr2 KO (n=8) male mice were pretreated with SB222200 60 min prior to the icv administration of GR 64349 (600 pmol). Blood samples were collected before (basal) and at 15 and 60 min after SB222200 administration, and at 15, 30 and 60 min after the injection of GR 64349 (**Figure 21**).

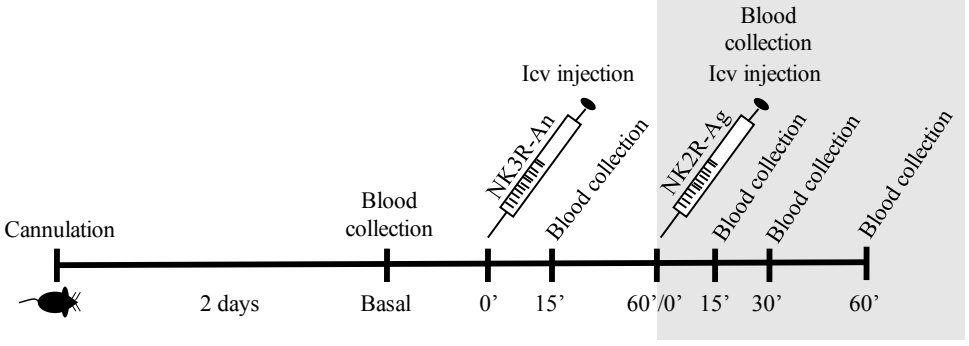

Figure 21. Experimental scheme of experiment 1 (bis).

9.1.1.2. Experiment 2: Expression of *NK1R*, *NK3R*, *NKB, Kiss1*, *GnRH* and *Pdyn* in the medial basal hypothalamus of Tacr2 KO mice

To confirm effective ablation of *Tacr2* and to determine whether the Tacr2 KO mice display compensatory changes in the expression of key elements involved in the central control of the reproductive axis, we measured the expression levels of the mRNAs encoding NK1R (*Tacr1*), NK2R (*Tacr2*), NK3R (*Tacr3*), NKB (*Tac2*), Kisspeptin (*Kiss1*), GnRH and dynorphin (*Pdyn*) in the medial basal hypothalamus (MBH) of WT (n=6-7) and Tacr2 KO (n=6-7) female and male mice.

9.1.1.3. Experiment 3: Phenotypic evaluation of pubertal maturation in Tacr2 KO mice

After weaning, 3-week-old WT (n=18-22) and Tacr2 KO (n=16-28) male and female mice were checked for phenotypic markers of puberty onset on a daily basis. Somatic and reproductive indices of pubertal development were monitored as detailed above (see "Phenotypic evaluation of pubertal maturation" section).

9.1.1.4. Experiment 4: Assessment of reproductive capacity of adult Tacr2 KO mice

WT (n=12) and Tacr2 KO (n=12) adult virgin female mice were monitored daily by vaginal cytology for at least 3-4 weeks to characterize the estrous cyclicity. Fertility studies were performed by breeding adult Tacr2 KO mice of either sex with fertile WT counterparts (the number of animals used is described in detail in the corresponding figure legend). Litter size, time lapse until successful pregnancy in females and pregnancy rates were monitored to fully characterizate the fertility in this model. Social sex preference tests were conducted in WT (n=8-10) and Tacr2 KO (n=12-15) male and female mice. In addition, female urine sniffing test was conducted in WT (n=20) and Tacr2 KO (n=17) male mice. Finally, histological analysis were performed in the testes from adult WT (n=5) and Tacr2 KO (n=5) male mice and in the ovaries and the uterus from adult WT (n=5) and Tacr2 KO (n=5) female mice to evaluate the reproductive function.

9.1.1.5. Experiment 5: Assessment of pulsatile LH secretion in Tacr2 KO female mice

Assessment of pulsatile LH secretion was conducted in WT (n=8-9) and Tacr2 KO (n=9-10) female mice. To avoid the potential confounding factor posed by dynamic fluctuations of endogenous estrogen levels, 4-5 month old female mice were subjected to bilateral ovariectomy (OVX) under isoflurane anesthesia, followed by 2-week replacement with physiological levels of estradiol (E_2), according to previous references[8,235]. After the standard

habituation period (*see above section "Sample collection"*), serial tail-tip blood samples were collected at 5-min intervals during 3 hours (**Figure 22**). The number of pulses as well as the basal and mean LH levels were measured. For OVX+E_2 mice, LH pulses were defined as those displaying an increase of 20% over the preceding two points; formula adapted from previous references[236,237]. Basal LH levels were calculated using the mean of the values preceding each peak, whereas mean LH levels were estimated as the aritmetic mean of all LH values over the study period.

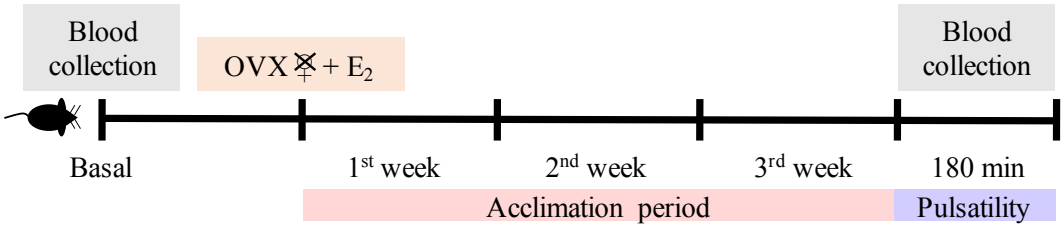

Figure 22. Experimental scheme of experiment 5.

9.1.1.6. Experiment 6: Determining mean LH levels in Tacr2 KO mice

To determine the mean LH levels in our Tacr2 KO model, tail-blood (4µl) was collected every 15 minutes for 45 minutes (time 0, 15, 30 and 45) and the replicate values were averaged for determination of group means. Blood LH content was analyzed using a super-sensitive ELISA, as described in a previous section (see "LH ELISA"). For assessing the LH secretion in response to ovariectomy, WT (n=6) and Tacr2 KO (n=7) female mice underwent surgery to bilaterally remove the ovaries under isoflurane anaesthesia. Blood samples were collected before surgery, and 2, 7 and 14 days after surgery, as mentioned previously.

9.1.2. Experimental set #2: Characterization of metabolic and related parameters in Tacr2 KO mice

Alike kisspeptins, for which distinct metabolic roles have been recently proposed[238,239], evidence strongly suggested that TAC pathways putatively participate in the control of key aspects of metabolism, such as body weight and composition, feeding behavior and glucose homeostasis[240,241]. Thus, a series of studies were applied to Tacr2 KO male and female mice for assessment of an eventual metabolic phenotype caused by ablation of NK2R signaling.

9.1.2.1. Experiment 7: Basic metabolic characterization of Tacr2 KO mice

Body weight gain and body composition were checked in WT (n=7-12) and Tacr2 KO (n=4-12) mice of both sexes at 2 and/or 6 months of age. Non-invasive measures of food intake, energy expenditure, respiratory quotient and locomotor activity (see "Evaluation of metabolic parameters" section) were conducted in adult WT (n=7-10) and Tacr2 KO (n=5-8) mice of both sexes fed with standard chow. Additionally, we carried out glucose and insulin tolerance tests (GTT and ITT) in adult WT (n=5-10) and Tacr2 KO (n=9-13) male mice fed either with standard (low-fat content; <8.5%) chow or a 45 % HFD, as shown in **Figure 23**.

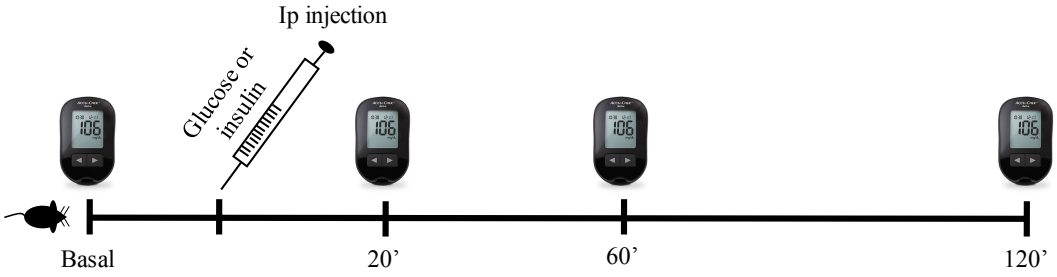

Figure 23. Experimental scheme for GTT and ITT of experiment 7.

9.1.2.2. Experiment 8: Assessment of body temperature in OVX Tacr2 KO female mice

Hot flushes, characterized by episodic and spontaneous activation of heat dissipation mechanisms (e.g., sweating, cutaneous vasodilatation and/or behavioral thermoregulation), occur in menopausal women as a result of estrogen withdrawal[242]. However, the etiology of hot flushes is still incomplete; yet, recent studies have described the involvement of NK3R signaling in that event[182,243]. To address the eventual specific role of NK2R signaling in this phenomenon, adult WT (n=5) and Tarc2 KO (n=5) female mice were subjected to OVX to mimic the withdrawal of estrogens as in menopausal women. The tail skin temperature was measured in OVX mice using a DST Nano-T probe attached to the surface of the tail, as described above.

9.1.2.3. Experiment 9: Assessment of LH responses to metabolic challenges in Tacr2 KO male mice

We assessed whether the lack of NK2R signaling modified LH responses to either chronic HFD exposure and/or a protocol of 24-hour fast. To this end, blood samples were collected as previous described in Experiment 6 from adult WT (n=5) and Tacr2 KO (n=13) male mice,

after challenge with an obesogenic diet (HFD 45%) for 10 weeks. Additionally, blood samples were collected from adult WT (n=12) and Tacr2 KO (n=18) male mice fed with standard diet that were subjected fasting during 24 hours. In this case, blood samples from tail-tip were collected before fasting and at 12, 18 and 24 h of fasting for hormone LH assays. In parallel, BW changes were checked at those times. LH content was analyzed by ELISA, as mentioned in Experiment 6.

9.1.2.4. Experiment 10: Monitoring systolic blood pressure

For assessment of the effect of the lack of NK2R on blood pressure, systolic blood pressure measurements were performed in conscious adult WT (n=5-10) and Tacr2 KO (n=5-9) mice of both sexes using a tail-cuff sphygmomanometer. Briefly, mice were kept warm with an overhead-heating lamp, and systolic blood pressure was recorded as a substantive pulse (**Figure 24**).

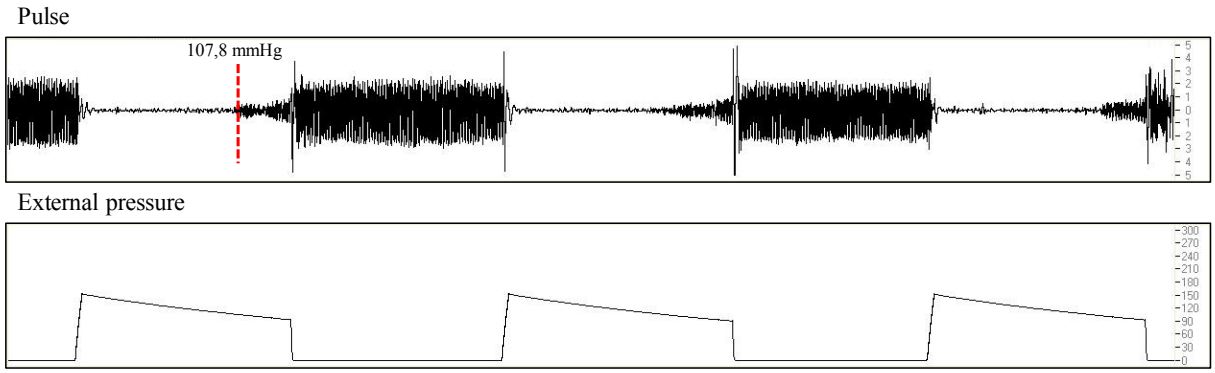

Figure 24. Diagram showing an example of blood pressure reading.

9.2. Part II: Exploring novel mediators for the effects of kisspeptins in the hypothalamus by proteomic analyses

9.2.1. Experimental set #3: New molecular mediators of kisspeptin actions

Considerable efforts have been devoted recently to elucidate how kisspeptins interplay with other central regulators of the reproductive brain. Additionally, it is worthy to note that *Gpr54* is not only expressed in GnRH neurons but also broadly in other cellular and tissue locations, which would suggest possible indirect effects of kisspeptins in the regulation of GnRH neurosecretion or, eventually, other biological functions. Here, we searched for novel molecular mediators of kisspeptin actions.

9.2.1.1. Experiment 11: Changes in hypothalamic proteomic profiles after acute central administration of Kp-10 in Kiss1 KO mice

To address how kisspeptins are interplaying with other networks in the control of reproductive function, we conducted proteomic analyses of hypothalamic (POA) tissues of Kiss1 KO mice after icv injection of Kp-10. Adult Kiss1 KO male mice (n=3-8) icv injected with vehicle (Veh) (0.9% saline) were used as controls. All animals were euthanized and POA was excised and processed for proteomic determinations (i.e., 2-DIGE or nano-HPLC associated to triple-TOP equipped with SWATH acquisition) as mentioned above.

9.2.1.2. Experiment 12: Effect of acute central administration of Kp-10 on astrocyte glial markers in Kiss1 KO mice

RT-qPCR and western blot analyses were performed for detecting the effect of Kp-10 on astrocyte glial markers, such as GFAP and Vimentin[244,245]. Adult Kiss1 KO male mice were icv injected with Kp-10 (n=3-4) or Veh (n=3). After 60 min, all animals were euthanized and POA was excised and processed for molecular analyses.

9.2.2. Experimental set #4: Molecular and functional studies in astrocyte Gpr54 signaling as putative mediator of kisspeptin actions

Based on the data from above proteomic and molecular analyses, we aimed to investigate the expression of kisspeptin receptor in astrocytes and its functionality in those cells through a comprehensive series of *in vitro* and *in vivo* analyses that include the use of primary astrocyte cultures and mouse models.

9.2.2.1. Experiment 13: *Gpr54* expression in primary astrocyte cultures and functional studies

To assess whether *Gpr54* is expressed in astrocytes and, subsequently, whether it is functional, primary astrocyte cultures from the hypothalamus of neonatal rats or mice were generated. *Gpr54* expression was addressed by PCR, as described in earlier sections. Once the expression of *Gpr54* was proven in both species, we conducted functional studies in those cultures. Astrocyte cultures from neonatal rats were incubated with Kp-10 (10^{-8} M) or vehicle (Veh) at different times (1, 10 and 30 minutes) for covering the activation of canonical pathways after Gpr54 stimulation. In addition, functional studies were conducted in astrocyte cultures from neonatal mice; these were incubated during 10 min with Kp-10 (10^{-8} M), based on the results from rat astrocyte cultures. Cortical astrocyte cultures from mice were also included in order

to compare the range of putative kisspeptin actions in astrocytes from different locations. In this study, astrocyte cultures were also incubated with epidermal grown factor (EGF) (50 ng/ml, Gibco), used as positive control[246].

9.2.2.2. Experiment 14: *In vivo* co-localization of Gpr54 and GFAP in mouse brain

To evaluate the astrocyte expression *in vivo* of *Gpr54* we used the RNAScope technology, which combines RNA *in situ* hybridization (ISH) method with immunofluorescence procedure. For performing this approach, brain sections were incubated with the probe for *Gpr54* (revealed in red) and the one for *GnRH* (revealed in far red). Additionally, immunohistochemistry against GFAP (revealed in green) was performed in the brain sections. To this end, three adult WT female mice at diestrus were studied. For each animal, two slides were taken: one covering the vascular organ of lamina terminalis (VOLT) and the anteroventral periventricular (AVPV) nucleus; and the second one for ARC and cortex. The image quantification was conducted as previously detailed (see "Images acquisition and qualitative analysis of RNAScope samples").

9.2.2.3. Experiment 15: Quantitative analysis of astrocyte markers in different models of Gpr54 signaling manipulation

Since we demonstrated that *Gpr54* is expressed in GFAP-positive cells and that kisspeptin seems to be able to modulate GFAP expression, we performed two different immune-histochemical analyses: immunofluorescence analysis for the detection of GFAP immuno-reactive astrocytes and a nickel-3,3'-diaminobenzidine (nickel-DAB) immunohistochemistry analysis for the detection of S100 calcium-binding protein B (S100ß), another astrocyte marker, in different mouse models of Gpr54 ablation (Gpr54 KO and Gpr54 KI mice models; see section "Animals -Mouse models-" above). To this end, WT (n=9), Gpr54 KI (n=8) and Gpr54 KO (n=9) male mice were anesthetized with ip injection of ketamine/xylazine mixture and perfused intracardially with 0.9% saline followed by 4% paraformaldehyde (PFA) in PBS (pH 7.6). After perfusion, brains were collected and processed for IHC analyses (see sections "Sample collection" and "Immunohistochemistry" above). For quantification, representative images of the ARC were delimited using as reference the mouse section from Allen Brain Atlas[230]. Both sides of bilateral images of ARC were counted on a similar number of sections per analyzed nucleus and animal, and replicate values were averaged for further determination of group means. GFAP staining was quantified measuring the intensity within a drawn region of interest and the number of cells (S100ß-labelled astrocytes) was counted manually, using ImageJ (**Figure 25**).

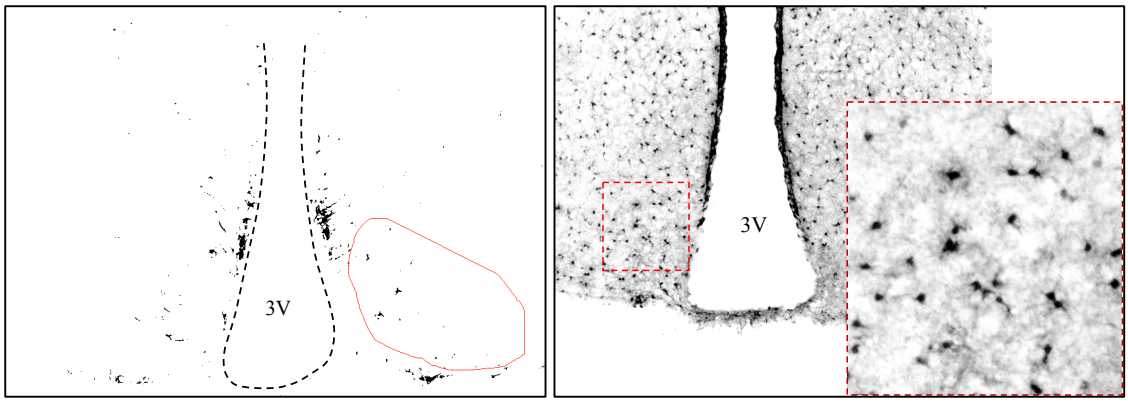

Figure 25. Image showing the drawn region of interest in the immunofluorescence (left) and the immunohistochemical (right) analyses.

9.3. Part III: Assessing the physiological roles of kisspeptin signaling in astrocytes: Characterization of a novel mouse line with selective ablation of Gpr54 in GFAP-positive cells.

9.3.1. Experimental set #5: Addressing of the role of kisspeptin signaling in astrocytes *in vivo* in the control of the reproductive axis

Considering that astrocytes play an important role in the control of the HPG axis through the release of growth factors, bioactive molecules and by their adhesiveness to GnRH neurons, and the novel herein identified expression of *Gpr54* in astrocytes, we generated a novel model for conditional ablation of kisspeptin signaling in astrocytes and conducted its reproductive characterization, as a means to elucidate the physiological role of such kisspeptin signaling in astrocytes in the control of reproduction.

9.3.1.1. Experiment 16: Validation of our new model, the G-KiRKO mouse

To provide a general validation of our G-KiRKO model, three complementary approaches were carried out. First, effective recombination denoting Cre activity was assessed by PCR in genomic DNA of different tissues from G-KiRKO mice. To this end, the pair of primers named Gpr54-Flox Fw (5' AGCGCAAGGCTCTGAAGCGGC 3') and GFAP.Cre:Gpr54 Rv (5' AACAACCCGTCGGATTCTCCG 3') were used to detect the presence of the recombination event (750-bp amplicon). Second, to assess whether Cre recombinase is functional in astrocytes, we used a reporter mouse line generated by crossing GFAP-Cre transgenic mice with YFP^{loxP} reporter mice, in which the expression of yellow fluorescent protein (YFP), the reporter signal, is blocked by a *loxP*-flanked STOP sequence. Double immunohistochemistry

was used to co-localize S100β, the cytosolic glial marker S100β[244], and YFP. The last validation approach was the generation of primary astrocyte cultures from the hypothalami of newborn (PND-1 up to PND-3) control (n=3-4) and G-KiRKO (n=3) mice for molecular analyses of *Gpr54* transcript by RT-qPCR. GFAP-Cre:Gpr54^{loxP} mice littermates lacking Cre expression were used as controls.

9.3.1.2. Experiment 17: Phenotypic evaluation of pubertal onset and estrous cyclicity in adult G-KiRKO mice

After weaning, 3-week-old Control (n=16-20) and G-KiRKO (n=12-16) male and female mice were checked for phenotypic markers of puberty onset on a daily basis, including the body weight gain, the age of vaginal opening and first estrus in females, and the age of balano-preputial separation in males. In addition, adult virgin Control (n=7) and G-KiRKO (n=12) female mice were monitored daily by vaginal cytology for at least 3-4 weeks to characterize the estrous cyclicity.

9.3.1.3. Experiment 18: Determining mean LH levels in adult G-KiRKO mice

To determine the mean LH levels in our G-KiRKO model, blood samples were collected, as previous described in Experiment 6, from adult Control (n=14-17) and G-KiRKO (n=10-11) male and female mice. Note that female blood samples were collected in the stage of diestrus. LH content was analyzed as detailed in a previous section (see "LH ELISA").

9.3.1.4. Experiment 19: Pharmacological studies in adult G-KiRKO mice

To further address the role of Gpr54 signaling in astrocytes, LH responses to kisspeptin (Kp-10) were studied in both G-KiRKO male and female mice. Control (n=14-17) and G-KiRKO (n=10-11) mice of both sexes were icv injected with Kp-10 (50 pmol). Blood samples were collected before injection (basal) and 15, 30 and 60 minutes after icv administration of Kp-10 (**Figure 26**). Blood LH content was analyzed as described above (see "LH ELISA" section).

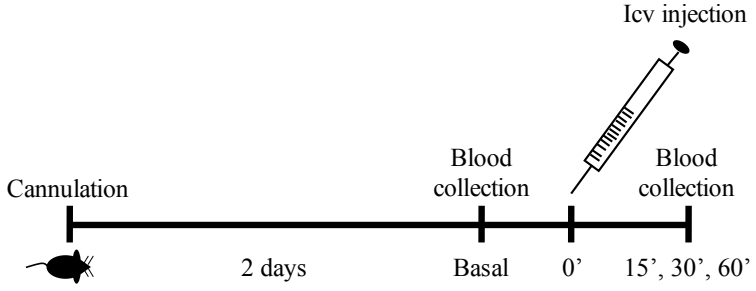

Figure 26. Experimental scheme of experiment 19.

9.3.1.5. Experiment 20: Quantitative analysis of GFAP immunoreactive in G-KiRKO mice

To assess whether the lack of Gpr54 signaling in astrocytes modified GFAP immunoreactivity, we performed immunohistochemical analysis in our G-KiRKO mice model. To this end, brains from adult Control (n=4) and G-KiRKO (n=4) male mice were collected and processed for IHC analyses (see "Sample collection" and "Immunohistochemistry" sections). GFAP staining quantification is described in Experiment 15.

9.3.2. Experimental set #6: Analysis of metabolic/reproductive interactions in G-KiRKO mice

Based on the data that kisspeptin signaling plays a role in the control of body weight and metabolic homeostasis, we decided to explore the potential role of Gpr54 signaling in GFAP-expressing cells on the metabolic control of reproductive function. To this end, weaned G-KiRKO mice were fed HFD (58% kcal from fat; reference D12331) for generation of diet-induced obesity.

9.3.2.1. Experiment 21: Phenotypic evaluation of pubertal maturation and estrous cyclicity in adult HFD-fed G-KiRKO mice

After weaning, 3-week-old Control (n=18-35) and G-KiRKO (n=9-17) male and female mice were exposed to HFD and checked for phenotypic markers of puberty onset on a daily basis. Somatic and reproductive indices of pubertal development, including body weight, vaginal opening, first estrus and balano-preputial separation, were recorded, following protocols similar to those described in Experiment 3. Adult virgin Control (n=7) and G-KiRKO (n=7) female mice, chronically exposed to HFD, were monitored daily by vaginal cytology for at least 3-4 weeks to characterize the estrous cyclicity.

9.3.2.2. Experiment 22: Assessment of LH responses to HFD exposure in G-KiRKO mice

To determine the high-fat diet effect on mean LH levels in our G-KiRKO model, blood LH levels in Control (n=15-16) and G-KiRKO (n=11-19) male and female mice fed with HFD were analyzed as previous described (see "Experiment 6").

9.3.2.3. Experiment 23: Pharmacological study for assessing the effect of Kp-10 on LH responses in G-KiRKO mice fed with HFD

Adult Control (n=15-16) and G-KiRKO (n=11-19) mice of both sexes, after challenge with an

obesogenic diet (HFD 58%) since the weaning, were icv injected with Kp-10 (50 pmol). Blood sample collection and LH content determinations were performed as previous mentioned in Experiment 19.

9.3.2.4. Experiment 24: Metabolic characterization of G-KiRKO mice fed with chow and HFD

To test the role of Gpr54 signaling in astrocytes in the control of key metabolic parameters, we carried out body composition analyses for determining fat and lean mass, at the age of 4-5 months old, in Control (n=7-12) and G-KiRKO (n=8-12) mice of both sexes fed with standard chow and HFD, as well as glucose and insulin tolerance tests (GTT and ITT). For the GTT and ITT, mice were fasted for 4 h and subsequently received an ip bolus of glucose or insulin, as described in previous sections.

9.3.2.5. Experiment 25: Quantitative analysis of GFAP immunoreactive after chronic and acute exposure to HFD in G-KiRKO mice

As has been previously reported, hypothalamic astrocytes display changes in response to chronic and acute exposure to high-fat diet[247]. In this context, we assessed whether the lack of Gpr54 signaling modified GFAP responses to either a 4-months of HFD exposure or a protocol of 3-day HFD exposure. To this end, Control (n=4-6) and G-KiRKO (n=4-6) male mice fed with 58% HFD during 4 months or during 3 days were used. Brains were collected and processed for IHC analyses (see “Sample collection” and “Immunohistochemistry” sections). Note that this experiment was performed using male instead of female mice, in order to avoiding changes in GFAP due to estradiol fluctuations during the estrous cycle. The image quantification was performed as described above in Experiment 15.

Results

Results

Part I: Addressing the physiological roles of NK2R in regulating the reproductive axis by characterizing a novel mouse line with congenital ablation of *Tacr2*.

Activation of NK2R evokes LH responses in adult mice: Comparison with other TACs & Kp-10

We explored the capacity of the agonist of NK2R, GR 64349, to evoke acute LH responses after icv administration in adult female and male control (wild-type) mice. These responses were compared with those elicited by the agonists of NK1R (GR 73632) and NK3R (Senktide), as well as kisspeptin-10 (Kp-10). As shown in **Figure 27**, activation of NK2R induced a significant elevation of serum LH levels, 30-min after icv injection of GR 64349 (salmon bars). These responses were comparable in magnitude to those elicited by NK1R (violet bars) and NK3R (blue bars) agonists, in both female and male control mice. The average increase in mean LH levels was approximately three-fold and two-fold at 30-min after NK2R activation, in female and male mice, respectively. Alike, adult female and male mice responded to a bolus of a low dose of Kp-10 (dark bars) with a robust four-fold increase in serum LH levels 30-min after the icv injection, which was significantly higher than any of the LH responses to the individual NKR agonists.

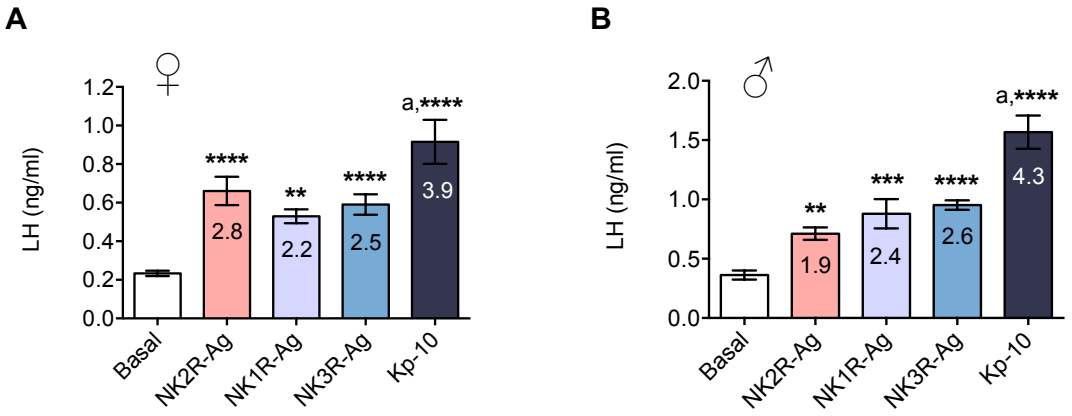

Figure 27. *LH responses to NK2R activation in control male and female mice.* The effects of acute icv administration of NK2R agonist (GR 64349; 600pmol), NK1R agonist (GR 73632; 3nmol), NK3R agonist (Senktide; 600pmol), and kisspeptin-10 (Kp-10; 50pmol) on LH release were monitored in intact control female (**A**) and male (**B**) mice. Blood samples for LH determination were obtained before (basal) and 30 min after injection of each compound. In addition to absolute levels, relative responses to TAC agonists and Kp-10 [expressed as degree of increase over corresponding mean control values (basal)] are shown in *insets*. LH values are shown as means ± SEM. Statistical significance was determined by one-way ANOVA: **P<0.01 vs basal, ***P<0.001 vs basal and ****P <0.0001 vs basal; ^{a} P <0.01-0.0001 corresponding to Kp-10 values. Number of determinations was as follows. **A**: n (basal)= 40; n (NK2R-Ag)= 10; n (NK1R-Ag)= 6; n (Senktide)= 10; n (Kp-10)= 10; **B**: n (basal)= 42; n (NK2R-Ag)= 10; n (NK1R-Ag)= 6; n (Senktide)= 10; n (Kp-10)= 12. Note that basal measurements for the different tests yielded similar values and were integrated for definition of representative basal LH levels.

LH responses to NK2R activation in adult Tacr2 KO mice: Comparison with other TACs and Kp-10

We also assessed the time-course of LH responses to the three NKR agonists and Kp-10 in Tacr2 KO mice and their corresponding controls. In line with genotyping results, female and male Tacr2 KO mice displayed absent *Tacr2* mRNA expression in the hypothalamus (**Figure 28**), which was detectable in control mice, thus validating the selective lack of NK2R in our model.

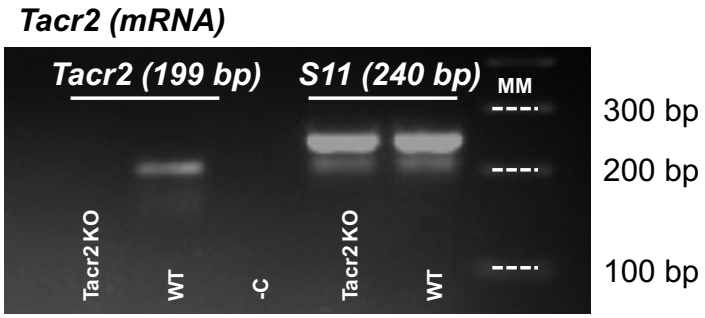

Figure 28. *Validation of the Tacr2 KO mouse line.* Representative gel of RT-qPCR analysis of *Tacr2* mRNA expression in medial basal hypothalamus (MBH) in WT and Tacr2 KO male mice. Ribosomal protein S11 was used as internal reference. Expected sizes for the RT-qPCR products are 199 bp for *Tacr2* and 240 bp for *S11*.

In clear contrast, hypothalamic expression of a number of genes encoding key regulators of the reproductive axis, including *Tacr1*, *Tacr3*, *Kiss1*, *GnRH*, *NKB* and *Pdyn*, were detectable in the hypothalamus of Tacr2 KO mice of both sexes, at levels comparable to those seen in control mice (**Figure 29**).

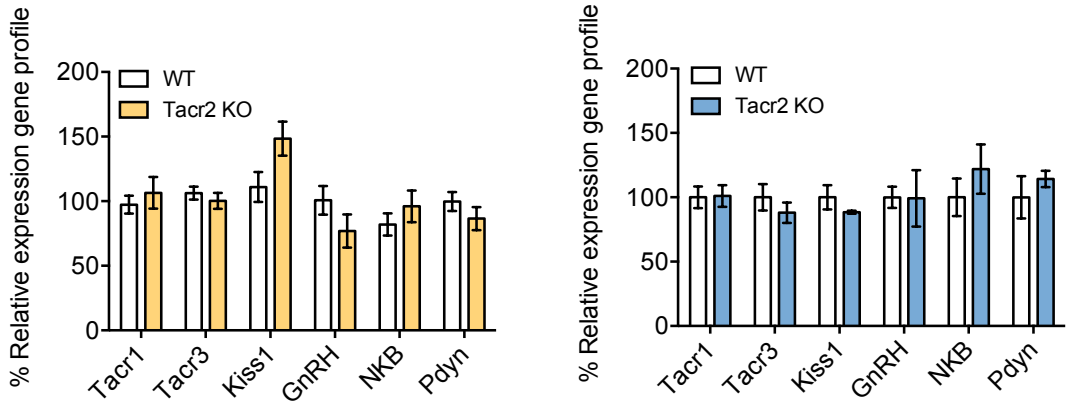

Figure 29. *Validation of the Tacr2 KO mouse line*. Relative expression levels of *Tacr1*, *Tacr3, Kiss1, GnRH, NKB* and *Pdyn* from MBH of WT (white) and Tacr2 KO female (yellow) and male (blue) mice, as assessed by quantitative RT-qPCR, are presented (female WT n= 6; female Tacr2 KO n= 6; male WT n= 7; male Tacr2 KO n= 7). Data are shown as means ± SEM.

In female mice, LH responses to the administration of NK2R agonist (GR 64349) were detectable, but significantly attenuated in Tacr2 KO mice, as defined by the lower LH levels at 15- and 30-min after agonist injection, and the overall decrease of integral (ΔAUC) LH responses for the 60-min period following administration of GR 64349 (**Figure 30**).

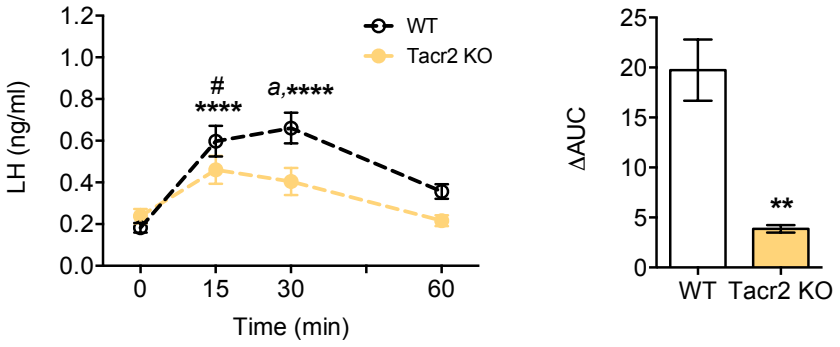

Figure 30. *Time-course LH responses to NK2R in Tacr2 KO female mice*. The effects of acute icv injection of NK2R agonist (GR 64349; 600pmol) on LH secretion were monitored in Tacr2 KO female mice. Blood samples for LH determination were obtained before (basal, 0) and 15, 30 and 60 min after injection. In addition to time course profiles, net increment of integral secretory responses to central administration of the NK2R agonist (represented as ΔAUC) over the 60-min study period are shown. Statistical significance was determined by two-way ANOVA followed by Bonferroni's post hoc test or Student t test: $^{\#}$P<0.05 vs. corresponding control values (basal); **P<0.01 vs. corresponding WT values; ****P<0.0001 vs. corresponding control values (basal); and ^{a} P< 0.01 vs. corresponding WT values at this time. Female WT n= 10; and female Tacr2 KO n= 8.

In contrast, LH responses to the other TAC receptor agonists and Kp-10 were not affected by *Tacr2* ablation, and were similar in magnitude to those of control female mice (**Figure 31**).

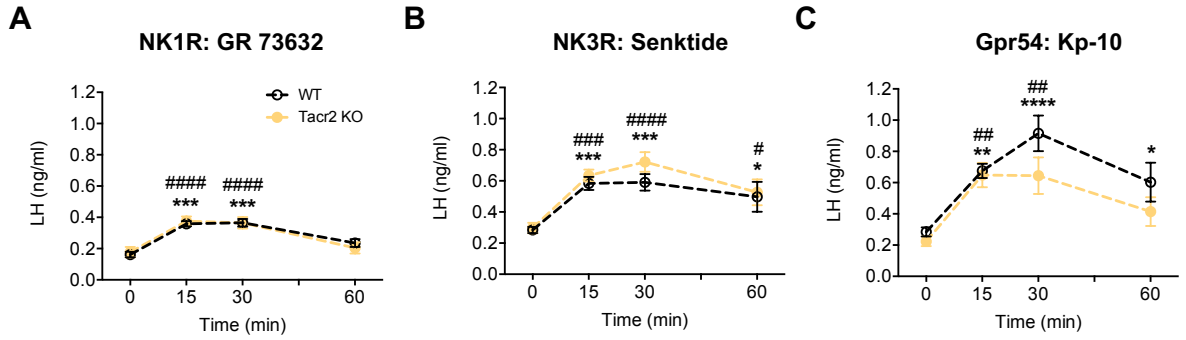

Figure 31. *Time-course LH responses to other TAC agonists and Kp-10 in Tacr2 KO female mice*. The effects of acute icv injection of NK1R agonist (GR 73632; 3nmol), NK3R agonist (Senktide; 600pmol), and kisspeptin-10 (Kp-10; 50pmol) on LH secretion were monitored in Tacr2 KO female mice. Blood samples for LH determination were obtained before (basal, 0) and 15, 30 and 60 min after each injection. Statistical significance was determined by two-way ANOVA followed by Bonferroni's post hoc tests: $^{*/\#}$*P*<0.05 vs. corresponding control values (basal); $^{**/\#\#}$P<0.01 vs. corresponding control values (basal); $^{***/\#\#\#}$P<0.001 vs. corresponding control values (basal); and $^{****/\#\#\#\#}$P<0.0001 vs. corresponding control values (basal). Female WT n= 6-11; and female Tacr2 KO n= 8-9.

On the hand, Tacr2 KO male mice displayed a grossly conserved LH responsiveness to the NK2R agonist, as denoted by time-course and integral analyses in **Figure 32**, except for a very modest decrease in serum LH levels over corresponding control values at 60-min after injection of GR 64349.

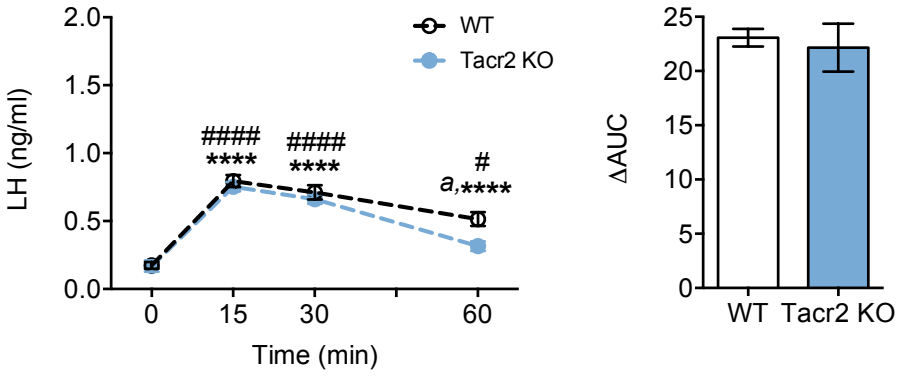

Figure 32. *Time-course LH responses to NK2R in Tacr2 KO male mice*. The effects of acute icv injection of NK2R agonist (GR 64349; 600pmol) on LH secretion were monitored in Tacr2 KO male mice. Blood samples for LH determination were obtained before (basal, 0) and 15, 30 and 60 min after injection. In addition to time course profiles, net increment of integral secretory responses to central administration of the NK2R agonist (represented as ΔAUC) over the 60-min study period are shown. Statistical significance was determined by two-way ANOVA followed by Bonferroni's post hoc tests: $^{\#}$P<0.05 vs. corresponding control values (basal); ****P<0.0001 vs. corresponding control values (basal); and ^{a} P< 0.01 vs. corresponding WT values at this time. Male WT n= 10; and male Tacr2 KO n= 11.

In addition, the stimulatory effects of the other TAC receptor agonists and Kp-10 on LH secretion were similar in Tacr2 KO and control male mice (**Figure 33**).

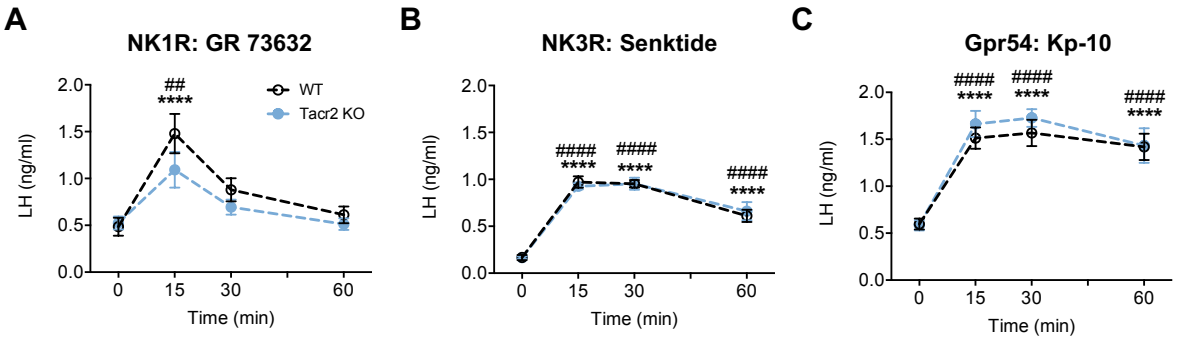

Figure 33. *Time-course LH responses to other TAC agonists and Kp-10 in Tacr2 KO male mice*. The effects of acute icv injection of NK1R agonist (GR 73632; 3nmol), NK3R agonist (Senktide; 600pmol), and kisspeptin-10 (Kp-10; 50pmol) on LH secretion were monitored in Tacr2 KO male mice. Blood samples for LH determination were obtained before (basal, 0) and 15, 30 and 60 min after each injection. Statistical significance was determined by two-way ANOVA followed by Bonferroni's post hoc tests: $^{\#\#}$P<0.01 vs. corresponding control values (basal); and $^{****/\#\#\#\#}$P<0.0001 vs. corresponding control values (basal). Male WT n= 6-12; and male Tacr2 KO n= 7-12.

The intriguing conservation of LH responses to the NK2R agonist in male mice congenitally lacking this receptor prompted us to explore the potential interplay between NKR2 and other TAC pathways in this model. In detail, male Tacr2 KO and control mice were pre-treated with the NK3R antagonist, SB 222200, and after 60-min, the animals were icv injected with an effective dose of the NK2R agonist, GR 64349. Control mice pre-treated with the NK3R antagonist displayed significant LH responses to NK2R activation. In contrast, LH responses to the NK2R agonist, GR 64349, were fully prevented by the concomitant blockade of NK3R in Tacr2 KO male mice (**Figure 34**).

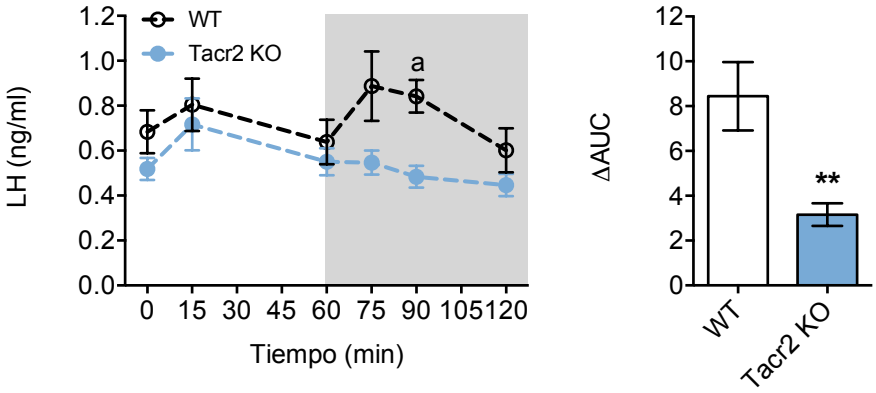

Figure 34. *Time-course LH responses to NK2R agonists after pre-treatment with NK3R antagonist in Tacr2 KO male mice (grey area)*. The effects of pre-treatment with the antagonist of NK3R (SB 222200; 7nmol) on LH responses to the NK2R agonist are displayed. In addition to time course profiles, net increment of integral secretory responses to central administration of the NK2R agonist (represented as ΔAUC) over the 120-min study period are shown. Statistical significance was determined by two-way ANOVA followed by Bonferroni's post hoc test or Student t test: $^{**}P<0.01$ vs. corresponding WT values; and $^{a}P< 0.05$ vs. corresponding WT values at this time. Male WT n= 4; and male Tacr2 KO n= 8.

Tacr2 KO mice display preserved puberty and fertility, but altered LH pulsatility

Puberty onset and reproductive parameters were monitored in Tacr2 KO mice of both sexes. Analysis of phenotypic markers of puberty revealed normal pubertal timing in Tacr2 KO male and female mice, as denoted by the conserved ages of vaginal opening (VO) and first estrus (FE) in females (**Figure 35**), and balano-preputial separation (BPS) in males (**Figure 36**). In addition, body weight (BW) gain during the pubertal transition was similar in KO and control mice (**Figures 35** and **36**).

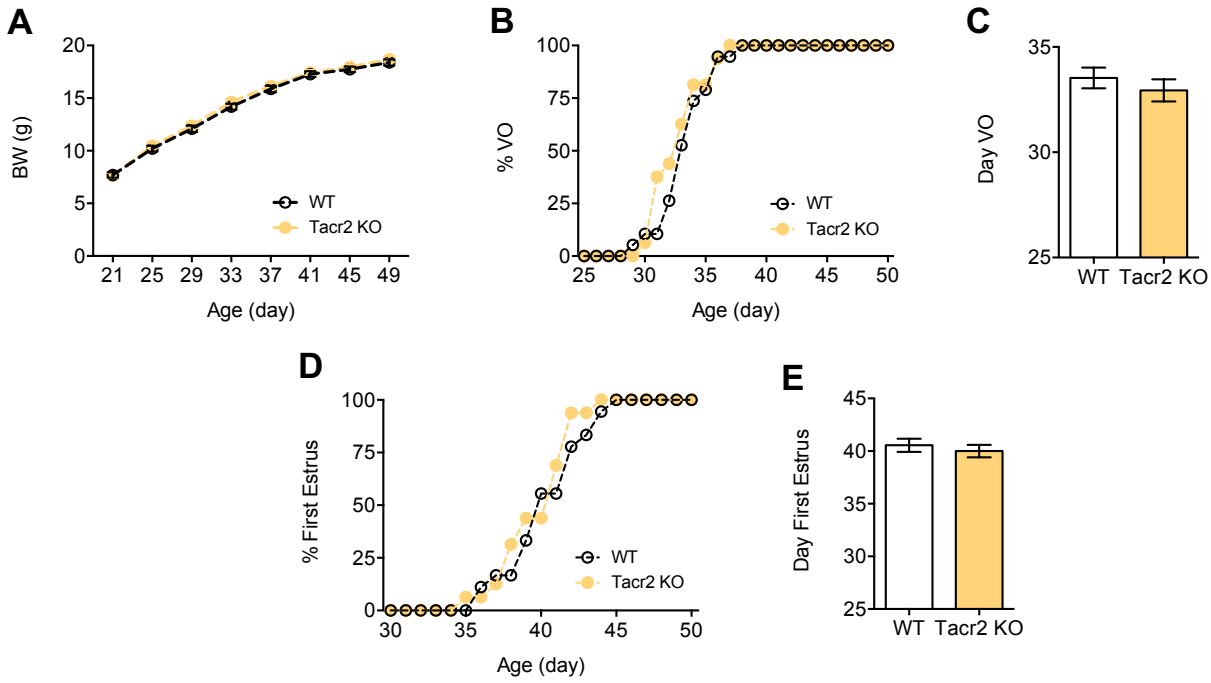

Figure 35. *Indices of pubertal maturation in Tacr2 KO female mice*. **A**, evolution of body weight (BW) gain from weaning (PND21) to adulthood is presented from WT (white) and Tacr2 KO (yellow) female mice (WT n= 18; Tacr2 KO n= 16). **B**, accumulated percentage of female mice displaying vaginal opening (VO) during the period of 3 weeks post weaning is shown; the average age of VO is presented in **C**. The accumulated percentage of female mice displaying first estrus (FE) and the average age of FE are shown in **D** and **E**.

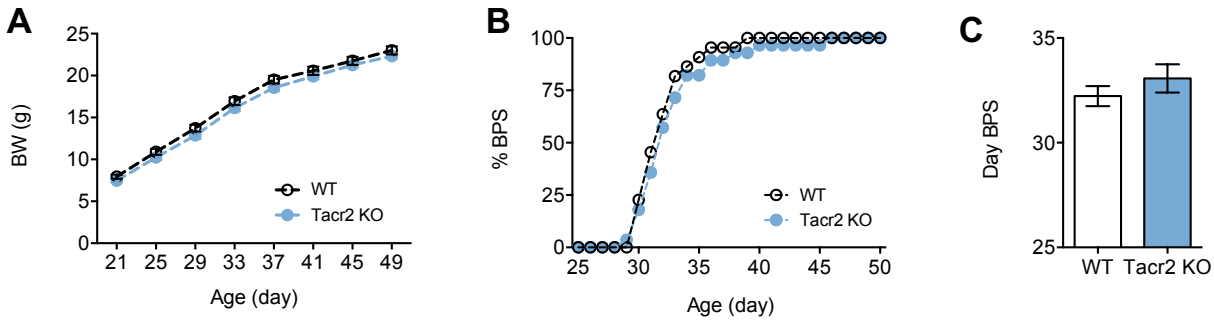

Figure 36. *Indices of pubertal maturation in Tacr2 KO male mice*. **A**, evolution of BW gain from weaning (PND21) to adulthood is presented from WT (white) and Tacr2 KO (blue) male mice (WT n= 22; Tacr2 KO n= 28). **B**, accumulated percentage of male mice displaying balano-preputial separation (BPS) during the period of 3 weeks post weaning is shown, while the average age of BPS is presented in **C**.

Additional parameters of the functioning of the reproductive axis were monitored in Tacr2 KO female mice. In detail, pulsatile LH secretion was assessed over a 180-min period, using frequent 5-min blood sampling and a super-sensitive LH ELISA. In addition, estrous cyclicity and fecundity were studied in Tacr2 KO female mice. In order to avoid the potential

interference of fluctuations of endogenous estrogen levels, LH pulsatility was evaluated in female mice of both genotypes following bilateral ovariectomy (OVX) and replacement with a physiological dose of estradiol (E_2). In this model of clamped E_2 levels, basal and mean LH levels were significantly lower in Tacr2 KO female mice. In contrast, the number of pulses was not significantly altered in null mice; if any, a trend for higher number of pulses over the 180-min period was observed (**Figure 37**).

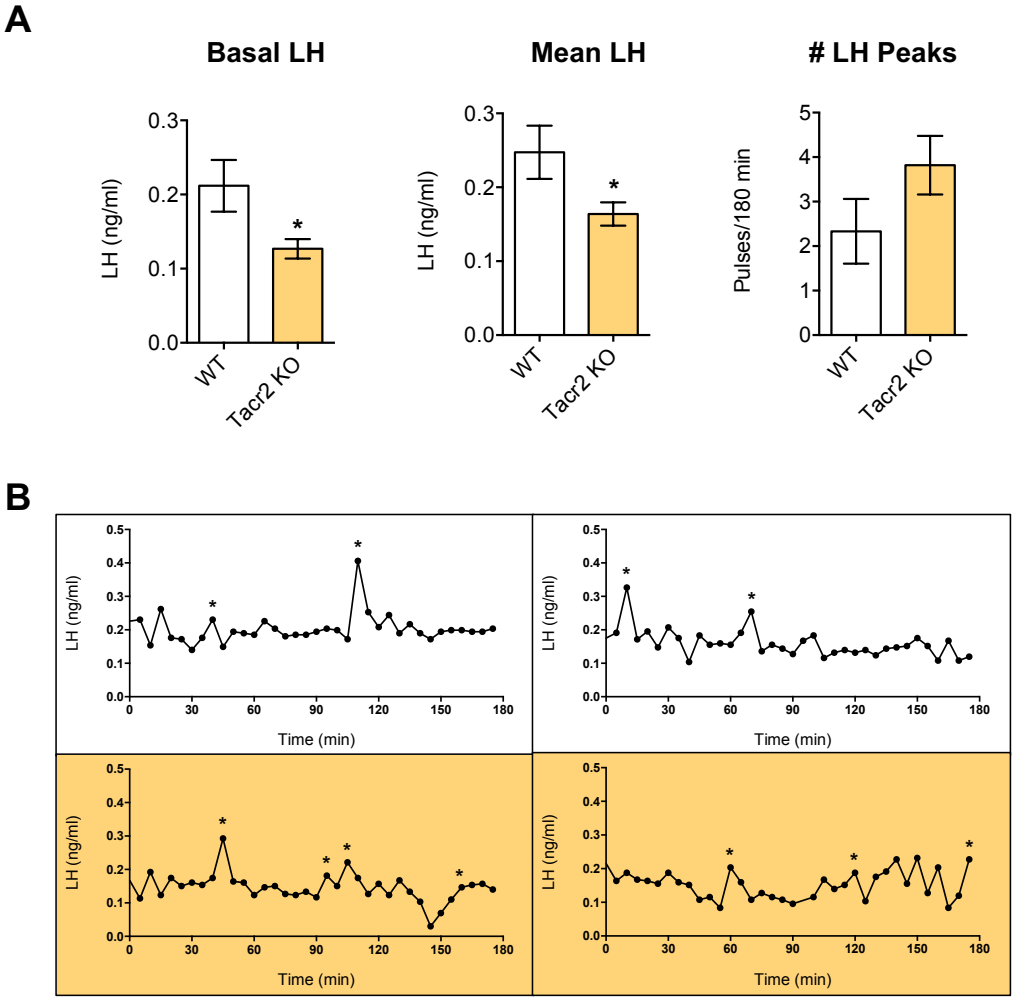

Figure 37. *LH pulsatility in Tacr2 KO mice.* **A**, bar graphs showing basal and mean LH levels, together with the numbers of LH pulses detected over a 3-h sampling period in WT and Tacr2 KO mice, ovariectomized (OVX) and supplemented with estradiol (E_2), are presented (WT n= 8-9; Tacr2 KO n= 9-10). **B**, two individual representative LH secretion profiles of OVX + E_2 WT and Tacr2 KO mice are shown.

Despite these alterations in LH pulsatility, estrous cyclicity was fully preserved in Tacr2 KO female mice, without any differences being observed in terms of total cycle length or stage distribution/frequency (**Figure 38**). Finally, fertility tests were conducted by crossing control or Tacr2 KO mice of either sex with control mice of the opposite sex. A non-significant trend

for increased breeding intervals was detected, especially for Tacr2 KO females, although due to inherent variability, this did not reach statistical significance. In addition, the litter size and pregnancy rate monitored in Tacr2 KO mice were similar to control mice (**Figure 39**).

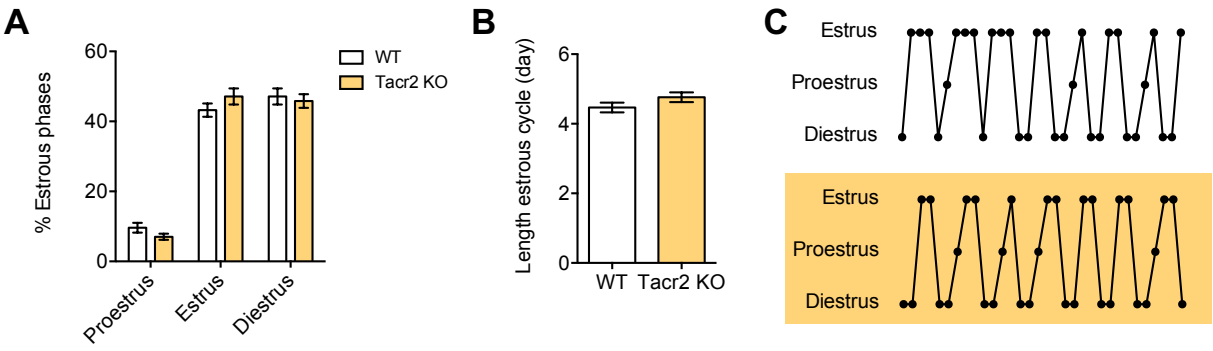

Figure 38. *Estrous cyclicity in Tacr2 KO mice.* **A**, bar graphs showing the percentual distribution of estrous cycle phases in WT and Tacr2 KO female mice are presented (WT n= 12; Tacr2 KO n= 12). **B**, the duration of the estrous cycle is displayed in WT and Tacr2 KO female mice. **C**, representative estrous cycle profiles in WT and Tacr2 KO female mice are shown.

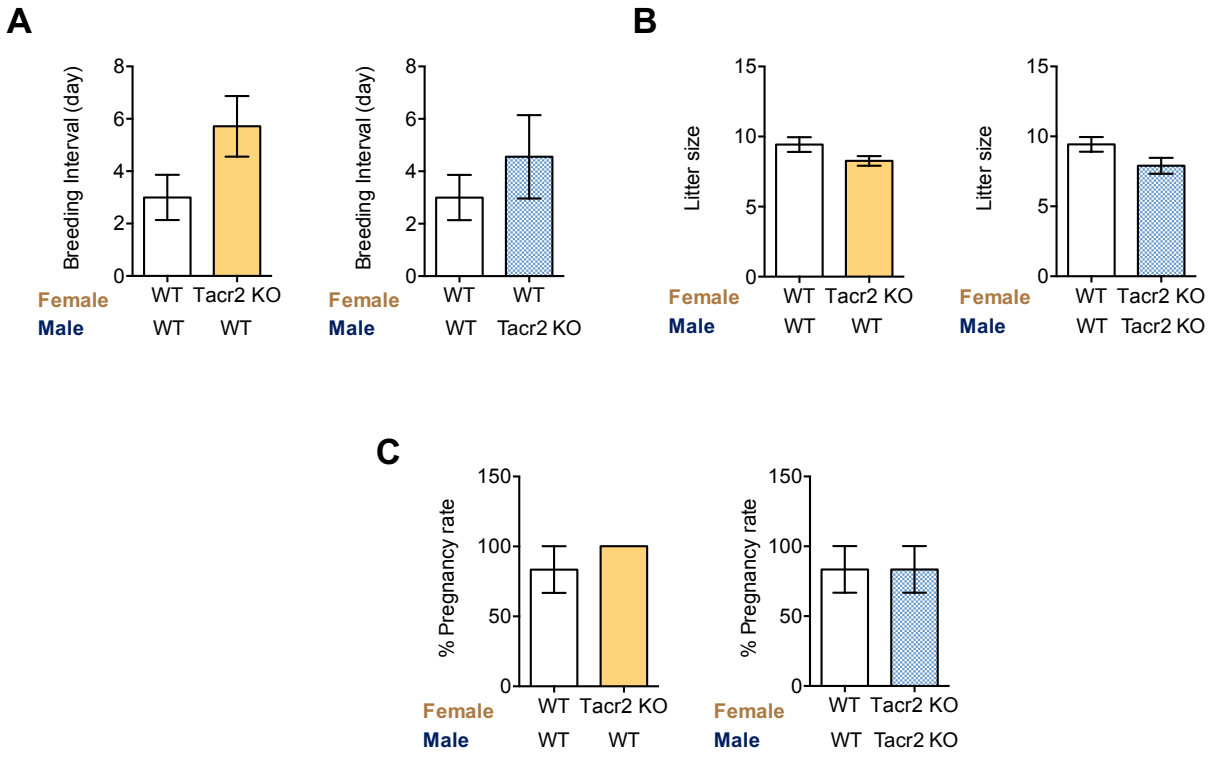

Figure 39. *Fertility parameters in Tacr2 KO mice.* **A**, breeding intervals in WT (white; n= 8) or Tacr2 KO (yellow; n= 14) female mice mated with WT males (left) and breeding intervals of WT female mice mated with WT (white; n= 8) or Tacr2 KO (blue; n= 9) male mice (right) are displayed. **B**, Litter size in WT or Tacr2 KO female mice mated with WT males (left) and WT female mice mated with WT or Tacr2 KO male mice (right). **C**, Pregnancy rate in WT or Tacr2 KO female mice mated with WT males (left) and WT female mice mated with WT or Tacr2 KO male mice (right). Data are presented as mean ± SEM.

In addition, gonadal histological analysis in Tacr2 KO males showed complete spermatogenesis and normal gross testicular histology. However, a closer observation revealed some histological alterations in 60% (3 out of 5) of KO animals examined. In these mice, elongated (i.e. advanced) spermatids were scarce in some tubules (**Figures 40** and **41**), multinucleated (symplastic) spermatids were found in many tubules (**Figures 40**), and atypical (enlarged) residual bodies were frequent (**Figure 42**). These last structures, corresponding to the cytoplasmic remnants of spermatids, are formed at stage VIII after the release of mature spermatids from the seminiferous epithelium and they are found in small numbers in WT animals at the next stages (IX-XI), disappearing thereafter from the epithelium (**Figures 42**) when they are phagocytized by Sertoli cells[248]. However, in the three affected Tacr2 KO mice, residual bodies were larger, more abundant (**Figures 42**), and remained longer in the seminiferous epithelium, as evidenced by their presence even at stages I-V (**Figures 42**). Altogether, these data suggest the existence of a defective function of Sertoli cells, in their interaction with spermatids, giving rise to symplastic giant cells, and in the processing of residual bodies.

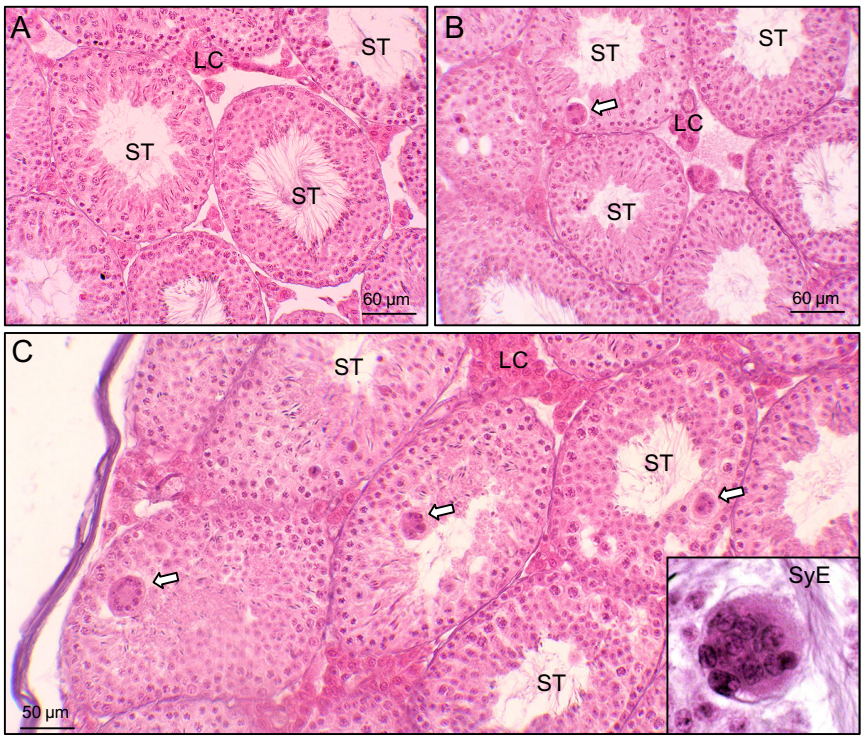

Figure 40. *Histology of the testis of Tacr2 KO mice.* Representative sections from the testis of WT (**A**) and Tacr2 KO (**B, C**) mice, showing grossly normal seminiferous tubules (ST) and interstitial Leydig cells (LC). In some KO testes, giant multinucleated cells (i.e., symplastic spermatids, arrows in **B, C** and SyE in the insert) can be observed.

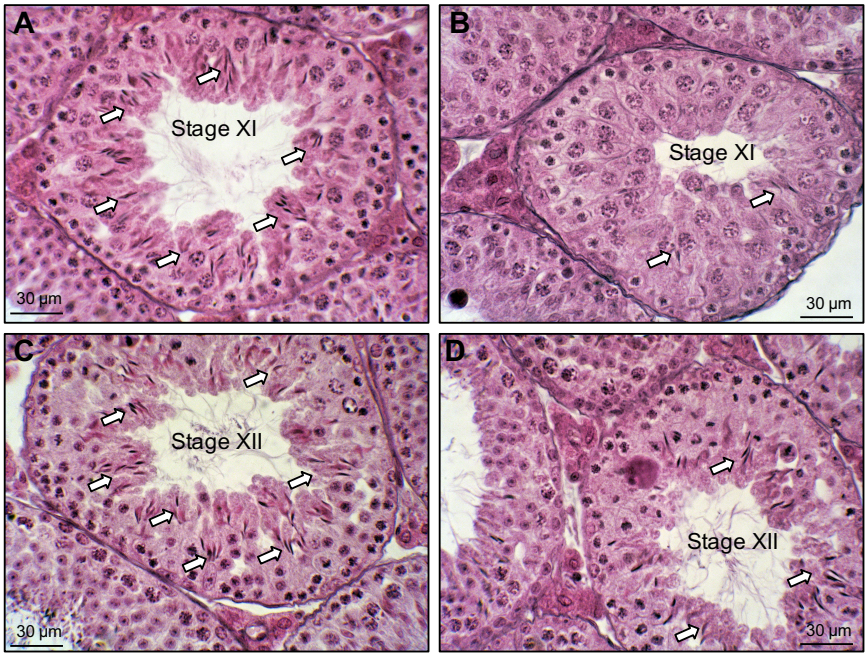

Figure 41. *Histology of the testis of Tacr2 KO mice*. Representative sections from WT (**A, C**) and Tacr2 KO (**B, D**) mouse testes showing the scarcity of advanced (i.e., elongated) spermatids (*arrows*) in some tubules from KO animals.

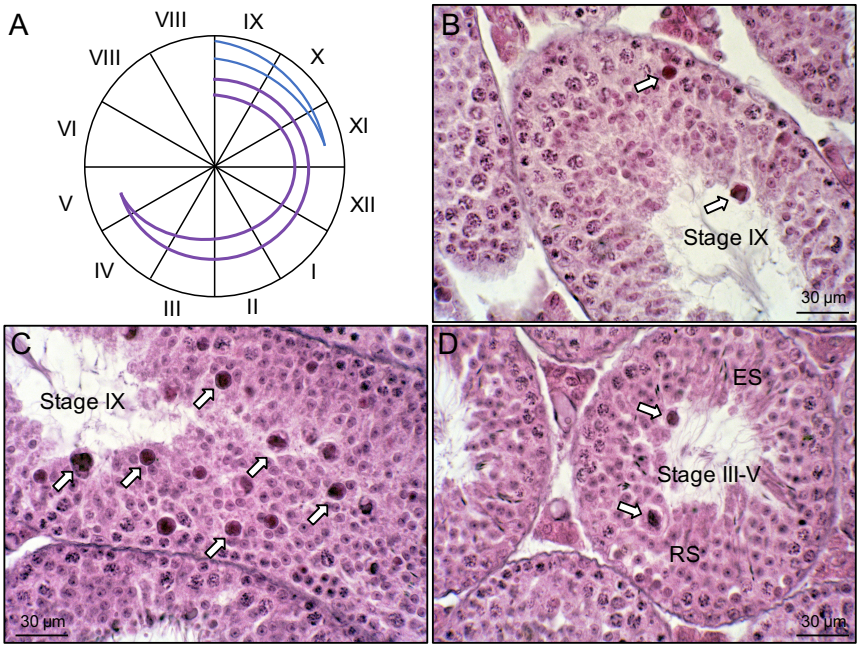

Figure 42. *Residual bodies in the seminiferous epithelium of Tacr2 KO mice*. In **A**, schematic drawing depicting the presence of residual bodies during the cycle of the seminiferous epithelium, after their formation at stage VIII, persisting up to stage XI in WT animals (blue lines), and up to stages IV-V in KO animals (purple lines). Residual bodies (arrows) were scarce in WT animals (**B**) and abundant in KO mice (**C**). In **D**, persistent residual bodies (arrows) can be observed at stages III-V, recognizable by the presence of both round (RS) and elongated (ES) spermatids.

In females, ovarian histological analysis showed normal cycling ovaries and uteri (**Figures 43**). Only one out of five Tacr2 KO mice showed some degree of endometrial hyperplasia with dilated uterine glands, containing inflammatory cells.

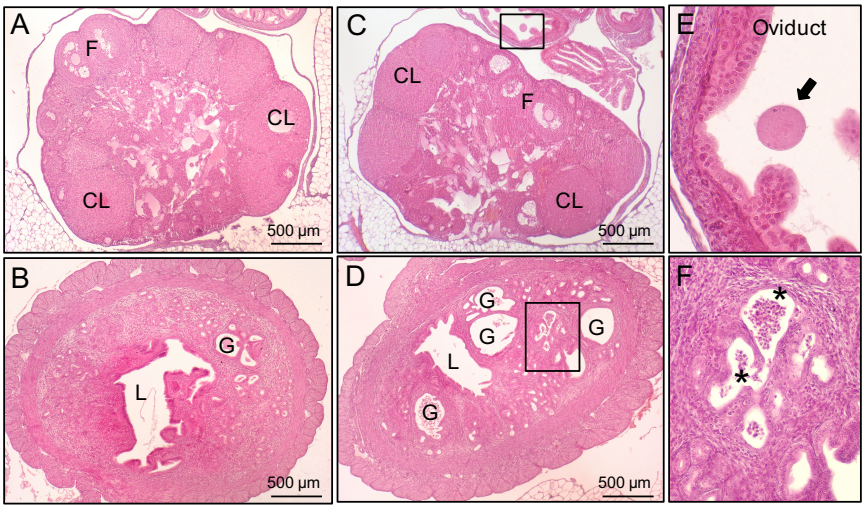

Figure 43. Representative sections from the ovary and uterus of WT (**A**, **B**) and Tacr2 KO (**C**-**F**) mice. Both types of animals showed normal cycling ovaries with abundant follicles (F) and corpora lutea (CL). Only one KO mice that showed normal ovary in metestrus, as evidenced by the presence of oocytes in the oviduct (**C**, **D**), showed early uterine hyperplasia with abundant and dilated endometrial glands (G) and intraglandular inflammatory cells (asterisks in **F**). L, uterine lumen.

In addition, we monitored changes in LH levels in Tacr2 KO mice in response to hormonal or nutritional manipulations, previously reported to modify LH secretion[151,249], such as ovariectomy and short-term fasting. In female control mice, LH concentrations rose shortly after OVX, with a significant elevation being detected already at day 2 after surgery, and massively increased LH concentrations by 7-days after OVX. A similar profile was detected in Tacr2 KO mice; yet, the elevation in LH levels detected at d-2 post-OVX was not statistically significant over the corresponding basal levels, in contrast to that observed in control mice. The body weight gained because of the ovariectomy was similar in Tacr2 KO and control mice (**Figure 44**).

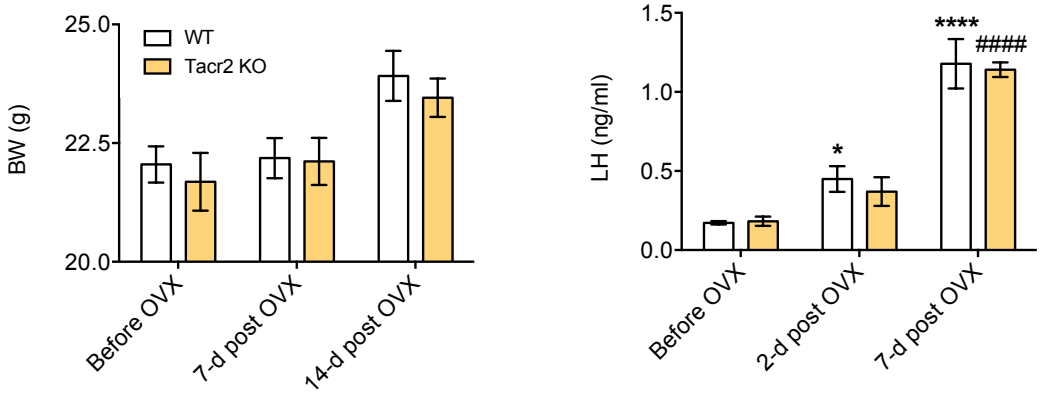

Figure 44. *Short-term LH responses to OVX in Tacr2 KO mice***.** In the left panel, BW changes (at 7- and 14-d post OVX) in WT and Tacr2 KO female mice are shown (WT n= 6; Tacr2 KO n= 7). In the right panel, LH responses to ovariectomy (at 2- and 7-d post OVX) in WT and Tacr2 KO female mice are shown. Data are presented as mean ± SEM. Statistical significance was determined by 2-way ANOVA followed by Bonferroni's post hoc test: $^{*}P<0.05$ and $^{****/####}P<0.0001$ vs. corresponding control values (basal, before OVX).

Additionally, in this same OVX Tacr2 KO mice we recorded the profile of tail skin temperature as a possible mouse model to study the mechanism of hot flushes. As shown in **Figure 45**, OVX WT and Tacr2 KO female mice exhibited a similar profile of skin temperature during 20 hours using the DST Nano-T probe attached to the surface of the tail. The average, minimum and maximum tail skin temperature monitored in OVX Tacr2 KO were comparable to those registered for WT littermate mice (**Figure 46**).

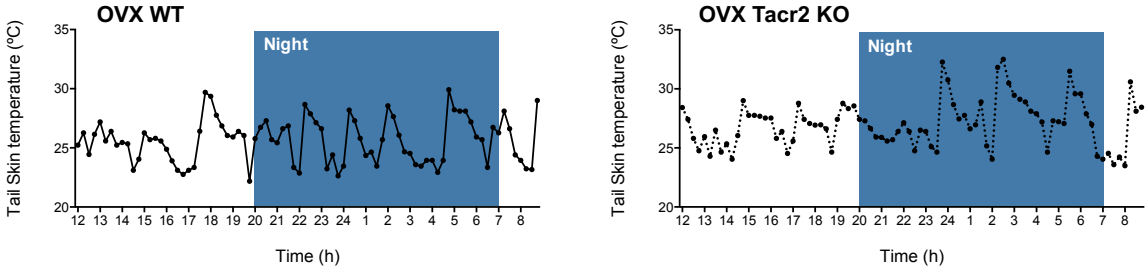

Figure 45. Representative tail skin temperature profiles in OVX WT and Tacr2 KO female mice.

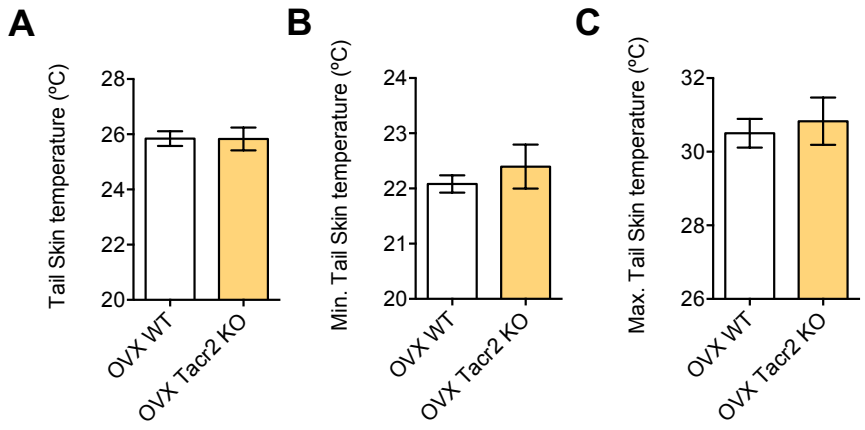

Figure 46. *Tail skin temperature in OVX Tacr2 KO.* **A**, average tail skin temperature during 20 hours of recording in Tacr2 KO (n= 5) and WT (n= 5) female mice. In **B** and **C**, minimum (min.) and maximum (max.) tail skin temperature recorded in Tacr2 KO and WT female mice, respectively. Data are presented as mean ± SEM.

Regarding the impact of nutritional manipulations, 24-h fasting was used to challenge KO mice in order to analyze whether the lack of *Tacr2* modifies the secretion of LH in conditions of energy deficit. In this experiment, LH levels were significantly lower in Tacr2 KO vs. control mice, as evidenced by time-course analyses and integral (AUC) values (**Figure 47**).

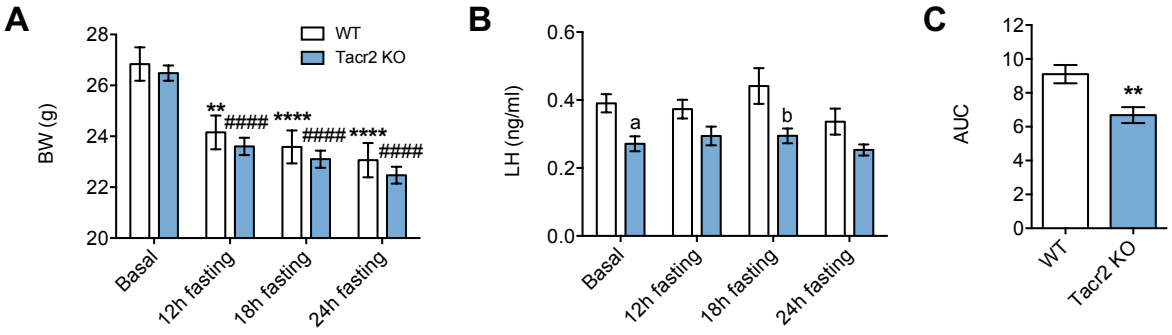

Figure 47. *Short-term LH responses to fasting in Tacr2 KO male mice***.** In **A** and **B**, BW changes and LH levels at timed intervals during a 24-h period after food deprivation are presented from Tacr2 KO male mice and their corresponding WT controls (WT n= 12; Tacr2 KO n= 18); the integral (AUC) secretory mass of LH during the 24-h period of fasting in WT and Tacr2 KO mice is shown in **C**. Data are presented as mean ± SEM. Statistical significance was determined by 2-way ANOVA followed by Bonferroni's post hoc test: $^{**}P<0.001$ vs. corresponding control values (basal) and/or WT values; $^{****/\#\#\#\#}P<0.0001$ vs. corresponding control values (basal): $^{a}P< 0.05$ vs. corresponding WT values at this time; and $^{b}P< 0.01$ vs. corresponding WT values at this time.

Tacr2 KO mice exhibit normal social interaction and sex preference behavior

To address whether NK2R signaling participates in the control of key aspects of sexual behavior, as reported previously for *Tacr1*[191], we applied female urine sniffing and sex preference tests to Tacr2 KO mice, following standard protocols. A three-chamber social sex preference test was applied to adult male and female null mice and their controls. In males, the stereotyped preference for the opposite (female) sex was documented; yet, no differences in any of the behavioral parameters explored, including velocity, distance moved and time spent in the vicinity of the same or opposite-sex mouse, were noted between control and KO mice (**Figure 48**).

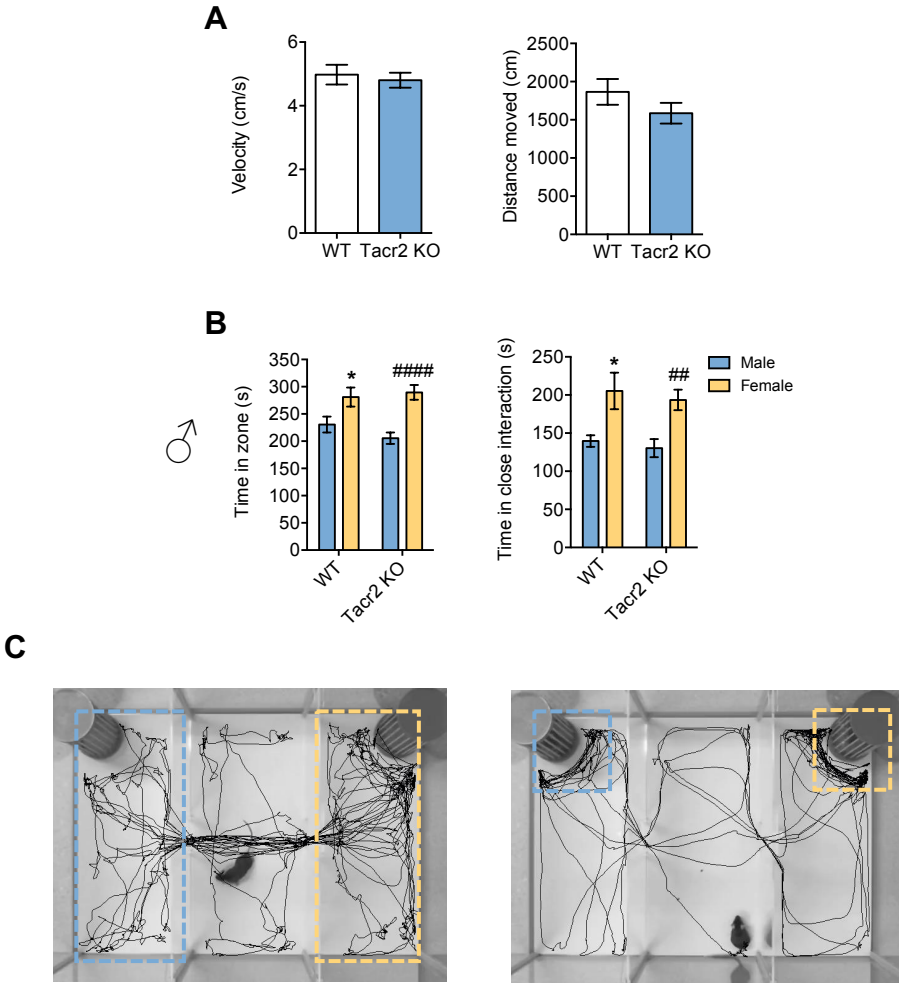

Figure 48. *Analysis of social sex preference behavior in Tacr2 KO male mice*. The three-chamber-social interaction paradigm testing sex preference was applied. **A**, mean velocity and distance covered, respectively, during the habituation for sex preference tests for WT and Tacr2 KO male mice are plotted (WT n= 8; Tacr2 KO n= 15). **B**, data of WT and Tacr2 KO males when tested for their preference of female over male odor are displayed (left); and data of close interaction in similar preference tests (right) are presented. **C**, representative images illustrating the results of sex preference test for Tacr2 KO male mouse are shown. Data are presented as mean ± SEM. Statistical significance was determined by Student t-tests: $^{*}P<0.05$ vs. corresponding male time values for WT; $^{\#\#}P<0.01$ vs. corresponding male time values for Tacr2 KO and $^{\#\#\#\#}P<0.0001$ vs. corresponding male time values for Tacr2 KO mice.

Likewise, no differences in terms of sex preference and social behavior were found between control and Tacr2 KO female mice (**Figure 49**).

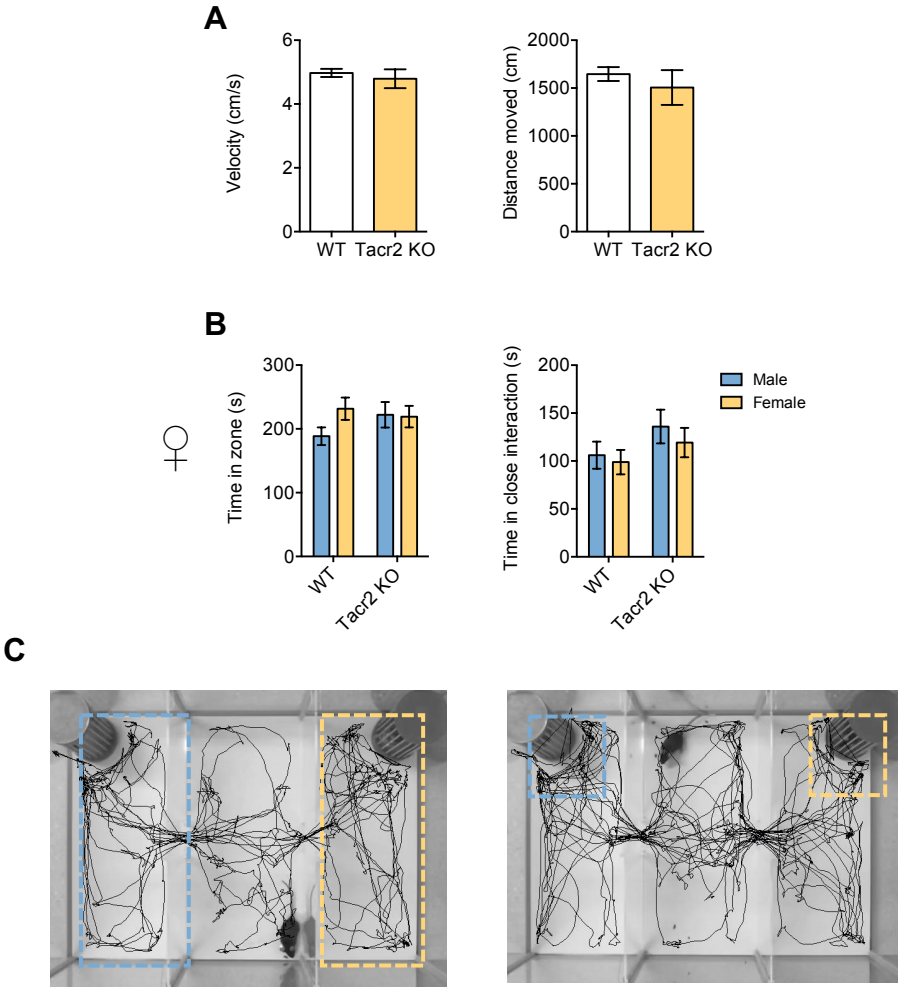

Figure 49. *Analysis of social sex preference behavior in Tacr2 KO female mice*. The three-chamber-social interaction paradigm testing sex preference was applied. **A**, mean velocity and distance covered, respectively, during the habituation for sex preference tests for WT and Tacr2 KO female mice are plotted (WT n= 10; Tacr2 KO n= 12). **B**, data of WT and Tacr2 KO females when tested for their preference of male over female odor are displayed (left); and data of close interaction in similar preference tests (right) are presented. **C**, representative images illustrating the results of sex preference test for Tacr2 KO female mouse are shown.

In the same vein, sniffing tests revealed no defect in Tacr2 KO male mice in terms of preference for female urine odors; if any, better focusing for close interaction with the female vs. neutral odor was observed in Tacr2 KO mice (**Figure 50**).

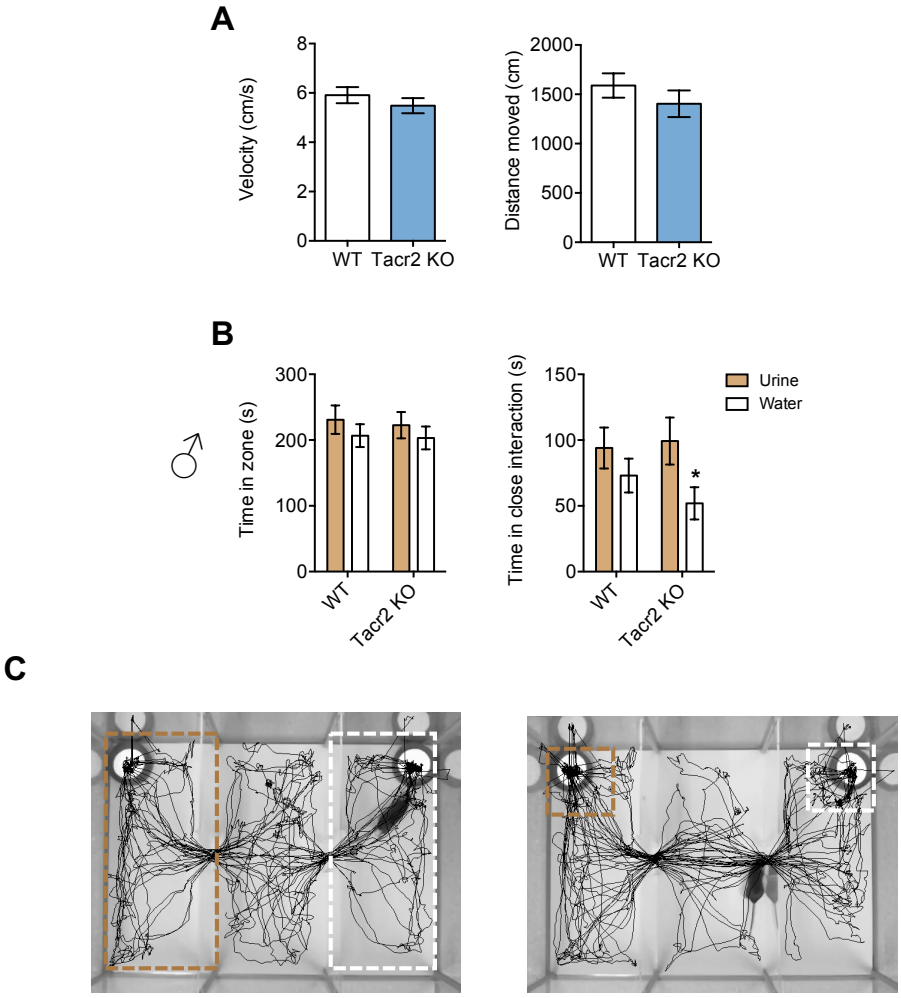

Figure 50. *Female urine sniffing tests (FUST).* The three-chamber-social interaction paradigm testing social odor preference was applied. **A**, mean velocity and distance covered, respectively, during the habituation for sex preference tests for WT (white) and Tacr2 KO (blue) male mice are plotted (WT n= 20; Tacr2 KO n= 17). **B**, data of WT and Tacr2 KO males when tested for their preference of female urine over non-social odor (water) (left); and data of close interaction in similar preference tests (right) are shown. **C**, representative images illustrating the results of female urine sniffing test are shown. Data are presented as mean ± SEM. Statistical significance was determined by Student t-tests: $^{*}P<0.05$ vs. corresponding values in mice exposed to urine.

Metabolic profiles of Tacr2 KO mice in lean and obesogenic conditions

To assess the impact of the lack of NK2R signaling on key metabolic parameters, we first monitored body weight gain in both female and male Tacr2 KO mice, at 2 and 6 months of age, which was similar to that of control littermates. In addition, body composition analyses at 2 months of age confirmed similar fat and lean mass in Tacr2 KO and control mice (**Figure 51**).

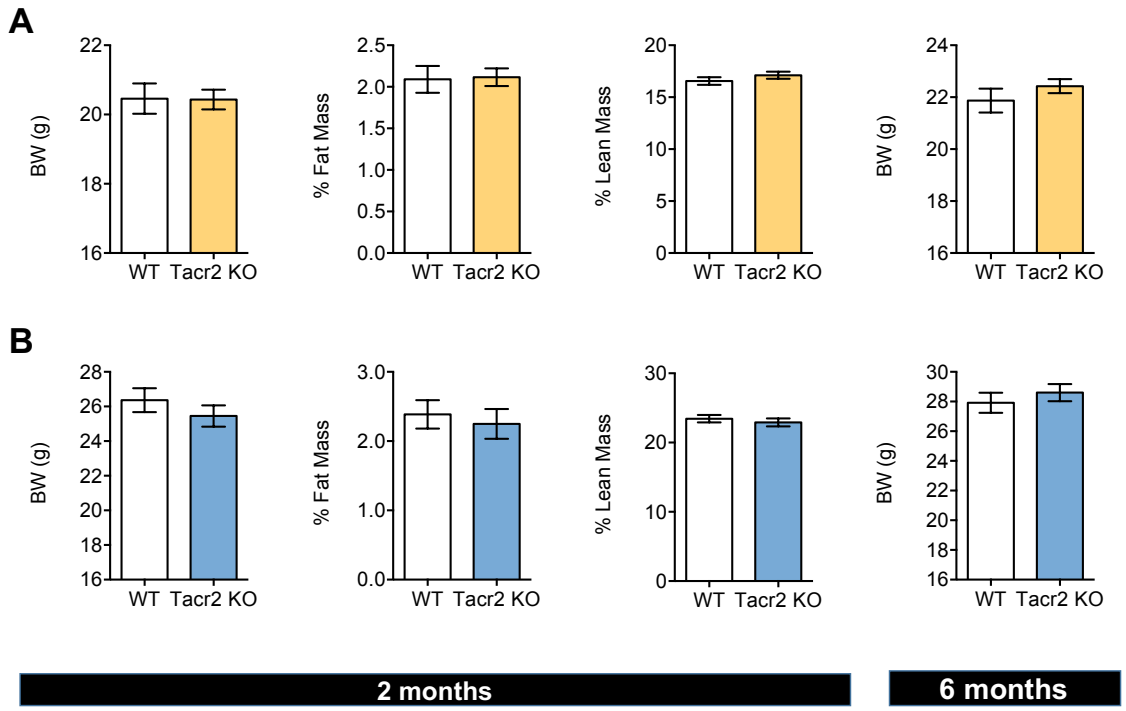

Figure 51. *Basic metabolic characterization of Tacr2 KO female and mice.* Metabolic parameters in WT (white) and Tacr2 KO female (yellow) and male (blue) mice are shown. **A**, body weight (BW) gain at 2 and 6 months of age in WT and Tacr2 KO females fed with standard diet; and body composition analyses and percentages of fat mass and lean mass at 2 months of age are presented from WT and Tacr2 KO female mice. (WT n= 7-12; Tacr2 KO n= 4-12). **B**, body weight (BW) gain at 2 and 6 months of age in WT and Tacr2 KO males fed with standard diet; and body composition analyses and percentages of fat mass and lean mass at 2 months of age are presented from WT and Tacr2 KO male mice. (WT n= 10-12; Tacr2 KO n= 8-12). Data are presented as mean ± SEM.

Alike, energy expenditure (EE) and respiratory quotient (RQ), as well as total and nocturnal locomotor activity, were similar in control and Tacr2 KO mice. No differences in terms of 24-h food intake and day/night feeding patterns were observed in Tacr2 KO mice either (**Figure 52**).

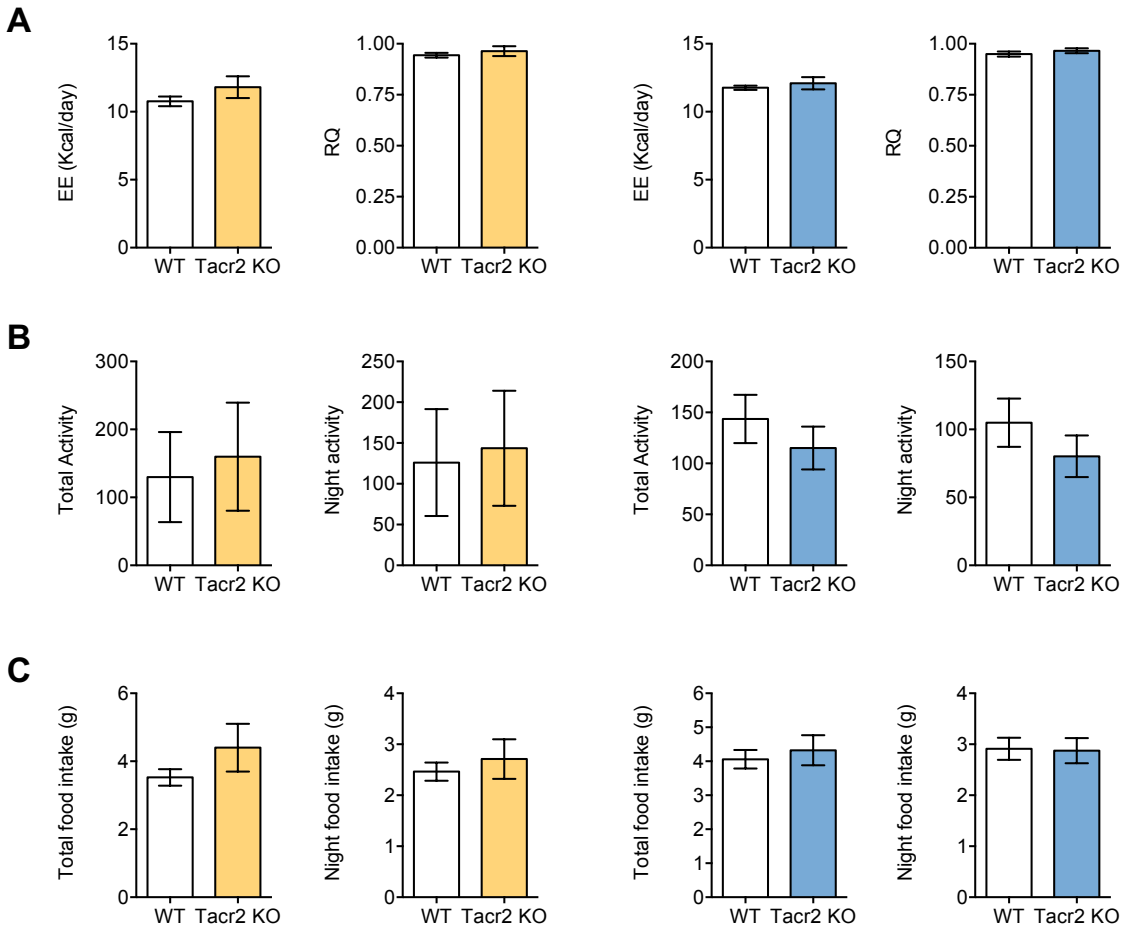

Figure 52. *Basic metabolic characterization of Tacr2 KO mice.* Metabolic parameters and feeding patterns in WT (white) and Tacr2 KO female (yellow) and male (blue) mice are shown. **A**, energy expenditure (EE), measured by indirect calorimetry; and respiratory quotient (RQ), both parameters measured over a 24-h period in WT and Tacr2 KO mice, are shown (Female WT n= 7; Tacr2 KO n= 5; and male WT n= 10; Tacr2 KO n= 8). **B**, total and nocturnal locomotor activity, measured over 24-h period, in WT and Tacr2 KO mice is represented (Female WT n= 4; Tacr2 KO n= 5; and male WT n= 9; Tacr2 KO n= 7). Finally, in **C**, spontaneous feeding patterns, defined by total and nocturnal food intake, monitored over 24-h period, in WT and Tacr2 KO mice are shown (Female WT n= 6; Tacr2 KO n= 4; male WT n= 10; Tacr2 KO n= 8). Data are presented as mean ± SEM.

Finally, measurement of blood pressure by a tail-cuff sphygmomanometer demonstrated that Tacr2 KO mice display values of systolic blood pressure similar to their control littermates (**Figure 53**).

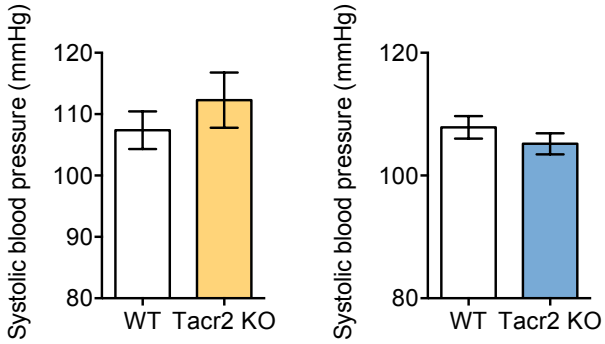

Figure 53. Systolic blood pressure (SBP), measured by a tail-cuff sphygmomanometer, in WT (white) and Tacr2 KO female (yellow) and male (blue) mice is displayed (Female WT n= 5; Tacr2 KO n= 5; male WT n= 10; Tacr2 KO n= 9).

Additional metabolic analyses, addressing glucose homeostasis, were conducted in control and Tacr2 KO male mice, after challenge with an obesogenic diet. Note that due to animal availability, these analyses were conducted only in males. Exposure to HFD for 10 weeks evoked a non-significant reduction of basal LH levels, which was associated to a significant increase in total body weight and basal glucose levels. Notably, whereas the rise of body weight induced by HFD was similar between control and Tacr2 KO mice, the elevation of basal glucose levels was significantly higher in Tacr2 KO males (**Figure 54**).

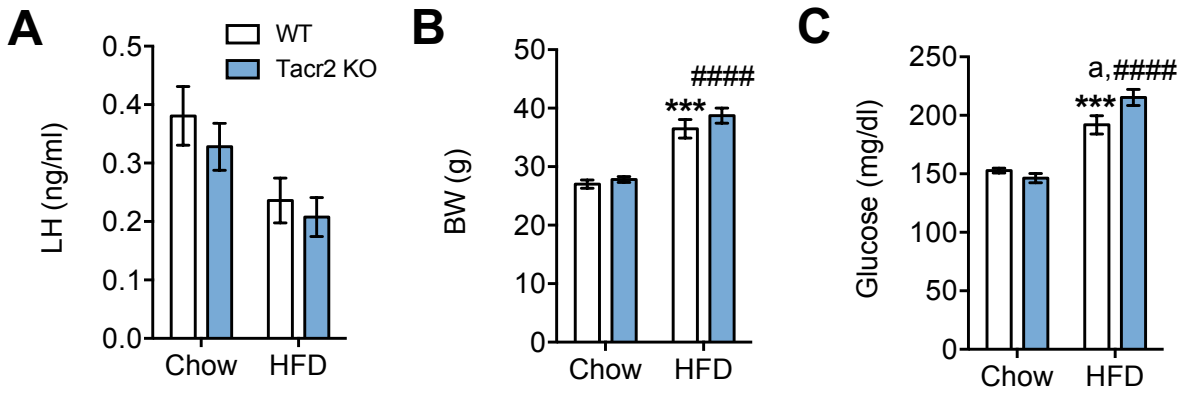

Figure 54. *Analysis of metabolic responses in Tacr2 KO male mice in lean and obesogenic conditions.* **A**, mean LH levels of WT and Tacr2 KO male mice fed with standard, chow diet or HFD (Chow; WT n= 12; Tacr2 KO n= 12; HFD: WT n= 5; Tacr2 KO n= 13). In **B** and **C**, body weight (BW) gain and basal glucose levels are presented from WT and Tacr2 KO mice, fed chow or HFD, at 6 months of age. Data are presented as mean ± SEM. Statistical significance was determined by 2-way ANOVA followed by Bonferroni's post hoc test: $^{***}P<0.001$ vs. corresponding control values; $^{\#\#\#\#}P<0.0001$ vs. corresponding control values and ^{a} $P<0.05$ Tacr2 KO vs. corresponding WT values in HFD.

Likewise, GTT denoted that glucose intolerance was induced by HFD, but this parameter, as assessed by integral AUG glucose values over the 120-min period after the glucose bolus, reached statistical significance only in Tacr2 KO mice (**Figure 55**).

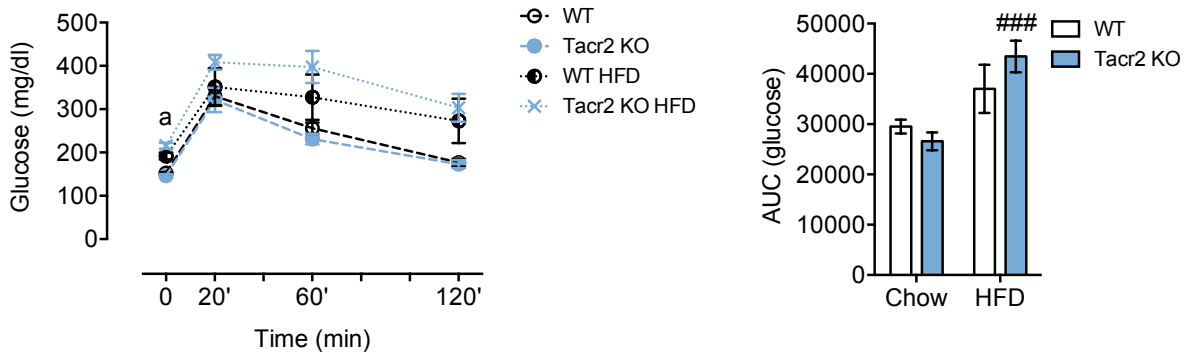

Figure 55. *Analysis of metabolic responses in Tacr2 KO male mice in lean and obesogenic conditions.* We show results from glucose tolerance tests (GTT), represented as 120-min time-course profile after intraperitoneal (ip) injection of a glucose bolus (left panel), and net increment of integral (AUC) glucose levels during GTT (right panel). Data are presented as mean ± SEM. Statistical significance was determined by 2-way ANOVA followed by Bonferroni's post hoc test: $^{###}P<0.001$ vs. corresponding control values; and ^{a} $P<0.05$ Tacr2 KO vs. corresponding WT values in HFD.

In contrast, no major alterations in insulin sensitivity, measured by ITT, were detected in Tacr2 null mice, irrespective of the diet regimen (**Figure 56**).

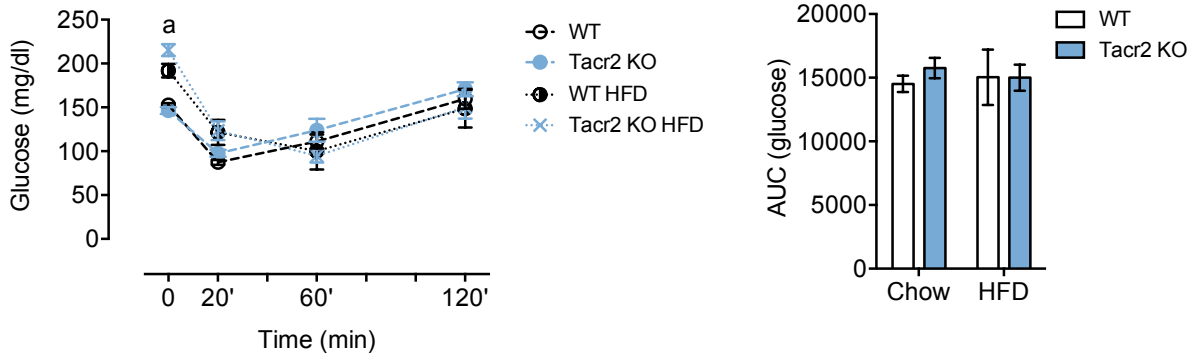

Figure 56. *Analysis of metabolic responses in Tacr2 KO male mice in lean and obesogenic conditions.* Results from insulin tolerance tests (ITT), represented as 120-min time-course profile after ip injection of an insulin bolus (left panel), and net increment of integral (AUC) glucose levels during ITT (right panel) are shown. Data are presented as mean ± SEM. Statistical significance was determined by 2-way ANOVA followed by Bonferroni's post hoc test: ^{a} $P<0.05$ Tacr2 KO vs. corresponding WT values in HFD.

Part II: Exploring novel mediators for the effects of kisspeptins in the hypothalamus by proteomic analyses

Identification of new downstream effectors of kisspeptin actions in the hypothalamus: Proteomic, functional and pathway enrichment analysis

We aimed to explore novel targets mediating kisspeptins actions in the hypothalamic preoptic area (POA) by using a genetically modified mouse line with inactivation of the *Kiss1* gene, termed here Kiss1 KO mice. The rationale for the use of this mouse line is that in this model endogenous levels of kisspeptin are null, hence, making easier to detect changes in the expression of kisspeptin-regulated proteins after exogenous Kp-10 challenge. For the identification of global changes in protein expression patterns after Kp-10 stimulation, we performed a first proteomic analysis based on a two-dimensional difference gel electrophoresis, 2D-DIGE. In this context, Kiss1 KO male mice icv injected with Kp-10 vs vehicle were compared. The image analysis revealed 30 differentially expressed proteins (**Figure 57)** which were identified by mass spectrometry. Ontology analysis applied to this set of differentially-expressed proteins revealed factors involved in cellular metabolism and energy balance, cell signaling, protein folding and synaptic plasticity. Of note, approximately 34% of these differentially expressed proteins were found to be involved in synaptic plasticity. Of note, analysis of the synaptic plasticity category showed that glial fibrillary acidic protein (GFAP) was one of the proteins modified in response to Kp-10, despite the fact that the kisspeptin receptor, Gpr54, had not been previously described to be expressed in GFAP-positive cells.

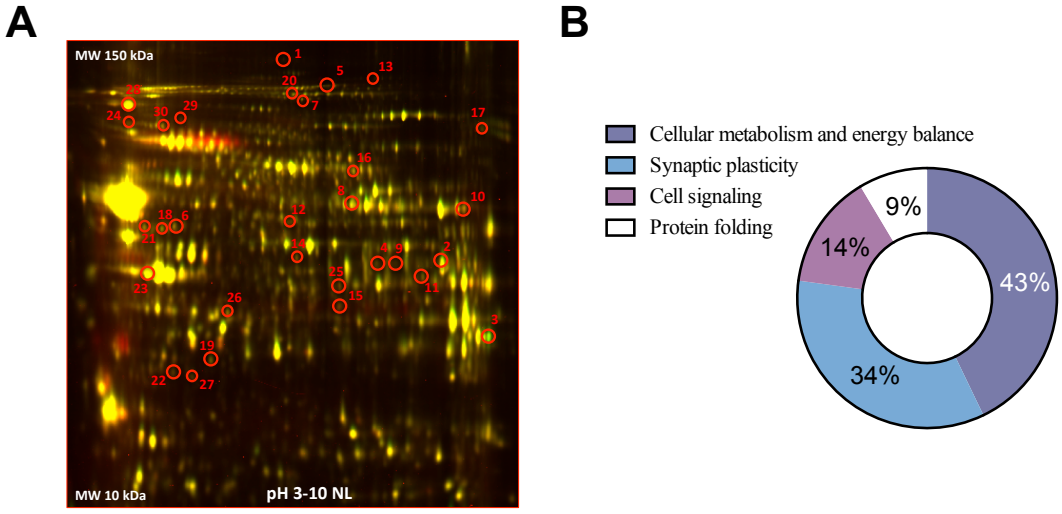

Figure 57. *Proteomic and gene ontology analysis*. **A**, 2D-DIGE map is showed. Encircled spots point differential protein expression in POA from Kiss1 KO mice after Kp-10 injection (n=3) vs. vehicle (n=3). Spots were identified by MALDI-MS/MS. **B**, pie chart presents the gene ontology (GO) of proteins enriched.

To deepen our proteomic analyses and to refine our initial 2D-DIGE approach, we repeated the differential proteomic analysis in Kiss1 KO mice, rising the number of animals per experimental group [Kp-10 injection (n=8) vs. vehicle (n=8)] and using a next-generation technology. For this purpose, we ran a high-performance liquid chromatography (nano-HPLC) associated with a mass spectrometer (triple-TOF) equipped with SWATH acquisition that would provide additional insight into the understanding of how kisspeptin acts in the hypothalamus (POA), and which are its major targets. Interestingly, we found that GFAP was again modified as we previously observed with the 2D-DIGE analysis. The significant proteins obtained were categorized and displayed in protein-protein interaction (PPI) networks, biological processes and cellular components using Cytoscape. The STRING database identified PPI networks of 77 differentially-expressed proteins, visualized in **Figure 58**. The most robust network of associations was observed around ribosomal proteins (RPs), while an independent network was identified around GFAP.

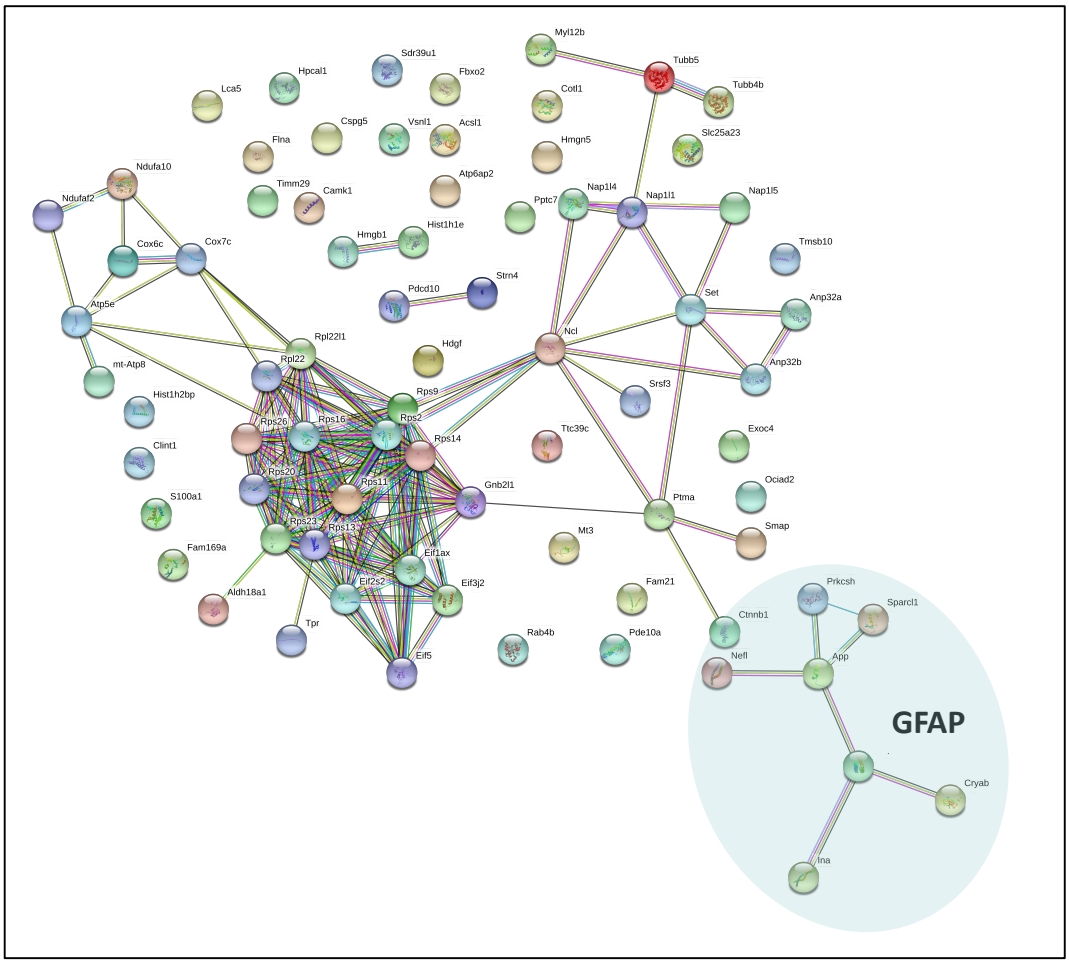

Figure 58. *Visualization of PPI networks using STRING.* The total number of differentially expressed proteins identified was 77. GFAP glial marker and the network around it is highlighted in the right down-side of the figure.

In addition, as indicated in **Table 8**, the GO enrichment analysis, performed to determine the putative functions of PPI networks, showed that, within the cellular components, there was a significant enrichment of regulated proteins belonging to the category of glial cell and astrocyte projections (**Figure 59**).

Table 8. GO pathway enrichment analysis of kisspeptin actions in Kiss1 KO male mice ($p<0.05$).

GOTerm: Cellular Component	Term. P Value	Associated Genes Found
Glial cell projection	3,06E-04	[App, Gfap, Mt3]
Astrocyte projection	5,93E-05	[App, Gfap, Mt3]
Respiratory chain complex	2,52E-03	[Cox7c, Ndufa10, Ndufb1-ps]
Inner mitochondrial membrane protein complex	8,76E-05	[Atp5e, Cox7c, Ndufa10, Ndufb1-ps, Timm29]
Mitochondrial respirasome	2,33E-03	[Cox7c, Ndufa10, Ndufb1-ps]
Ribosome	3,88E-12	[Mt3, Rack1, Rpl22, Rpl22l1, Rps11, Rps13, Rps14, Rps16, Rps2, Rps20, Rps23, Rps26, Rps9]
Cytosolic ribosome	6,70E-13	[Rack1, Rpl22, Rps11, Rps13, Rps14, Rps16, Rps2, Rps20, Rps23, Rps26, Rps9]
Ribosomal subunit	2,22E-10	[Rack1, Rpl22, Rps11, Rps13, Rps14, Rps16, Rps2, Rps20, Rps23, Rps26, Rps9]
Small ribosomal subunit	4,47E-13	[Rack1, Rps11, Rps13, Rps14, Rps16, Rps2, Rps20, Rps23, Rps26, Rps9]
Cytosolic small ribosomal subunit	1,67E-15	[Rack1, Rps11, Rps13, Rps14, Rps16, Rps2, Rps20, Rps23, Rps26, Rps9]
Dendritic shaft	1,18E-04	[App, Ctnnb1, Exoc4, Flna]

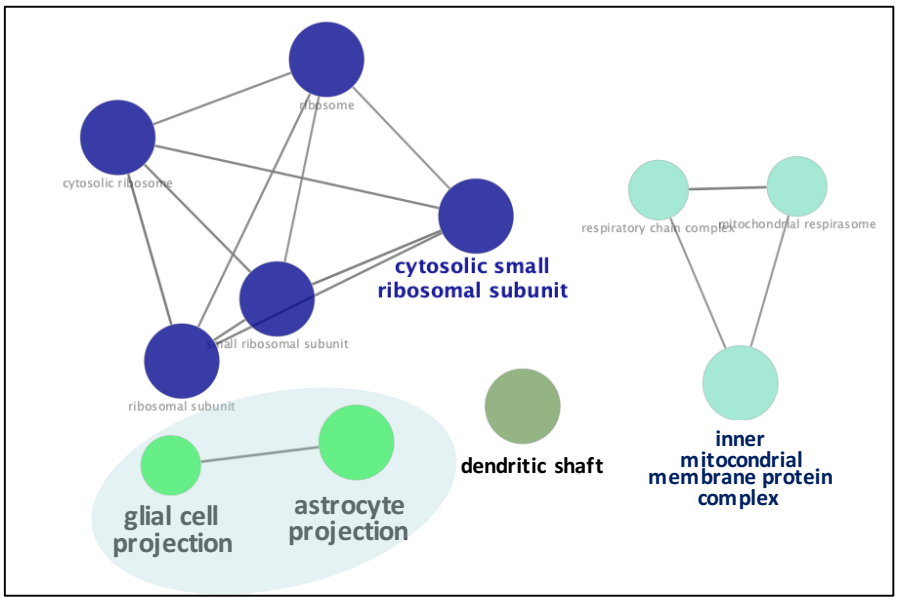

Figure 59. Cytoscape-ClueGO *diagram presenting the cellular components from POA of Kiss1 KO male mice after being icv injected with Kp-10.* Glial cell and astrocyte projections are highlighted in the bottom-left side of the GO representation.

In addition, for molecular function, the gene function classification of GO was mainly related to astrocyte development, positive regulation of neural precursor cell proliferation, structural constituent of the cytoskeleton, oxidative phosphorylation and regulation of oxidative stress-induced neuron death, as shown in **Figure 60**.

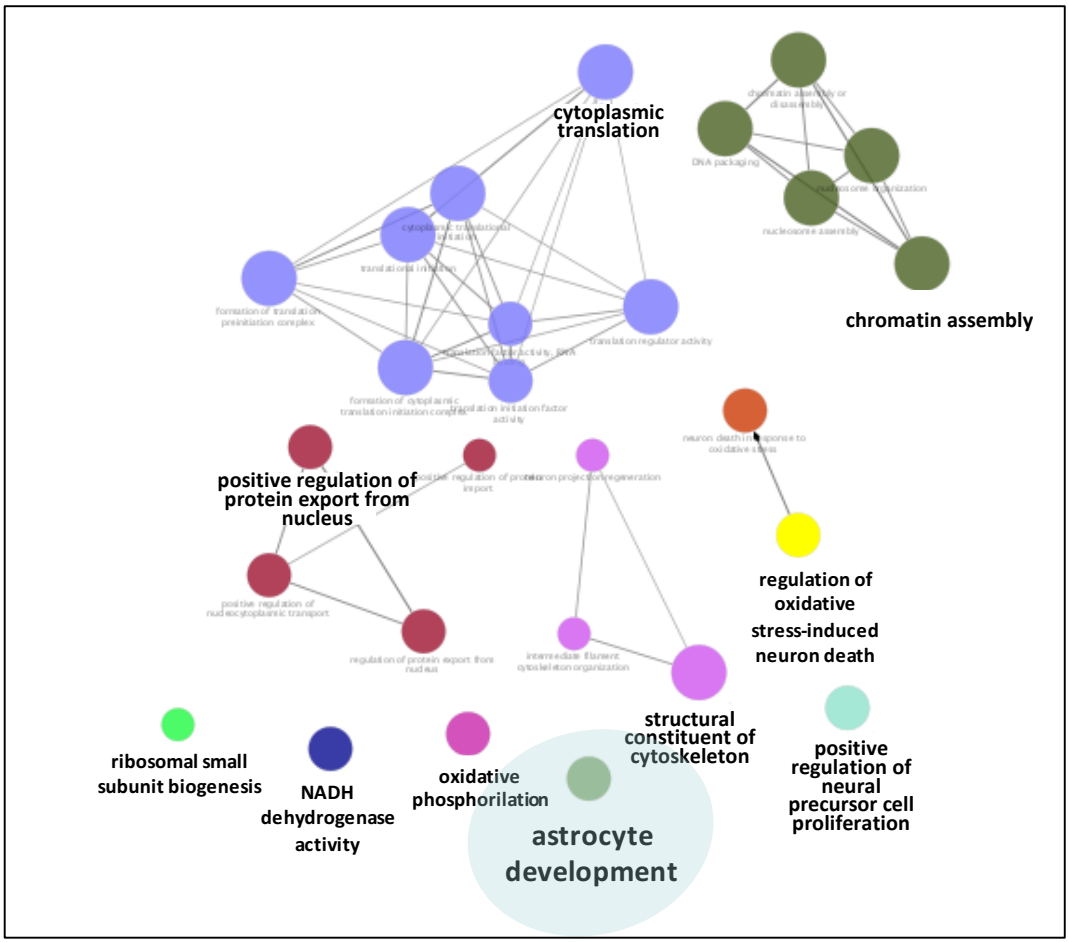

Figure 60. Cytoscape-ClueGO *diagram presenting the biological process from POA of Kiss1 KO male mice after being icv injected with Kp-10.* Astrocyte development is highlighted in the bottom of the GO representation.

From this same proteomic analysis, we extracted the raw SWATH-MS data for independent validation of GFAP, Amyloid Precursor Protein (APP) and Metallothionein 3 (MT3) that were differentially expressed and visualized in the PPI network. The data revealed that, distinctly, Kp-10 modulates GFAP expression, being this glial marker increased in Kiss1 KO male mice treated with Kp-10 vs. vehicle. Besides, the expression of *APP* and *MT3* was also modified by Kp-10 administration, although it was significantly decreased by Kp-10 administration (**Figure 61**).

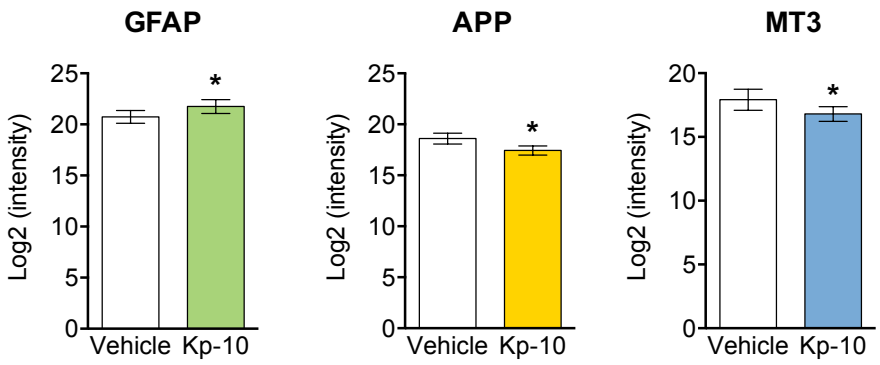

Figure 61. *Independent validation of GFAP, APP and MT3 proteins.* Bar graphs show the intensity of GFAP, APP and MT3 proteins in SWATH-MS proteomics data. Data are presented as mean ± SEM. Statistical significance was determined by Student t-tests: *P<0.05 vs. corresponding values in mice treated with vehicle.

Kisspeptin modulates glial markers expression

We further studied the expression patterns of glial markers, such as GFAP and vimentin, following icv Kp-10 injection in Kiss1 KO mice. The results of RT-qPCR analysis and western blot from POA revealed an increase in both, transcripts and proteins, suggesting a notable effect of Kp-10 over glial cells (**Figure 62**).

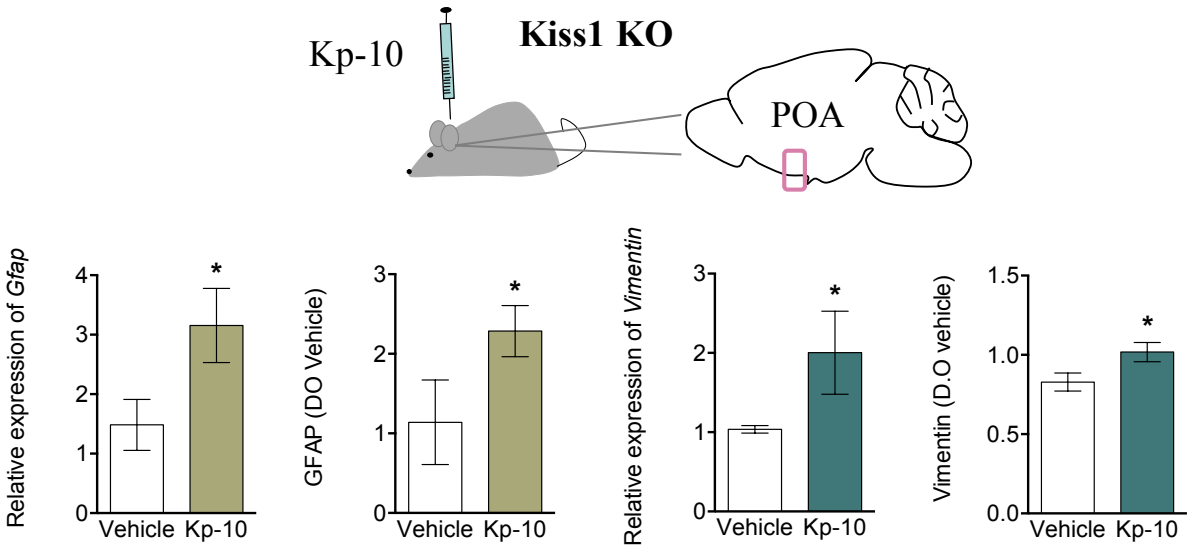

Figure 62. *Analysis of glial markers expression (mRNA and protein) from POA of Kiss1 KO male mice after Kp-10 stimulation.* Kiss1 KO mice after Kp-10 injection (n=3-4) vs. vehicle (n=3). Data are presented as mean ± SEM. Statistical significance was determined by Student t-test: *P<0.05 vs. corresponding values in mice treated with vehicle.

Supporting the above analysis, which showed changes in the expression of glial cell markers in the hypothalamus after Kp-10 stimulation, we carried out RT-qPCR analyses for detecting

Gpr54 expression in rodent astrocytes. The expression of *Gpr54* transcripts in primary cultures of astrocytes isolated from brains of neonatal rats and mice are shown in **Figure 63** and unambiguously demonstrate for the first time the expression of the gene encoding the kisspeptin receptor in astrocytes. In clear contrast, *Kiss1*, i.e., the gene encoding the ligand, is not expressed in cultured astrocytes from rats or mice.

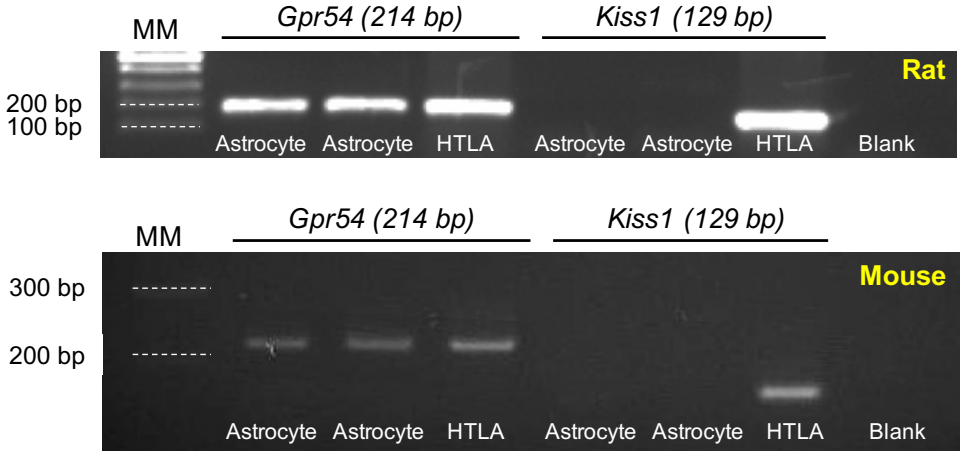

Figure 63. *Representative gels illustrating the expression of Gpr54, but not Kiss1 in primary astrocyte cultures from rodent hypothalamus.* The upper gel shows the expression of *Gpr54* in two different pools of hypothalamic astrocytes from neonatal rats. The lower gel shows the expression of *Gpr54* in two different pools of hypothalamic astrocyte from neonatal mice. Note that no amplicon was detected for *Kiss1*. Hypothalamic (HTLA) tissue was used as positive control for *Gpr54* and *Kiss1* expressions. MM, molecular markers. Blank, negative control. Expected sizes for the RT-qPCR products are 214 bp for *Gpr54* and 129 bp for *Kiss1*.

Functional studies in primary astrocyte cultures exposure to Kp-10

Based on the above findings, we generated primary astrocyte cultures from neonatal rats and mice to evaluate the downstream signaling pathways activated by kisspeptin. As shown in **Figure 64**, 10 min of Kp-10 treatment was able to induce the phosphorylation of ERK/MAP kinase, as a key element of the canonical kisspeptin signaling pathway[143], in primary rat hypothalamic astrocyte culture, whereas there were not significant differences, in the phosphorylation of Akt, albeit a trend was observed. Additionally, in primary astrocyte cultures from neonatal mice, Kp-10 treatment was also able to stimulate the phosphorylation of ERK/MAP kinase in hypothalamic astrocytes, but not in cortical astrocytes. Moreover, Kp-10 did not stimulate the phosphorylation of Akt in hypothalamic or cortical astrocytes (**Figure 65**).

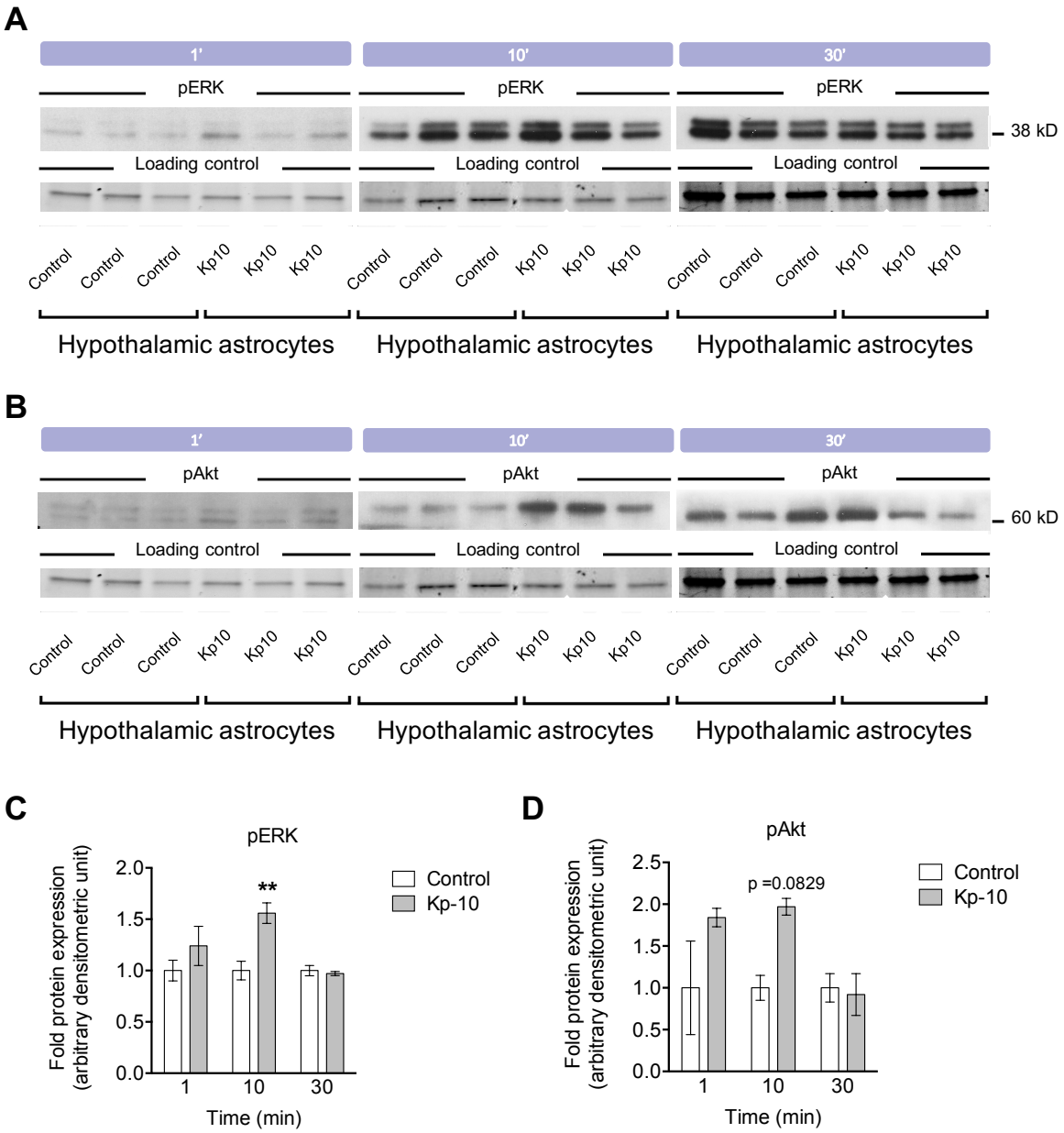

Figure 64. *Western blot analysis of phosphorylated ERK (pERK) and Akt (pAkt) in primary rat hypothalamic astrocytes*. **A**, blots illustrating the effect of Kp-10 treatment (10^{-8} M) at 1, 10 and 30 min on ERK phosphorylation. **B**, blots illustrating the effect of Kp-10 treatment at 1, 10 and 30 min on Akt phosphorylation. In **C** and **D**, bar graphs show the quantification of the effect of Kp-10 over pERK and pAkt. Astrocyte cultures treated with vehicle were used as a negative control. Values from Kp-10 were expressed relative to control values (loading control). Data are presented as mean ± SEM. Statistical significance was determined by 2-way ANOVA followed by Bonferroni's post hoc test: $^{**}P<0.01$ corresponding values in astrocytes treated with vehicle.

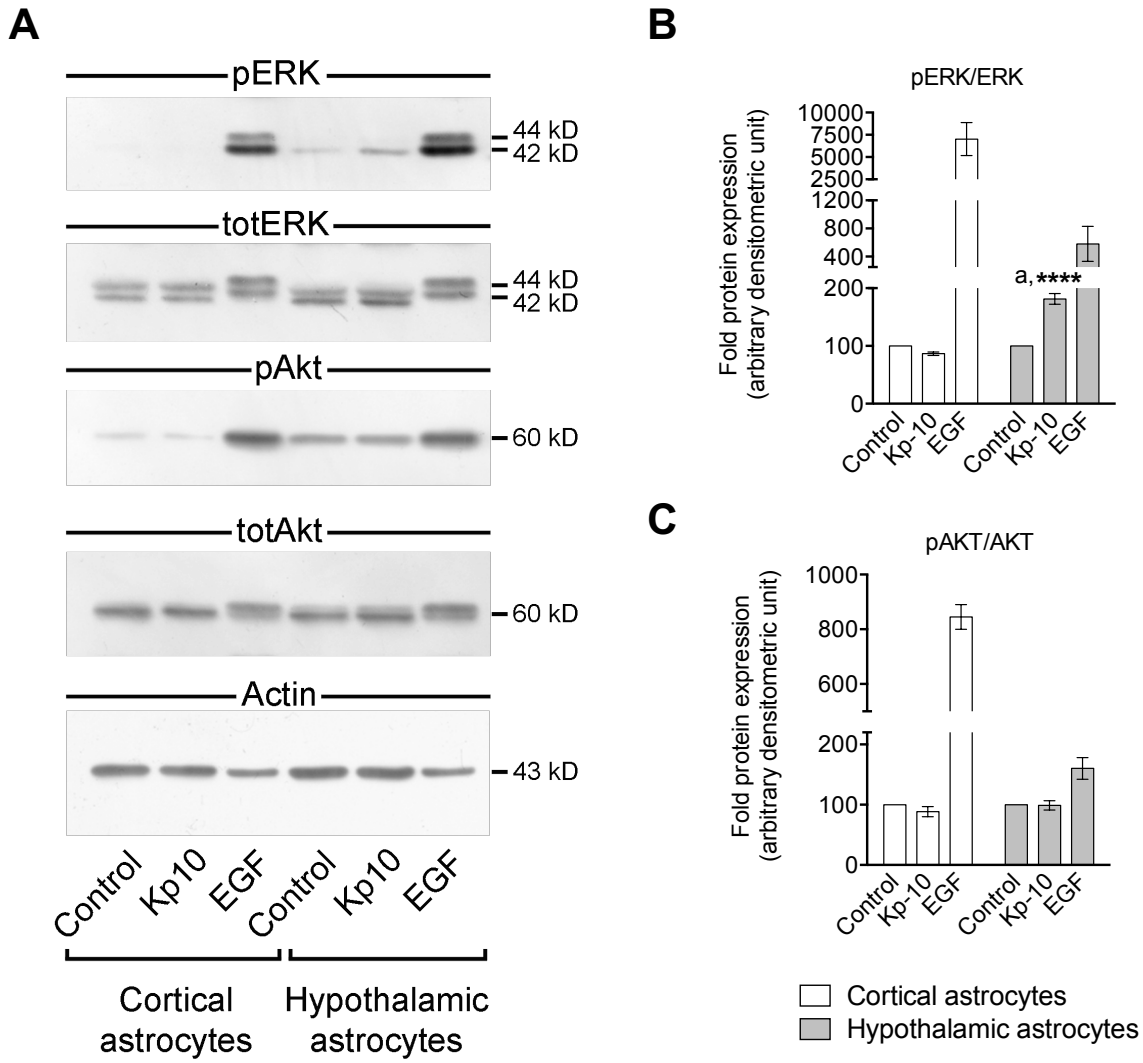

Figure 65. *Western blot analysis of pERK, total ERK (totERK), pAkt, total Akt (totAkt) and actin in primary mouse cerebrocortical and hypothalamic astrocytes treated with Kp-10 (10^{-8} M) or Epidermal Growth Factor (EGF, 50 ng/ml) used as a positive control.* **A**, gel illustrating the effect of Kp-10 or EGF at 10 min on pERK, total ERK (totERK), pAkt and total Akt (totAkt). In **B** and **C**, bar graphs show the effect of Kp-10 over the ratio pERK/totERK and pAkt/Akt, respectively. Astrocyte treated with vehicle were used as a negative control. Values from Kp-10 and EGF were expressed relative to control values (actin). Data are presented as mean ± SEM. Statistical significance was determined by 2-way ANOVA followed by Bonferroni's post hoc test: ****P<0.0001 corresponding values in astrocytes treated with Kp-10 vs. vehicle and ^{a} P<0.0001 corresponding values in hypothalamic astrocytes vs. cortical astrocytes.

Kisspeptin receptor, Gpr54, is co-expressed with GFAP in mouse brain

Considering our *in vitro* data, we sought to determine whether co-localization of GFAP and *Gpr54* expression is detected *in vivo*. To this end, we have implemented, in collaboration with the teams of Dr. Ariane Shariff and Prof. Vincent Prevot, in the University of Lille, France, double labelling analyses using RNAScope *in situ* hybridization (to detect *Gpr54* mRNA) and

immunohistochemistry (to detect GFAP-positive cells). As shown in **Figure 66**, our data conclusively demonstrate the co-expression of *Gpr54* in GFAP-positive cells in mouse brain tissue sections from C57BL/6 female mice (sampled at diestrus). In this same experiment, as positive control, the co-expression of *GnRH* and *Gpr54* transcripts already reported was also demonstrated, as shown in **Figure 66**.

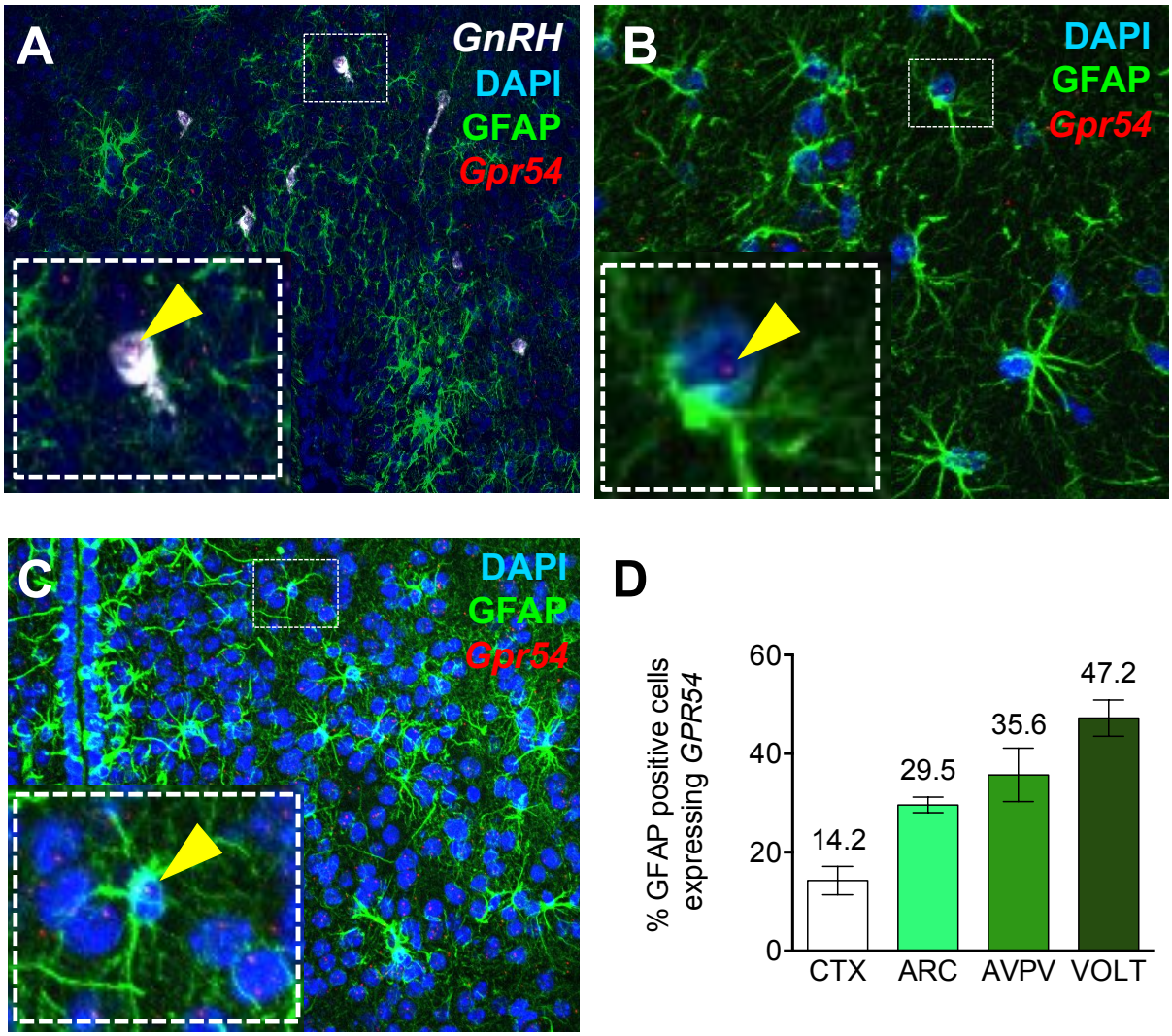

Figure 66. Dual *RNAScope ISH combined with immunohistochemistry in mouse brain tissue sections.* **A**, images illustrating the detection of GFAP protein, and *GnRH* and *Gpr54* mRNAs, in the vascular organ of lamina terminalis (VOLT), in addition to the co-expression of *GnRH* and *Gpr54* mRNAs (used as positive control). **B**, dual positive staining for GFAP-fibers and *Gpr54* mRNA in cortex; and in **C**, dual positive staining for GFAP-fibers and *Gpr54* mRNA in AVPV. **D,** chart showing the qualitative analysis of percentage of GFAP-fiber co-localizing with *Gpr54* mRNA**.** Control was totally clean. Objective 20X. Data are presented as mean ± SEM.

Qualitative analysis of the RNAScope ISH combined with immunohistochemistry allowed the examination of *Gpr54*-GFAP positive cells around key hypothalamic areas involved in the central control of the reproductive axis, such as VOLT, AVPV and ARC; in addition, the cortex was used as putative control. As displayed in **Figure 66**, there was an enrichment in the % of co-location of *Gpr54* and GFAP in VOLT and AVPV, both hypothalamic areas in which GnRH and Kiss1 neurons population are identified. To a lesser extent, this co-location was also found in ARC, where the terminals of GnRH neurons are projecting into the median eminence and the other prominent Kiss1 neuronal population is found. Finally, in the cortex, even though there was detectable co-location between *Gpr54* expression and GFAP, the percentage of GFAP-positive cells expressing *Gpr54* was lower than in the other areas of interest.

The glial marker GFAP, but not S100β, is altered in response to Gpr54 signaling alterations

Our previous data documented the expression of *Gpr54* in rodent astrocytes and its co-localization in GFAP-positive cells *in vivo*. Hence, to further explore the functional role of Gpr54 signaling in astrocytes, we used two models of congenital ablation of Gpr54, named herein Gpr54 KO and Gpr54 KI mouse lines, to explore changes in astrocyte markers. The models used were Gpr54 KO, with global congenital ablation of Gpr54 and hence central hypogonadism, and Gpr54 KI, which has the same background as Gpr54 KO but due to the selective re-introduction of Gpr54 expression only in GnRH neurons, does not display hypogonadotropic hypogonadism. We analyzed changes in GFAP labelling by immunofluorescence in the hypothalamus of these two lines.

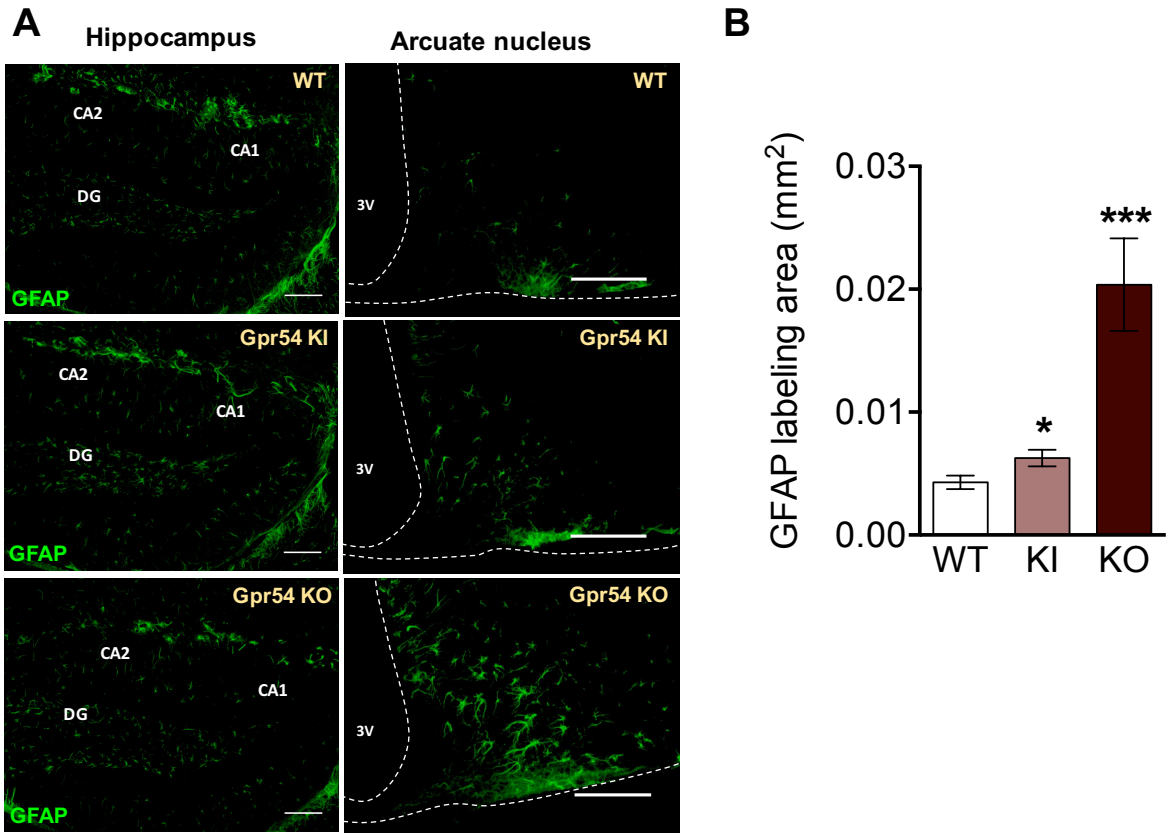

Figure 67. *Disrupting Gpr54 signaling increases GFAP in Gpr54 KI and Gpr54 KO mice.* **A**, representative fluorescent images showing GFAP-labelled astrocytes in arcuate nucleus sections of WT, Gpr54 KI (KI) and Gpr54 KO (KO) mice. Hippocampus images are shown as control area without being altered by Gpr54 signaling perturbations. Scale bar = 100 µm. **B**, bar graph shows the astrocyte reactivity quantified and referred as values of fluorescent intensity using ImageJ. Data are presented as mean ± SEM. Statistical significance was determined by Student t-tests: $^{*}P<0.05$ vs. corresponding values in wild-type mice.

These studies documented clear differences in terms of changes in GFAP immunoreactivity when Gpr54 is absent (**Figure 67**). Thus, global elimination of Gpr54 induced a marked increase in GFAP labelling in the ARC, but not in the hippocampus. A significant elevation in GFAP immunoreactivity was also observed in the ARC of Gpr54 KI mice, albeit the magnitude of this increase was substantially lower than that of Gpr54 KO.

In contrast, another astrocytic marker protein, S100 calcium binding protein B (S100β), analyzed by DAB immunohistochemistry, displayed no significant alterations in either Gpr54 KO or KI models (**Figure 68**).

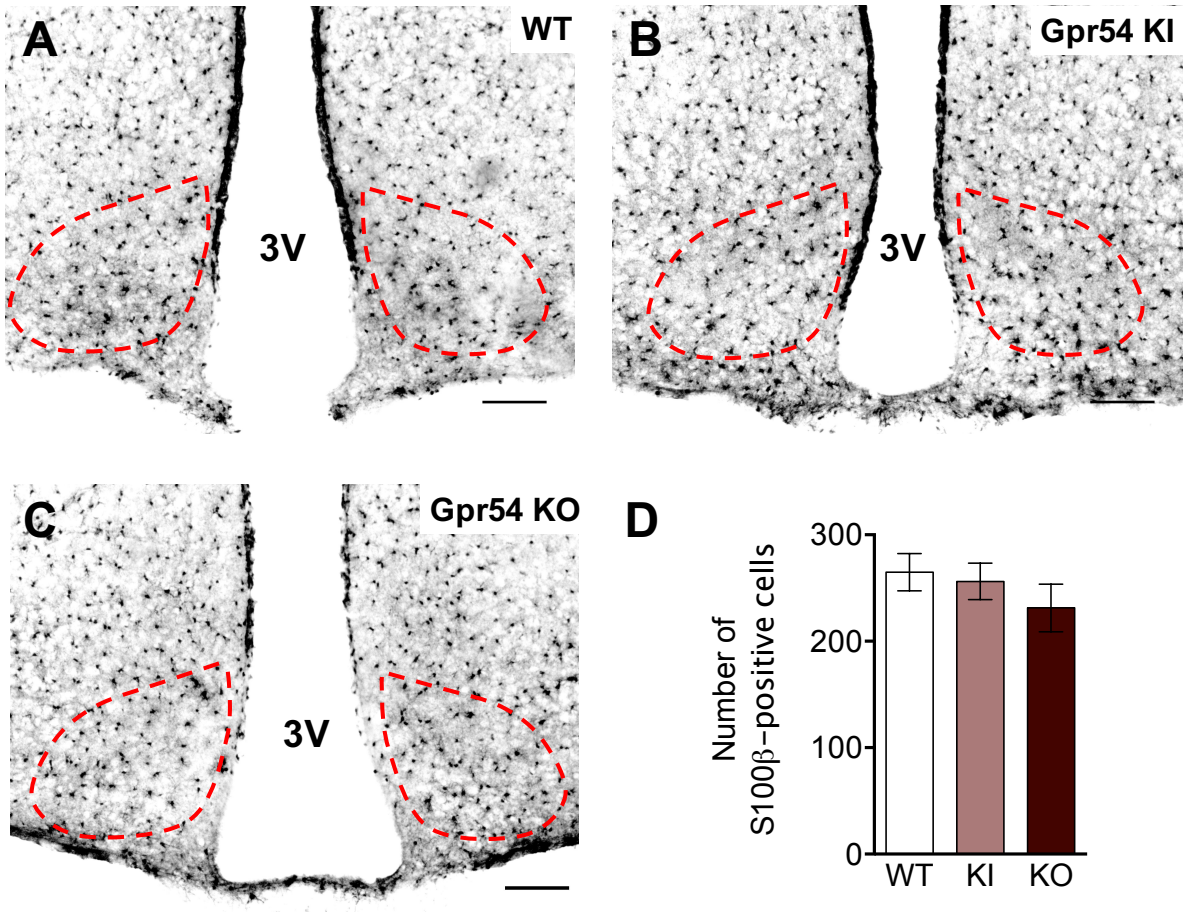

Figure 68. DAB *immunohistochemistry analysis of S100β.* In **A-C**, representative images show S100β-labelled astrocytes in arcuate nucleus sections (indicated as red line) of WT, Gpr54 KI (KI) and Gpr54 KO (KO) mice, respectively. Scale bar = 100 µm. **D**, bar graph shows the number of S100β-positive cells in ARC. Data are presented as mean ± SEM.

Part III: Assessing the physiological roles of kisspeptin signaling in astrocytes: Characterization of a novel mouse line with selective ablation of *Gpr54* in GFAP-positive cells.

To further evaluate the role of kisspeptin signaling in astrocytes, we have generated a new mouse line with a selective deletion of kisspeptin receptor, *Gpr54*, in astrocytes (GFAP-positive cells); this new line is named herein as G-KiRKO (for **G**FAP-specific **Ki**ss1 **R**eceptor **KO**).

Validation of the G-KiRKO mouse model

Since we documented the expression of *Gpr54* in astrocytes, we generated G-KiRKO mice, using the Cre-loxP technology, for addressing the role of Gpr54 in those cells *in vivo*. These mice were the result of crossing a mouse line expressing the Cre recombinase under the control of the promoter of *GFAP* with a Gpr54 floxed mouse line, as described in the Methods section. To validate G-KiRKO line, we implemented PCR assays for detecting the recombinant event that would denote Cre recombinase activity. The screening assay shown in **Figure 69**, demonstrate the presence of recombinant events in the brain of G-KiRKO mice, predominantly in POA and to lesser extent in MBH. We also detected recombinant events in the testes and, weakly, in other tissues (e.g., BAT), albeit qRT-PCR assays pointed out that *Gpr54* expression was not compromised in those same tissues (**Figure 69**).

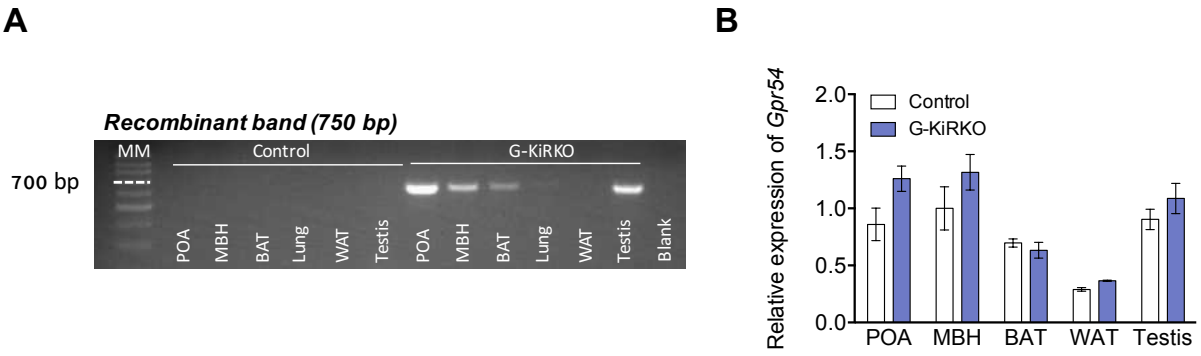

Figure 69. *Screening of G-KiRKO mouse model*. (**A**) PCR products for detecting genomic recombinant events produced by Cre activity (750 bp band). (**B**) The profile of *Gpr54* expression in different tissues of G-KiRKO mice, as assessed by quantitative RT-qPCR, are shown (Control n= 3; G-KiRKO n= 3). Data are presented as mean ± SEM.

Further, we evaluated the Cre recombinase activity in astrocytes *in vivo*, as another way to complete the validation of our model. To do that, we used a reporter mouse line, named YFP-GFAP Cre line, generated by crossing the GFAP-Cre line, namely, the same one that we

previously used for the generation of G-KiRKO model, with a line in which *YFP* (yellow fluorescent protein) gene, blocked by a *loxP*-flanked STOP sequence, is expressed upon Cre activity. As shown in **Figure 70**, using this reported mouse line, we co-localized S100β, the astrocyte marked chosen because its cytosolic location, with YFP signal.

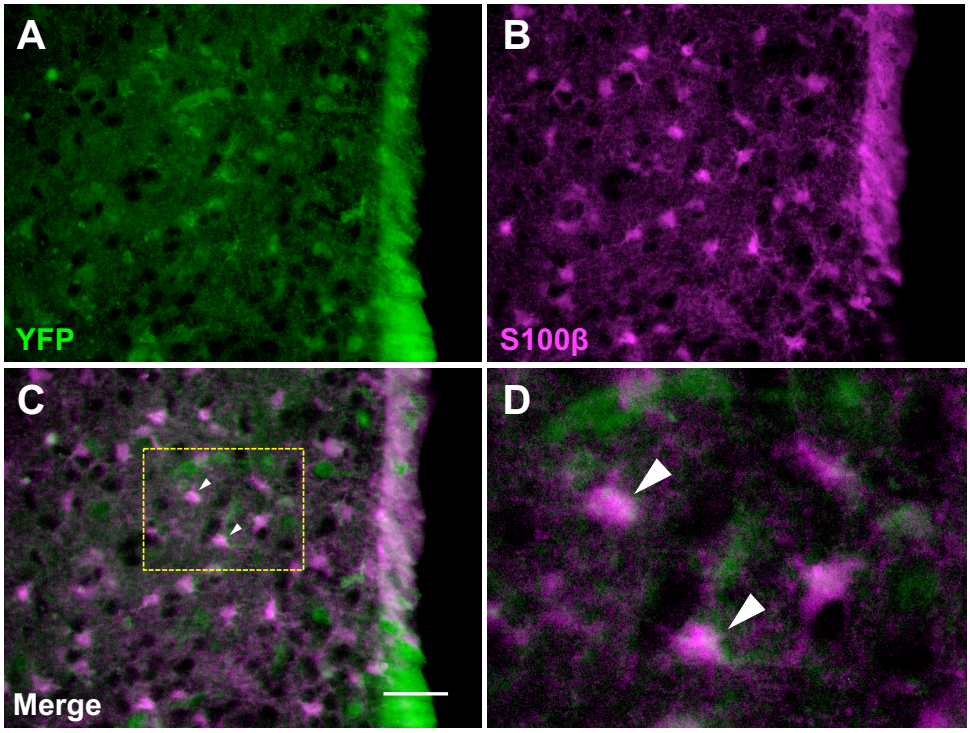

Figure 70. *Double immunofluorescence of YFP-GFAP Cre reporter mouse model*. In **A-B**, representative images show YFP- (green) and S100β-labelled (magenta) cells in arcuate nucleus sections, respectively. In **C**, the merge image of **A** and **B** that point the co-location between YFP- and S100β-labelled cells. The zoom of a limited area (yellow line) from **C** is shown in **D**, in which two astrocytes are co-expressing YFP and S100β. Scale bar = 100 µm.

The last and more definitive approach for validating our model included primary astrocyte cultures from G-KiRKO neonatal mice (**Figure 71**). Marked down-regulation of *Gpr54* expression was observed in astrocytes from G-KiRKO mice in comparison with control astrocytes that would confirm the validity of our mouse line for effective ablation of *Gpr54* expression in astrocytes *in vivo*. In addition, the expression of *Kiss1* gene was analyzed for discarding neuron contamination in those astrocyte cultures, as our previous data demonstrated that *Kiss1* is not expressed in astrocytes. No amplification of Kiss1 mRNA was detected in astrocyte cultures from WT or G-KiRKO mice. Overall, these three validation strategies unambiguously demonstrate that Cre recombinase is properly active in astrocytes, leading to conditional ablation of *Gpr54*, thus, confirming the validation of G-KiRKO model.

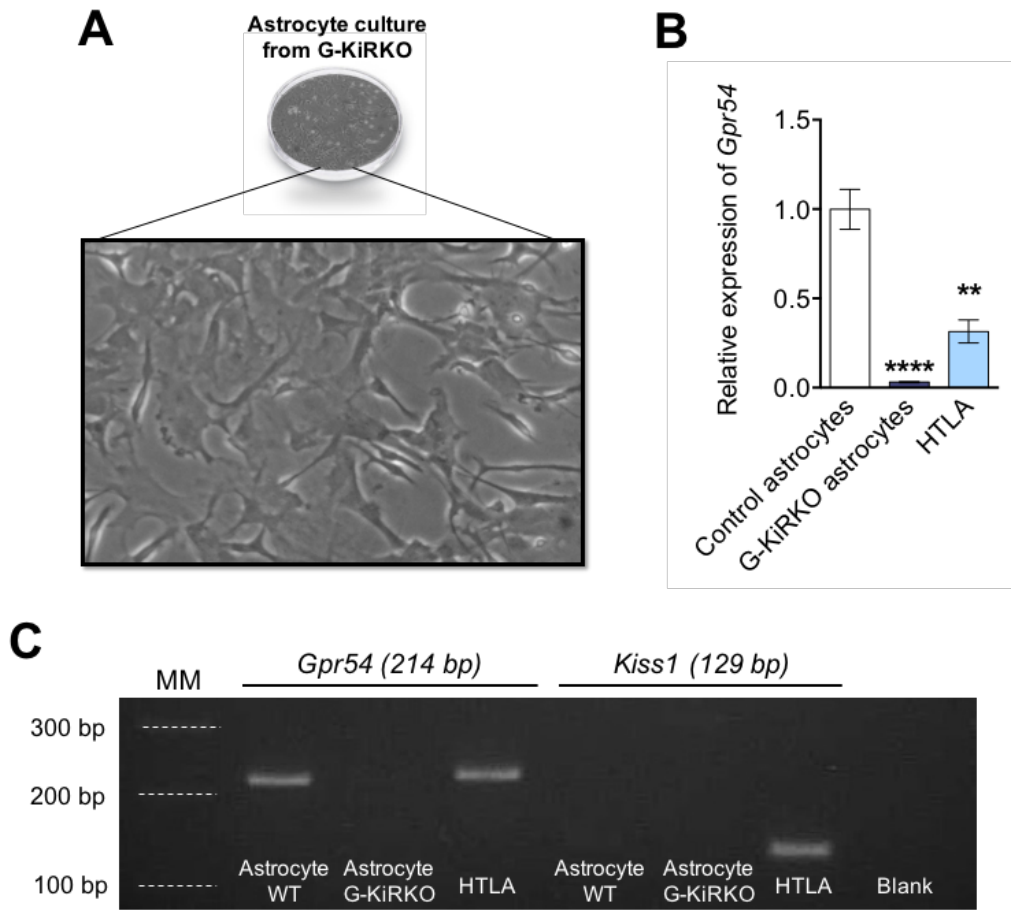

Figure 71. *Removal of Gpr54 in GFAP-positive cells.* **A**, image of primary astrocyte culture from neonatal G-KiRKO mice is shown. **B**, bar graph shows *Gpr54* mRNA expression measured by RT-qPCR from hypothalamic astrocytes of G-KiRKO mice. POA from WT mice was used as positive control. The level of Gpr54 mRNA was normalized using the level of S11 mRNA. **C,** representative gel illustrating the expression of *Gpr54* and *Kiss1* from hypothalamic astrocytes of control and G-KiRKO mice. Expected sizes for the PCR products are 240 bp for *Gpr54* and 129 bp for *Kiss1*. Data are presented as mean ± SEM. Statistical significance was determined by Student t-tests: $^{*}P<0.05$ vs. corresponding values in control astrocytes.

G-KiRKO mice display preserved puberty and reproductive parameters but increased LH responses to Kp-10 stimulation

Puberty onset and reproductive parameters were monitored in G-KiRKO mice of both sexes. Analysis of phenotypic markers of puberty revealed normal pubertal timing in G-KiRKO male and female mice, as denoted by the conserved ages of vaginal opening (VO) and first estrus (FE) in females (**Figure 72**), and balano-preputial separation (BPS) in males (**Figure 73**). Additionally, body weight (BW) gain in G-KiRKO mice during the pubertal transition was similar to control mice (**Figure 72** and **73**).

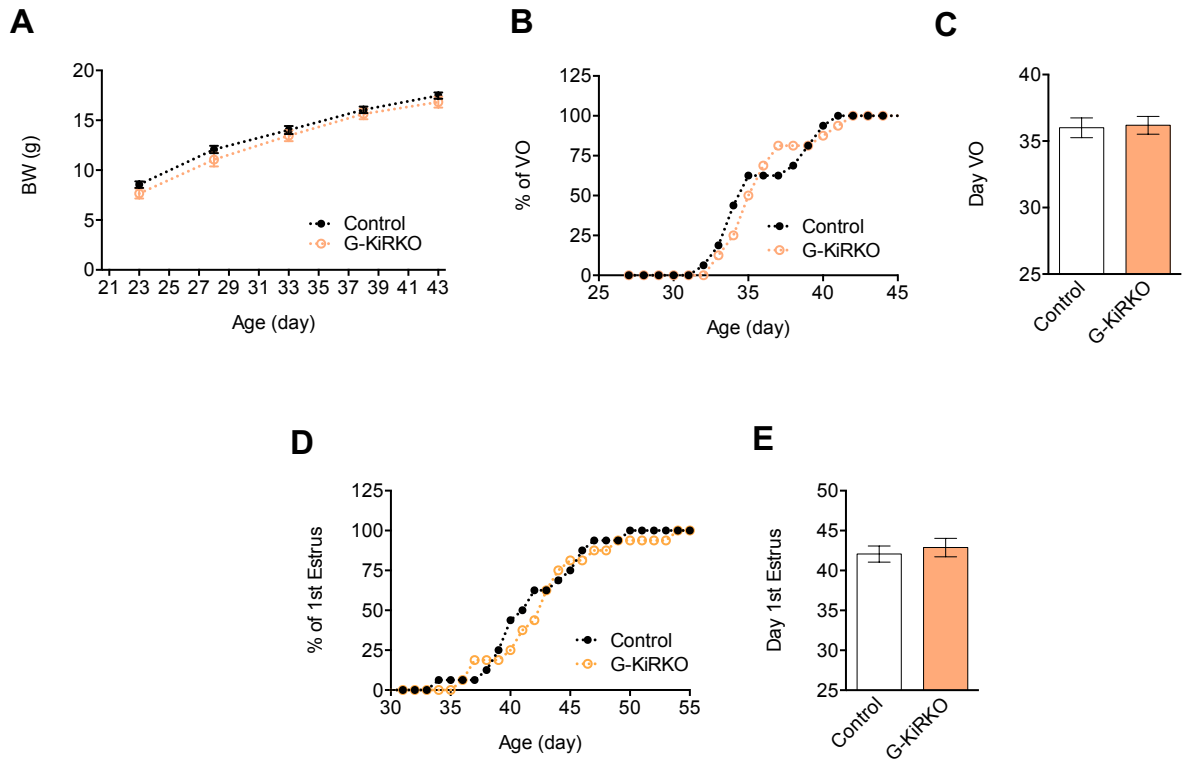

Figure 72. *Indices of pubertal maturation in G-KiRKO female mice*. **A**, evolution of body weight (BW) gain from weaning (PND21) to adulthood is presented from control (white) and G-KiRKO (orange) female mice (Control n= 16; Control n= 16). **B**, the accumulated percentage of female mice displaying vaginal opening (VO) during the period of 3 weeks post weaning is shown; the average age of VO is presented in **C**. The accumulated percentage of female mice displaying first estrus (FE) and the average age of FE are shown in **D** and **E**. Data are presented as mean ± SEM.

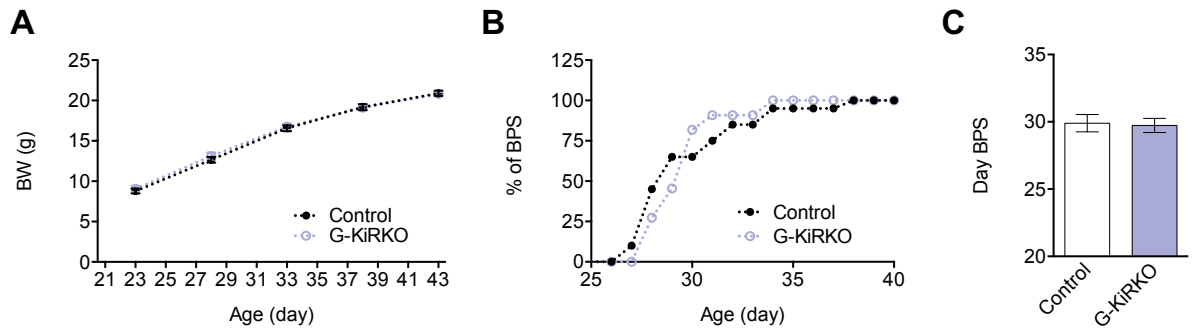

Figure 73. *Indices of pubertal maturation in G-KiRKO male mice*. **A**, evolution of BW gain from weaning (PND21) to adulthood is presented from control (white) and G-KiRKO (purple) male mice (Control n= 20; G-KiRKO n= 12). **B**, the accumulated percentage of male mice displaying balano-preputial separation (BPS) during the period of 3 weeks post weaning is shown, while the average age of BPS is presented in **C**. Data are presented as mean ± SEM.

In contrast, although no alterations were observed in the pubertal transition to acquire the sexual maturation, icv stimulation with Kp-10 (50 pmol/mouse) in adult G-KiRKO mice produced an over-response in terms of LH secretion in both sexes (**Figure 74** and **75**).

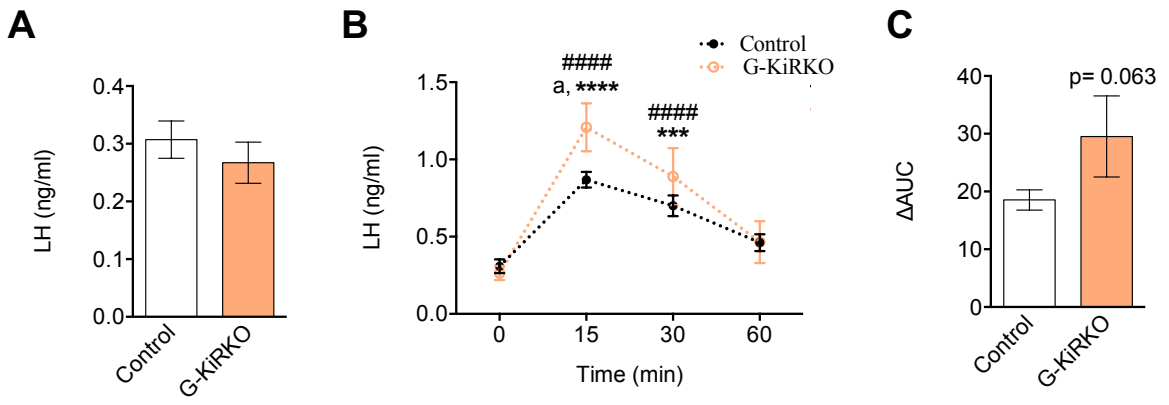

Figure 74. *LH response to Kp-10 in adult G-KiRKO female mice*. **A**, mean basal LH levels are presented in Control (n= 17) and G-KiRKO (n= 10) mice. **B**, LH secretion as 60-min time-course profile after icv injection of Kp-10 (include dose in pmol); in **C,** net increment of integral (AUC) LH secretion over the 60-min period after Kp-10 injection. Data are presented as mean ± SEM. Statistical significance was determined by 2-way ANOVA followed by Bonferroni's post hoc test for time-course analyses: ***P<0.001 vs. corresponding control values; ****/####P<0.0001 vs. corresponding control values; and [a] P<0.05 G-KiRKO vs. corresponding WT values; and by Student t-tests: P= 0.0063 vs. corresponding values in control mice.

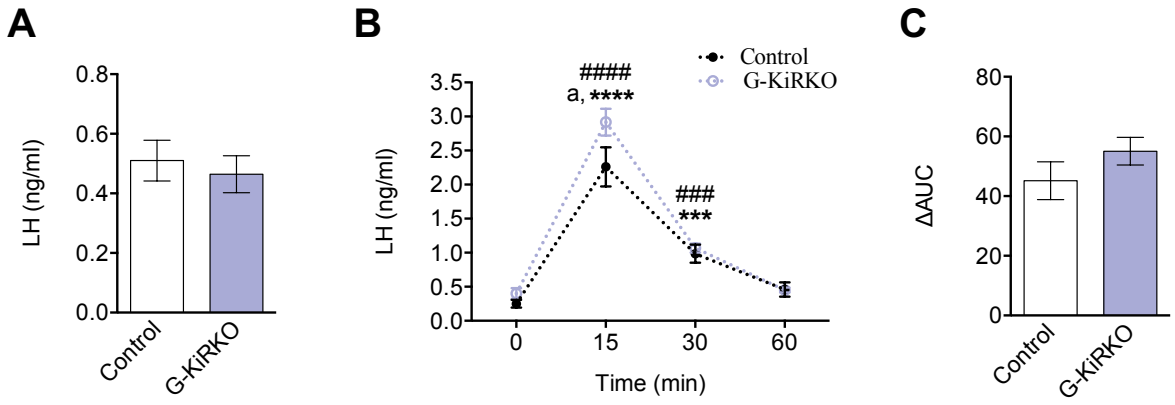

Figure 75. *LH response to Kp-10 in adult G-KiRKO male mice*. **A**, mean basal LH levels are presented in Control (n= 14) and G-KiRKO (n= 11) mice. **B**, LH secretion is shown as 60-min time-course profile after icv injection of Kp-10 (include dose in pmol); in **C,** net increment of integral (AUC) LH secretion over the 60-min period after Kp-10 injection. Data are presented as mean ± SEM. Statistical significance was determined by 2-way ANOVA followed by Bonferroni's post hoc test for time-course analyses: ***/###P<0.001 vs. corresponding control values; ****/####P<0.0001 vs. corresponding control values; and [a] P< 0.05G-KiRKO vs. corresponding WT values.

Monitoring of estrous cyclicity in adult G-KiRKO female mice failed to reveal an overt perturbation in the sequence of phases of ovarian cyclicity (**Figure 76**). Yet, a statistically shorter length of estrous cycle was observed in G-KiRKO mice as compared to controls.

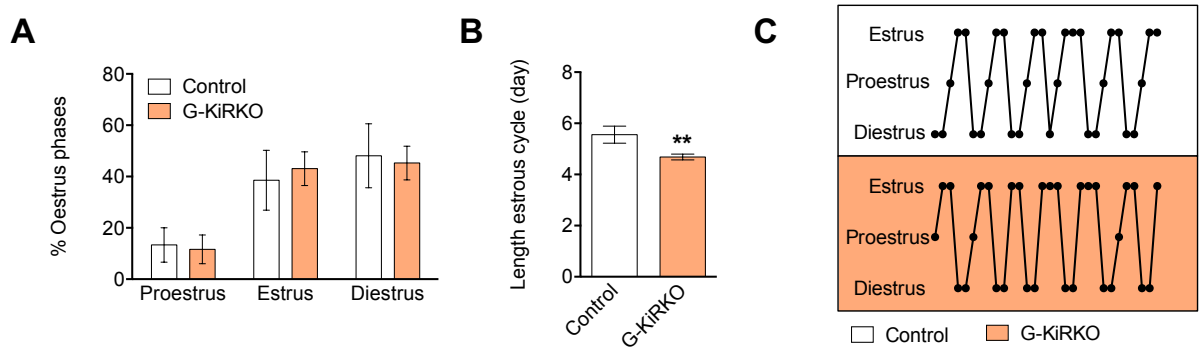

Figure 76. *Reproductive parameters in G-KiRKO mice.* **A**, bar graphs showing the percentual distribution of estrous cycle phases in Control and G-KiRKO female mice are presented (Control n= 7; G-KiRKO n= 12). The duration of the estrous cycle is displayed in **B**, while in **C**, representative estrous cycle profiles in Control and G-KiRKO female mice are shown. Data are presented as mean ± SEM. Statistical significance was determined by Student t-tests: $^{**}P<0.01$ vs. corresponding values in control mice.

Metabolic profiles of G-KiRKO mice in lean conditions

To assess the impact of the congenital absence of Gpr54 signaling in astrocytes on key metabolic parameters, we first monitored body weight gain in both female and male G-KiRKO mice at 4-5 months of age, which was similar to that of control littermates. Moreover, body composition analyses, including the assessment of fat mass and lean body mass were conducted in G-KiRKO, which showed no differences either in comparison with control mice (**Figure 77**).

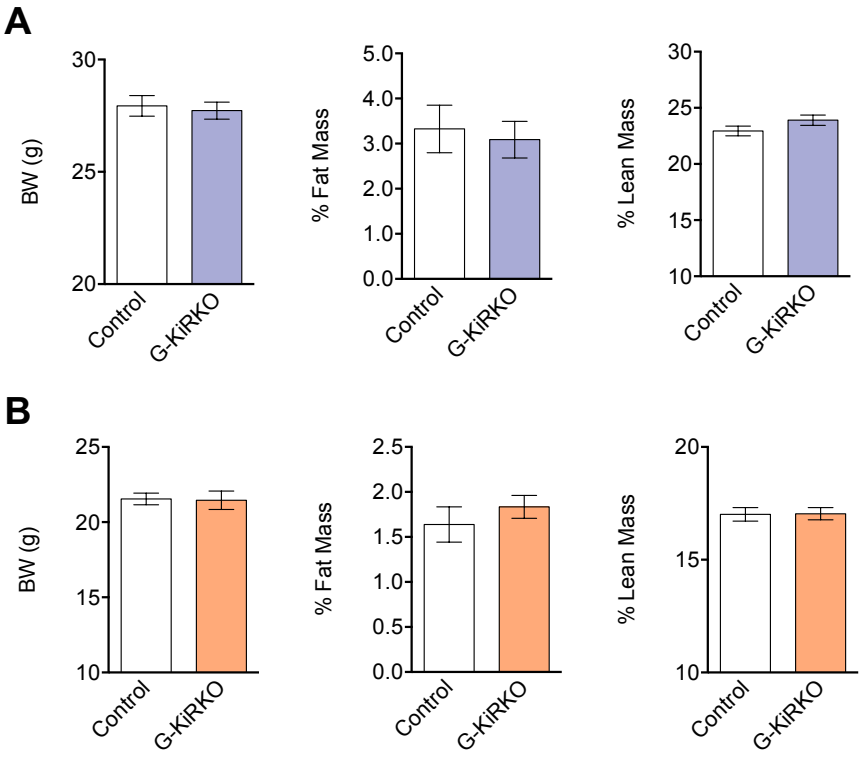

Figure 77. *Basic metabolic characterization of G-KiRKO mice.* Metabolic parameters in Control (white), G-KiRKO male (purple) and G-KiRKO female (orange) mice are shown. **A**, body weight (BW) gain and body composition analyses as percentage of fat mass and lean mass in Control (n=12) and G-KiRKO (n=8) male mice are presented. **B**, body weight (BW) gain and body composition analyses as percentages of fat mass and lean mass in Control (n=7) and G-KiRKO (n=12) female mice are presented. Data are presented as mean ± SEM.

Additionally, metabolic analyses related to glucose homeostasis were conducted in control and G-KiRKO mice. Notably, although basal glucose levels were similar in Control and G-KiRKO mice of both sexes, the results from GTT revealed a subtle improvement of the response to a glucose bolus in G-KiRKO mice, as denoted by time-course profiles shown in **Figure 78** and **79**, in which the integral AUG glucose values over the 120-min period after the glucose bolus were significantly lower in G-KiRKO male versus their control littermates. In contrast, no alterations in insulin sensitivity, measured by ITT, were detected in G-KiRKO male and female mice (**Figure 78 and 79**).

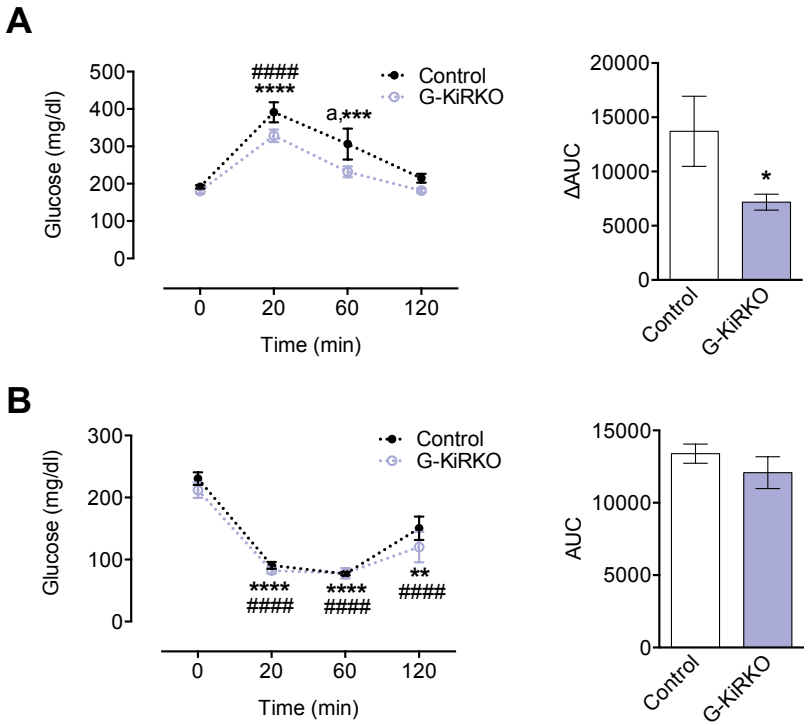

Figure 78. *Analysis of metabolic responses in G-KiRKO male mice in lean conditions.* **A,** results from glucose tolerance tests (GTT), represented as 120-min time-course profile after ip injection of a glucose bolus, and net increment of integral (AUC) glucose levels during GTT are shown. **B**, results from insulin tolerance tests (ITT), represented as 120-min time-course profile after ip injection of an insulin bolus (left panel), and net increment of integral (AUC) glucose levels during ITT (right panel), are shown. Data are presented as mean ± SEM. Statistical significance was determined by 2-way ANOVA followed by Bonferroni's post hoc test: ***P<0.001 vs. corresponding control values (time 0); $^{****/\#\#\#\#}$P<0.0001 vs. corresponding control values and ^{a}P<0.05 G-KiRKO vs. corresponding control values; and by Student t-tests: *P<0.01 vs. corresponding values in control mice.

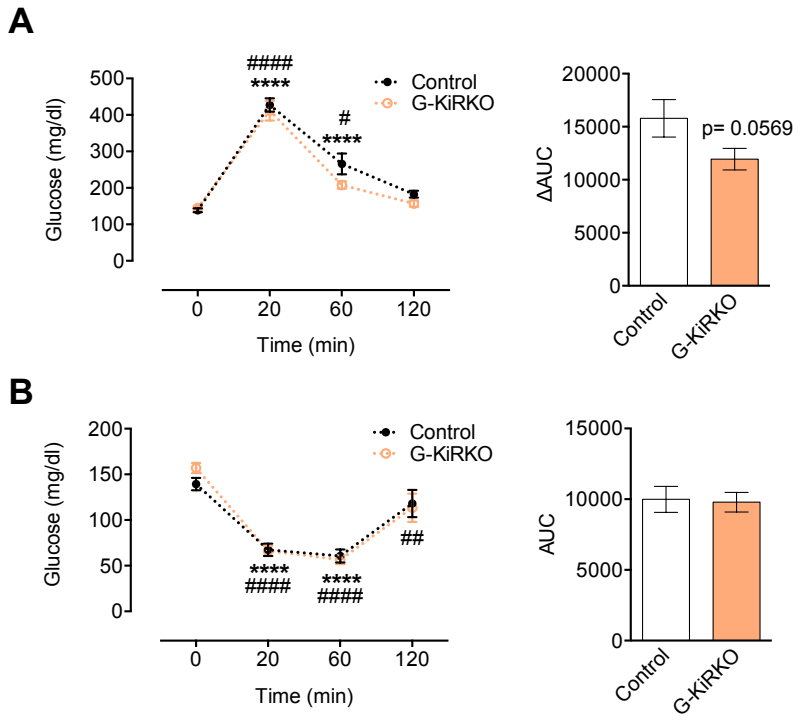

Figure 79 (see previous page)**.** *Analysis of metabolic responses in G-KiRKO female mice in lean conditions.* **A,** results from glucose tolerance tests (GTT), represented as 120-min time-course profile after ip injection of a glucose bolus, and net increment of integral (AUC) glucose levels during GTT, are shown. **B**, results from insulin tolerance tests (ITT), represented as 120-min time-course profile after ip injection of an insulin bolus (left panel), and net increment of integral (AUC) glucose levels during ITT (right panel), are shown. Data are presented as mean ± SEM. Statistical significance was determined by 2-way ANOVA followed by Bonferroni's post hoc test: $^{\#}P<0.05$ vs. corresponding control values (time 0); $^{\#\#}P<0.01$ vs. corresponding control values; $^{****/\#\#\#\#}P<0.0001$ vs. corresponding control values and $^{a}P<0.05$ G-KiRKO vs. corresponding control values; and by Student t-tests: P=0.0569 vs. corresponding values in control mice.

Reproductive assessment of G-KiRKO mice in conditions of metabolic stress

The metabolic status has a clear impact on the timing of puberty and reproductive function[18]. In order to explored whether the lack of Gpr54 signaling in astrocytes has any effect under conditions of metabolic stress, weaned G-KiRKO mice were fed with 58% HFD. Balano-preputial separation (BPS), a marker of puberty onset, was monitored in G-KiRKO male mice. As shown in **Figure 80**, although HFD produced a delay in the time of BPS, G-KiRKO male mice showed similar values as their control littermates under the same diet condition. In addition, the body weight gain was also similar in G-KiRKO male mice than in control ones.

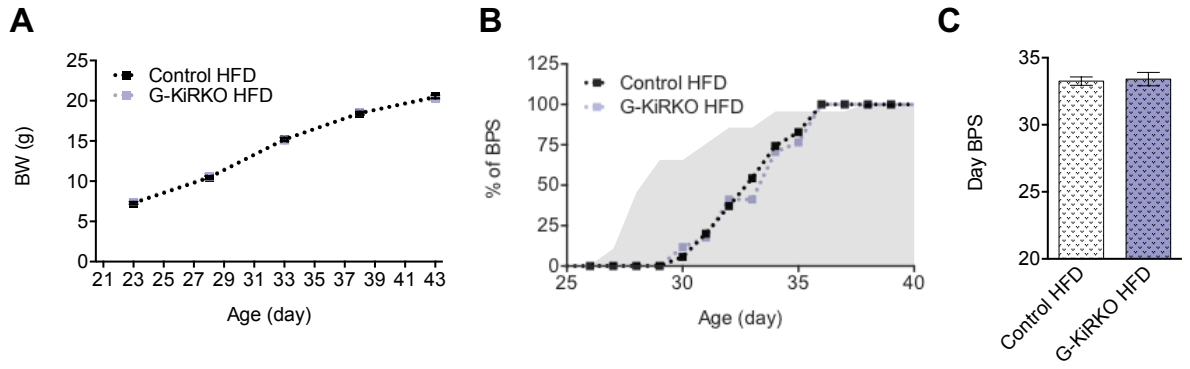

Figure 80. *Indices of pubertal maturation in G-KiRKO male mice fed with HFD*. **A**, evolution of BW gain from weaning (PND21) to adulthood is presented from control (white) and G-KiRKO (purple) male mice (Control n= 35; G-KiRKO n= 17). **B**, the accumulated percentage of male mice displaying balano-preputial separation (BPS) during the period of 3 weeks post weaning is shown. The average age of BPS is presented in **C**. Data are presented as mean ± SEM. Grey shadow indicates the values corresponding to control mice fed with standard diet (chow).

In the case of female mice, the age of vaginal opening (VO) and first estrus, external markers of puberty onset, were advanced as a consequence of HFD exposure (**Figure 81**). Notwithstanding, we observed that HFD-fed G-KiRKO mice presented a delay in the VO in comparison to HFD-fed control mice. In contrast, no differences were detected in term of first estrus in KO mice versus controls. Furthermore, the body weight gained in G-KiRKO female mice was similar than in control mice.

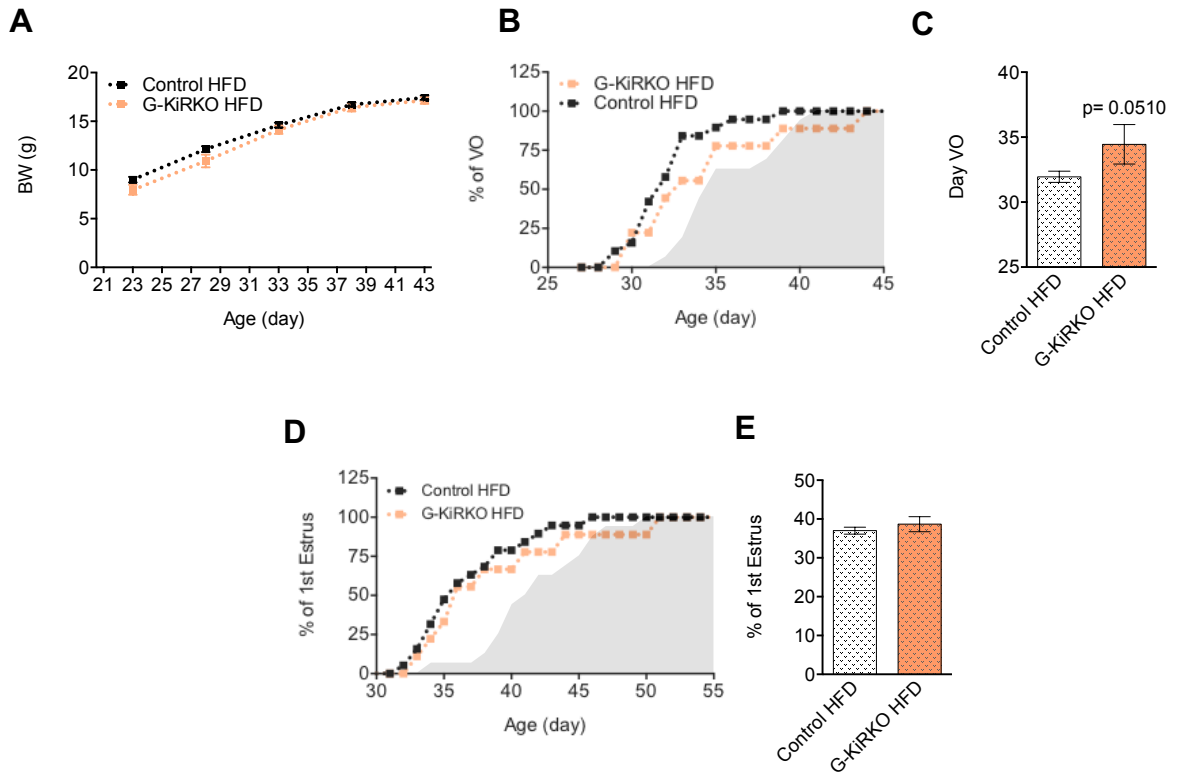

Figure 81. *Indices of pubertal maturation in G-KiRKO female mice fed with HFD*. **A**, evolution of BW gain from weaning (PND21) to adulthood is presented from control (white) and G-KiRKO (orange) female mice (Control n= 18; G-KiRKO n= 9). **B**, the accumulated percentage of female mice displaying vaginal opening (VO) during the period of 3 weeks post weaning is shown. The average age of VO is presented in **C**. The accumulated percentage of female mice displaying first estrus (FE) and the average age of FE are shown in **D** and **E**. Data are presented as mean ± SEM. Statistical significance was determined by Student t-tests: P= 0.0510 vs. corresponding values in control mice. Grey shadow indicates the values corresponding to control mice fed with standard diet (chow).

In adulthood, G-KiRKO male mice fed with HFD displayed no significant alterations in terms of basal LH secretion neither in the LH responses to icv injection with Kp-10 (indicate dose in pmol/mouse), represented as 60-min time-course profile after Kp-10 injection (**Figure 82**).

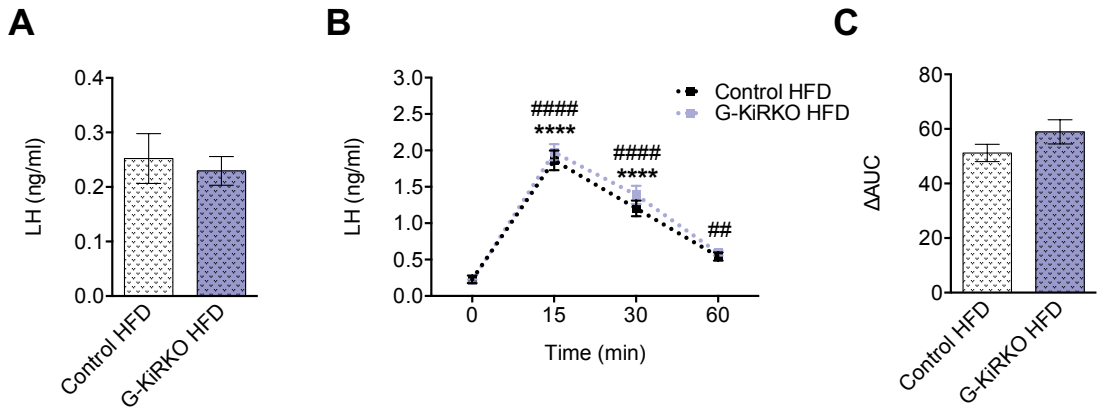

Figure 82. *LH response to Kp-10 in adult G-KiRKO male mice fed with HFD*. **A**, mean LH levels are presented in Control (n= 16) and G-KiRKO (n= 19) mice. **B**, LH secretion is shown as 60-min time-course profile after icv injection of Kp-10 (include dose in pmol); in **C,** net increment of integral (AUC) LH secretion over the 60-min period after Kp-10 injection. Data are presented as mean ± SEM. Statistical significance was determined by 2-way ANOVA followed by Bonferroni's post hoc test: $^{\#\#}$P<0.01 vs. corresponding control values and $^{****/\#\#\#\#}$P<0.0001 vs. corresponding control values.

In contrast, HFD-fed G-KiRKO female showed an overresponse to Kp-10 in terms of LH secretion, reminiscent of what we already observed in physiological conditions, in which lean G-KiRKO mice also displayed higher LH secretory responses after stimulation with Kp-10 (**Figure 83**). In addition, although the estrous cyclicity was preserved in G-KiRKO female, high-fat diet exposure induced estrous cycle irregularities in G-KiRKO female mice. These alterations were evidenced by longer cycle length and a higher number of days in diestrus and reduced number of days in estrus in G-KiRKO mice (**Figure 84**).

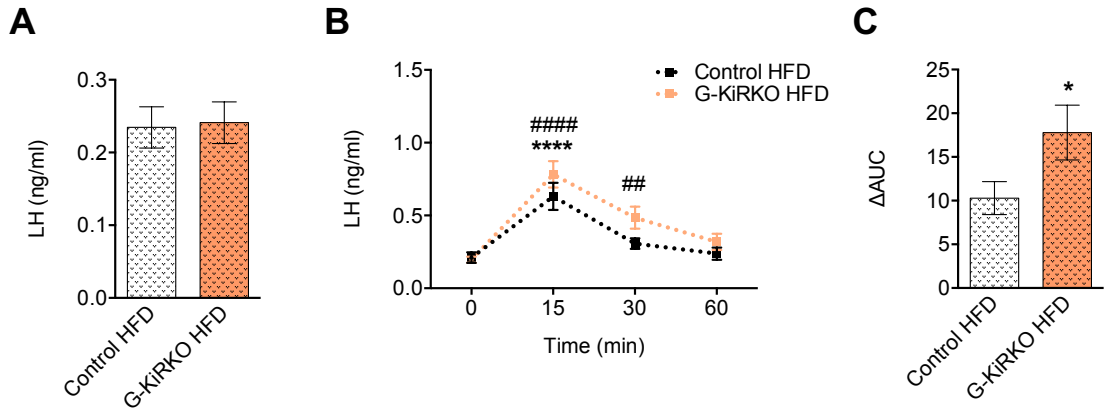

Figure 83. *LH response to Kp-10 in adult G-KiRKO female mice fed with HFD*. **A**, mean LH levels are presented in Control (n= 15) and G-KiRKO (n= 11) mice. **B**, show LH secretion as 60-min time-course profile after icv injection of Kp-10 (include dose in pmol), and, in **C,** net increment of integral (AUC) of LH secretion over the 60-min period after Kp-10 injection. Data are presented as mean ± SEM. Statistical significance was determined by 2-way ANOVA followed by Bonferroni's post hoc test: $^{\#\#}$P<0.01 vs. corresponding control values and $^{****/\#\#\#\#}$P<0.0001 vs. corresponding control values; and by Student t-tests: *P<0.05 vs. corresponding values in control mice fed with HFD.

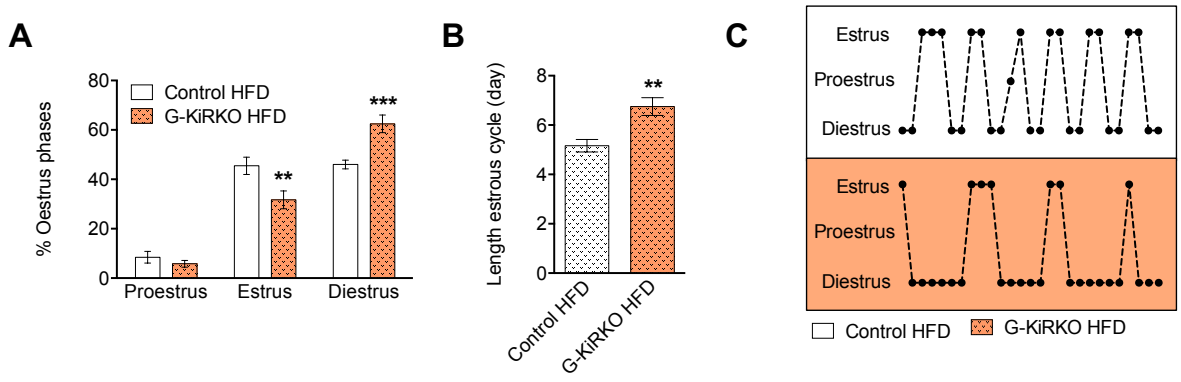

Figure 84. *Reproductive parameters in G-KiRKO female mice fed with HFD.* **A**, bar graphs showing the percentual distribution of estrous cycle phases in Control and G-KiRKO female mice are presented (Control n= 7; G-KiRKO n= 7). The duration of the estrous cycle is displayed in **B**, while in **C**, representative estrous cycle profiles in Control and G-KiRKO female mice are shown. Data are presented as mean ± SEM. Statistical significance was determined by 2-way ANOVA followed by Bonferroni's post hoc test: $^{**}P<0.01$ vs. corresponding values in control mice and $^{***}P<0.001$ vs. corresponding values in control mice; and by Student t-test: $^{**}P<0.01$ vs. corresponding values in control mice fed with HFD.

Metabolic profiles of HFD-fed G-KiRKO mice

At the age of 4-5 months, G-KiRKO mice fed with HFD were monitored for various metabolic parameters, such as body weight gain and body composition. All these parameters remained unaltered in G-KiRKO mice from both sexes (**Figure 85**).

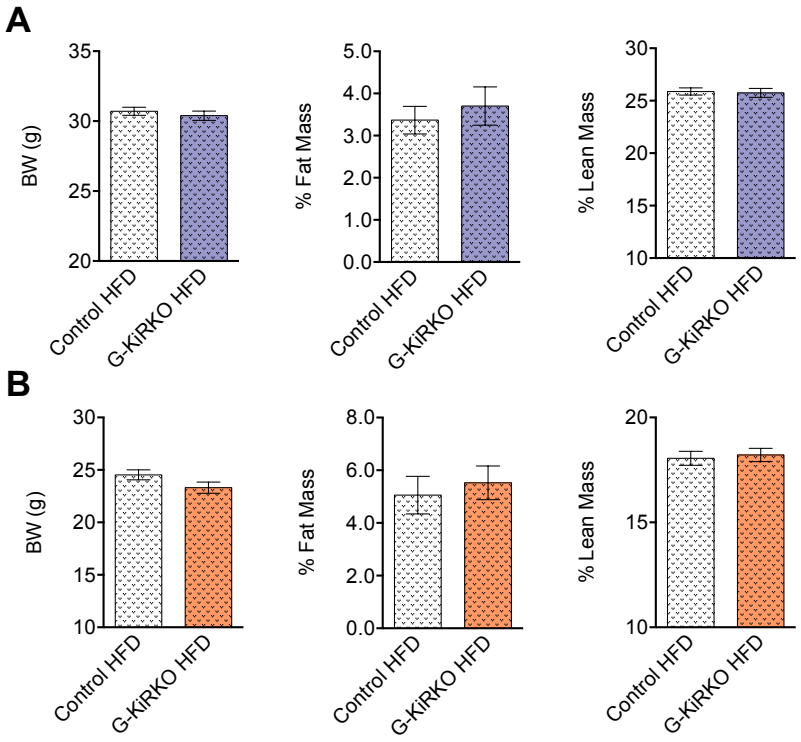

Figure 85 (see previous page)**.** *Basic metabolic characterization of G-KiRKO mice fed with HFD.* Metabolic parameters in Control (white), G-KiRKO male (purple) and G-KiRKO female (orange) mice are shown. **A**, body weight (BW) gain and body composition analyses as percentage of fat mass and lean mass in Control (n= 20-33) and G-KiRKO (n= 13-19) male mice are presented. **B**, body weight (BW) gain and body composition analyses as percentage of fat mass and lean mass in Control (n= 10-19) and G-KiRKO (n= 6-11) female mice are presented. Data are presented as mean ± SEM.

Furthermore, in order to complete the metabolic phenotypic characterization of this model under HFD condition, glucose homeostasis, as measured by GTT and ITT was assessed. Despite basal glucose levels of G-KiRKO male mice were similar to control mice, the levels of glucose during the GTT were lower than those observed for control mice, revealing a conserved and improved response to glucose bolus, already registered in conditions of normal feeding (**Figure 86**). In contrast, no differences in terms of ITT were detected between HFD-fed G-KiRKO males and their corresponding controls.

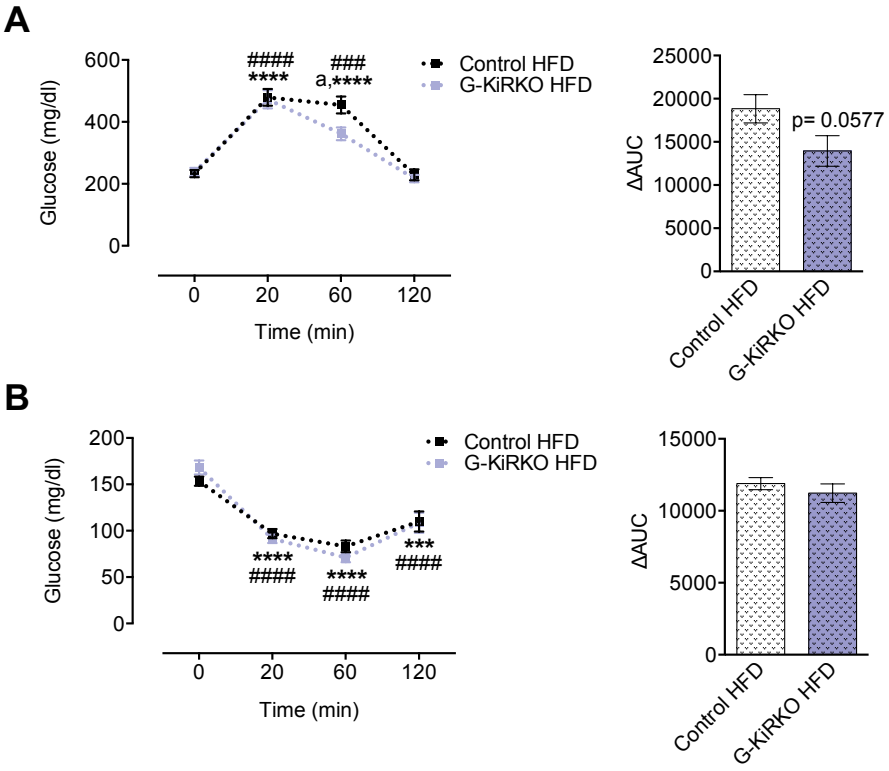

Figure 86. *Analysis of metabolic responses in G-KiRKO male mice fed with HFD.* **A,** results from glucose tolerance tests (GTT), represented as 120-min time-course profile after ip injection of a glucose bolus, and net increment of integral (AUC) glucose levels during GTT, are shown. **B**, results from insulin tolerance tests (ITT), represented as 120-min time-course profile after ip injection of an insulin bolus (left panel), and net increment of integral (AUC) glucose levels during ITT (right panel), are shown. Data are presented as mean ± SEM. Statistical significance was determined by 2-way ANOVA followed by Bonferroni's post hoc test: $^{***/\#\#\#}P<0.001$ vs. corresponding control values (time 0); $^{****/\#\#\#\#}P<0.0001$ vs. corresponding control values and $^{a}P<0.05$ G-KiRKO vs. corresponding values in control mice; and by Student t-tests: P= 0.0577 vs. corresponding values in control mice.

On the other hand, HFD-fed G-KiRKO female mice displayed no differences in basal glucose levels, neither in the response to glucose bolus, despite being on HFD since weaning (**Figure 87**). Similarly, ITT profiles were similar between G-KiRKO and control female mice, fed HFD.

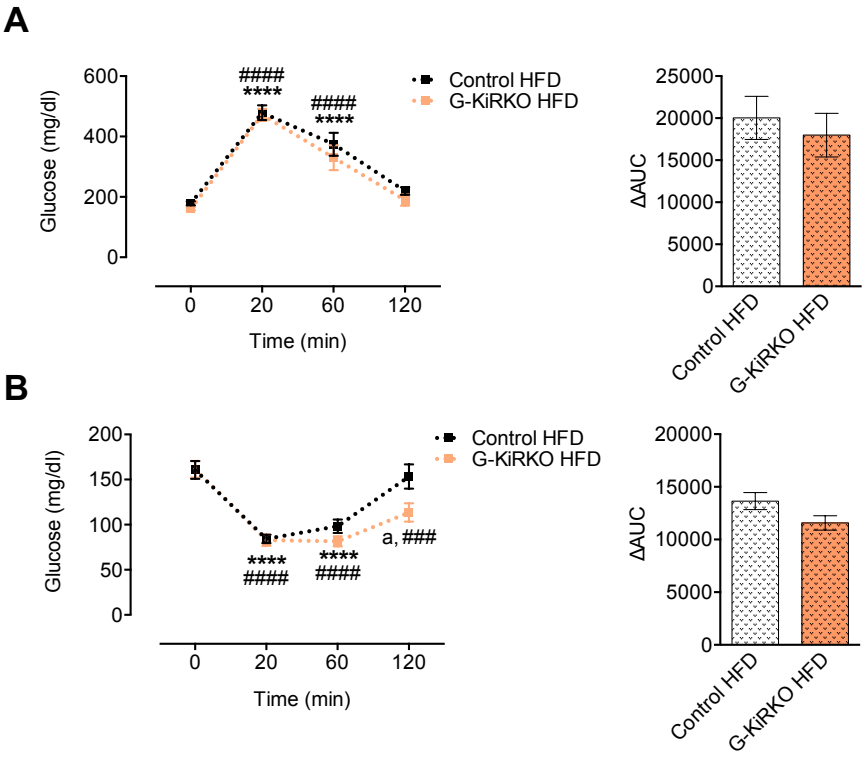

Figure 87. *Analysis of metabolic responses in G-KiRKO female mice fed with HFD.* **A,** results from glucose tolerance tests (GTT), represented as 120-min time-course profile after ip injection of a glucose bolus, and net increment of integral (AUC) glucose levels during GTT, are shown. **B**, results from insulin tolerance tests (ITT), represented as 120-min time-course profile after ip injection of an insulin bolus (left panel), and net increment of integral (AUC) glucose levels during ITT (right panel), are shown. Data are presented as mean ± SEM. Statistical significance was determined by 2-way ANOVA followed by Bonferroni's post hoc test: $^{###}P<0.001$ vs. corresponding control values (time 0); $^{****/####}P<0.0001$ vs. corresponding control values and $^{a}P<0.01$ G-KiRKO vs. corresponding values in control mice.

GFAP immunoreactivity in HFD-fed G-KiRKO male mice

Previous studies in rodents have documented that either acute or chronic exposure to HFD causes reactive gliosis and an increase of *GFAP* expression in the hypothalamus[221]. In order to explore the involvement of Gpr54 signaling in the astrocytic response to HFD, GFAP immunoreactivity was quantified in the ARC nucleus of G-KiRKO male mice fed HFD. However, under the same diet condition, G-KiRKO male mice showed similar values as their control littermates (**Figure 88**). By contrast, while acute exposure to HFD, consisting of feeding for 3-days with 58% HFD, failed to change GFAP labelling in the ARC of control

mice, GFAP immunoreactivity was significantly decreased in the ARC of G-KiRKO male mice after 3-day feeding with 58% HFD (**Figure 89**).

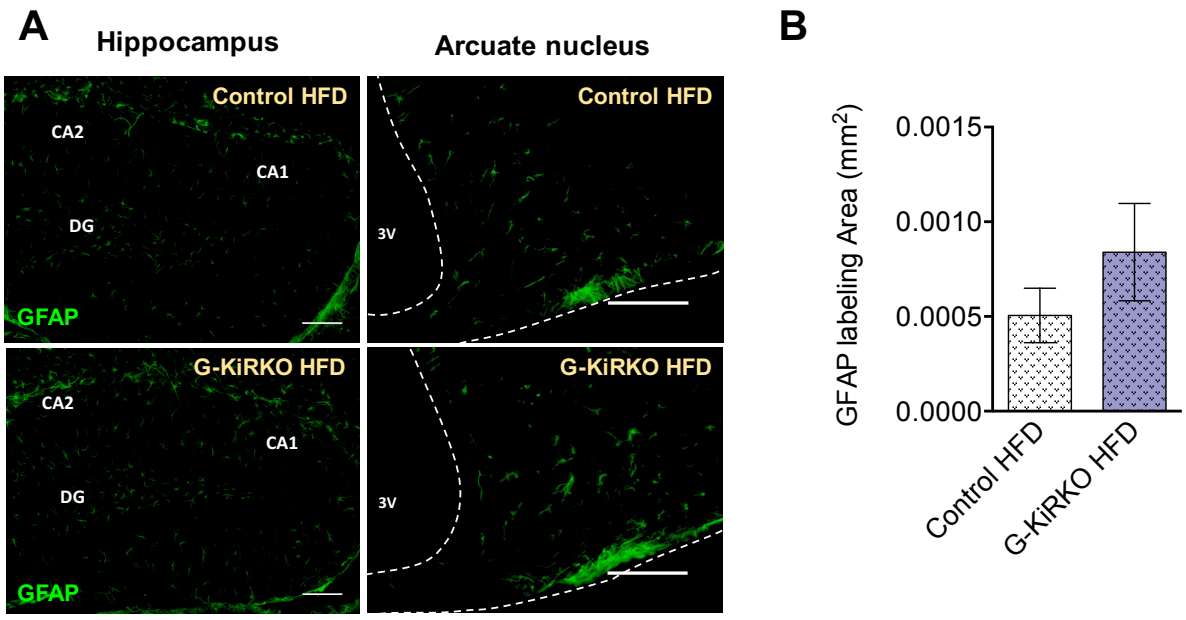

Figure 88. *GFAP immunoreactivity in chronically HFD-fed G-KiRKO male mice.* **A,** representative fluorescent images showing GFAP-labelled astrocytes in arcuate nucleus sections of Control (n= 6) and G-KiRKO (n= 6) mice. Hippocampus images are shown as control area without being altered by Gpr54 signaling perturbations. Scale bar = 100 µm. **B**, bar graph shows the astrocyte reactivity quantified and referred as values of fluorescent intensity using ImageJ. Data are presented as mean ± SEM.

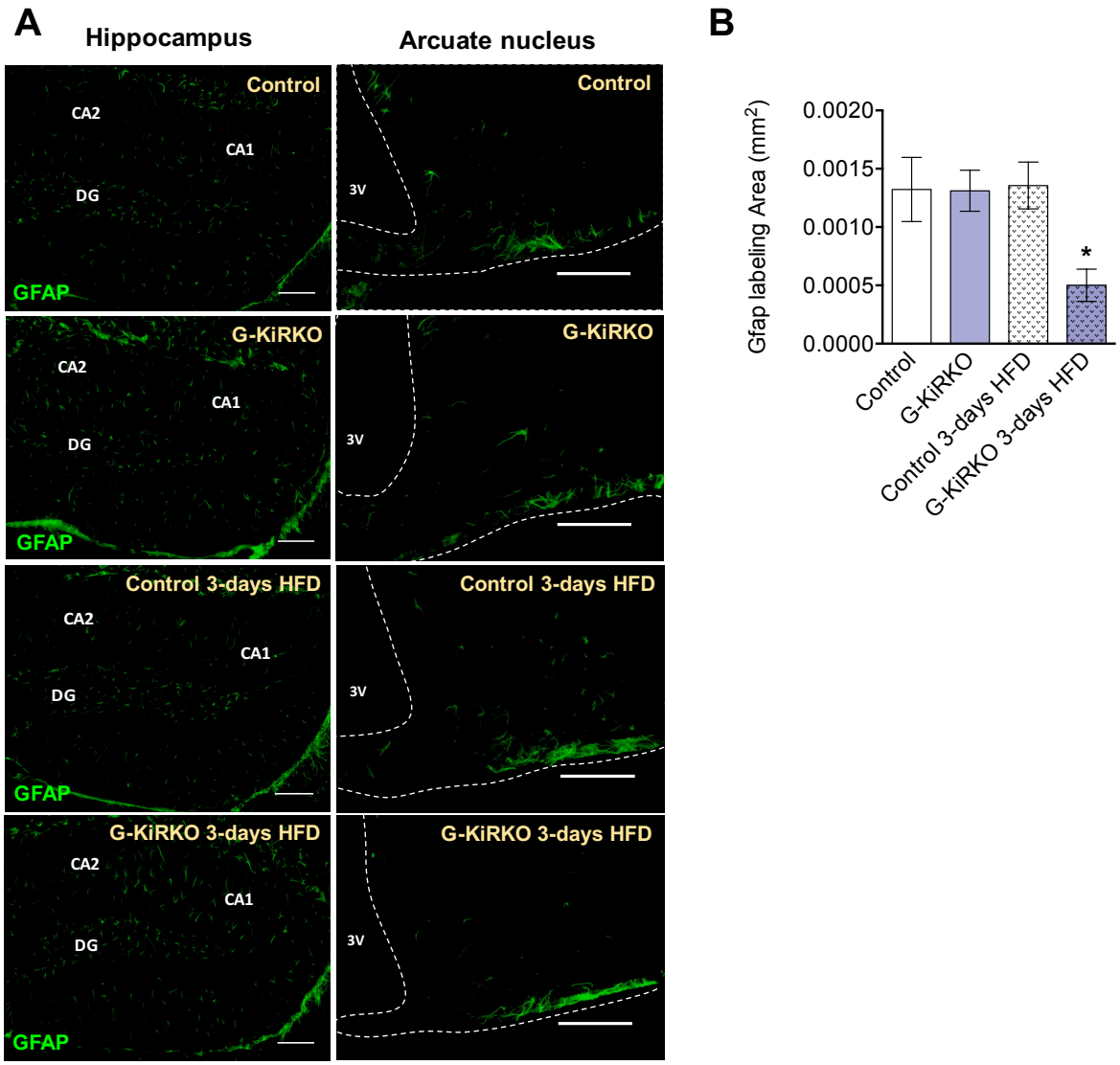

Figure 89. *GFAP immunoreactivity in G-KiRKO male mice fed HFD for 3 days.* **A,** representative fluorescent images showing GFAP-labelled astrocytes in arcuate nucleus sections of Control (n=4-5) and G-KiRKO (n=4-5) mice fed with chow diet or HFD for 3 days. Hippocampus images are shown as control area without being altered by Gpr54 signaling perturbations. Scale bar = 100 µm. **B**, bar graph shows the astrocyte reactivity quantified and referred as values of fluorescent intensity using ImageJ. Data are presented as mean ± SEM. Statistical significance was determined by one-way ANOVA followed by Bonferroni's post hoc test: $^{*}P<0.05$ G-KiRKO 3-day HFD vs. corresponding values in control mice.

Discussion

Discussion

Our understanding of the central pathways that regulate GnRH neurons and, thereby, contribute to the control of reproductive axis, remains incomplete. Nonetheless, in recent years, kisspeptins have been shown to play a major physiological role in the precise regulation of GnRH secretion and the reproductive axis, as solidly documented by an overwhelming number of physiological, pharmacological and genetic studies in humans and rodents[6,7]. Among other features, these studies have revealed the complex interplay of kisspeptins with different neurotransmitters and effector systems, whose nature is yet to be fully exposed. Amid them, compelling evidence has previously shown that, not only NKB and its receptor, NK3R, but also other members of the tachykinin family, participate in the control of GnRH neurosecretion and of different aspects of reproductive function, seemingly via close interaction with the kisspeptin pathway[8,9,12,13,170,188,189]. However, due to the intense crosstalk and partial redundancy of the elements of TAC signaling, as defined by multiple ligands (SP, NKA, NKB) and receptors (NK1R, NK2R, NK3R), teasing apart the individual roles of the specific TAC pathways has been difficult and remained to date elusive. In this context, the putative physiological role of NKA/NK2R signaling in the control of reproduction persists particularly ill-defined and its characterization has been so far mostly based on pharmacological analyses or studies in murine models with congenital ablation of the *Tac1* gene, which encodes both SP and NKA. In the same vein, our current knowledge about the mechanisms and down-stream targets whereby kisspeptins conducts their central regulatory actions is rather incomplete. Thus, the identification and characterization of novel co-transmitters and effector pathways are important, since these may provide a deeper understanding of the mode of action of kisspeptins and of their roles in the regulation of reproductive function.

In the above context, this Doctoral Thesis has explored (i) the role of NK2R signaling in the control of reproductive function, by characterizing a novel mouse line with a congenital ablation of the *Tacr2* gene; and (ii) novel mediators for the effects of kisspeptins in the hypothalamus, by implementing proteomic analyses in a suitable genetic model. The latter analyses led also to (iii) the assessment of the physiological roles of kisspeptin signaling in astrocytes, as putative novel mechanism for regulating the reproductive axis, using, among other approaches, a novel mouse line with a selective ablation of *Gpr54*, the gene encoding the canonical kisspeptin receptor, in GFAP-positive cells.

For sake of concision and to ease understanding of our Discussion, this section has been divided into two subsections, corresponding to the first and second-third objectives of this Thesis,

respectively, with their corresponding graphical summaries, followed by a final joint section of Conclusions.

Roles of NKA/NK2R signaling pathway and interplay with other TAC and kisspeptins

A large body of evidence, including the analysis of human mutations and murine models of inactivation of the genes encoding TAC ligands and receptors, has highlighted the relevance of the TAC system in the control of reproductive function. However, the particular roles of the different components of the TAC pathways are not equally elucidated, due to species differences, putative compensatory responses and the divergent characterization of different mouse lines with genetic inactivation of the various TAC ligands or receptors. In particular, little is known about the involvement of the NK2R pathway in the control of reproduction. In this context, this Thesis reports the first systematic characterization of a novel murine line in which the *Tacr2* gene has been ablated, thus allowing to dissect out the putative roles of NK2R signaling in the control of different aspects of reproductive function, from puberty onset and gonadotropin secretory profiles, to sexual behavior.

Our data refine and complement recent studies addressing the role of NKA in the control of puberty and reproduction in the mouse[13]. In line with previous reports, central administration of the agonist of NK2R, GR 64349, evoked unambiguous LH responses in control male and female mice, which our current data document that are similar in magnitude to those evoked by agonists of other TAC receptors, such as NK1R and NK3R[124]. This pharmacological evidence supports the involvement of NK2R signaling in the stimulatory control of the gonadotropin axis. Intriguingly, however, despite the proven ablation of *Tacr2* expression in our model, LH responses to the selective NK2R agonist were only partially blunted in female Tacr2 KO mice, while in null males, LH secretion in response to the NKA agonist, GR 64349, was only marginally reduced at late time-points. Possibly, some degree of promiscuity at the receptor level of the agonist used can explain the partially preserved LH responses, as these might derive from the collateral activation of other TAC receptors. This is further supported by the fact that LH responses to the NK2R agonist could be totally blocked in Tacr2 KO males pretreated with the pharmacological antagonist of NK3R. In the same vein, the phenotypic impact of genetic ablation of *Tac1*, encoding SP and NKA, has been recently shown to be augmented by the concomitant elimination of *Tac2*, encoding NKB[178]. In any event, it is interesting to note that the impact of *Tacr2* elimination on LH secretory responses to the NKA agonist was higher in females, suggesting that the degree of redundancy and compensation among the TAC pathways is lower than in males. This suggests a greater physiological

relevance of NK2R signaling in the control of the female (vs. male) gonadotropic axis. In good agreement, the reproductive impact of individual or combined *Tac1* and *Tac2* ablation was higher in females[175,178,189], suggesting that the female reproductive axis, at least at central levels, is more sensitive to alterations in TAC signaling.

Inactivating mutations of the NKB/NK3R systems cause failure of puberty of central origin in humans, whereas mice with genetic inactivation of various elements of the TAC signaling pathways display variable, but milder alterations, which in general were stronger in females. Yet, congenital ablation of *Tacr3* (encoding NK3R) failed to alter puberty onset in either male or female mice[250], while the pubertal phenotype of Tacr1 null mice has not been reported. Our current dataset expands those previous observations and demonstrate normal timing of puberty in Tacr2 null mice of either sex. Interestingly, ablation of *Tac1* or combined elimination of *Tac1/Tac2* did cause overt alterations of puberty in male and female mice[178], suggesting that the joint absence of several tachykinins is needed to overtly perturb puberty onset in rodents of both sexes. The fact that individual elimination of *Tacr3* or *Tacr2* did not alter pubertal timing in mice further emphasizes the functional redundancy of the TAC system also in terms of pubertal control; a contention that might be confirmed by compound ablation of all TAC receptors in future studies. At a physiological level, these data suggest that the biological effects of the different tachykinins will depend on the expression level of the three TAC receptors in a given cell target.

Similar redundancy appears to operate in terms of maintenance of fertility, so that both male and female Tacr2 null mice produced litters when crossed with WT counterparts and displayed grossly normal reproductive indices, such as preserved estrous cyclicity in females. This is in line with the preserved fertility of Tacr1 KO mice[191], whereas Tacr3 KO females were sub-fertile[250]. In contrast, individual or compound ablation of the genes encoding tachykinins, *Tac1* and *Tac2*, resulted in subfertility, with the greatest perturbation being observed in compound Tac1/Tac2 null female mice, which displayed infertility in 80% of the individuals[178]. Of note, preservation of fertility in mice lacking NK2R signaling was not seemingly attained by developmental compensation, as suggested by the conserved hypothalamic expression of key central elements of the reproductive axis, such as the genes encoding NKB, the TAC receptors, NK1R and NK3R, Kiss1, dynorphin and GnRH. Along this line, functional (LH) responses to other activators of the GnRH/gonadotropin axis, such as agonists of SP, NKB and kisspeptin, were maintained in Tacr2 KO mice. Therefore, given that pharmacological activation of NK2R can activate the gonadotropic axis, it is tenable that the lack of overt reproductive phenotypes

in Tacr2 KO mice might derive from the crosstalk and redundancy among the different TAC pathways, rather than a potential compensation via over-expression of complementary regulatory pathways. Admittedly, however, other compensatory events (e.g., adaptative connectivity) cannot be ruled out on the basis of our current data.

Notwithstanding, while gross fertility was preserved, fecundity of Tacr2 null mice, especially of females, appeared to be modestly compromised, as suggested by their longer breeding intervals than controls. In the same line, Tacr2 KO female mice displayed altered patterns of LH pulsatility, as defined by lower mean and basal LH levels than corresponding control females, although the number of LH pulses over the 3-h period of sampling was preserved. These data point out that, despite the potential redundancy among the TAC pathways, NK2R plays a genuine role in defining specific aspects of LH pulsatility. Of note, previous evidence had demonstrated that, although the stimulatory effects of NKA on GnRH/LH secretion requires a preserved kisspeptin signaling[13], *Tacr2* is not expressed in Kiss1 (or GnRH) neurons, suggesting a primary site of action of NKA on upstream afferents to Kiss1 neurons[10]. These might include Tac1 neurons in the ventromedial hypothalamus (VMH), which express *Tacr2*, as well as unidentified neurons from the ARC and VMH[13]. This is in contrast with the proposed network for the stimulatory effects of NKB, which would take place directly on ARC KNDy neurons, by auto-or para-synaptic loops. Interestingly, this KNDy neuronal population has been proposed as an essential component of the GnRH pulse generator, which likely dictates not only the pulse interval but also other features of the secretory profile of GnRH. On the basis of our data, the NKA/NK2R pathway appears to play a relevant role in defining the basal inter-pulse levels of GnRH/LH secretion.

In addition, the mechanisms controlling the GnRH pulses are seemingly involved also in the generation of hot flushes, since KNDy neurons play a facilitating role in the tail skin vaso-dilation and mediate the estradiol effects on thermal regulation[251]. Specifically, the thermo-regulatory vasodilation action of KNDy neurons, contributing to hot flushes, appears to be conducted via activation of glutamatergic NK3R neurons located in the median preoptic nucleus (MnPO) of rodents[243,252]. Supporting the relevance of the role of NK3R signaling in hot flushes, human studies have documented that infusion of NKB induces hot flushes, while administration of NK3R antagonists reduces their number and frequency[184,253]. However, the potential involvements of other TAC signaling pathways in the generation of hot flushes had not been addressed to date. Our current dataset demonstrate that ablation of *Tacr2* in OVX

female mice failed to alter tail skin temperature, thus arguing against a major role of the NKA/NK2R pathway in this phenomenon.

In contrast, subtle alterations were noticed when analyzing single-point LH levels in Tacr2 KO mice subjected to manipulations known to perturb the normal functioning of the gonadotropic axis. On one hand, short-term responses to ovariectomy appeared to be marginally blunted in Tacr2 KO female mice, as LH levels at 2-days after OVX were not significantly increased over basal levels, in contrast with the significant rise detected in control animals. On the other hand, the secretory mass of LH over a 24-h period of fasting, a manipulation known to suppress LH secretion, was significantly lower in Tacr2 KO male mice than in their corresponding controls. A tenable explanation for both findings is that the ablation of a stimulatory pathway, such as NK2R, would result in a partially defective activation of the GnRH/LH system immediately after lifting the negative feedback of sex steroids by OVX, but a greater suppression of LH secretion in conditions driving an inhibitory input to the reproductive axis, such as fasting. Admittedly, however, the net differences caused by *Tacr2* ablation were rather modest and, in fact, the absence of NK2R signaling did not prevent (but rather modestly attenuated) LH secretory patterns. This further emphasizes the detectable, but moderate physiological role of this TAC pathway in the control of the gonadotropic axis.

In addition to neuroendocrine responses, basic aspects of social and sexual behavior were explored in Tacr2 KO mice. Initial analyses in mice congenitally deficient for *Tac1* or *Tacr1* evidenced that the SP/NK1R pathway plays a role in emotional behavior[254,255], and previous studies had documented that ablation of *Tacr1*, but not of *Tac1*, results in diminished attraction by female pheromones and blunted sexual behavior[191]. In clear contrast, our current analyses failed to detect any defects in the exploration of female urine by Tacr2 KO male mice. Similarly, social sex preference was not affected by congenital ablation of *Tacr2*, even in male mice, in which the stereotyped preference for the female was fully preserved in Tacr2 null animals. Albeit more incisive sex behavioral tests were not applied (e.g., assessing lordosis or copulatory efficiency) due to the lack of behavioral phenotypes in our initial analyses, our current data strongly suggest that, contrary to NK1R, NK2R pathways are dispensable for the manifestation of basic adult social and sex preference behavior in mice.

Interestingly, histological analysis of the testis from Tacr2 KO mice strongly suggested the existence of a defective function of Sertoli cells, in their interaction with spermatids, in our model of congenital ablation of NK2R signaling. This perturbation manifested in the

appearance of symplastic giant cells and the defective processing of residual bodies, which accumulated in the seminiferous tubules of Tacr2 KO male mice, therefore pointing out a role of NK2R signaling in this function. These findings provide physiological support to previous pharmacological data suggesting a role of tachykinins in the control of rodent Sertoli cells *in vitro*[256]; yet, no study had previously documented the possible function of NK2R signaling in the control of Sertoli cell function in a physiological setting. Of note, in those previous studies, NKA, ligand of NK2R, was more potent than SP in the modulation of Sertoli cell secretory activity[256], in line with our current results. On the other hand, the fact that male Tacr2 KO were devoid of overt central alterations of the HPG axis, as denoted by the lack of changes in neuro-endocrine responses, further emphasizes the relevance of local, testicular NKR2 signaling. In any event, it must be stressed that despite these detectable alterations in testicular histology, male fertility was not compromised in our model, suggesting that Sertoli cells are still properly supporting the division and differentiation of germ cells even in the absence of NKR2. Admittedly, the lack of an overt reproductive phenotype in Tacr2 KO males might result also from compensatory mechanisms and/or redundancy within the TAC system. In clear contrast, in female Tacr2 KO animals, the histological analysis revealed apparently normal cycling ovaries and uteri, in accordance with their grossly preserved fertility and the absence of any detectable behavioral phenotype in terms of sex preference.

Alike kisspeptins, for which distinct metabolic roles have been recently proposed[238,239], previous evidence strongly suggested that TAC pathways putatively participate in the control of key aspects of metabolism, such as body weight and composition, feeding behavior and glucose homeostasis. In detail, initial studies using Tacr1 KO mice revealed a potential metabolic role of NK1R signaling in metabolic responses to obesogenic insults, as Tacr1 deficient animals showed reduced body weight gain and circulating levels of leptin and insulin, as well as improved glucose homeostasis in response to HFD[240]. In good agreement, later analyses in Tac1 null mice have documented a role of SP signaling in metabolic responses to obesity, so that congenital ablation of *Tac1* conferred resistance to obesity and improved glucose tolerance and insulin sensitivity under HFD[241,257]. Of note, ablation of *Tac1* might positively impact metabolic profiles by elimination of SP and/or NKA, the latter being mediated by NK2R. However, our current data argue against this possibility, since NK2R-deficient mice, under normal diet, displayed similar body weight gain and composition that their paired-fed littermates, neither they showed alterations in energy expenditure, respiratory quotient and food intake. Moreover, while exposure to HFD caused an increase in body weight

that was similar in control and Tacr2 KO male mice, basal glucose levels were higher in Tacr2 null animals fed HFD, which also displayed worse indices of glucose intolerance, without changes in insulin sensitivity. Altogether, this evidence suggests that, if any, the role of NKA/NK2R signaling in the control of metabolism is opposite to that of SP/NK1R, both being seemingly engaged in a reciprocal manner in the modulation of glucose homeostasis, especially in obesogenic conditions.

As a final note, in spite of previous pharmacological evidence suggesting a putative role of NKA in the control of cardiovascular function[258], our current analyses failed to detect any alteration in blood pressure in our Tacr2 KO mice, which was in the normotensive range in both sexes. These findings are in line with previous pharmacological studies showing that blockade of NK2R did not cause changes in blood pressure or heart rate in conscious rats[259]. Deeper analyses in our genetic model are deemed to assess whether other parameters of cardiovascular function might be altered in the congenital absence of NK2R.

A synoptic summary of the phenotypic features of male and female Tacr2 KO mice, in comparison with similar features in murine models of genetic manipulation of other members of the TAC system are presented in **Tables 9** and **10** (see page 133).

Novel hypothalamic targets of kisspeptins: Evidence for Gpr54 signaling in astrocytes

As mentioned above, the initial recognition of the crucial role of the Gpr54/Kiss1 system in the control of reproductive function, prompted the active search for the identification of potential downstream targets mediating kisspeptin actions in the brain[6]. Accordingly, considerable advancements have been made in the elucidation of the set of partners, co-transmitters and mediators of kisspeptin biological effects, fueled by the generation of various genetically modified mouse models and the implementation of multiple preclinical studies. Nevertheless, despite the above-mentioned efforts, characterization of the underlying pathways for kisspeptin actions in the hypothalamus remains incomplete.

In this Thesis, we aimed to identify novel hypothalamic targets of kisspeptin actions using robust proteomic approaches, enriched with PPI networks and GO analysis. Our strategy included the initial use of quantitative 2D-DIGE, for identification of differentially expressed proteins in the preoptic hypothalamic area (POA) of Kiss1 KO mice, after central (icv) injection with Kp-10. Our line of reasoning for such approach was that the Kiss1 null line, in which endogenous kisspeptin is absent, provides an excellent background where to reveal targets up- or down-regulated after challenge with exogenous kisspeptin. Our 2D-DIGE

analyses revealed changes in the POA levels of proteins involved in cellular metabolism and energy balance, in agreement with the proposed role of kisspeptin signaling in the control of body weight and metabolic homeostasis[238]. In addition, our proteomic approach pointed out also changes in proteins implicated in the cell signaling and protein folding, which might be explained as a result of the already demonstrated variety of intracellular cascades that are mediating kisspeptin actions[143]. Interestingly, we found that among the differentially expressed proteins related to synaptic plasticity, the levels of the glial fibrillary acidic protein (GFAP), a marker of astrocytes[260], were altered in response to Kp-10 stimulation. To our knowledge, this is the first evidence supporting the capacity of kisspeptins to modulate protein levels in non-neuronal brain cells, supposedly in astrocytes, as prominent subtype of glial cells. Of note, at the beginning of this work, no data on Gpr54 expression in glial cells had been presented.

Supporting the above findings, GO enrichment analysis applied on our second, independent high-throughput approach, using SWATH label-free proteomics, surfaced protein-protein interaction networks, cellular components and molecular functions, in which either GFAP or other astrocyte features/markers were modified in the POA of male Kiss1 KO mice in response to Kp-10 administration. In detail, three main protein clusters were identified by proteomic results. The most robust cluster included ribosomal proteins (RPs) and others factors involved in protein synthesis, possibly as reflection of the activation or maintenance of a functional proteome needed for mediating kisspeptin effects. This finding is also in line with the fact that our 2D-DIGE analyses revealed proteins involved in cell signaling and protein folding. In addition, in another cluster, we found nucleosome assembly proteins and nuclear proteins that are also involved in the regulation of cell signaling.

However, the most striking cluster for us was that in which GFAP was spotted, as interactive element with other proteins, in an independent node. In this cluster, we identified proteins, such as the small heat shock protein αB-crystallin (CRYAB), which enables astrocytes to become activated, and the metallothionein 3 (MT3), a zinc-binding metallothionein that contributes to actin polymerization in astrocytes and/or the amyloid precursor protein (APP), which is reportedly induced in reactive glial cells[261-263]. Besides their physiological relevance, these data provide a sort of internal validation for the proposal of a previously unnoticed effect of kisspeptins on astrocyte/glial cells, as putative mediators for at least part of their reproductive (or eventually another) biological actions. In this context, previous compelling evidence had highlighted the participation of glia cells in the control of GnRH neuro-secretion, mainly via the release of bioactive molecules and other mechanisms, including juxtacrine interactions at

the level of GnRH neurons[206,216]. Yet, no evidence had been presented so far on a putative role of glial cells as transducers of the effects of kisspeptins on GnRH cells, or on any other brain target/function.

This novel kisspeptin-glial pathway was further supported by detailed analyses of the raw SWATH data, which documented significant changes not only of GFAP, but also of APP and MT3 proteins, albeit of disparate nature: while GFAP content increased, hypothalamic APP and MT3 levels decreased after Kp-10 stimulation. In the same line, the results from our RT-qPCR and western blot analyses for GFAP and Vimentin, also expressed in astrocytes[245], further documented the capacity of kisspeptins to modulate astrocyte protein expression, therefore suggesting, although not conclusively proving, that astrocytes express the kisspeptin receptor.

In order to provide direct evidence for this putative pathway, we assessed the expression of *Gpr54* in primary astrocyte cultures from brains of neonatal rats and mice. Our RT-qPCR data not only unambiguously documented the expression of the gene encoding the kisspeptin receptor in rodent astrocytes, which to the best of our knowledge had not previously reported, but also demonstrated the lack of *Kiss1* expression in astrocytes *in vitro*. The later would argue against any potential neuronal contamination in our cultures, as spurious source of *Gpr54* expression, since *Kiss1* gene expression appears to be circumscribed to neuronal populations located in AVPV, ARC and periventricular nucleus of the hypothalamus in rodents[226,264], which might be tenable sources for kisspeptin input to glial cells.

In addition, our experiments also permitted confirmation of the functionality of Gpr54 in astrocyte cultures, by analyzing ERK1/2 and Akt levels after Kp-10 challenge *in vitro*, as biological readout[265,266]. In fact, in cultures of hypothalamic astrocytes from rats, we detected increased phosphorylation of ERK, and a trend for enhanced phosphorylation of Akt, in response to Kp-10, suggesting that the mechanism by which kisspeptin acts on astrocytes is mainly via ERK/MAP kinase cascade, analogous to that described for mediating the kisspeptin effects in GnRH neurons[143]. Likewise, our studies in mouse astrocytes *in vitro* demonstrated activation of ERK/MAP kinase pathway after Kp-10 challenge also in this species, although no detectable phosphorylation of Akt caused by kisspeptin was observed in mouse cultures. In any event, the fact that Kp-10 was effective in inducing ERK phosphorylation in hypothalamic but not cortical astrocytes in the mouse suggests some specificity in the responsiveness to kisspeptin depending of astrocyte location. In this sense, it is worthy to stress that the

hypothalamus is the region where Kiss1 and GnRH neuron populations are located, suggesting that hypothalamic astrocytes eventually wrapping or in close interaction with Kiss1 and/or GnRH neurons are those more responsive to kisspeptin, as eventual contributing mechanism for the control of GnRH secretion[6,205]. Altogether, these results not only confirm the functionality of Gpr54 in astrocytes, but also point out some differences in the pathways involved in the response to Kp-10 in astrocytes between the rat and mouse, as well as in the responsiveness to kisspeptin depending on astrocyte location within the CNS.

In line with the above expression and functional data *in vitro,* our co-localization analyses also documented the co-expression of *Gpr54* in GFAP-positive cells in the mouse brain. To our knowledge, in the CNS, *Gpr54* expression had been only documented so far in neurons, without previous evidence for a non-neuronal location of the kisspeptin receptor *in vivo*[138]. Interestingly, the co-expression of GFAP and *Gpr54* was notably higher in those areas where GnRH and Kiss1 neurons are located, reinforcing the idea that (a) kisspeptin responsiveness in astrocytes may vary according to the brain area; and (b) kisspeptin signaling in astrocytes may contribute to convey at least part of the regulatory actions of kisspeptins to GnRH neurons. While the existence of indirect neuronal pathways (e.g., glutamatergic or GABA-ergic) whereby kisspeptins can modulate GnRH neuro-secretion had been previously proposed[125], this is the first demonstration for a functional kisspeptin-glial pathway, with putative roles in the control of GnRH neurons and, thereby, the reproductive axis.

Further exploration of the nature and physiological role of such kisspeptin-glial network involved analyses in genetically modified mouse models with selective manipulations in kisspeptin signaling. In a first approach, we analyzed GFAP and S100β immunoreactivity, as another putative astrocyte marker, in specific brain areas of two mouse lines with genetic inactivation of Gpr54, namely the Gpr54 KO and Gpr54 KI mouse lines. In the former, kisspeptin signaling is totally abrogated by congenital elimination of *Gpr54*, which causes also severe hypogonadism. In the latter, whole-body Gpr54 ablation is associated to re-introduction (i.e., knock-in: KI) of *Gpr54* expression selectively in GnRH neurons; accordingly, kisspeptin signaling is absent in all cells except for GnRH neurons and gonadal function is grossly preserved[124,267]. Interesting, changes in GFAP-immunoreactive were detected in the ARC in both models, suggesting that prevention of kisspeptin actions in cells other than GnRH neurons can perturb expression of this bona fide marker of astrocytes. It must be stressed, however, that the increase in GFAP-immunoreactive detected in Gpr54 KO mice was much larger than in Gpr54 KI animals, suggesting that a majority of this effect is indirect and mediated via

suppression of gonadal function, in line with previous data showing an increase in the number of astrocytes in the medial basal hypothalamus of adult hypogonadal mice, due to defective gonadal steroids levels[268]. Nonetheless, the fact that Gpr54 KI mice displayed significantly altered GFAP levels is compatible with a primary action of kisspeptin signaling in the control of key astrocyte markers. Notably, this effect was prominent only in the ARC, in line with our co-localization analyses showing abundant co-expression of GFAP and Gpr54 in this area. Intriguingly, however, the changes in GFAP in our Gpr54 null models were not paralleled by similar alterations in S100β, suggesting that, rather than the unspecific perturbation of astrocyte function, elimination of kisspeptin signaling may alter specific functions of these glial cells.

In order to gain a more direct assessment of the physiological roles of kisspeptin signaling in astrocytes, we have generated and characterized, as part of this Thesis, the first mouse model with conditional ablation of *Gpr54* targeted to GFAP-positive cells. This line, that we termed G-KiRKO (for **G**FAP cell-specific **Ki**sspeptin **R**eceptor **KO**), provides a very powerful tool for interrogating the actual roles of kisspeptin actions in astrocytes in a physiological setting. In this model, Cre recombinase activity, driven by the *GFAP* promoter, permits excision of *loxP* flanked *Gpr54* coding regions in a cell-specific manner. Notably, while evidence for prominent Cre-mediated recombination was obtained in the POA, other hypothalamic areas, such as the MBH, and peripheral tissues (e.g., the testis) displayed also recombinase activity. However, our RT-qPCR analyses demonstrated preserved *Gpr54* mRNA levels in those tissues, therefore suggesting the marginal impact of such eventual deletion in these tissues. In fact, this GFAP-Cre mouse line had been previously used for astrocyte-preferential excision of various genes[224,225,269], even assuming that due to the features of endogenous GFAP expression, other cells might be also targeted. Importantly, confirmation for effective targeting of astrocytes was obtained by the use of a YFP-GFAP Cre reporter mouse line, in which YFP is activated in the presence of Cre recombinase activity and it was shown to be co-localized with the astrocyte marker, S100β, and also by our expression analyses in isolated astrocytes from G-KiRKO mice, which demonstrated negligible expression of *Gpr54* in primary astrocyte cultures from our conditional KO line. Altogether, these features solidly document the capacity of our approach to ablate the kisspeptin receptor from hypothalamic astrocytes.

Despite the effective ablation of *Gpr54* in astrocytes, phenotypic characterization of male and female G-KiRKO mice revealed rather modest alterations in basal conditions, i.e., under normal nutrition. Thus, G-KiRKO mice of both sexes displayed normal timing of puberty, as denoted by preserved ages of vaginal opening and first estrus in females and preputial

separation in males, conserved basal LH levels and preserved fertility. This is in contrast with recent data, showing that the timing of puberty onset was delayed and fertility was compromised in mice that lack the insulin receptor in GFAP cells[113]. Nonetheless, despite that G-KiRKO mice had normal puberty timing and they were fertile, they displayed enhanced LH secretory responses to the central administration of Kp-10 in both sexes. This finding would suggest that Gpr54 signaling in astrocytes might play a suppressive role in the modulation of kisspeptin effects on GnRH neurons, which nevertheless would not translate into overt alterations of puberty or fertility *in vivo*, except for a marginal shortening of the length of the ovarian cycle. Of note, the enhancement of LH responses to Kp-10 administration observed in G-KiRKO mice was more evident in females than in males, suggesting a possible sexual difference in the effects of kisspeptin signaling in astrocytes.

Astrocytes have recently emerged as mayor players in the brain control of body weight and glycemic homeostasis[114,218]. Yet, G-KiRKO mice of both sexes failed to show overt differences in adult body weight or composition vs. control animals fed a normal diet. However, G-KiRKO mice displayed improved glycemic responses to glucose overload in GTT, without detectable changes in insulin sensitivity. This observation suggests that kisspeptin signaling in astrocytes participates in the control of glucose homeostasis, with a predicted function as factor favoring glucose intolerance in basal conditions. While the mechanisms for such phenomenon are yet to be clarified, this putative function appears to be more evident in males, in which AUC responses to a glucose bolus in GTT were more clearly diminished (as index of improved glucose tolerance) than in females. Of note, opposite alterations, namely, a worsening of glucose tolerance, were detected in mice with conditional ablation of insulin receptors in GFAP cells[114], suggesting a reciprocal role of insulin and kisspeptin signaling in astrocytes in the control of peripheral glucose homeostasis.

Basic reproductive and metabolic characterization was conducted also in G-KiRKO mice of both sexes subjected to a condition of metabolic stress, caused by chronic exposure to HFD. Feeding HFD is known to cause reactive changes in astrocytes, which are putatively involved in mediating at least part of reproductive and metabolic deregulations associated to obesity[222,270]. In line with previous reports, in our study, HFD exposure caused an acceleration of puberty onset in control female mice. However, conditional ablation of *Gpr54* in astrocytes partially prevented such effect, suggesting that the astrocytic responses to HFD, tenably involved in causing pubertal advancement, are partially prevented in the absence of kisspeptin signaling. Notably, this effect was more evident in terms of vaginal opening, which denotes

initiation of puberty, than in terms of age of first estrus, which is an index of ovulation and attainment of fertility, suggesting that perturbed astrocyte function caused by *Gpr54* ablation is possibly more relevant in terms of pubertal activation rather than completion. In addition, female G-KiRKO mice displayed also alterations of estrous cyclicity under HFD conditions. This phenomenon, which was not detected under normal feeding, suggests that females devoid of kisspeptin signaling in astrocytes are more susceptive to the deleterious effects of HFD on adult ovarian function[271].

In addition, the beneficial effect of ablation of *Gpr54* in astrocytes in terms of glucose tolerance was lost in G-KiRKO female mice fed HFD. This intriguing observation, whose underlying mechanism is yet to be defined, denotes a complex interplay between kisspeptin astrocyte signaling and nutritional conditions in the control of glucose homeostasis. Finally, G-KiRKO males showed a defective hypothalamic GFAP-responses to 3-days high-fat feeding, but not to chronic HFD exposure; conditions that are known to cause reactive gliosis[222]. This observation further points out that specific ablation of kisspeptin signaling alters astrocyte responses to a strong nutritional stressor, as HFD, whose plethora of functional consequences warrant future investigation.

Summary tables

Summary tables

We have summarized here the comparison of phenotypic features of Tacr2 KO mouse with other genetic models of altered TAC signaling. The major phenotypic features of female (**Table 9**) and male (**Table 10**) Tacr2 KO mouse, as compared to those described previously for other genetically-modified mouse lines, with congenital ablation of the genes encoding TACs (*Tac1* and *Tac2*) or other TAC receptors (*Tacr1* and *Tacr3*), are synoptically presented as follows:

Table 9. Comparison of phenotypic features of Tacr2 KO female mouse with other genetic models of altered TAC signaling.

♀	Tacr2 KO	Tac1 KO	Tac2 KO	Tac1/Tac2 KO	Tacr1 KO	Tacr3 KO
Puberty onset	Normal	Delayed	Delayed	Delayed	-	Normal
Reproductive impairment	Altered LH secretion. Fertile but modest impairment (increased breeding interval)	Sub-fertile	Sub-fertile	80% infertile & disrupted LH pulses	Fertile	Sub-fertile
Sexual behavior	Normal	Normal	-	-	Diminished pheromone-induced sexual behavior	-
Metabolic parameters	-	Resistance to obesity, improved glucose tolerance & reduced insulin resistance under HFD	-	-	-	-

Table 10. Comparison of phenotypic features of Tacr2 KO male mouse with other genetic models of altered TAC signaling.

♂	Tacr2 KO	Tac1 KO	Tac2 KO	Tac1/Tac2 KO	Tacr1 KO	Tacr3 KO
Puberty onset	Normal	Delayed	Normal	Delayed	-	Normal
Reproductive impairment	Fertile but slight increase in breeding interval	Fertile	Fertile	Fertile	Fertile	Fertile
Sexual behavior	Normal	Normal	-	-	Deficit of sexual interaction & diminished pheromone-induced sexual behavior	-
Metabolic parameters	Enhanced elevation of basal glucose levels under high-fat-diet	Resistance to obesity, improved glucose tolerance & reduced insulin resistance under high-fat-diet	-	-	Improved glucose clearance	-

Graphical abstract

Graphical summary

The major findings of the present Doctoral Thesis can be summarized as follows:

Roles of NKA/NK2R signaling pathway and interplay with other TAC and kisspeptins

We have documented here that the global disruption of *Tacr2* gene, which results in ablation of NK2R, leads to discernible, albeit discrete deficits in the functioning of the reproductive axis, defined by (i) suppression of basal and mean LH levels; (ii) trend for lengthening of breeding intervals; and (iii) altered LH secretory pattern in response to manipulations known to perturb the normal functioning of the gonadotropic axis (e.g., ovariectomy and fasting). In addition, congenital ablation of *Tacr2* results in (iv) moderate worsening of basal glucose levels in response to high-fat feeding; and (v) defective function of Sertoli cells; without causing a gross perturbation of the timing of puberty onset, fertility and basic social sex behavior.

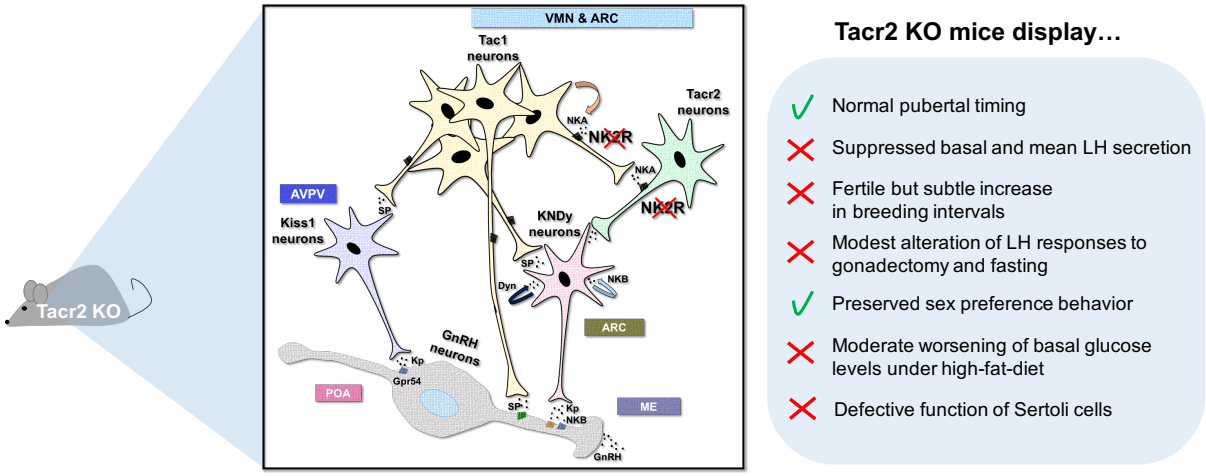

Figure 90. Schematic drawing outlining the putative role of NK2R signaling in the regulation of reproductive axis, as revealed by studies in our Tacr2 KO mouse line.

Novel hypothalamic targets of kisspeptins: Evidence for Gpr54 signaling in astrocytes

We have demonstrated here a novel functional kisspeptin signaling pathway in astrocytes, whereby kisspeptin can modulate glial cell markers in the hypothalamus. Congenital ablation of *Gpr54* in GFAP-cells *in vivo* failed to cause major reproductive alterations in basal conditions, apart from enhancement of LH responses to exogenous kisspeptin, which denotes a putative repressive role of this glial pathway on GnRH responsiveness to kisspeptin, together with a modest improvement of glycemic homeostasis. However, elimination of kisspeptin signaling from GFAP cells altered reproductive responses to a nutritional stressor, such as HFD. In detail, challenge G-KiRKO mice with HFD prevented the advancement in the age of vaginal opening (VO) and altered the cyclicity of estrous cycle. Under this condition, the enhanced LH secretory responses to Kp-10 was conserved too. By contrary, other reproductive and metabolic parameters remained without being altered.

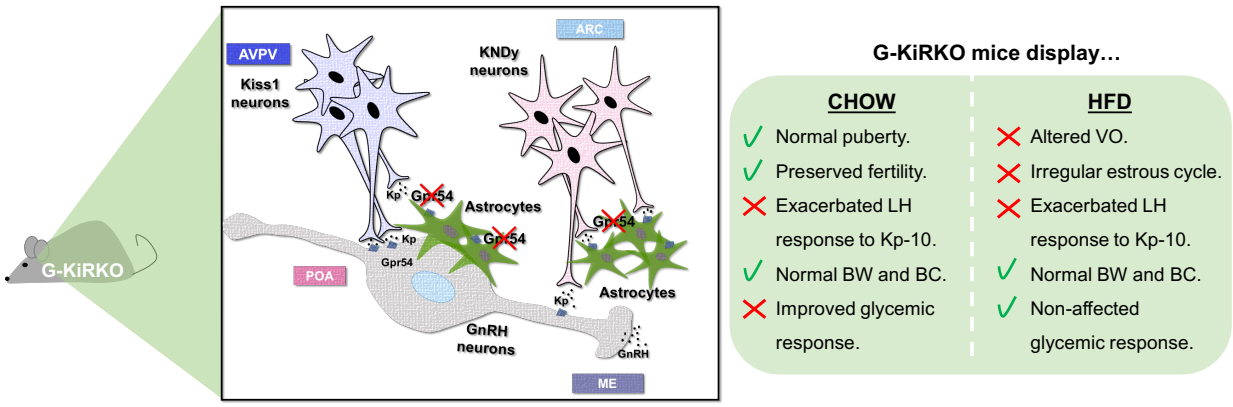

Figure 91. Schematic drawing outlining the putative role of kisspeptin signaling in astrocytes in the regulation of reproductive axis, as revealed by studies in our G-KiRKO mouse line.

Conclusions

Conclusions

The major conclusions of this Doctoral Thesis are the following:

1. Congenital ablation of the tachykinin receptor, NK2R, namely the canonical receptor for NKA, causes discernible, albeit moderate deficits in the functioning of the reproductive axis, including the suppression of basal and mean LH levels, trend for lengthening of breeding intervals and defective function of Sertoli cells, together with a moderate perturbation of glucose homeostasis in obesogenic conditions, but without preventing normal fertility or social sex behavior. These findings reveal a modest, albeit detectable role of NK2R signaling in the control of the reproductive axis, with partially overlapping and redundant functions with other tachykinin receptors.

2. Our data are the first to document the capacity of kisspeptins to activate hypothalamic glial responses *in vivo* and the existence of a previously unsuspected, functional kisspeptin receptor pathway in astrocytes, which utilizes canonical signaling factors, such as ERK, and regulates glial cell markers. Effective disruption of kisspeptin signaling in astrocytes *in vivo* induced only modest alterations in the functioning of the reproductive axis in basal conditions, denoted by enhancement of LH secretion after kisspeptin stimulation, but perturbed some reproductive responses to metabolic stress induced by HFD, including altered pubertal timing and estrous cyclicity in female mice, and attenuated indices of reactive gliosis after short-term exposure to high fat content diet

Bibliography

Bibliography

1. Fink, G. in *Neuroendocrinology in Physiology and Medicine* (eds. Conn, P. M. & Freeman, M. E.) 14, 107–133 (Humana Press, 2000).
2. Schwartz, N. B. in *Neuroendocrinology in Physiology and Medicine* (eds. Conn, P. M. & Freeman, M. E.) 139, 135–145 (Humana Press, 2000).
3. Carmel, P. W., Araki, S. & Ferin, M. Pituitary Stalk Portal Blood Collection in Rhesus Monkeys: Evidence for Pulsatile Release of Gonadotropin-Releasing Hormone (GnRH). *Endocrinology* 99, 243–248 (1976).
4. Tsutsumi, R. & Webster, N. J. G. GnRH Pulsatility, the Pituitary Response and Reproductive Dysfunction. *Endocrine Journal* 56, 729–737 (2009).
5. Bilban, M. Kisspeptin-10, a KiSS-1/metastin-derived decapeptide, is a physiological invasion inhibitor of primary human trophoblasts. *Journal of Cell Science* 117, 1319–1328 (2004).
6. Pinilla, L., Aguilar, E., Dieguez, C., Millar, R. P. & Tena-Sempere, M. Kisspeptins and Reproduction: Physiological Roles and Regulatory Mechanisms. *Physiological Reviews* 92, 1235–1316 (2012).
7. Terasawa, E., Guerriero, K. A. & Plant, T. M. in *Kisspeptin Signaling in Reproductive Biology* (eds. Kauffman, A. S. & Smith, J. T.) 784, 253–273 (Springer New York, 2013).
8. Navarro, V. M. *et al.* Regulation of Gonadotropin-Releasing Hormone Secretion by Kisspeptin/Dynorphin/Neurokinin B Neurons in the Arcuate Nucleus of the Mouse. *J. Neurosci.* 29, 11859–11866 (2009).
9. Navarro, V. M. *et al.* The Integrated Hypothalamic Tachykinin-Kisspeptin System as a Central Coordinator for Reproduction. *Endocrinology* 156, 627–637 (2015).
10. León, S. & Navarro, V. M. Novel Biology of Tachykinins in Gonadotropin-Releasing Hormone Secretion. *Semin Reprod Med* 37, 109–118 (2019).
11. León, S. *et al.* Redundancy in the central tachykinin systems safeguards puberty onset and fertility. 51, 523–36 (2019).
12. Maguire, C. A. *et al.* Tac1 Signaling Is Required for Sexual Maturation and Responsiveness of GnRH Neurons to Kisspeptin in the Male Mouse. *Endocrinology* 158, 2319–2329 (2017).
13. León, S. *et al.* Characterization of the Role of NKA in the Control of Puberty Onset and Gonadotropin Release in the Female Mouse. *Endocrinology* 160, 2453–2463 (2019).
14. Spergel, D. J., Krüth, U., Shimshek, D. R., Sprengel, R. & Seeburg, P. H. Using reporter genes to label selected neuronal populations in transgenic mice for gene promoter, anatomical, and physiological studies. *Progress in Neurobiology* 63, 673–686 (2001).
15. Morris, J. A., Jordan, C. L. & Breedlove, S. M. Sexual differentiation of the vertebrate nervous system. *Nat Neurosci* 7, 1034–1039 (2004).
16. Roa, J. *et al.* Hypothalamic Expression of KiSS-1 System and Gonadotropin-Releasing Effects of Kisspeptin in Different Reproductive States of the Female Rat. *Endocrinology* 147, 2864–2878 (2006).

17. Opel, H. The Hypothalamus and Reproduction in the Female. *Poultry Science* 58, 1607–1618 (1979).
18. Roa, J. & Tena-Sempere, M. Connecting metabolism and reproduction: Roles of central energy sensors and key molecular mediators. *Molecular and Cellular Endocrinology* 397, 4–14 (2014).
19. Boulant, J. A. Role of the Preoptic-Anterior Hypothalamus in Thermoregulation and Fever. *Clinical Infectious Diseases* 31, S157–S161 (2000).
20. Saper, C. B. & Lowell, B. B. The hypothalamus. *CURBIO* 24, R1111–R1116 (2014).
21. Hill, Y. X. A. J. W. Cross-talk between metabolism and reproduction: the role of POMC and SF1 neurons. 1–13 (2012).
22. Hoffman, G. E., Phelps, C. J., Khachaturian, H. & Sladek, J. R., Jr. in *Morphology of Hypothalamus and Its Connections* (eds. Ganten, D. & Pfaff, D.) 7, 161–196 (Springer Berlin Heidelberg, 1986).
23. Schally, A. V. *et al.* Isolation and properties of the FSH and LH-releasing hormone. *Biochemical and Biophysical Research Communications* 43, 393–399 (1971).
24. Matsuo, H., Baba, Y., Nair, R. M. G., Arimura, A. & Schally, A. V. Structure of the porcine LH- and FSH-releasing hormone. I. The proposed amino acid sequence. *Biochemical and Biophysical Research Communications* 43, 1334–1339 (1971).
25. Schally, A. V. *et al.* Gonadotropin-Releasing Hormone: One Polypeptide Regulates Secretion of Luteinizing and Follicle-Stimulating Hormones. *Science* 173, 1036–1038 (1971).
26. Millar, R. P. *et al.* Gonadotropin-Releasing Hormone Receptors. *Endocrine Reviews* 25, 235–275 (2016).
27. Okubo, K. & Nagahama, Y. Structural and functional evolution of gonadotropin-releasing hormone in vertebrates. *Acta Physiologica* 193, 3–15 (2008).
28. Desaulniers, A. T., Cederberg, R. A., Lents, C. A. & White, B. R. Expression and Role of Gonadotropin-Releasing Hormone 2 and Its Receptor in Mammals. *Front. Endocrinol.* 8, 1366 (2017).
29. Miyamoto, K. *et al.* Identification of the second gonadotropin-releasing hormone in chicken hypothalamus: evidence that gonadotropin secretion is probably controlled by two distinct gonadotropin-releasing hormones in avian species. *Proc Natl Acad Sci USA* 81, 3874–3878 (1984).
30. Kauffman, A. S. & Rissman, E. F. A Critical Role for the Evolutionarily Conserved Gonadotropin-Releasing Hormone II: Mediation of Energy Status and Female Sexual Behavior. *Endocrinology* 145, 3639–3646 (2004).
31. Yamamoto, N., Oka, Y. & Kawashima, S. Lesions of Gonadotropin-Releasing Hormone-lmmunoreactive Terminal Nerve Cells: Effects on the Reproductive Behavior of Male Dwarf Gouramis. *Neuroendocrinology* 65, 403–412 (1997).
32. Whitlock, K. E. Origin and development of GnRH neurons. *Trends in Endocrinology & Metabolism* 16, 145–151 (2005).
33. King, J. C. & Anthony, E. L. P. LHRH neurons and their projections in humans

and other mammals: Species comparisons. *Peptides* 5, 195–207 (1984).
34. Colombo, J. A., Whitmoyer, D. I. & Sawyer, C. H. Local changes in multiple unit activity induced by electrochemical means in preoptic and hypothalamic areas in the female rat. *Brain Research* 71, 35–45 (1974).
35. Clark, M. E. & Mellon, P. L. The POU homeodomain transcription factor Oct-1 is essential for activity of the gonadotropin-releasing hormone neuron-specific enhancer. *Mol. Cell. Biol.* 15, 6169–6177 (1995).
36. Maeda, K.-I. *et al.* Neurobiological mechanisms underlying GnRH pulse generation by the hypothalamus. *Brain Research* 1364, 103–115 (2010).
37. Flier, J. S., Underhill, L. H., Marshall, J. C. & Kelch, R. P. Gonadotropin-Releasing Hormone: Role of Pulsatile Secretion in the Regulation of Reproduction. *N Engl J Med* 315, 1459–1468 (1986).
38. Pohl, C. R., Richardson, D. W., Hutchison, J. S., Germak, J. A. & Knobil, E. Hypophysiotropic signal frequency and the functioning of the pituitary-ovarian system in the rhesus monkey. *Endocrinology* 112, 2076–2080 (1983).
39. Rispoli, L. A. & Nett, T. M. Pituitary gonadotropin-releasing hormone (GnRH) receptor: Structure, distribution and regulation of expression. *Animal Reproduction Science* 88, 57–74 (2005).
40. Pawson, A. J. *et al.* Inhibition of Human Type I Gonadotropin-Releasing Hormone Receptor (GnRHR) Function by Expression of a Human Type II GnRHR Gene Fragment. *Endocrinology* 146, 2639–2649 (2005).
41. Millar, R. *et al.* A novel mammalian receptor for the evolutionarily conserved type II GnRH. *Proc Natl Acad Sci USA* 98, 9636–9641 (2001).
42. Millar, R. P. GnRHs and GnRH receptors. *Animal Reproduction Science* 88, 5–28 (2005).
43. Millar, R. P., Pawson, A. J., Morgan, K., Rissman, E. F. & Lu, Z.-L. Diversity of actions of GnRHs mediated by ligand-induced selective signaling. *Frontiers in Neuroendocrinology* 29, 17–35 (2008).
44. Hall, J. E. *Guyton y Hall. Tratado de fisiología médica*. (Elsevier, 2016).
45. Childs, G. V. in *Morphology of Hypothalamus and Its Connections* (eds. Ganten, D. & Pfaff, D.) 7, 49–97 (Springer Berlin Heidelberg, 1986).
46. Hearn, M. T. W. & Gomme, P. T. Molecular architecture and biorecognition processes of the cystine knot protein superfamily: part I. The glycoprotein hormones. *Journal of Molecular Recognition* 13, 223–278 (2000).
47. Stilley, J. A. W. *et al.* FSH Receptor (FSHR) Expression in Human Extragonadal Reproductive Tissues and the Developing Placenta, and the Impact of Its Deletion on Pregnancy in Mice1. *Biology of Reproduction* 91, 247–15 (2014).
48. Ziecik, A. J., Derecka-Reszka, K. & Rzucidło, S. J. Extragonadal gonadotropin receptors, their distribution and function. *J Physiol Pharmacol* 43, 33–49 (1992).
49. Ascoli, M. & Narayan, P. *Chapter 2 – The Gonadotropin Hormones and Their Receptors*. *Yen & Jaffe's Reproductive Endocrinology: Physiology, Pathophysiology, and Clinical Management* 27–44.e8 (Elsevier, 2013).
50. Ascoli, M., Fanelli, F. & Segaloff, D. L. The Lutropin/Choriogonadotropin Receptor, A 2002 Perspective. *Endocrine Reviews* 23, 141–174 (2016).

51. Zheng, M., Shi, H., Segaloff, D. L. & Van Voorhis, B. J. Expression and Localization of Luteinizing Hormone Receptor in the Female Mouse Reproductive Tract1. *Biology of Reproduction* 64, 179–187 (2001).
52. Bliss, S. P., Navratil, A. M., Xie, J. & Roberson, M. S. GnRH signaling, the gonadotrope and endocrine control of fertility. *Frontiers in Neuroendocrinology* 31, 322–340 (2010).
53. Schwartz, N. B. & McCobmack, C. E. Reproduction: Gonadal Function and its Regulation. *Annual Review of physiology* 34, 425–472 (1972).
54. Johnson, M. H. *Essential Reproduction*. (2007).
55. Gougeon, A. Dynamics of follicular growth in the human: a model from preliminary results. *Human Reproduction* 1, 81–87 (1986).
56. Baker, T. G. A quantitative and cytological study of germ cells in human ovaries. *Proc. R. Soc. Lond. B.* 158, 417–433 (1997).
57. Hillier, S. G. Gonadotropic control of ovarian follicular growth and development. *Molecular and Cellular Endocrinology* 179, 39–46 (2001).
58. Mbemya, G. T., Vieira, L. A., Canafistula, F. G., Pessoa, O. D. L. & Rodrigues, A. P. R. Reports on in vivo and in vitro contribution of medicinal plants to improve the female reproductive function. *Reprodução & Climatério* 32, 109–119 (2017).
59. Caligioni, C. S. *Assessing Reproductive Status/Stages in Mice*. 1–11 (John Wiley & Sons, Inc., 2001).
60. Parkening, T., Collins, T. & Smith, E. Plasma and pituitary concentrations of luteinizing hormone, follicle-stimulating hormone and prolactin in aged, ovariectomized CD-1 and C57BL/6 mice. *Experimental Gerontology* 17, 437–443 (1982).
61. *Comparative Anatomy and Histology*. 1–461 (Elsevier, 2012).
62. Ravindranath, N., Dettin, L. & Dym, M. in *Introduction to Mammalian Reproduction* (ed. Tulsiani, D. R. P.) 91, 1–19 (Springer US, 2003).
63. Hansson, V. *et al.* Regulation of Seminiferous Tubular Function by FSH and Androgen. *Reproduction* 44, 363–375 (1975).
64. Ying, S.-Y. Inhibins, Activins, and Follistatins: Gonadal Proteins Modulating the Secretion of Follicle-Stimulating Hormone. *Endocrine Reviews* 9, 267–293 (1988).
65. Luo, L., Chen, H., Stocco, D. M. & Zirkin, B. R. Leydig Cell Protein Synthesis and Steroidogenesis in Response to Acute Stimulation by Luteinizing Hormone in Rats1. *Biology of Reproduction* 59, 263–270 (1998).
66. Sullivan, R. & Mieusset, R. The human epididymis: its function in sperm maturation. *Hum. Reprod. Update* 22, 574–587 (2016).
67. Cosentino, M. J. & Cockett, A. T. K. Review article: Structure and function of the epididymis. *Urol. Res.* 14, 229–240 (1986).
68. *Knobil and Neill's Physiology of Reproduction*. (Elsevier, 2015).
69. Santen, R. J. Is aromatization of testosterone to estradiol required for inhibition of luteinizing hormone secretion in men? *J. Clin. Invest.* 56, 1555–1563 (1975).
70. Skorupskaite, K., George, J. T. & Anderson, R. A. The kisspeptin-GnRH pathway in human reproductive health and disease. *Hum. Reprod. Update* 20, 485–500

(2014).
71. Hellier, V. *et al.* Female sexual behavior in mice is controlled by kisspeptin neurons. *Nature Communications* 1–12 (2018).
72. Fergani, C. & Navarro, V. M. Expanding the role of tachykinins in the neuroendocrine control of reproduction. *Reproduction* 153, R1–R14 (2016).
73. Krnjevic, K. & Phillis, J. W. Actions of Certain Amines on Cerebral Cortical Neurones. *British Journal of Pharmacology and Chemotherapy* 20, 471–490 (2012).
74. Barnes, G. N. & Slevin, J. T. Ionotropic Glutamate Receptor Biology: Effect on Synaptic Connectivity and Function in Neurological Disease. *Current Medicinal Chemistry* 10, 2059–2072 (2003).
75. Maffucci, J. A. & Gore, A. C. in 274, 69–127 (Elsevier, 2009).
76. Mahesh, V. B. & Brann, D. W. Regulatory role of excitatory amino acids in reproduction. *Endocr* 28, 271–280 (2005).
77. Iremonger, K. J., Constantin, S., Liu, X. & Herbison, A. E. Glutamate regulation of GnRH neuron excitability. *Brain Research* 1364, 35–43 (2010).
78. Zanisi, M. & Messi, E. Sex steroids and the control of LHRH secretion. *The Journal of Steroid Biochemistry and Molecular Biology* 40, 155–163 (1991).
79. Wang, L., Burger, L. L., Greenwald-Yarnell, M. L., Myers, M. G., Jr. & Moenter, S. M. Glutamatergic Transmission to Hypothalamic Kisspeptin Neurons Is Differentially Regulated by Estradiol through Estrogen Receptor α in Adult Female Mice. *J. Neurosci.* 38, 1061–1072 (2018).
80. Chu, Z. & Moenter, S. M. Endogenous Activation of Metabotropic Glutamate Receptors Modulates GABAergic Transmission to Gonadotropin-Releasing Hormone Neurons and Alters Their Firing Rate: A Possible Local Feedback Circuit. *J. Neurosci.* 25, 5740–5749 (2005).
81. Micevych, P. & Sinchak, K. Estradiol regulation of progesterone synthesis in the brain. *Molecular and Cellular Endocrinology* 290, 44–50 (2008).
82. Park, J. Y., Pillinger, M. H. & Abramson, S. B. Prostaglandin E2 synthesis and secretion: The role of PGE2 synthases. *Clinical Immunology* 119, 229–240 (2006).
83. Breyer, R. M., Bagdassarian, C. K., Myers, S. A. & Breyer, M. D. Prostanoid receptors: subtypes and signaling
. *Annu. Rev. Pharmacol. Toxicol.* 41, 661–690 (2001).
84. Clasadonte, J. *et al.* Prostaglandin E2 release from astrocytes triggers gonadotropin-releasing hormone (GnRH) neuron firing via EP2 receptor activation. *Proc Natl Acad Sci USA* 108, 16104–16109 (2011).
85. Tsutsui, K. *et al.* A Novel Avian Hypothalamic Peptide Inhibiting Gonadotropin Release. *Biochemical and Biophysical Research Communications* 275, 661–667 (2000).
86. Tsutsui, K. *et al.* Gonadotropin-inhibitory hormone (GnIH) and its control of central and peripheral reproductive function. *Frontiers in Neuroendocrinology* 31, 284–295 (2010).
87. Watanabe, M. The role of GABA in the regulation of GnRH neurons. 1–9 (2014).
88. Bicknell, R. J. Endogenous opioid peptides and hypothalamic neuroendocrine

neurones. *Journal of Endocrinology* 107, 437–446 (1985).
89. Goodman, R. L. *et al.* Evidence That Dynorphin Plays a Major Role in Mediating Progesterone Negative Feedback on Gonadotropin-Releasing Hormone Neurons in Sheep. *Endocrinology* 145, 2959–2967 (2004).
90. Weems, P. W. *et al.* Evidence That Dynorphin Acts Upon KNDy and GnRH Neurons During GnRH Pulse Termination in the Ewe. *Endocrinology* 159, 3187–3199 (2018).
91. Mcdonald, J. K. Role of Neuropeptide Y in Reproductive Function. *Annals of the New York Academy of Sciences* 611, 258–272 (1990).
92. Revisiting the reproductive functions of neuropeptide Y. 1–12 (2002).
93. Saif. Estrogen Signaling Multiple Pathways to Impact Gene Transcription. 1–12 (2006).
94. Carmeci, C., Thompson, D. A., Ring, H. Z., Francke, U. & Weigel, R. J. Identification of a Gene (GPR30) with Homology to the G-Protein-Coupled Receptor Superfamily Associated with Estrogen Receptor Expression in Breast Cancer. *Genomics* 45, 607–617 (1997).
95. Otto, C. *et al.* GPR30 Does Not Mediate Estrogenic Responses in Reproductive Organs in Mice. *Biology of Reproduction* 80, 34–41 (2009).
96. Micevych, P. E., May Wong, A. & Mittelman-Smith, M. A. *Estradiol Membrane-Initiated Signaling and Female Reproduction*. 84, 1211–1222 (John Wiley & Sons, Inc., 2011).
97. Herbison, A. E. & Pape, J.-R. New Evidence for Estrogen Receptors in Gonadotropin-Releasing Hormone Neurons. *Frontiers in Neuroendocrinology* 22, 292–308 (2001).
98. Petersen, S. L., Ottem, E. N. & Carpenter, C. D. Direct and Indirect Regulation of Gonadotropin-Releasing Hormone Neurons by Estradiol1. *Biology of Reproduction* 69, 1771–1778 (2003).
99. Wolfe, A. Estrogenic regulation of the GnRH neuron. 1–11 (2012).
100. Brinton, R. D. *et al.* Progesterone receptors: Form and function in brain. *Frontiers in Neuroendocrinology* 29, 313–339 (2008).
101. Sleiter, N. *et al.* Progesterone Receptor A (PRA) and PRB-Independent Effects of Progesterone on Gonadotropin-Releasing Hormone Release. *Endocrinology* 150, 3833–3844 (2009).
102. Skinner, D. C. *et al.* The negative feedback actions of progesterone on gonadotropinreleasing hormone secretion are transduced by the classical progesterone receptor. *Proc Natl Acad Sci USA* 95, 10978–10983 (1998).
103. Fu, R. *et al.* Novel evidence that testosterone promotes cell proliferation and differentiation via G protein-coupled receptors in the rat L6 skeletal muscle myoblast cell line. *J. Cell. Physiol.* 227, 98–107 (2011).
104. Pitteloud, N. *et al.* Inhibition of Luteinizing Hormone Secretion by Testosterone in Men Requires Aromatization for Its Pituitary But Not Its Hypothalamic Effects: Evidence from the Tandem Study of Normal and Gonadotropin-Releasing Hormone-Deficient Men. *The Journal of Clinical Endocrinology & Metabolism* 93, 784–791 (2008).

105. Knight, P. G. Roles of inhibins, activins, and follistatin in the female reproductive system. *Frontiers in Neuroendocrinology* 17, 476–509 (1996).
106. DiVall, S. A. *et al.* Insulin Receptor Signaling in the GnRH Neuron Plays a Role in the Abnormal GnRH Pulsatility of Obese Female Mice. *PLoS ONE* 10, e0119995–13 (2015).
107. Bruning, J. C. Role of Brain Insulin Receptor in Control of Body Weight and Reproduction. *Science* 289, 2122–2125 (2000).
108. McKibbin, P. E., McCarthy, H. D., Shaw, P. & Williams, G. Insulin deficiency is a specific stimulus to hypothalamic neuropeptide Y: A comparison of the effects of insulin replacement and food restriction in streptozocin-diabetic rats. *Peptides* 13, 721–727 (1992).
109. Hill, J. W. *et al.* Direct Insulin and Leptin Action on Pro-opiomelanocortin Neurons Is Required for Normal Glucose Homeostasis and Fertility. *Cell Metabolism* 11, 286–297 (2010).
110. Kim, H. H., DiVall, S. A., Deneau, R. M. & Wolfe, A. Insulin regulation of GnRH gene expression through MAP kinase signaling pathways. *Molecular and Cellular Endocrinology* 242, 42–49 (2005).
111. Evans, M. C., Rizwan, M., Mayer, C., Boehm, U. & Anderson, G. M. Evidence that Insulin Signalling in Gonadotrophin-Releasing Hormone and Kisspeptin Neurones does not Play an Essential Role in Metabolic Regulation of Fertility in Mice. *Journal of Neuroendocrinology* 26, 468–479 (2014).
112. Qiu, X. *et al.* Delayed Puberty but Normal Fertility in Mice With Selective Deletion of Insulin Receptors From Kiss1 Cells. *Endocrinology* 154, 1337–1348 (2013).
113. Manaserh, I. H. *et al.* Ablating astrocyte insulin receptors leads to delayed puberty and hypogonadism in mice. *PLoS Biol* 17, e3000189–22 (2019).
114. García-Cáceres, C. *et al.* Astrocytic Insulin Signaling Couples Brain Glucose Uptake with Nutrient Availability. 166, 867–880 (2016).
115. Zhang, Y. & Chua, S. *Leptin Function and Regulation*. 8, 351–369 (American Cancer Society, 2011).
116. Coleman, D. L. Obese and diabetes: Two mutant genes causing diabetes-obesity syndromes in mice. *Diabetologia* 14, 141–148 (1978).
117. Chehab, F. F., Lim, M. E. & Lu, R. Correction of the sterility defect in homozygous obese female mice by treatment with the human recombinant leptin. *Nat Genet* 12, 318–320 (1996).
118. Tschöp, M., Smiley, D. L. & Heiman, M. L. Ghrelin induces adiposity in rodents. *Nature* 407, 908–913 (2000).
119. Martini, A. C. *et al.* Comparative Analysis of the Effects of Ghrelin and Unacylated Ghrelin on Luteinizing Hormone Secretion in Male Rats. *Endocrinology* 147, 2374–2382 (2006).
120. Terasawa, E. & Fernandez, D. L. Neurobiological Mechanisms of the Onset of Puberty in Primates. *Endocrine Reviews* 22, 111–151 (2016).
121. Ojeda, S. R. *et al.* Minireview: The Neuroendocrine Regulation of Puberty: Is the Time Ripe for a Systems Biology Approach? *Endocrinology* 147, 1166–1174

(2006).
122. Avendaño, M. S., Vazquez, M. J. & Tena-Sempere, M. Disentangling puberty: novel neuroendocrine pathways and mechanisms for the control of mammalian puberty. *Hum. Reprod. Update* 23, 737–763 (2017).
123. Wiemann, J. N., Clifton, D. K. & Steiner, R. A. Pubertal Changes in Gonadotropin-Releasing Hormone and Proopiomelanocortin Gene Expression in the Brain of the Male Rat. *Endocrinology* 124, 1760–1767 (1989).
124. León, S. *et al.* Direct Actions of Kisspeptins on GnRH Neurons Permit Attainment of Fertility but are Insufficient to Fully Preserve Gonadotropic Axis Activity. *Nature Publishing Group* 6, 1235–14 (2016).
125. Pielecka-Fortuna, J. & Moenter, S. M. Kisspeptin Increases γ-Aminobutyric Acidergic and Glutamatergic Transmission Directly to Gonadotropin-Releasing Hormone Neurons in an Estradiol-Dependent Manner. *Endocrinology* 151, 291–300 (2010).
126. Roa, J. *et al.* Desensitization of gonadotropin responses to kisspeptin in the female rat: analyses of LH and FSH secretion at different developmental and metabolic states. *Am J Physiol Endocrinol Metab* 294, E1088–E1096 (2008).
127. Clarkson, J., Han, S.-K., Liu, X., Lee, K. & Herbison, A. E. Neurobiological mechanisms underlying kisspeptin activation of gonadotropin-releasing hormone (GnRH) neurons at puberty. *Molecular and Cellular Endocrinology* 324, 45–50 (2010).
128. Clarkson, J. & Herbison, A. E. Postnatal Development of Kisspeptin Neurons in Mouse Hypothalamus; Sexual Dimorphism and Projections to Gonadotropin-Releasing Hormone Neurons. *Endocrinology* 147, 5817–5825 (2006).
129. Takumi, K., Iijima, N. & Ozawa, H. Developmental Changes in the Expression of Kisspeptin mRNA in Rat Hypothalamus. *J Mol Neurosci* 43, 138–145 (2010).
130. Roa, J. & Tena-Sempere, M. Energy balance and puberty onset: emerging role of central mTOR signaling. *Trends in Endocrinology & Metabolism* 21, 519–528 (2010).
131. Kotani, M. *et al.* The Metastasis Suppressor Gene KiSS-1 Encodes Kisspeptins, the Natural Ligands of the Orphan G Protein-coupled Receptor GPR54. *J. Biol. Chem.* 276, 34631–34636 (2001).
132. Seminara, S. B. *et al.* The GPR54 gene as regulator of puberty. *N Engl J Med* 349, 1614–1627 (2003).
133. Lee, J. H. *et al.* KiSS-1, a Novel Human Malignant Melanoma Metastasis-Suppressor Gene. *JNCI Journal of the National Cancer Institute* 88, 1731–1737 (1996).
134. Li, D., Yu, W. & Liu, M. Regulation of KiSS1 gene expression. *Peptides* 30, 130–138 (2009).
135. Lehman, M. N., Merkley, C. M., Coolen, L. M. & Goodman, R. L. Anatomy of the kisspeptin neural network in mammals. *Brain Research* 1364, 90–102 (2010).
136. Pineda, R., Plaisier, F., Millar, R. P. & Ludwig, M. Amygdala Kisspeptin Neurons: Putative Mediators of Olfactory Control of the Gonadotropic Axis. *Neuroendocrinology* 104, 223–238 (2017).

137. Lass, G. *et al.* Optogenetic stimulation of kisspeptin neurones within the posterodorsal medial amygdala increases LH pulse frequency in female mice. *bioRxiv* 497164 (2018).
138. Herbison, A. E., d'Anglemont de Tassigny, X., Doran, J. & Colledge, W. H. Distribution and Postnatal Development of Gpr54Gene Expression in Mouse Brain and Gonadotropin-Releasing Hormone Neurons. *Endocrinology* 151, 312–321 (2010).
139. Tena-Sempere, M. GPR54 and kisspeptin in reproduction. *Hum. Reprod. Update* 12, 631–639 (2006).
140. Horikoshi, Y. *et al.* Dramatic Elevation of Plasma Metastin Concentrations in Human Pregnancy: Metastin as a Novel Placenta-Derived Hormone in Humans. *The Journal of Clinical Endocrinology & Metabolism* 88, 914–919 (2003).
141. Makri, A., Pissimissis, N., Lembessis, P., Polychronakos, C. & Koutsilieris, M. The kisspeptin (KiSS-1)/GPR54 system in cancer biology. *Cancer Treatment Reviews* 34, 682–692 (2008).
142. Navenot, J.-M., Wang, Z., Chopin, M., Fujii, N. & Peiper, S. C. Kisspeptin-10-Induced Signaling of GPR54 Negatively Regulates Chemotactic Responses Mediated by CXCR4: a Potential Mechanism for the Metastasis Suppressor Activity of Kisspeptins. *Cancer Res* 65, 10450–10456 (2005).
143. Castaño, J. P. *et al.* Intracellular signaling pathways activated by kisspeptins through GPR54: Do multiple signals underlie function diversity? *Peptides* 30, 10–15 (2009).
144. Adachi, S. *et al.* Involvement of Anteroventral Periventricular Metastin/Kisspeptin Neurons in Estrogen Positive Feedback Action on Luteinizing Hormone Release in Female Rats. *J. Reprod. Dev.* 53, 367–378 (2007).
145. Han, S. Y., McLennan, T., Czieselsky, K. & Herbison, A. E. Selective optogenetic activation of arcuate kisspeptin neurons generates pulsatile luteinizing hormone secretion. *Proc Natl Acad Sci USA* 112, 13109–13114 (2015).
146. Kauffman, A. S. *et al.* Sexual Differentiation of Kiss1Gene Expression in the Brain of the Rat. *Endocrinology* 148, 1774–1783 (2007).
147. Smith, J. T. *et al.* Differential Regulation of KiSS-1 mRNA Expression by Sex Steroids in the Brain of the Male Mouse. *Endocrinology* 146, 2976–2984 (2005).
148. Comninos, A. N. *et al.* Kisspeptin signaling in the amygdala modulates reproductive hormone secretion. *Brain Struct Funct* 221, 2035–2047 (2015).
149. Aggarwal, S. *et al.* Medial Amygdala Kiss1 Neurons Mediate Female Pheromone Stimulation of Luteinizing Hormone in Male Mice. *Neuroendocrinology* 108, 172–189 (2019).
150. Adekunbi, D. A. *et al.* Role of amygdala kisspeptin in pubertal timing in female rats. *PLoS ONE* 12, e0183596 (2017).
151. Castellano, J. M. *et al.* KiSS-1 System and Restoration of Pubertal Activation of the Reproductive Axis by Kisspeptin in Undernutrition. *Endocrinology* 146, 3917–3925 (2005).
152. Cravo, R. M. *et al.* Characterization of Kiss1 neurons using transgenic mouse

models. *NSC* 173, 37–56 (2011).
153. Qiu, X. *et al.* Insulin and Leptin Signaling Interact in the Mouse Kiss1 Neuron during the Peripubertal Period. *PLoS ONE* 10, e0121974 (2015).
154. Donato, J., Jr. *et al.* Leptin's effect on puberty in mice is relayed by the ventral premammillary nucleus and does not require signaling in Kiss1 neurons. *J. Clin. Invest.* 121, 355–368 (2011).
155. Cravo, R. M. *et al.* Leptin Signaling in Kiss1 Neurons Arises after Pubertal Development. *PLoS ONE* 8, e58698–7 (2013).
156. Forbes, S., Li, X. F., Kinsey-Jones, J. & O'Byrne, K. Effects of ghrelin on Kisspeptin mRNA expression in the hypothalamic medial preoptic area and pulsatile luteinising hormone secretion in the female rat. *Neuroscience Letters* 460, 143–147 (2009).
157. Frazão, R. *et al.* Estradiol modulates Kiss1 neuronal response to ghrelin. *Am J Physiol Endocrinol Metab* 306, E606–E614 (2014).
158. Satake, H., Aoyama, M., Sekiguchi, T. & Kawada, T. Insight into Molecular and Functional Diversity of Tachykinins and their Receptors. *PPL* 20, 615–627 (2013).
159. Steinhoff, M. S., Mentzer, von, B., Geppetti, P., Pothoulakis, C. & Bunnett, N. W. Tachykinins and Their Receptors: Contributions to Physiological Control and the Mechanisms of Disease. *Physiological Reviews* 94, 265–301 (2014).
160. Maggi, C. A. The mammalian tachykinin receptors. *General Pharmacology: The Vascular System* 26, 911–944 (1995).
161. de Croft, S., Boehm, U. & Herbison, A. E. Neurokinin B Activates Arcuate Kisspeptin Neurons Through Multiple Tachykinin Receptors in the Male Mouse. *Endocrinology* 154, 2750–2760 (2013).
162. Goodman, R. L. *et al.* Kisspeptin Neurons in the Arcuate Nucleus of the Ewe Express Both Dynorphin A and Neurokinin B. *Endocrinology* 148, 5752–5760 (2007).
163. Noritake, K.-I. *et al.* Involvement of Neurokinin Receptors in the Control of Pulsatile Luteinizing Hormone Secretion in Rats. *J. Reprod. Dev.* 57, 409–415 (2011).
164. Ruiz-Pino, F. *et al.* Neurokinin B and the Control of the Gonadotropic Axis in the Rat: Developmental Changes, Sexual Dimorphism, and Regulation by Gonadal Steroids. *Endocrinology* 153, 4818–4829 (2012).
165. Topaloglu, A. K. *et al.* TAC3 and TACR3 mutations in familial hypogonadotropic hypogonadism reveal a key role for Neurokinin B in the central control of reproduction. *Nat Genet* 41, 354–358 (2008).
166. Hrabovszky, E. Neuroanatomy of the Human Hypothalamic Kisspeptin System. *Neuroendocrinology* 99, 33–48 (2014).
167. Navarro, V. M. *et al.* Interactions between kisspeptin and neurokinin B in the control of GnRH secretion in the female rat. *Am J Physiol Endocrinol Metab* 300, E202–E210 (2011).
168. Debeljuk, L. & Lasaga, M. Modulation of the hypothalamo-pituitary-gonadal axis and the pineal gland by neurokinin A, neuropeptide K and neuropeptide γ.

Peptides 20, 285–299 (1999).
169. Shamgochian, M. D. & Leeman, S. E. Substance P stimulates luteinizing hormone secretion from anterior pituitary cells in culture. *Endocrinology* 131, 871–875 (1992).
170. Garcia-Galiano, D. *et al.* Kisspeptin Signaling Is Indispensable for Neurokinin B, but not Glutamate, Stimulation of Gonadotropin Secretion in Mice. *Endocrinology* 153, 316–328 (2012).
171. Ramaswamy, S. *et al.* Neurokinin B Stimulates GnRH Release in the Male Monkey (Macaca mulatta) and Is Colocalized with Kisspeptin in the Arcuate Nucleus. *Endocrinology* 151, 4494–4503 (2010).
172. Fergani, C. *et al.* NKB signaling in the posterodorsal medial amygdala stimulates gonadotropin release in a kisspeptin-independent manner in female mice. *eLife* 7, e12572 (2018).
173. Navarro, V. M. *et al.* Role of Neurokinin B in the Control of Female Puberty and Its Modulation by Metabolic Status. *J. Neurosci.* 32, 2388–2397 (2012).
174. Young, J. *et al.* TAC3 and TACR3Defects Cause Hypothalamic Congenital Hypogonadotropic Hypogonadism in Humans. *The Journal of Clinical Endocrinology & Metabolism* 95, 2287–2295 (2010).
175. True, C., Nasrin Alam, S., Cox, K., Chan, Y.-M. & Seminara, S. B. Neurokinin B Is Critical for Normal Timing of Sexual Maturation but Dispensable for Adult Reproductive Function in Female Mice. *Endocrinology* 156, 1386–1397 (2015).
176. Yang, J. J., Caligioni, C. S., Chan, Y.-M. & Seminara, S. B. Uncovering Novel Reproductive Defects in Neurokinin B Receptor Null Mice: Closing the Gap Between Mice and Men. *Endocrinology* 153, 1498–1508 (2012).
177. Gianetti, E. *et al.* TAC3/TACR3 mutations reveal preferential activation of gonadotropin-releasing hormone release by neurokinin B in neonatal life followed by reversal in adulthood. *The Journal of Clinical Endocrinology & Metabolism* 95, 2857–2867 (2010).
178. León, S. *et al.* Tachykinin signaling is required for the induction of the preovulatory LH surge and normal LH pulses. *Neuroendocrinology* (2020).
179. Lehman, M. N., Coolen, L. M. & Goodman, R. L. Minireview: Kisspeptin/Neurokinin B/Dynorphin (KNDy) Cells of the Arcuate Nucleus: A Central Node in the Control of Gonadotropin-Releasing Hormone Secretion. *Endocrinology* 151, 3479–3489 (2010).
180. Navarro, V. M. & Tena-Sempere, M. Neuroendocrine control by kisspeptins: role in metabolic regulation of fertility. *Nat Rev Endocrinol* 8, 40–53 (2011).
181. Clarkson, J. *et al.* Definition of the hypothalamic GnRH pulse generator in mice. *Proc Natl Acad Sci USA* 114, E10216–E10223 (2017).
182. Rance, N. E., Dacks, P. A., Mittelman-Smith, M. A., Romanovsky, A. A. & Krajewski-Hall, S. J. Modulation of body temperature and LH secretion by hypothalamic KNDy (kisspeptin, neurokinin B and dynorphin) neurons: A novel hypothesis on the mechanism of hot flushes. *Frontiers in Neuroendocrinology* 34, 211–227 (2013).
183. Krajewski-Hall, S. J., Blackmore, E. M., McMinn, J. R. & Rance, N. E. Estradiol

alters body temperature regulation in the female mouse. *Temperature* 5, 56–69 (2017).
184. Jayasena, C. N. *et al.* Neurokinin B Administration Induces Hot Flushes in Women. *Nature Publishing Group* 5, 1–7 (2015).
185. Lasaga, M. & Debeljuk, L. Tachykinins and the hypothalamo–pituitary–gonadal axis: An update. *Peptides* 32, 1972–1978 (2011).
186. Coiro, V. *et al.* Luteinizing hormone response to an intravenous infusion of substance P in normal men. *Metabolism* 41, 689–691 (1992).
187. Hrabovszky, E. *et al.* Substance P Immunoreactivity Exhibits Frequent Colocalization with Kisspeptin and Neurokinin B in the Human Infundibular Region. *PLoS ONE* 8, e72369 (2013).
188. Ruiz-Pino, F. *et al.* Effects and Interactions of Tachykinins and Dynorphin on FSH and LH Secretion in Developing and Adult Rats. *Endocrinology* 156, 576–588 (2015).
189. Simavli, S. *et al.* Substance P Regulates Puberty Onset and Fertility in the Female Mouse. *Endocrinology* 156, 2313–2322 (2015).
190. Dornan, W. A., Malsbury, C. W. & Penney, R. B. Facilitation of lordosis by injection of substance P into the midbrain central gray. *Neuroendocrinology* 45, 498–506 (1987).
191. Berger, A. *et al.* Diminished pheromone-induced sexual behavior in neurokinin-1 receptor deficient (TACR1 −/−) mice. *Genes, Brain and Behavior* 11, 568–576 (2012).
192. Kalra, P. S. Diverse effects of tachykinins on luteinizing hormone release in male rats: mechanism of action. *Endocrinology* 131, 1195–1201 (1992).
193. Candenas, L. *et al.* Tachykinins and tachykinin receptors: effects in the genitourinary tract. *Life Sciences* 76, 835–862 (2005).
194. Ravina, C. G. *et al.* A role for tachykinins in the regulation of human sperm motility. *Human Reproduction* 22, 1617–1625 (2007).
195. Candenas, M. L. *et al.* Changes in the Expression of Tachykinin Receptors in the Rat Uterus During the Course of Pregnancy1. *Biology of Reproduction* 65, 538–543 (2001).
196. Pennefather, J. N., Patak, E., Pinto, F. M. & Candenas, M. L. Mammalian tachykinins and uterine smooth muscle: the challenge escalates. *European Journal of Pharmacology* 500, 15–26 (2004).
197. Patak, E. *et al.* Tachykinins and tachykinin receptors in human uterus. *British Journal of Pharmacology* 139, 523–532 (2003).
198. Pennefather, J. N., Zeng, X.-P., Gould, D., Hall, S. & Burcher, E. Mammalian tachykinins stimulate rat uterus by activating NK-2 receptors. *Peptides* 14, 169–174 (1993).
199. Debeljuk, L., Rao, J. N. & Bartke, A. Tachykinins and their possible modulatory role on testicular function: a review. *International Journal of Andrology* 26, 202–210 (2003).
200. Chiwakata, C. *et al.* Tachykinin (substance-P) gene expression in Leydig cells of the human and mouse testis. *Endocrinology* 128, 2441–2448 (1991).

201. Araque, A., Carmignoto, G. & Haydon, P. G. Dynamic Signaling Between Astrocytes and Neurons. *Annual Review of physiology* 63, 795–813 (2001).
202. Jäkel, S. & Dimou, L. Glial Cells and Their Function in the Adult Brain: A Journey through the History of Their Ablation. *Front. Cell. Neurosci.* 11, 81–17 (2017).
203. Mong, J. A., Glaser, E. & McCarthy, M. M. Gonadal Steroids Promote Glial Differentiation and Alter Neuronal Morphology in the Developing Hypothalamus in a Regionally Specific Manner. *J. Neurosci.* 19, 1464–1472 (1999).
204. Clasadonte, J. & Prevot, V. The special relationship: glia–neuron interactions in the neuroendocrine hypothalamus. *Nature Publishing Group* 1–20 (2017).
205. Ojeda, S. R., Lomniczi, A. & Sandau, U. Contribution of glial-neuronal interactions to the neuroendocrine control of female puberty. *European Journal of Neuroscience* 32, 2003–2010 (2010).
206. Ojeda, S. R., Lomniczi, A. & Sandau, U. S. Glial-Gonadotrophin Hormone (GnRH) Neurone Interactions in the Median Eminence and the Control of GnRH Secretion. *Journal of Neuroendocrinology* 20, 732–742 (2008).
207. Rage, F., Lee, B. J., Ma, Y. J. & Ojeda, S. R. Estradiol Enhances Prostaglandin E2 Receptor Gene Expression in Luteinizing Hormone-Releasing Hormone (LHRH) Neurons and Facilitates the LHRH Response to PGE2 by Activating a Glia-to-Neuron Signaling Pathway. *J. Neurosci.* 17, 9145–9156 (1997).
208. Sandau, U. S. *et al.* The Synaptic Cell Adhesion Molecule, SynCAM1, Mediates Astrocyte-to-Astrocyte and Astrocyte-to-GnRH Neuron Adhesiveness in the Mouse Hypothalamus. *Endocrinology* 152, 2353–2363 (2011).
209. Garcia-Segura, L. M. & McCarthy, M. M. Minireview: Role of Glia in Neuroendocrine Function. *Endocrinology* 145, 1082–1086 (2004).
210. Witkin, J. W., Ferin, M., Popilskis, S. J. & Silverma, A.-J. Effects of Gonadal Steroids on the Ultrastructure of GnRH Neurons in the Rhesus Monkey: Synaptic Input and Glial Apposition. *Endocrinology* 129, 1083–1092 (1991).
211. Baroncini, M. *et al.* Morphological Evidence for Direct Interaction Between Gonadotrophin-Releasing Hormone Neurones and Astroglial Cells in the Human Hypothalamus. *Journal of Neuroendocrinology* 19, 691–702 (2007).
212. Pirttimaki, T. M. & Parri, H. R. Astrocyte Plasticity. *Neuroscientist* 19, 604–615 (2013).
213. Kohama, S. G., Goss, J. R., McNeill, T. H. & Finch, C. E. Glial fibrillary acidic protein mRNA increases at proestrus in the arcuate nucleus of mice. *Neuroscience Letters* 183, 164–166 (1995).
214. Cashion, A. B., Smith, M. J. & Wise, P. M. The Morphometry of Astrocytes in the Rostral Preoptic Area Exhibits a Diurnal Rhythm on Proestrus: Relationship to the Luteinizing Hormone Surge and Effects of Age. *Endocrinology* 144, 274–280 (2003).
215. Ojeda, S. R., Urbanski, H. F., Costa, M. E., Hill, D. F. & Moholt-Siebert, M. Involvement of transforming growth factor alpha in the release of luteinizing hormone-releasing hormone from the developing female hypothalamus. *Proc Natl Acad Sci USA* 87, 9698–9702 (1990).
216. Sharif, A., Baroncini, M. & Prevot, V. Role of Glia in the Regulation of

Gonadotropin-Releasing Hormone Neuronal Activity and Secretion. *Neuroendocrinology* 98, 1–15 (2013).
217. Glanowska, K. M. & Moenter, S. M. Endocannabinoids and prostaglandins both contribute to GnRH neuron-GABAergic afferent local feedback circuits. *Journal of Neurophysiology* 106, 3073–3081 (2011).
218. Kim, J. G. *et al.* Leptin signaling in astrocytes regulates hypothalamic neuronal circuits and feeding. *Nat Neurosci* 17, 908–910 (2014).
219. Fuente-Martín, E. *et al.* Ghrelin Regulates Glucose and Glutamate Transporters in Hypothalamic Astrocytes. *Nature Publishing Group* 6, 14875–15 (2016).
220. Thaler, J. P. *et al.* Obesity is associated with hypothalamic injury in rodents and humans. *J. Clin. Invest.* 122, 153–162 (2012).
221. Buckman, L. B., Thompson, M. M., Moreno, H. N. & Ellacott, K. L. J. Regional astrogliosis in the mouse hypothalamus in response to obesity. *J. Comp. Neurol.* 521, 1322–1333 (2013).
222. García-Cáceres, C., Yi, C.-X. & Tschöp, M. H. Hypothalamic Astrocytes in Obesity. *Endocrinology and Metabolism Clinics of North America* 42, 57–66 (2013).
223. Hsuchou, H. *et al.* Obesity induces functional astrocytic leptin receptors in hypothalamus. *Brain* 132, 889–902 (2008).
224. Zhuo, L. *et al.* hGFAP-cre transgenic mice for manipulation of glial and neuronal function in vivo. *genesis* 31, 85–94 (2001).
225. Malatesta, P. *et al.* Neuronal or Glial Progeny. *Neuron* 37, 751–764 (2003).
226. d'Anglemont de Tassigny, X. *et al.* Hypogonadotropic hypogonadism in mice lacking a functional Kiss1 gene. *Proc Natl Acad Sci USA* 104, 10714–10719 (2007).
227. Steyn, F. J. *et al.* Development of a Methodology for and Assessment of Pulsatile Luteinizing Hormone Secretion in Juvenile and Adult Male Mice. *Endocrinology* 154, 4939–4945 (2013).
228. Bilkei-Gorzo, A., Racz, I., Michel, K. & Zimmer, A. Diminished Anxiety- and Depression-Related Behaviors in Mice with Selective Deletion of the Tac1 Gene. *J. Neurosci.* 22, 10046–10052 (2002).
229. Malkesman, O. *et al.* The Female Urine Sniffing Test: A Novel Approach for Assessing Reward-Seeking Behavior in Rodents. *Biological Psychiatry* 67, 864–871 (2010).
230. Wang, Q. *et al.* The Allen Mouse Brain Common Coordinate Framework: A 3D Reference Atlas. *Cell* 181, 936–953.e20 (2020).
231. Pinilla, L., Rodriguez-Padilla, M. L., Sanchez-Criado, J., Gaytán, F. & Aguilar, E. Mechanism of reproductive deficiency in spontaneously hypertensive rats. *Physiology & Behavior* 51, 99–104 (1992).
232. Ortea, I., Ruiz-Sánchez, I., Cañete, R., Caballero-Villarraso, J. & Cañete, M. D. Identification of candidate serum biomarkers of childhood-onset growth hormone deficiency using SWATH-MS and feature selection. *Journal of Proteomics* 175, 105–113 (2018).
233. Szklarczyk, D. *et al.* STRING v11: protein–protein association networks with

increased coverage, supporting functional discovery in genome-wide experimental datasets. *Nucleic Acids Research* 47, D607–D613 (2018).

234. Doncheva, N. T., Morris, J. H., Gorodkin, J. & Jensen, L. J. Cytoscape StringApp: Network Analysis and Visualization of Proteomics Data. *J. Proteome Res.* 18, 623–632 (2018).
235. Roa, J. *et al.* The Mammalian Target of Rapamycin as Novel Central Regulator of Puberty Onset via Modulation of Hypothalamic Kiss1 System. *Endocrinology* 150, 5016–5026 (2009).
236. Clarkson, J. *et al.* Definition of the hypothalamic GnRH pulse generator in mice. *Proc Natl Acad Sci USA* 114, E10216–E10223 (2017).
237. Esparza, L. A., Schafer, D., Ho, B. S., Thackray, V. G. & Kauffman, A. S. Hyperactive LH Pulses and Elevated Kisspeptin and NKB Gene Expression in the Arcuate Nucleus of a PCOS Mouse Model. *Endocrinology* 161, 377 (2020).
238. Velasco, I. *et al.* Gonadal hormone-dependent vs. -independent effects of kisspeptin signaling in the control of body weight and metabolic homeostasis. *Metabolism* 98, 84–94 (2019).
239. Wolfe, A. & Hussain, M. A. The Emerging Role(s) for Kisspeptin in Metabolism in Mammals. *Front. Endocrinol.* 9, 1731 (2018).
240. Karagiannides, I. *et al.* Substance P (SP)-Neurokinin-1 Receptor (NK-1R) Alters Adipose Tissue Responses to High-Fat Diet and Insulin Action. *Endocrinology* 152, 2197–2205 (2011).
241. Maguire, C. A., Leon, S., Carroll, R. S., Kaiser, U. B. & Navarro, V. M. Altered circadian feeding behavior and improvement of metabolic syndrome in obese Tac1-deficient mice. *Int J Obes* 41, 1798–1804 (2017).
242. Kronenberg, F. Hot Flashes: Epidemiology and Physiologya. *Annals of the New York Academy of Sciences* 592, 52–86 (1990).
243. Mittelman-Smith, M. A., Krajewski-Hall, S. J., McMullen, N. T. & Rance, N. E. Neurokinin 3 Receptor-Expressing Neurons in the Median Preoptic Nucleus Modulate Heat-Dissipation Effectors in the Female Rat. *Endocrinology* 156, 2552–2562 (2015).
244. Zhang, Z. *et al.* The Appropriate Marker for Astrocytes: Comparing the Distribution and Expression of Three Astrocytic Markers in Different Mouse Cerebral Regions. *BioMed Research International* 2019, 1–15 (2019).
245. Schnitzer, J., Franke, W. W. & Schachner, M. Immunocytochemical demonstration of vimentin in astrocytes and ependymal cells of developing and adult mouse nervous system. *Journal of Cell Biology* 90, 435–447 (1981).
246. Martinez, R. & Gomes, F. C. A. Neuritogenesis Induced by Thyroid Hormone-treated Astrocytes Is Mediated by Epidermal Growth Factor/Mitogen-activated Protein Kinase-Phosphatidylinositol 3-Kinase Pathways and Involves Modulation of Extracellular Matrix Proteins. *J. Biol. Chem.* 277, 49311–49318 (2002).
247. Buckman, L. B. *et al.* Evidence for a novel functional role of astrocytes in the acute homeostatic response to high-fat diet intake in mice. *Molecular Metabolism* 4, 58–63 (2015).
248. Creasy, D. *et al.* Proliferative and Nonproliferative Lesions of the Rat and Mouse

Male Reproductive System. *Toxicol Pathol* 40, 40S–121S (2012).
249. Navarro, V. M. *et al.* Developmental and Hormonally Regulated Messenger Ribonucleic Acid Expression of KiSS-1 and Its Putative Receptor, GPR54, in Rat Hypothalamus and Potent Luteinizing Hormone-Releasing Activity of KiSS-1 Peptide. *Endocrinology* 145, 4565–4574 (2004).
250. Yang, J. J., Caligioni, C. S., Chan, Y.-M. & Seminara, S. B. Uncovering novel reproductive defects in neurokinin B receptor null mice: closing the gap between mice and men. *Endocrinology* 153, 1498–1508 (2012).
251. Mittelman-Smith, M. A., Williams, H., Krajewski-Hall, S. J., McMullen, N. T. & Rance, N. E. Role for kisspeptin/neurokinin B/dynorphin (KNDy) neurons in cutaneous vasodilatation and the estrogen modulation of body temperature. *Proc Natl Acad Sci USA* 109, 19846–19851 (2012).
252. Krajewski-Hall, S. J., Miranda Dos Santos, F., McMullen, N. T., Blackmore, E. M. & Rance, N. E. Glutamatergic Neurokinin 3 Receptor Neurons in the Median Preoptic Nucleus Modulate Heat-Defense Pathways in Female Mice. *Endocrinology* 160, 803–816 (2019).
253. Skorupskaite, K., George, J. T., Veldhuis, J. D., Millar, R. P. & Anderson, R. A. Neurokinin 3 Receptor Antagonism Reveals Roles for Neurokinin B in the Regulation of Gonadotropin Secretion and Hot Flashes in Postmenopausal Women. *Neuroendocrinology* 106, 148–157 (2018).
254. Cao, Y. Q. *et al.* Primary afferent tachykinins are required to experience moderate to intense pain. *Nature* 392, 390–394 (1998).
255. Santarelli, L. Genetic and pharmacological disruption of neurokinin 1 receptor function decreases anxiety-related behaviors and increases serotonergic function. *Proc Natl Acad Sci USA* 98, 1912–1917 (2001).
256. Rao, J. N., Debeljuk, L. & Bartke, A. Effects of tachykinins on the secretory activity of rat Sertoli cells in vitro. *Endocrinology* 136, 1315–1318 (1995).
257. Karagiannides, I. *et al.* Role of Substance P in the Regulation of Glucose Metabolism via Insulin Signaling-Associated Pathways. *Endocrinology* 152, 4571–4580 (2011).
258. Kaczyńska, K., Jampolska, M. & Szereda-Przestaszewska, M. The role of vagal pathway and NK 1and NK 2receptors in cardiovascular and respiratory effects of neurokinin A. *Clin Exp Pharmacol Physiol* 43, 818–824 (2016).
259. Giuliani, S. *et al.* Effect of a tachykinin NK2 receptor antagonist, nepadutant, on cardiovascular and gastrointestinal function in rats and dogs. *European Journal of Pharmacology* 415, 61–71 (2001).
260. Eng, L. F. Glial fibrillary acidic protein (GFAP): the major protein of glial intermediate filaments in differentiated astrocytes. *Journal of Neuroimmunology* 8, 203–214 (1985).
261. Kuipers, H. F. *et al.* Phosphorylation of αB-crystallin supports reactive astrogliosis in demyelination. *Proc Natl Acad Sci USA* 114, E1745–E1754 (2017).
262. Banati, R. B., Gehrmann, J., Wießner, C., Hossmann, K. A. & Kreutzberg, G. W. Glial Expression of the β-Amyloid Precursor Protein (APP) in Global Ischemia. *J Cereb Blood Flow Metab* 15, 647–654 (2016).

263. Lee, S.-J., Seo, B.-R. & Koh, J.-Y. Metallothionein-3 modulates the amyloid β endocytosis of astrocytes through its effects on actin polymerization. *Mol Brain* 8, 1–12 (2015).
264. Gottsch, M. L. *et al.* A Role for Kisspeptins in the Regulation of Gonadotropin Secretion in the Mouse. *Endocrinology* 145, 4073–4077 (2004).
265. Szereszewski, J. M. *et al.* GPR54 Regulates ERK1/2 Activity and Hypothalamic Gene Expression in a Gαq/11 and β-Arrestin-Dependent Manner. *PLoS ONE* 5, e12964 (2010).
266. Terasaka, T. *et al.* Mutual interaction of kisspeptin, estrogen and bone morphogenetic protein-4 activity in GnRH regulation by GT1-7 cells. *Molecular and Cellular Endocrinology* 381, 8–15 (2013).
267. Kirilov, M. *et al.* Dependence of fertility on kisspeptin–Gpr54 signaling at the GnRH neuron. *Nature Communications* 4, 1–11 (2013).
268. McQueen, J. K. & Wilson, H. The Development of Astrocytes Immunoreactive for Glial Fibrillary Acidic Protein in the Mediobasal Hypothalamus of Hypogonadal Mice. *Molecular and Cellular Neuroscience* 5, 623–631 (1994).
269. Marino, S., Vooijs, M., van Der Gulden, H., Jonkers, J. & Berns, A. Induction of medulloblastomas in p53-null mutant mice by somatic inactivation of Rb in the external granular layer cells of the cerebellum. *Genes Dev* 14, 994–1004 (2000).
270. Buckman, L. B. *et al.* Evidence for a novel functional role of astrocytes in the acute homeostatic response to high-fat diet intake in mice. *Molecular Metabolism* 4, 58–63 (2015).
271. Skaznik-Wikiel, M. E., Swindle, D. C., Allshouse, A. A., Polotsky, A. J. & McManaman, J. L. High-Fat Diet Causes Subfertility and Compromised Ovarian Function Independent of Obesity in Mice. *Obstetrical & Gynecological Survey* 71, 532–533 (2016).